# EXPLOITATION OF SYNERGISTIC EFFECTS BETWEEN PLANT- DERIVED COMPOUNDS AND ANTIMICROBIAL PEPTIDES FOR BIOTECHNOLOGICAL PURPOSES

**Shurooq Ismail**

# EXPLOITATION OF SYNERGISTIC EFFECTS BETWEEN PLANT-DERIVED COMPOUNDS AND ANTIMICROBIAL PEPTIDES FOR BIOTECHNOLOGICAL PURPOSES

**Shurooq Ismail**

Dottorato in Biotecnologie – XXXV ciclo

Università di Napoli Federico II

# EXPLOITATION OF SYNERGISTIC EFFECTS BETWEEN PLANT-DERIVED COMPOUNDS AND ANTIMICROBIAL PEPTIDES FOR BIOTECHNOLOGICAL PURPOSES

**Shurooq Ismail**

Dottorato in Biotecnologie – XXXV ciclo

Università di Napoli Federico II

Dottorando: Shurooq Ismail

Relatore: Prof. Angela Arciello

Coordinatore: Prof. Marco Moracci

Settore Scientifico Disciplinare: BIO-10

*I dedicate this thesis to:*

*My beloved Parents **Muhammad** and **Afaf**; my role models in life who gave me all their love, trust, compassion, and support.*

*My dear sisters **Noor**, **Rawan**, **Duá**, **Nidá**, **Aya** and **Jasneem**, as well as my precious brother, **Abdullah**.*
*You all made my life full of love and happiness.*

( وَعَلَّمَكَ مَا لَمْ تَكُن تَعْلَمُ ۚ وَكَانَ فَضْلُ اللَّهِ عَلَيْكَ عَظِيمًا )

صدق الله العظيم (النساء: 113)

*'And Allah has revealed to you the Book and wisdom and has taught you that which you did not know. And ever has the favor of Allah upon you been great.'*

*(Surah An-Nisa :113)*

# INDEX

## ABSTRACT

The discovery of penicillin by Sir Alexander Fleming in 1928 started the golden age of natural product antibiotic discovery that peaked in the mid-1950s. Since then, a gradual decline in antibiotic discovery as well as the development and evolution of drug resistance in many human pathogens has led to the current antimicrobial resistance crisis. Plants are one of the dominant creatures on earth and represent the primitive rich source of antimicrobial natural products. Indeed, plants adapt and encounter diverse environmental challenges since their existence. For this reason, they have evolved sophisticated and effective defense mechanisms against predators, abiotic stress, and diseases. Due to this adaptive process, plants can produce a massive chemical arsenal of secondary metabolites effective in combating even the most dangerous infections. Here, a bio-guided purification of *Centaurea hyalolepis* and *Ephedra foeminea* extracts were performed for the first time to identify bioactive compounds. The molecular structure of the identified compounds was determined by nuclear magnetic resonance (NMR) spectroscopy and mass spectrometry (MS) analyses. Six compounds were isolated and identified from *E. foeminea* extracts including both monoterpenoid phenols carvacrol and thymol, in addition to four acylated kaempferol glycosides. Regarding *C. hyalolepis* extracts, three sesquiterpene lactones were isolated and identified as cnicin, 11β,13-dihydrosalonitenolide and salonitenolide. Among the identified compounds,kaempferol-3-*O*-*α*-L-(2”,4”-di-*E*-*p*-coumaroyl)-rhamnopyranoside which was found to be endowed with pronounced antibacterial properties and significant anti-biofilm activity against *S. aureus* bacterial strains. Moreover, significant additive effects were observed when this compound was tested in combination with r(P)ApoBL$^{Pro}$ peptide against the tested *S. aureus* MRSA WKZ-2 and *A. baumannii* ATCC 17878 bacterial strains. Preliminary experiments were also performed to load this compound on hydroxyethyl cellulose (HEC) films cross-linked with citric acid, thus developing an active food packaging system that might be able to prevent food spoilage. Altogether, the achieved results open interesting perspectives to the applicability of the identified plant-derived compounds in several fields, such as biomedical, pharmaceutical, cosmeceutical, as well as in food preservation and active packaging areas.

## RIASSUNTO

La scoperta della penicillina da parte di Alexander Fleming nel 1928 ha dato inizio all'età d'oro della scoperta degli antibiotici da prodotti naturali che raggiunse il picco a metà degli anni '50. Da allora, un graduale declino nella scoperta di nuovi antibiotici in concomitanza con lo sviluppo e l'evoluzione della resistenza ai farmaci in molti agenti patogeni umani ha portato all'attuale crisi dovuta ad una massiva resistenza agli agenti antimicrobici. Le piante sono tra le creature dominanti sulla Terra e rappresentano una fonte primitiva e ricca di prodotti naturali antimicrobici. In effetti, le piante si sono adattate ad affrontare diverse sfide ambientali sin dalla loro esistenza. Per questo motivo, hanno sviluppato sofisticati ed efficaci meccanismi di difesa contro predatori, stress abiotici e malattie. Grazie a questo processo di adattamento, le piante possono produrre un enorme arsenale chimico di metaboliti secondari efficaci nel combattere anche le infezioni più pericolose. Nel presente lavoro di tesi, è stata eseguita per la prima volta una purificazione bio-guidata degli estratti di *Centaurea hyalolepis* ed *Ephedra foeminea*, al fine di identificare i principali composti bioattivi in essi contenuti. La struttura molecolare dei composti identificati è stata determinata mediante spettroscopia di risonanza magnetica nucleare (NMR) e analisi di spettrometria di massa (MS). Sei composti sono stati isolati e identificati da estratti di *E. foeminea*, inclusi i fenoli monoterpenici carvacrolo e timolo, oltre a quattro glicosidi acilati del kaempferolo. Nel caso degli estratti di *C. hyalolepis*, tre lattoni sesquiterpenici sono stati isolati e identificati come cnicina, 11β,13-diidrosalonitenolide e salonitenolide. Tra i composti identificati, il kaempferolo-3-*O*-*α*-L-(2”,4”-di-*E*-*p*-cumaril)-ramnopiranoside è risultato dotato di spiccate proprietà antibatteriche e significativa attività anti-biofilm nei confronti del batterio *S. aureus*. Inoltre, sono stati osservati significativi effetti additivi quando questo composto è stato testato in combinazione con il peptide antimicrobico r(P)ApoB$_L^{Pro}$ contro i ceppi batterici *S. aureus* MRSA WKZ-2 e *A. baumannii* ATCC 17878. Sono stati, inoltre, eseguiti esperimenti preliminari per caricare questo composto su film di idrossietilcellulosa (HEC) reticolati con acido citrico, con l’intento di sviluppare un sistema di confezionamento alimentare attivo che potrebbe essere in grado di prevenire il deterioramento di campioni alimentari. Nel complesso, i risultati raggiunti aprono

prospettive interessanti all'applicabilità dei composti di origine vegetale qui identificati in diversi campi, come quello biomedico, farmaceutico, cosmeceutico, così come nelle aree della conservazione degli alimenti e del *packaging* alimentare attivo.

# CHAPTER 1

# General Introduction

Shurooq Ismail
Department of Chemical Sciences, PhD in Biotechnology
University of Naples Federico II

# General Introduction

## 1.1 Plant-derived Compounds as Antimicrobial Agents

Natural products embrace chemical compounds with several biological properties that allow their applicability in biomedicine, veterinary medicine, agriculture, and industry. Natural products comprise molecules derived from the secondary metabolism of animals, plants, bacteria, algae, and fungi [1,2]. Plants represent up to 80% of the total biomass of ecosystems and they are a primitive source of antimicrobial natural products [3]. Through their evolution, plants have evolved sophisticated and effective defense mechanisms against predators, abiotic stress, and diseases. Due to this adaptive process, plants became able to produce a rich arsenal of secondary metabolites able to combat even the most dangerous infections [4]. Since ancient times, plant-derived compounds were used as flavorings, preservatives, and as antioxidant and antimicrobial agents in traditional medicine [5]. It was reported that Sumerians employed thyme for its beneficial impact on health [6]. Moreover, the ancient Egyptian population used *Aloe vera*, castor bean, garlic, hemp, anise, and mustard for their nutritive and healing properties [7]. Hence, plants represent a source of priceless therapeutic compounds that could be identified by using modern technologies that could allow to investigate the basis of this folkloric medicinal heritage and to discover therapeutic instruments suitable for nowadays challenges.

Several secondary metabolites produced by plants, such as tannins, terpenoids, alkaloids, polyphenols, and flavonoids, were found to be endowed with antimicrobial properties *in vitro* against both Gram-positive and Gram-negative bacteria. Some of these phytochemicals were also found to alter or to influence the resistance mechanisms in bacteria [8]. Plant-derived compounds might also help conventional antimicrobials to penetrate into bacterial cells more effectively. Massive studies were conducted to investigate the antimicrobial activity of several plant extracts, in order to identify alternatives to conventional antibiotics [5]. Among identified compounds, the essential oil allicin from garlic, which was found to exert (i) antibacterial properties against a variety of Gram-positive and Gram-negative bacteria, including multidrug-resistant *Escherichia coli* strains, (ii) antifungal activity against *Candida albicans* (iii) anti-parasitic properties against human intestinal protozoan parasites, and (iv) antiviral activity [9]. Garlic total extract was also found to impair *Pseudomonas aeruginosa's* capacity for quorum sensing, thus making bacterial cells more vulnerable to the

bactericidal effects of tobramycin antibiotic and to polymorphonuclear leukocytes [10,11]. Similarly, *Nigella sativa* extracts were found to successfully eradicate the pathogenic yeast *Candida albicans*. Garlic and black cumin were traditionally used to treat urinary tract infections, and it was demonstrated that they are more effective than cefalexin, cotrimoxazole, and nalidixic acid in the treatment of infections [5]. Peppermint (*Mentha piperita*) oil was found to be more powerful than chlorhexidine in preventing the formation of biofilm by *Streptococcus* mutants and *Streptococcus pyogenes* [12]. It is challenging to assign the observed antibacterial activity to a specific element of plant extracts due to the concomitant presence of carbohydrates, peptides, alkaloids, glycosides, flavonoids, terpenoids, tannins, reducing sugars, soluble phenols, and saponin glycosides [13]. Possible mechanisms of the antimicrobial activity of some plant-derived compounds are summarized in **Figure 1** [14].

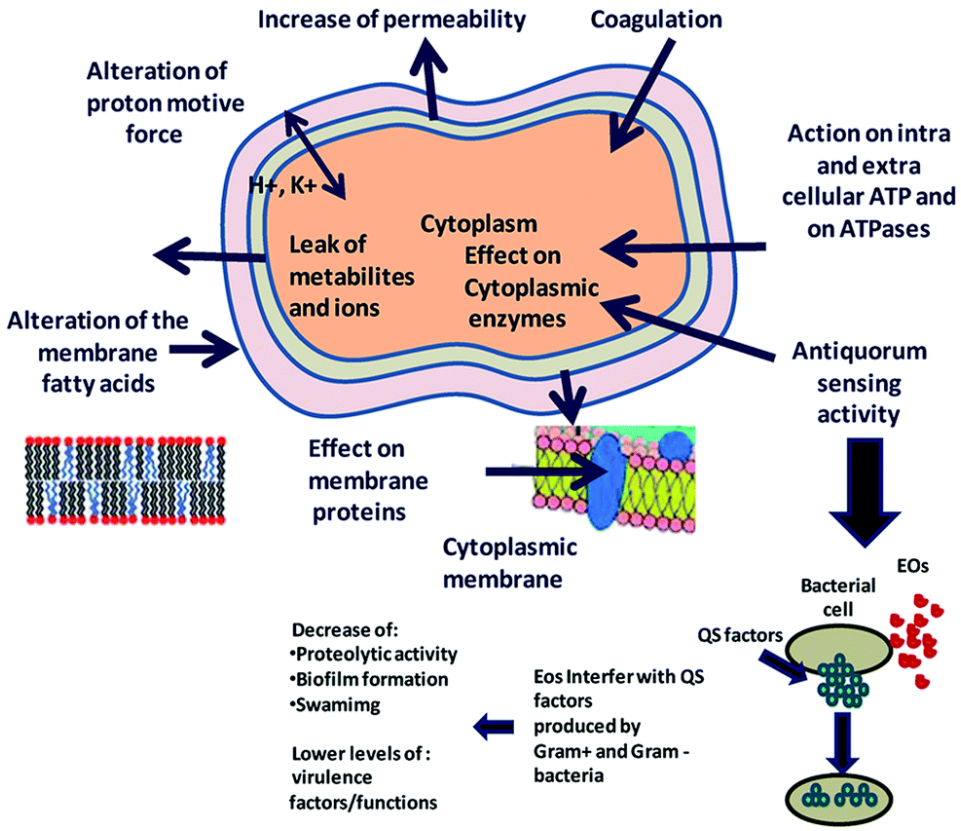


**Figure 1.** Targets of the antimicrobial activity of plant metabolites and their proposed mechanism of action from Bazaka *et al.*, 2015.

About 200,000 plant secondary metabolites were identified so far, and, among them, 170,000 had distinct chemical structures [15]. Alkaloids, terpenoids, and polyphenols are among the plant secondary metabolites endowed with antimicrobial properties [16]. Although only few studies described the antibacterial potentiality of pure alkaloids, several reports described the antimicrobial activity of plant extracts that contain alkaloids as primary constituents [17,18]. Terpenoids do not generally exhibit considerable antibacterial action, according to several *in vitro* investigations [19]. However, due to their hydrophobic properties and low molecular weight, they might contribute to enhance the antibacterial activity of other bioactive compounds [20]. Plant-derived polyphenols are divided into several subfamilies: flavonoids, hydrolysable tannins, lignans, phenolic acids and stilbenes. Based on the structure of the flavonoid group, other subfamilies can be identified: anthocyanidins, flavanones, flavones, flavonols and isoflavones. Examples of flavonoids with antimicrobial activity are quercetin, kaempferol, morin, and myricetin [21].

According to Lai and Roy, 2004 [5], the hydroxyl (-OH) groups of phenolic compounds might interact with bacterial cell membranes determining membrane alterations and the consequent leakage of cellular components [22]. It was reported that the antibacterial properties are significantly influenced by the presence and the position of the (-OH) group in phenolic compounds [23]. An example is represented by the antimicrobial activity of essential oils thymol and carvacrol that are structurally similar but, when tested *in vitro*, they showed different antibacterial properties against Gram-positive and Gram-negative bacteria. These variations are correlated to the fact that the (-OH) group in thymol is located in the meta position, whereas it is located in the ortho position in carvacrol [23]. In addition, double bonds were found to be key structural determinants of antimicrobial activity. Indeed, citronellol was found to be less effective than geraniol and nerol because it has only one double bond, whereas geraniol and nerol had two double bonds and exhibited stronger antibacterial effects [24,25]. Berberine, an isoquinoline alkaloid that was found in the roots of Berberis species, was found to be able to accumulate into the cells and to intercalate into DNA, with a consequent inhibition of several enzymes involved in DNA replication and protein synthesis, such as gyrase, topoisomerase IV and RNA polymerase [26,27]. Generally, plants' secondary metabolites were found to be characterized by diverse antimicrobial mechanism of actions, including the ability to form complexes with extracellular and insoluble proteins, and with

membrane proteins of targeted microbes. Membrane disruption and inhibition of bacterial enzymes were also described. Some secondary metabolites were found to function as proton exchangers that reduce the pH gradient across the cytoplasmic membrane, thus determining cell death. Some plant secondary metabolites have been also found to prevent biofilm formation or detach the already existing one [28-32].

## 1.2 Plants' Natural Compounds to Overcome Antimicrobial Resistance (AMR)

Antimicrobial Resistance (AMR) is the ability of microorganisms to adapt and thrive in the presence of compounds previously able to influence their survival [33]. This is a worrying phenomenon for human health and, if this issue is not resolved, conventional antibiotics used with great effectiveness in the past might be no longer able to provide humans with protection against bacterial infections [21]. Bacteria adapt to the presence of antibiotics by mutations, horizontal gene transfer or modifications of gene expression. Once antibiotic resistance is acquired, it could be transmitted to future bacterial generations either by cell division or by horizontal gene transfer [34]. Antibiotic abuse in health sector, agricultural practices, as well as, the modern and convenient transportation methods of people, animals, and goods have greatly contributed to the development of antimicrobial resistance in recent years [33].

The lack in the discovery of new antibiotics made the situation worse, thus urge the need to develop effective alternatives to conventional antibiotics. To fight antibiotic resistance, several strategies have been explored. Among these, the synergistic interactions between natural substances and antibiotics had attracted considerable attention [34]. Indeed, antibiotics and phytochemicals acting in synergism might represent a promising therapeutic approach. Plant-derived compounds and their isolated phytochemicals were found to be active on almost all the targets of multidrug resistant microbes (MDR) [34]. While some plant-derived compounds have direct antimicrobial activity against antibiotic-resistant bacteria, some of them are able to increase the effectiveness of antibiotics in different ways, *i.e.*, (i) by altering bacterial membrane and facilitating antibiotics entry, (ii) by blocking efflux pumps (EPs), or (iii) by disrupting biofilms [21]. Targets of natural products from different sources in MDR bacteria are summarized in **Figure 2**.

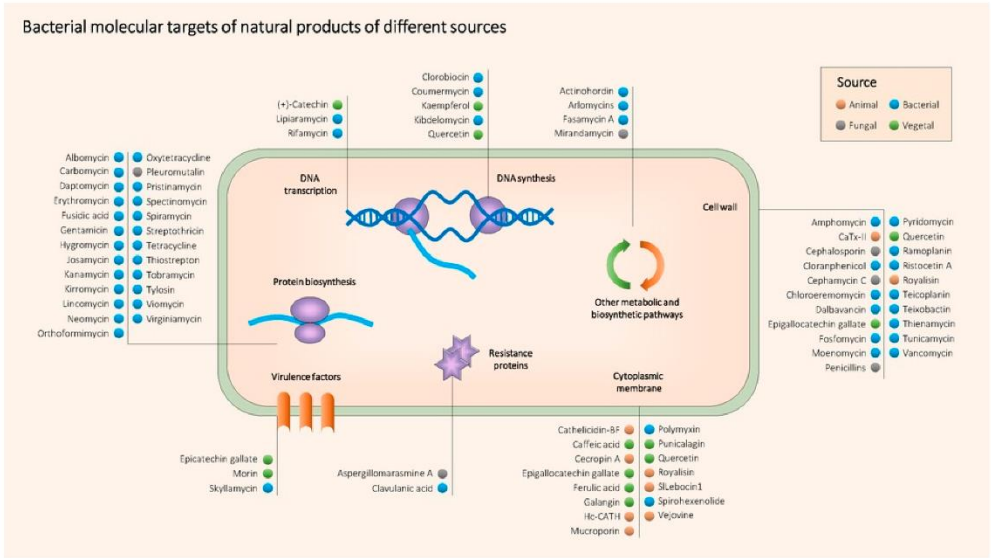


**Figure 2**. Molecular targets of antimicrobial natural compounds. Plant-derived compounds are represented in green. From Álvarez-Martínez *et al.,* 2020.

The chemical structures of common plant-derived compounds tested in combination with antibiotics are listed in **Figure 3** [34]. The plant-derived compounds kaempferol and quercetin are two flavonols with pronounced antimicrobial activity, which were found to enhance the efficacy of rifampicin antibiotic against MDR bacterial strains. This activity was attributed to the flavonols' ability to inhibit topoisomerases activity, with the consequent inhibition of DNA synthesis leading to cell death [35]. In addition, flavonol Epicatechin gallate (ECg) was found to enhance the sensitivity of MDR strains to penicillin or oxacillin. This is probably due to ECg ability to manipulate plasma membrane fluidity. ECg was also found to alter MDR strains sensitivity to β-lactam antibiotics through the alteration of PBP2a enzyme responsible for the resistance phenotype. Furthermore, ECg was found to be able to inhibit biofilm formation and to induce the decrease in the expression of proteins that are related to virulence factors [36]. Some phytochemicals were found to have a remarkable ability to block different efflux pumps of MDR Gram-positive or Gram-negative bacteria. For instance, capsaicin, indirubin, kaempferol rhamnoside, and olympicin-A were found to be able to disrupt NorA efflux pump of *S. aureus* SA-1199-B [37-41]. 4-hydroxytetralone, ursolic acid and its derivatives were found to be able to inhibit YojI efflux pump in MDR *E. coli* [42]. Berberine and palmatine were found to inhibit MexAB-OprM in a clinically isolatesd MDR strain of *P. aeruginosa* [43].

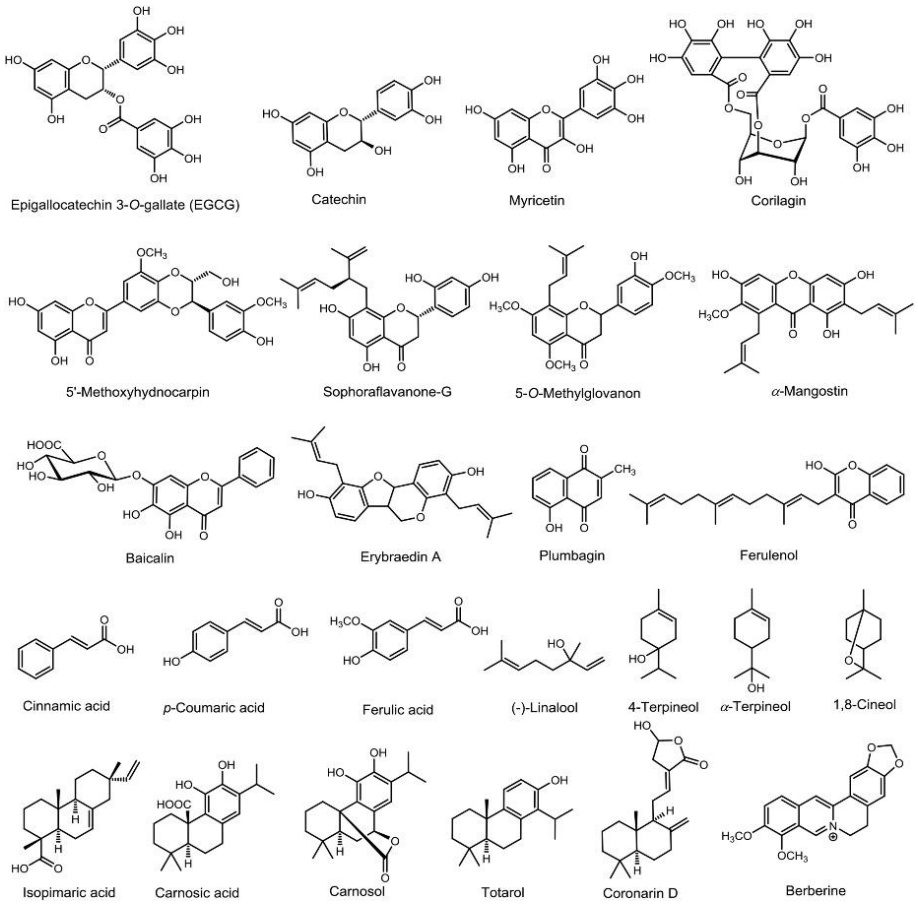


**Figure 3.** Chemical structure of plant-derived compounds tested in combinations with antibiotics, from Ayaz *et al*., 2019.

## 1.3 Antimicrobial Peptides (AMPs)

Antimicrobial peptides (AMPs) were discovered to be as a part of the innate immune system in all organisms. Therefore, they are also known as Host Defense Peptides (HDPs) [44]. Indeed, AMPs are able to exert not only direct antimicrobial effects, but they were also found to be endowed with multiple biological properties, such as antibiofilm, immunomodulatory, anticancer, cell signaling, cell differentiation, chemotaxis and wound healing properties. [45]. AMPs are generally short peptides with a length of about 12-50 residues, and with a net positive charge [45]. They are also rich in hydrophilic and hydrophobic amino acids; a fundamental feature conferred their diverse biological properties. AMPs typically have an overall positive net charge ranging from +2 to +9 [45]. Based on their secondary structure, AMPs can be divided into three groups: (i) those with α-helical, (ii) β-sheet, or (iii)

extended/random-coil structure. The first two classes comprise the majority of AMPs [46]. AMPs direct microbicidal activity mainly targets bacterial membrane [47]. Interactions between AMPs and bacterial membrane are generally mediated by electrostatic forces between the positively charged AMPs and the negatively charged bacterial surface [48,49]. The membrane of both Gram-positive and Gram-negative bacteria is abundant in negatively charged phospholipids. Additionally, lipopolysaccharides (LPS) and teichoic acids provide additional negative charge to bacterial surface, thus strengthening the interaction with AMPs [46][49]. Three models were proposed to explain AMPs mechanism of action, namely the barrel-stave model, toroidal pore model, and carpet model [50,51], which are schematically represented in **Figure 4.**

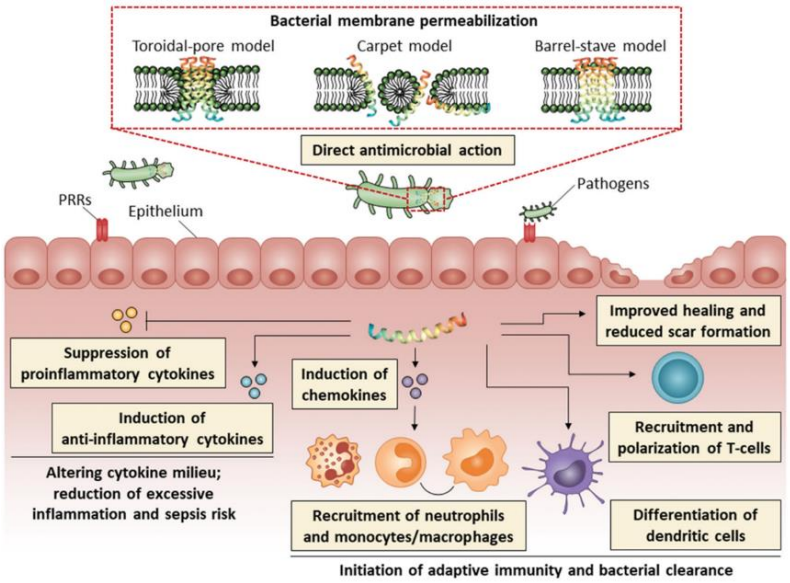


**Figure 4.** Schematic representation of AMPs mechanism of action from Kosikowska and Lesner, 2016.

AMPs can also weaken or thicken the bacterial membrane (membrane thinning / thickening concept) or cluster the phospholipid head groups in the membrane (charged lipid-clustering model) [52]. They were also described as non-membranolytic peptides that target intracellular components and inhibit vital cell processes, such as protein folding, enzyme activity, DNA, RNA, and protein synthesis, and cell wall production [53-57].

In recent years, Pane *et al*. created a valuable bioinformatic tool to identify AMPs in the sequences of human precursor proteins and to quantitatively predict their antibacterial activity [58]. This method led to the discovery of hundreds of putative AMPs in human secretory proteins. Apolipoprotein B was also identified as a source of AMPs. Two versions of the identified peptide were recombinantly produced. They were named r(P)ApoB$_L^{Pro}$ and r(P)ApoB$_S^{Pro}$ peptides. They are 38 and 26 residues long, respectively [66]. P refers to the presence of a Pro residue at the N-terminus of each peptide released upon acidic hydrolysis of an Asp-Pro bond, whereas L and S refer to a longer or a shorter version of the produced peptide. Produced peptides were found to be endowed with broad-spectrum antimicrobial activity, while being neither toxic nor hemolytic towards human and murine eukaryotic cells [59]. Additionally, both ApoB-derived peptides were found to be able to synergistically act in combination with EDTA or conventional antibiotics, thus providing intriguing possibilities to their applicability in pharmaceutical and cosmeceutical industries [59]. Additionally, peptides derived from ApoB exhibited strong anti-biofilm properties, being able to stop biofilm from forming, adhere to an existing one, and even detach preformed biofilm. Significant anti-biofilm effects were also found against bacterial strains such as methicillin-resistant *Staphylococcus aureus*, which were found to be resistant to peptides' direct antibacterial activity [59]. ApoB-derived peptides were also found to be endowed with anti-inflammatory properties being able to decrease the release of nitric oxide (NO) and interleukin-6 (IL-6) in mice macrophages upon stimulation with LPS [59]. Peptides were also found to exhibit antifungal properties and to be effective in a mouse model of skin infection [60]. These findings collectively open interesting perspectives to the applicability of ApoB-derived peptides in several fields, such as pharmaceutical, cosmeceutical, agricultural, and food preservation areas.

### 1.4 Biofilm Formation and Its Impact on Food

Food contaminations are caused by bacteria, viruses, parasites or chemical substances that can enter human body through consumption. Numerous diseases caused by contaminated food samples can provoke permanent disability and even death. It was estimated that about 600 million people worldwide get sick by eating contaminated food each year [61]. Food contaminations are verified at any stage during the farm-to-fork chain and are responsible for illness and intoxication [62]. During food processing and manufacturing, food

residues may accumulate on surfaces of devices that encounters food, with consequent bacterial adhesion due to poor sanitation of surfaces [63].

Foodborne bacteria are also able to form biofilm. Biofilm development occurs on several surfaces, either biotic (*i.e.,* meat, oral cavity, intestine, urogenital tract, skin, *etc*.) or abiotic (*i.e.,* floors, walls, drains, equipment, or food-contacting surfaces) [64]. Among foodborne pathogens which are able to form biofilm, *Listeria monocytogenes*, *Micrococcus* spp., *Staphylococcus* spp., *Clostridium* spp., *Bacillus* spp., *Lactobacillus* spp., *Brochothrix thermosphacta*, *Salmonella enterica*, *Escherichia coli*, *Serratia* spp., *Campylobacter* spp., and *Pseudomonas* spp. [65,66]. **Table 1** summarizes the most common foodborne pathogens and their effects food safety [66].

**Table 1.** Summary of common foodborne pathogens forming biofilm and their effects on food safety from Bai *et al.,* 2021.

| Pathogen | Gram Stain | Spore Forming | Foods Involved | Infectious Dose | Disease Symptoms |
|---|---|---|---|---|---|
| *Listeria monocytogenes* | Positive | No | Ready-to-eat meat, dairy, fish, fruits, and vegetables. Foods with high protein content, such as deli meat, fish, and cheese. | <100–$10^{11}$ CFU (colony forming unit) depending on individual immunological health [31,32]. | To healthy children and adults, flu-like symptoms include diarrhea, fever, vomiting, joint pain, headache. Invasive systemic disease in the immunocompromised host. Miscarriage and stillbirth in pregnant women. Meningitis or encephalitis in newborns and elderly. |
| *Staphylococcus aureus* | Positive | No | Milk products, meat, and hand-prepared foods. | *S. aureus* cells: $10^5$–$10^8$ CFU/g. Toxin: 1 ng/g [33]. | Vomiting, diarrhea, and sometimes toxic shock symptoms including fever, low blood pressure, and even death. |
| *Escherichia coli* | Negative | No | Meat products, such as ground beef and sausage, fruits and vegetables. | Cause both food poisoning and infection. As low as 50–100 CFU of Enterohemorrhagic *E. coli* (EHEC) can cause infection [34]. Approximately $10^3$–$10^5$ CFU is needed to cause diseases [35]. However, as low as 1–100 CFU is also implicated depending on the serovars involved [36]. | Vomiting, diarrhea, bloody diarrhea, hemorrhagic colitis, hemolytic uremic syndrome. |
| *Salmonella enterica* | Negative | No | Poultry products, meat, fish, vegetables, nuts, flours, milk, and drinking water. | | Typhoid fever, fever, vomiting, diarrhea, abdominal pain. It causes invasive disease in immunocompromised patients. |
| *Pseudomonas aeruginosa* | Negative | No | Not a common foodborne pathogen but may present in water, soil, plants, and foods. It contributes to the polymicrobial biofilm formation with other foodborne pathogens to be a food safety concern. | An opportunistic pathogen and infectious dose are highly variable; $10^3$–$10^9$ CFU [37]. | Cause serious diseases in burn and cystic fibrosis patients with fever, chills, coughs with yellow, green, or bloody discharge. Gastroenteritis and diarrhea in some patients. |

Over 80% of chronic infectious disorders are associated to biofilm formation. Furthermore, traditional antibiotic treatments were found to be ineffective in curing these biofilm-associated infections [67, 68]. Biofilm plays the role of a structural barrier protecting microorganisms from adverse environmental factors, such as severe temperature values, pH, high salinity, pressure changes, inadequate nutrition, antibiotics, *etc*. [69]. Biofilm mode of growth causes not only bacterial resistance to antibiotics but also to disinfection, with serious consequences on both health and economy [70]. In this scenario, it

appears fundamental to establish effective strategies to eradicate biofilm forming bacteria from food production and processing environments. However, this requires a deep understanding of physiological and pathophysiological bases of biofilm-forming bacteria [66]. In **Figure 5,** they are schematically reported the major stages of biofilm development [71]. The stages are: (i) the initial or reversible attachment to the surface indicative of the transition from planktonic life to the biofilm mode [71]. (ii) The irreversible attachment, which includes the development of the extracellular matrix. (iii) The microcolony formation, which implies the adherence of bacteria enhancing the release polymeric compounds that function as a "glue" to fix microorganisms on various surfaces. (iv)The biofilm maturation with the transformation into a three-dimensional spatially coordinated structure through a signaling system known as Quorum Sensing (QS), and (v) the dispersion of biofilm characterized by the detachment of bacterial cells that look for novel surfaces to adhere to, thus beginning a novel round of biofilm production [71].

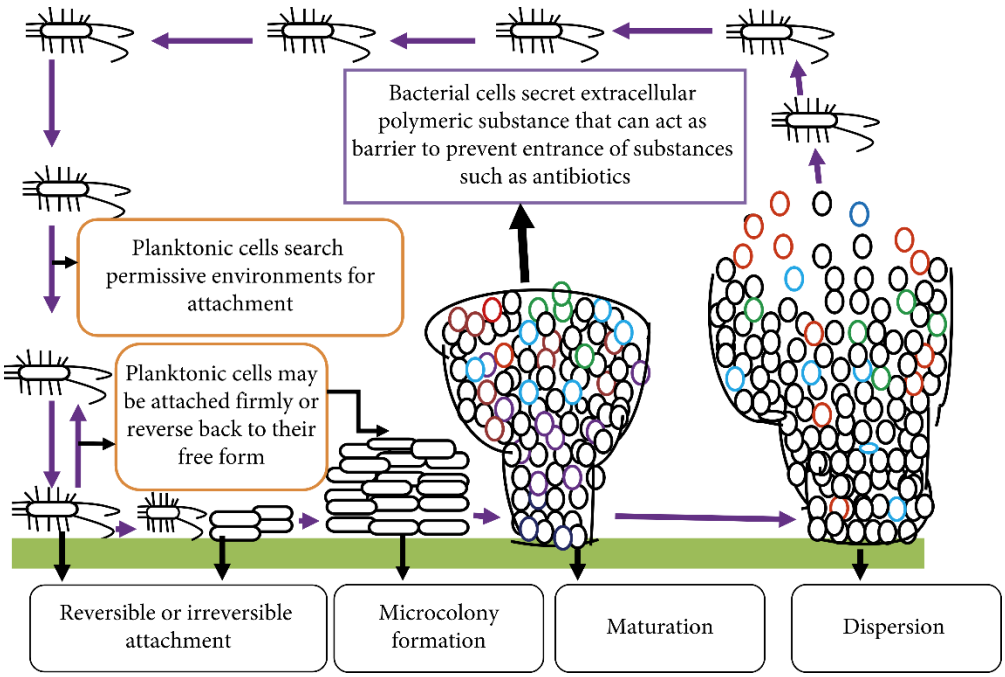


**Figure 5.** Stages of biofilm formation from Abebe, 2020.

## 1.5 Aims of the Thesis

The main aim of this PhD project is to purify and isolate novel plant-derived compounds endowed with multiple biological activities. Once identified, these compounds were characterized for their biological properties moreover; their ability to act in synergism with ApoB-derived HDPs was exploited [58]. A bio-guided purification procedure allowed the purification of phytochemical constituents of wild plants, which were then isolated, identified, and tested in combination with HDPs endowed with antimicrobial activities towards food-borne pathogens. Herewith, **chapter 1** comprises a general introduction to the experimental part of this project. Consequently, **chapters 2-5** report the isolation and identification of plant-derived compounds and the attempt to develop a suitable active food packaging system. **Chapter 6** comprises a general discussion on the main achieved results. The detailed content of the main chapters of the thesis are listed below:

- **Chapter 2:** screening of several wild plant extracts to evaluate their antimicrobial and anti-biofilm activities against a panel of Gram-positive and Gram-negative bacterial strains.
- **Chapter 3:** bio-guided purification procedure to isolate the active compounds of ***Centaurea hyalolepis*** extract, and their identification through NMR and MS analyses.
- **Chapter 4:** bio-guided purification procedure to isolate the active compounds of ***Ephedra foeminea*** extract, and their identification through NMR and MS analyses. Among the identified compounds, **(kaempferol-3-*O*-*α*-L-(2",4"-di-*E*-*p*-coumaroyl)-rhamnopyranoside)** which showed strong activity against MDR (*S. aureus* MRSA WKZ-2) bacterial strain and was characterized for its antibacterial, anti-biofilm, and anticancer properties. Molecular docking analyses were performed as well to predict the possible targets of its mechanism of action. Analyses of synergistic effects between the identified compound and r(P)ApoBL peptide were also performed.
- **Chapter 5:** development of an active food packaging system based on the employment of hydroxyethyl cellulose (HEC) films cross-linked with citric acid. The physiochemical properties of the prepared films was also described.

# 5. References


[1] Katz, L.; Baltz, R. H. Natural product discovery: past, present, and future. *Journal of Industrial Microbiology and Biotechnology*. **2016**, *43*(2-3), 155-176.https://doi.org/10.1007/s10295-015-1723-5

[2] Tajkarimi, M. M.; Ibrahim, S. A.; Cliver, D. O. Antimicrobial herb and spice compounds in food. *Food control*,**2010**, *21*(9), 1199-1218. https://doi.org/10.1016/j.foodcont.2010.02.003

[3] Bar-On, Y. M.; Phillips, R.; Milo, R. The biomass distribution on Earth. *Proceedings of the National Academy of Sciences*. **2018**, *115*(25), 6506-6511.https://doi.org/10.1073/pnas.1711842115

[4] Muthamilarasan, M., Prasad, M. Plant innate immunity: An updated insight into defense mechanism. *J Biosci* ,**2013**,*38*, 433–449. https://doi.org/10.1007/s12038-013-9302-2

[5] Lai, P. K.; Roy, J. Antimicrobial and chemopreventive properties of herbs and spices. *Current medicinal chemistry*,**2004**, *11*(11), 1451-1460. https://doi.org/10.2174/0929867043365107

[6] Tapsell, Linda C.; Hemphill, Ian; Cobiac, Lynne; Sullivan, David R.; Fenech, Michael; Patch, Craig S.; Roodenrys, Steven; Keogh, Jennifer B.; Clifton, Peter M.; Williams, Peter G.; Fazio, Virginia A.; and Inge, Karen E. Health benefits of herbs and spices: the past, the present, the future **2006.** https://ro.uow.edu.au/hbspapers/1397

[7] Franke, H.; Scholl, R.; Aigner, A. Ricin and *Ricinus communis* in pharmacology and toxicology-from ancient use and "*Papyrus Ebers*" to modern perspectives and "poisonous plant of the year 2018". *Naunyn-Schmiedeberg's Arch Pharmacol* **2019**,*392*, 1181–1208. https://doi.org/10.1007/s00210-019-01691-6

[8] Kyaw, B. M.; Lim, C. S. Bactericidal antibiotic-phytochemical combinations against methicillin resistant *Staphylococcus aureus*. *Brazilian Journal of Microbiology*,**2012**, *43*, 938-945. https://doi.org/10.1590/S1517-83822012000300013

[9] Ankri, S.; Mirelman, D. Antimicrobial properties of allicin from garlic. *Microbes and infection*,**1999**, *1*(2), 125-129. https://doi.org/10.1016/S1286-4579(99)80003-3

[10] Bjarnsholt, T.; Jensen, P. Ø.; Rasmussen, T. B.; Christophersen, L.; Calum, H.; Hentzer, M.; Hougen H. P.; Rygaard J.; Moser C.; Eberl L.; Høiby N.; Givskov, M. Garlic blocks quorum sensing and promotes rapid clearing of pulmonary *Pseudomonas aeruginosa* infections. *Microbiology*,**2005**, *151*(12), 3873-3880. https://doi.org/10.1099/mic.0.27955-0

[11] Rasmussen, T. B.; Bjarnsholt, T.; Skindersoe, M. E.; Hentzer, M.; Kristoffersen, P.; Kote, M.; Nielsen J.; Eberl L., ;Givskov, M. Screening for quorum-sensing inhibitors (QSI) by use of a novel genetic system, the QSI selector. *Journal of bacteriology*,**2005**, *187*(5), 1799-1814. https://doi.org/10.1128/JB.187.5.1799-1814.2005

[12] Singh, M. K.; Singh, N. Comparison of antimicrobial activity of herbs & spices and their phytochemical determination. *International Journal of Green Pharmacy (Medknow Publications & Media Pvt. Ltd.)*, **2011**,*5*(3). 10.4103/0973-8258.91232

[13] Okwu, M. U.; Olley, M.; Akpoka, A. O.; Izevbuwa, O. E. Methicillin-resistant *Staphylococcus aureus* (MRSA) and anti-MRSA activities of extracts of some medicinal plants: A brief review. *AIMS microbiology*,**2019**, *5*(2), 117–137. https://doi.org/10.3934/microbiol.2019.2.117

[14] Bazaka, K.; Jacob, M. V.; Chrzanowski, W.; Ostrikov, K. Anti-bacterial surfaces: natural agents, mechanisms of action, and plasma surface modification. *Rsc Advances*,**2015***, 5*(60), 48739-48759. 10.1039/C4RA17244B

[15] Harvey, A.; Edrada-Ebel, R.; Quinn, R. The re-emergence of natural products for drug discovery in the genomics era. *Nat Rev Drug Discov* ,**2015**,14, 111–129. https://doi.org/10.1038/nrd4510

[16] Radulovic, N. S.; Blagojevic, P. D.; Stojanovic-Radic, Z. Z.; Stojanovic, N. M. Antimicrobial plant metabolites: structural diversity and mechanism of action. *Current medicinal chemistry*,**2013**, *20*(7), 932-952. https://doi.org/10.2174/092986713805219136

[17] Çoban, İ., Toplan; G. G., Özbek; B., Gürer, Ç. U.; Sarıyar, G. Variation of alkaloid contents and antimicrobial activities of Papaver rhoeas L. growing in Turkey and northern Cyprus. *Pharmaceutical biology*,**2017**, *55*(1), 1894-1898.https://doi.org/10.1080/13880209.2017.1340964

[18] Nugraha, A. S.; Damayanti, Y. D.; Wangchuk, P.; Keller, P. A. Anti-infective and anti-cancer properties of the Annona species: their ethnomedicinal uses, alkaloid diversity, and pharmacological activities. *Molecules*, **2019**,*24*(23), 4419. https://doi.org/10.3390/molecules24234419

[19] Tian, J.; Ban, X.; Zeng, H.; He, J.; Huang, B.; Wang, Y. Chemical composition and antifungal activity of essential oil from Cicuta virosa L. var. latisecta Celak. *International Journal of Food Microbiology*,**2011,** *145*(2-3), 464-470. https://doi.org/10.1016/j.ijfoodmicro.2011.01.023

[20] Tariq, S.; Wani, S.; Rasool, W.; Shafi, K.; Bhat, M. A.; Prabhakar, A.; Shalla A. H.; Rather, M. A. A comprehensive review of the antibacterial, antifungal and antiviral potential of essential oils and their chemical constituents against drug-resistant microbial pathogens. *Microbial pathogenesis*, **2019** *134*, 103580.https://doi.org/10.1016/j.micpath.2019.103580.

[21] Álvarez-Martínez, F. J.; Barrajón-Catalán, E.; Micol, V. Tackling antibiotic resistance with compounds of natural origin: A comprehensive review. *Biomedicines*, **2020**, *8*(10), 405. https://doi.org/10.3390/biomedicines8100405

[22] Xue, J.; Davidson, P. M.; Zhong, Q. Thymol nanoemulsified by whey protein-maltodextrin conjugates: The enhanced emulsifying capacity and antilisterial properties in milk by propylene glycol. *Journal of agricultural and food chemistry*,**2013**, *61*(51), 12720-12726. https://doi.org/10.1021/jf4043437

[23] Dorman, H. D.; Deans, S. G. Antimicrobial agents from plants: antibacterial activity of plant volatile oils. *Journal of applied microbiology*, **2000**,*88*(2), 308-316.https://doi.org/10.1046/j.1365-2672.2000.00969.x

[24] Ultee, A.; Bennik, M. H. J.; Moezelaar, R. J. A. E. M. The phenolic hydroxyl group of carvacrol is essential for action against the food-borne pathogen *Bacillus cereus*. *Applied and environmental microbiology*, **2002**,*68*(4), 1561-1568.https://doi.org/10.1128/AEM.68.4.1561-1568.2002

[25] Gochev, V.; Dobreva, A.; Girova, T.; Stoyanova, A. Antimicrobial activity of essential oil from *Rosa alba*. *Biotechnology & Biotechnological Equipment*, **2010** *24*(sup1), 512-515. https://doi.org/10.1080/13102818.2010.10817892

[26] Iwasa, K.; Moriyasu, M.; Yamori, T.; Turuo, T.; Lee, D. U.; Wiegrebe, W. In vitro cytotoxicity of the protoberberine-type alkaloids. *Journal of natural products*, **2001**,*64*(7), 896-898.https://doi.org/10.1021/np000554f

[27] Yi, Z. B.; Yu, Y.; Liang, Y. Z.; Zeng, B. Evaluation of the antimicrobial mode of berberine by LC/ESI-MS combined with principal component analysis. *Journal of pharmaceutical and biomedical analysis*,**2007**, *44*(1), 301-304.https://doi.org/10.1016/j.jpba.2007.02.018

[28] Cowan, M. M. Plant products as antimicrobial agents. *Clinical microbiology reviews*,**1999**, *12*(4), 564-582.https://doi.org/10.1128/CMR.12.4.564

[29] Kurek, A. N. N. A.; Grudniak, A. M.; Kraczkiewicz-Dowjat, A.; Wolska, K. I. New antibacterial therapeutics and strategies. *Polish Journal of Microbiology*, **2011**,*60*(1), 3. http://www.pjmonline.org/wpcontent/uploads/archive/vol6012011003.pdf

[30] Garcia, A.; Rhoden, S. A.; Bernardi-Wenzel, J.; Orlandelli, R. C., Azevedo, J. L.; Pamphile, J. A. Antimicrobial activity of crude extracts of endophytic fungi isolated from medicinal plant *Sapindus saponaria* L. *Journal of applied pharmaceutical science*,**2012**, *2*(10), 035-040.10.7324/JAPS.2012.21007

[31] Fowler, Z. L.; Baron, C. M.; Panepinto, J. C.; Koffas, M. A. Melanization of flavonoids by fungal and bacterial laccases. *Yeast*, **2011**,*28*(3), 181-188. https://doi.org/10.1002/yea.1829

[32] Gyawali, R.; Ibrahim, S. A. Natural products as antimicrobial agents. *Food control*,**2014**, *46*, 412-429.https://doi.org/10.1016/j.foodcont.2014.05.047

[33] Dadgostar, P. Antimicrobial resistance: implications and costs. *Infection and drug resistance*,**2019** *12*, 3903. 10.2147/IDR.S234610

[34] Ayaz, M.; Ullah, F.; Sadiq, A.; Ullah, F.; Ovais, M.; Ahmed, J.; Devkota, H. P. Synergistic interactions of phytochemicals with antimicrobial agents: Potential strategy to counteract drug resistance. *Chemico-Biological Interactions*. **2019,** *308*, 294-303. https://doi.org/10.1016/j.cbi.2019.05.050

[35] Daglia, M. Polyphenols as antimicrobial agents. *Curr. Opin. Biotechnol.* **2012**, *23*, 174–181. https://doi.org/10.1016/j.copbio.2011.08.007

[36] Bernal, P.; Lemaire, S.; Pinho, M.G.; Mobashery, S.; Hinds, J.; Taylor, P.W. Insertion of epicatechin gallate into the cytoplasmic membrane of methicillin-resistant *Staphylococcus aureus* disrupts penicillin-binding protein (pbp) 2a-mediated beta-lactam resistance by delocalizing pbp2. *J. Biol. Chem.* **2010**, *285*, 24055–24065.https://doi.org/10.1074/jbc.M110.114793

[37] Kalia, N.P.; Mahajan, P.; Mehra, R.; Nargotra, A.; Sharma, J.P.; Koul, S.; Khan, I.A. Capsaicin, a novel inhibitor of the nora efflux pump, reduces the intracellular invasion of *Staphylococcus aureus*. *J. Antimicrob. Chemother.* **2012**, *67*, 2401–2408.https://doi.org/10.1093/jac/dks232

[38] Ponnusamy, K.; Ramasamy, M.; Savarimuthu, I.; Paulraj, M.G. Indirubin potentiates ciprofloxacin activity in the nora efflux pump of *Staphylococcus aureus*. *Scand. J. Infect. Dis.* **2010**, *42*, 500–505. https://doi.org/10.3109/00365541003713630

[39] Holler, J.G.; Christensen, S.B.; Slotved, H.C.; Rasmussen, H.B.; Guzman, A.; Olsen, C.E.; Petersen, B.; Molgaard, P. Novel inhibitory activity of the *Staphylococcus aureus* nora efflux pump by a kaempferol rhamnoside

isolated from *Persea lingue* nees. *J. Antimicrob. Chemother.* **2012**, *67*, 1138–1144.https://doi.org/10.1093/jac/dks005

[40] Shiu, W.K.; Malkinson, J.P.; Rahman, M.M.; Curry, J.; Stapleton, P.; Gunaratnam, M.; Neidle, S.; Mushtaq, S.; Warner, M.; Livermore, D.M.; et al. A new plant-derived antibacterial is an inhibitor of efflux pumps in *Staphylococcus aureus*. *Int. J. Antimicrob. Agents,* **2013**, *42*, 513–518. https://doi.org/10.1016/j.ijantimicag.2013.08.007

[41] Bame, J.R.; Graf, T.N.; Junio, H.A.; Bussey, R.O., III; Jarmusch, S.A.; El-Elimat, T.; Falkinham, J.O., III; Oberlies, N.H.; Cech, R.A.; Cech, N.B. Sarothrin from *Alkanna orientalis* is an antimicrobial agent and efflux pump inhibitor. *Planta Med.* **2013**, *79*, 327–329.10.1055/s-0032-1328259

[42] Dwivedi, G.R.; Maurya, A.; Yadav, D.K.; Khan, F.; Darokar, M.P.; Srivastava, S.K. Drug resistance reversal potential of ursolic acid derivatives against nalidixic acid- and multidrug-resistant *Escherichia coli*. *Chem. Biol. Drug Des.* **2015**, *86*, 272–283. https://doi.org/10.1111/cbdd.12491

[43] Aghayan, S.S.; Mogadam, H.K.; Fazli, M.; Darban-Sarokhalil, D.; Khoramrooz, S.S.; Jabalameli, F.; Yaslianifard, S.; Mirzaii, M. The effects of berberine and palmatine on efflux pumps inhibition with different gene patterns in *Pseudomonas aeruginosa* isolated from burn infections. *Avicenna J. Med. Biotechnol.* **2017**, *9*, 2–7. https://www.ncbi.nlm.nih.gov/pmc/articles/PMC5219818/

[44] Gordon, Y. J.; Romanowski, E. G.; McDermott, A. M. A review of antimicrobial peptides and their therapeutic potential as anti-infective drugs. *Current eye research*,**2005**, *30*(7), 505-515. https://doi.org/10.1080/02713680590968637

[45] Kosikowska, P.; Lesner, A. Antimicrobial peptides (AMPs) as drug candidates: a patent review (2003–2015). *Expert opinion on therapeutic patents*,**2016**, *26*(6), 689-702. https://doi.org/10.1080/13543776.2016.1176149

[46] Mahlapuu, M.; Björn, C.; Ekblom, J. Antimicrobial peptides as therapeutic agents: Opportunities and challenges. *Critical reviews in biotechnology*,**2020**, *40*(7), 978-992. https://doi.org/10.1080/07388551.2020.1796576

[47] Hancock, R.; Nijnik, A.; Philpott, D. Modulating immunity as a therapy for bacterial infections. *Nat Rev Microbiol,***2012,** 10, 243–254. https://doi.org/10.1038/nrmicro2745

[48] Yeung, A. T., Gellatly, S. L.; Hancock, R. E. Multifunctional cationic host defence peptides and their clinical applications. *Cellular and Molecular Life Sciences*,**2011** *68*(13), 2161-2176. https://doi.org/10.1007/s00018-011-0710-x

[49] Ebenhan, T.; Gheysens, O.; Kruger, H. G.; Zeevaart, J. R.; Sathekge, M. M. Antimicrobial peptides: their role as infection-selective tracers for molecular imaging. *BioMed research international*, **2014**,*2014*. https://doi.org/10.1155/2014/867381

[50] Matsuzaki, K. Membrane Permeabilization Mechanisms. In: Matsuzaki, K. (eds) Antimicrobial Peptides. *Advances in Experimental Medicine and Biology*,**2019,** vol 1117. Springer, Singapore. https://doi.org/10.1007/978-981-13-3588-4_2

[51] Rončević, T.; Puizina, J.; Tossi, A. Antimicrobial peptides as anti-infective agents in pre-post-antibiotic era?. *International journal of molecular sciences*, **2019**, *20*(22), 5713.https://doi.org/10.3390/ijms20225713

[52] Grage, S. L.; Afonin, S.; Kara, S., Buth, G.; Ulrich, A. S. Membrane thinning and thickening induced by membrane-active amphipathic peptides. *Frontiers in cell and developmental biology*,**2016**, *4*, 65. https://doi.org/10.3389/fcell.2016.00065

[53] Yeaman, M. R.; Yount, N. Y. Mechanisms of antimicrobial peptide action and resistance. *Pharmacological reviews*,**2003**, *55*(1), 27-55. https://doi.org/10.1124/pr.55.1.2

[54] Jenssen, H.; Hamill, P.; Hancock, R. E. Peptide antimicrobial agents. *Clinical microbiology reviews*,**2006,** *19*(3), 491-511. https://doi.org/10.1128/CMR.00056-05

[55] Yount, N. Y.;Yeaman, M. R. Immunocontinuum: perspectives in antimicrobial peptide mechanisms of action and resistance. *Protein and peptide letters*,**2005**, *12*(1), 49-67. https://doi.org/10.2174/0929866053405959

[56] Cudic, M.; Otvos Jr, L. Intracellular targets of antibacterial peptides. *Current drug targets*,**2002**, *3*(2), 101-106. https://doi.org/10.2174/1389450024605445

[57] Brogden, K. Antimicrobial peptides: pore formers or metabolic inhibitors in bacteria?. *Nat Rev Microbiol* ,**2005**, *3*, 238–250. https://doi.org/10.1038/nrmicro1098

[58] Pane, K.; Durante, L.; Crescenzi, O.; Cafaro, V.; Pizzo, E.; Varcamonti, M.; Notomista, E. Antimicrobial potency of cationic antimicrobial peptides can be predicted from their amino acid composition: Application to the detection of "cryptic" antimicrobial peptides. *Journal of Theoretical Biology*, **2017**, 419, 254–265. https://doi.org/10.1016/j.jtbi.2017.02.012

[59] Gaglione, R.; Dell'Olmo, E.; Bosso, A.; Chino, M.; Pane, K.; Ascione, F.; Itri, F.; Caserta, S.; Amoresano, A.; Lombardi, A.; Haagsman, H.P.; Piccoli, R.; Pizzo, E.; Veldhuizen, E.J.A.; Notomista, E.; Arciello, A. Novel human bioactive peptides identified in apolipoprotein B: evaluation of their therapeutic potential. *Biochemical Pharmacology,***2017**, *130*, 34-50. https://doi.org/10.1016/j.bcp.2017.01.009

[60] Dell'Olmo, E.; Gaglione, R.; Cesaro, A.; Cafaro, V.; Teertstra, W. R.; de Cock, H.; Notomista, E; Haagsman H.P. ; Veldhuizen E.J.A.; Arciello, A. Host defence peptides identified in human apolipoprotein B as promising antifungal agents. *Applied microbiology and biotechnology*,**2021** *105*(5), 1953-1964.https://doi.org/10.1007/s00253-021-11114-3

[61] World Health Organization (WHO), *Food Safety*, World Health Organization (WHO), Geneva, Switzerland, **2022**, https://www.who.int/news-room/fact-sheets/detail/food-safety

[62] Yang, SC., Lin, CH., Aljuffali, I.A. *et al.* Current pathogenic *Escherichia coli* foodborne outbreak cases and therapy development. *Arch Microbiol,***2017** 199, 811–825. https://doi.org/10.1007/s00203-017-1393-y

[63] Lindsay, D.; Von Holy, A. Bacterial biofilms within the clinical setting: what healthcare professionals should know. *Journal of Hospital Infection*,**2006** *64*(4), 313-325.https://doi.org/10.1016/j.jhin.2006.06.028

[64] Flemming, H. C.; Wingender, J.; Szewzyk, U.; Steinberg, P.; Rice, S. A.; Kjelleberg, S. Biofilms: an emergent form of bacterial life. *Nature Reviews Microbiology*,**2016** *14*(9), 563-575. https://doi.org/10.1038/nrmicro.2016.94

[65] Mazaheri, T.; Cervantes-Huamán, B.R.H.; Bermúdez-Capdevila, M.; Ripolles-Avila, C.; Rodríguez-Jerez, J.J. *Listeria monocytogenes* biofilms in

the food industry: Is the current hygiene program sufficient to combat the persistence of the pathogen? *Microorganisms* **2021**, *9*, 181. https://doi.org/10.3390/microorganisms9010181

[66] Bai, X.; Nakatsu, C. H.; Bhunia, A. K. Bacterial biofilms and their implications in pathogenesis and food safety. *Foods*,**2021**, *10*(9), 2117. https://doi.org/10.3390/foods10092117

[67] Li, X. H.; Lee, J. H. Antibiofilm agents: A new perspective for antimicrobial strategy. *Journal of Microbiology*,**2017** *55*(10), 753-766. https://doi.org/10.1007/s12275-017-7274-x

[68] Pinto, R. M.; Soares, F. A.; Reis, S., Nunes; C.; Van Dijck, P. Innovative strategies toward the disassembly of the EPS matrix in bacterial biofilms. *Frontiers in microbiology*, **2020,***11*, 952. https://doi.org/10.3389/fmicb.2020.00952

[69] Yin, W.; Wang, Y.; Liu, L.; He, J. Biofilms: the microbial “protective clothing” in extreme environments. *International journal of molecular sciences,***2019** *20*(14), 3423.https://doi.org/10.3390/ijms20143423

[70] Bridier, A., Briandet, R., Thomas, V.; Dubois-Brissonnet, F. Resistance of bacterial biofilms to disinfectants: a review. *Biofouling*,**2011**, *27*(9), 1017-1032. https://doi.org/10.1080/08927014.2011.626899

[71] Abebe G. M. The Role of Bacterial Biofilm in Antibiotic Resistance and Food Contamination", *International Journal of Microbiology*, **2020** vol. 2020, Article ID 1705814, 10 pages, 2020. https://doi.org/10.1155/2020/1705814

# CHAPTER 2

# Identification of Wild Plant Extracts Endowed with Antimicrobial and Anti-biofilm Activities

Shurooq Ismail

Department of Chemical Sciences, PhD in Biotechnology

University of Naples Federico II

# Identification of Wild Plant Extracts Endowed with Antimicrobial and Anti-biofilm Activities

## 1. Introduction

Through centuries, nature was fundamental for humankind life prosperity on earth. Since their existence, humans used plants as the natural resource for their food, animal feeds and medical treatments of various diseases [1]. Prevention and treatment of several diseases were achieved by using conventional medicinal plants that are known for their antimicrobial, antifungal, anti-inflammatory and antiviral as well as anticancer characteristics [2]. This wide range of activities is correlated to different plant-derived active chemical components, such as essential oils and secondary metabolites, including alkaloids, terpenoids, tannins and flavonoids [2,3]. According to the published literature in phytochemistry, several secondary metabolites are endowed with antimicrobial properties exerted through diverse antimicrobial mechanisms of actions, including the ability to form complexes with extracellular and soluble proteins as well as with membrane proteins of targeted microbes. Antimicrobial activity is also mediated by the ability to cause membrane disruption and bacterial enzymes inhibition [4-7].

Among targeted enzymes, gyrase, topoisomerase IV and RNA polymerase are commonly reported [8,9]. Active plant-derived compounds vary in quantity and activity depending on plant species and environmental conditions. Based on the interesting pharmacological features of plants, most people in developing countries are dependent on traditional herbal medicine, which is considered less harmful in terms of side effects with respect to traditional medicine. Humans used only a small percentage (1-10%) of plant species present on earth [10,11]. Researchers employed the basic knowledge acquired from traditional folk medicine to analyze the chemical composition of the used plants, in order to clarify molecular bases of their beneficial properties. However, the analysis of wild plants, which are not used in folk medicine, could reveal novel compounds rich in biological properties suitable for applicability in several fields [3].

Indeed, humans used plants for centuries to cure several diseases and health related troubles, and this practice was passed to generations without a deep scientific understanding of the mechanisms of action responsible of these beneficial effects. For this reason, researchers focused their attention on the analysis of extracts obtained

from several plants, since they could represent a precious source of active compounds with interesting pharmaceutical properties to be exploited as active molecules of formulations to be employed in several fields, such as biomedical, cosmeceutical and food industries.

In this chapter, a preliminary survey of nine wild Palestinian plants with potential antimicrobial activity was performed. The Minimal Inhibitory Concentration (MIC) was determined by using the broth microdilution assays. In addition to the crystal violet assays, which were used to evaluate the antibiofilm activity of the screened plant, extracts. The achieved results were the basis of selecting the plants for further analyses.

## 2. Methods

**2.1 Materials.** All the reagents were purchased from Sigma-Merck (Milan, Italy), unless specified otherwise.

**2.2 Plant Collection and Identification.** Nine plants (*Ephedra aphylla, Ephedra foeminea, Verbascum sinuatum, Centaurea hyalolepis, Ruta chalepensis, Parietaria judaica L., Heliotropium maris, Withainia somnifera L., Aizon hispanicum L.*) were selected and collected from different locations in West Bank, Palestine (**Figure 1**). Dr. Ghadeer Omar, a plant taxonomist from the Department of Biology and Biotechnology of An-Najah National University, Palestine, carried out plants' identification. Once collected, plants were pressed until drying. Further, chemically treated, mounted on herbarium sheets and provided with voucher numbers corresponding to those deposited at An-Najah National University herbarium.

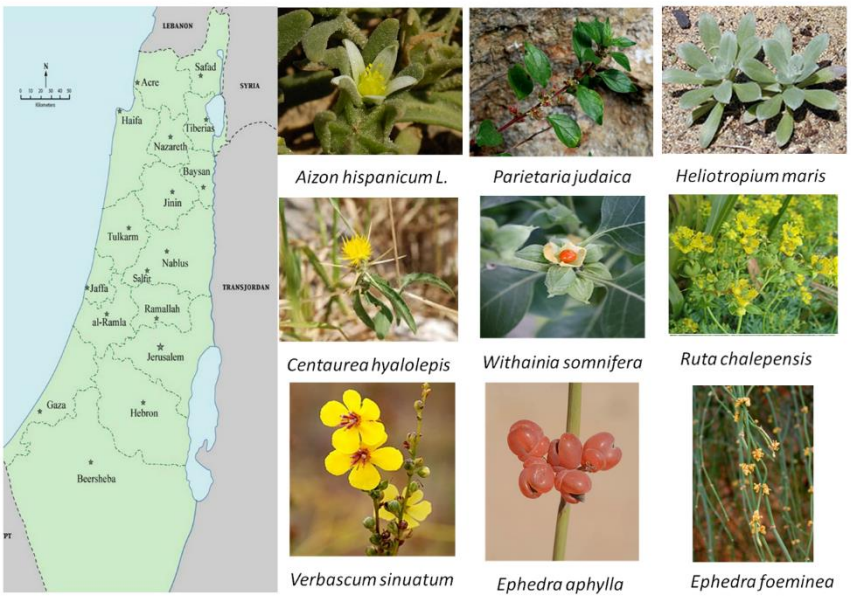


**Figure 1.** Selected and screened plants collected from different Palestinian cites.

**2.3 Plant Extracts Preparation.** Plants aerial parts were washed, air-dried, ground into powder and stored at room temperature. Extraction was performed in water, ethanol or methanol solvents. Aqueous extraction was achieved by using 10 grams of each plant powder, which were soaked in 100 mL of boiled distilled water for one week by routinely shaking at 4 °C. Mixtures were then centrifuged for 15 min at 5,000 rpm at 4°C to remove fine particles. Supernatants were lyophilized by using a freeze-dryer and stored at -80°C to be used later.

When needed, water extracts were dissolved in 75% dimethyl sulfoxide (DMSO) at a concentration of 250 mg/mL. Ethanol and methanol extracts were prepared by using 10 grams of each plant powder, which were soaked in 100 mL of 70% ethanol/methanol for one week by routinely shaking at 4°C. Mixtures were then centrifuged for 15 min at 5,000 rpm at 4°C to remove fine particles. Supernatant extract was then dried and concentrated by using a rotary evaporator at 50 °C. Methanolic and ethanolic extracts were dissolved in 75% DMSO at a final concentration of 250 mg/mL.

**2.4 Bacterial strains and growth conditions.** Three bacterial strains were used to evaluate the antibacterial and antibiofilm characteristics of the studied plant extracts, *i.e.*, *Staphylococcus aureus* ATCC 29213*, Escherichia coli* ATCC 25922 and *Salmonella typhimurium* ATCC 14028. American type culture collection (ATCC) numbers represent the standard strain numbers assigned to these microorganisms. Bacterial strains were grown in Muller Hinton Broth (MHB; Becton Dickinson Difco, Franklin Lakes, NJ, USA) and on Tryptic Soy Agar (TSA; Oxoid Ltd., Hampshire, UK). In all experiments, bacteria were inoculated and grown overnight in MHB at 37°C. The next day, bacteria were transferred to a fresh MHB tube and grown to mid-logarithmic phase.

**2.5 Antimicrobial Activity Assays.** To test extracts antimicrobial activity, bacterial cells were diluted to $2x10^6$ CFU/mL in Nutrient Broth (NB; Difco, Becton Dickinson, Franklin Lakes, NJ, USA) along with increasing concentrations of each tested compound or extract. In each case, starting from a stock solution, two-fold serial dilutions were prepared according to broth microdilution method [12]. $MIC_{100}$ values were determined as the lowest extract concentration responsible for no visible bacterial growth after overnight incubation.

**2.6 Anti-Biofilm Activity by Crystal Violet Assay**. To evaluate plant extracts effects on biofilm formation, bacteria were grown overnight in MHB, and then diluted to $1×10^8$ CFU/mL in 0.5X MHB medium containing increasing extract concentrations (starting from sub-$MIC_{100}$ values). Incubations with the extracts were carried out for 24 h, to test their effects on biofilm formation. Bacterial biofilms were formed for 24h at 37˚C and, at the end of the incubation, crystal violet assays were performed. To this purpose, the planktonic culture was removed from the wells, and washed three times with sterile PBS prior to staining with 0.04% crystal violet for 20 min. Three successive washes with sterile PBS were carried out to eliminate the excess of the dye. Finally, the crystal violet was solubilized with 33% acetic acid and samples optical

absorbance values were determined at 630 nm by using a microtiter plate reader (FLUOstar Omega, BMG LABTECH, Germany) [13].

**2.7 Statistical analyses**. Statistical analyses were performed by using a Student's t-test. Significant differences were indicated as *P < 0.05, **P < 0.01 or ***P < 0.001. Graphs were performed with the GraphPad Prism 8 software.

# 3. Results

## 3.1 Antimicrobial activity of selected extracts.

To identify extracts endowed with antimicrobial properties, 9 aqueous extracts and 8 alcoholic extracts of wild plants were tested for their antibacterial and anti-biofilm capabilities against Gram-positive and Gram-negative food borne pathogens. Firstly, the antimicrobial activity of the aqueous plant extracts was tested against *S. aureus* ATCC 29213, *E. coli* ATCC 25922 and *S. typhimurium* ATCC 14028 bacterial strains by using broth microdilution assays [12] to determine the minimal inhibitory concentration (MIC) values. The aqueous plant extracts were found to exhibit antibacterial activity ($MIC_{100}$ values ranging from 8 to 33 mg/mL) against all the tested bacterial strains. Both Gram-positive and Gram-negative tested strains were found to be susceptible to *C. hyalolepis* aqueous extract with the best $MIC_{100}$ value found to be 8 mg/mL (**Table 1**).

**Table 1**. $MIC_{100}$ and $MIC_{90}$ (*) values (mg/mL) determined for aqueous plant extracts against Gram-positive and Gram-negative bacterial strains.

| Aqueous Plant Extracts $MIC_{100}$ (mg/mL) | | | |
|---|---|---|---|
| | ***S. aureus*** **ATCC 29213** | ***E. coli*** **ATCC 25922** | ***S. typhimurium*** **ATCC 14028** |
| ***Aizon hispanicum*** | 33* | 33 | 33 |
| ***Withainia somnifera*** | 16 | 16 | 16 |
| ***Heliotropium maris*** | 16 | 16 | 16 |
| ***Parietaria judaica*** | 33 | 16 | 16 |
| ***Ruta chalepensis*** | 16 | 16 | 16 |
| ***Centaurea hyalolepis*** | 8 | 8 | 8 |
| ***Verbascum sinuatum*** | 16 | 16 | 16 |
| ***Ephedra aphylla*** | 16 | 16 | 16 |
| ***Ephedra foeminea*** | 33 | 16 | 16 |

Minimal inhibitory concentration (MIC) values were also determined for ethanolic and methanolic plant extracts. The ethanolic plant extracts exhibited the best antibacterial activity against all the tested bacterial strains with *S. aureus* ATCC 29213 found to be the most susceptible to *E. foeminea* extract with $MIC_{100}$ value found to be 2 mg/mL (**Table 2**). The most active methanolic plant extracts were found to be those from *E. aphylla* and *E. foeminea* that exhibited

significant antimicrobial activity against *S. aureus* ATCC 29213 with $MIC_{100}$ values of 4 mg/mL (**Table 3**).

**Table 2**. $MIC_{100}$ values (mg/mL) determined for ethanolic plant extracts against Gram-positive and Gram-negative bacterial strains.

| Ethanol Plant Extracts $MIC_{100}$ (mg/mL) | | | |
|---|---|---|---|
| | ***S. aureus* ATCC 29213** | ***E. coli* ATCC 25922** | ***S. typhimurium* ATCC 14028** |
| ***Verbascum sinuatum*** | 16 | 16 | 16 |
| ***Withainia somnifera*** | 8 | 8 | 8 |
| ***Ephedra aphylla*** | 8 | 16 | 16 |
| ***Ephedra foeminea*** | 2 | 16 | 16 |

**Table 3**. $MIC_{100}$ values (mg/mL) determined for methanolic plant extracts against Gram-positive and Gram-negative bacterial strains.

| Methanol Plant Extracts $MIC_{100}$ (mg/mL) | | | |
|---|---|---|---|
| | ***S. aureus* ATCC 29213** | ***E. coli* ATCC 25922** | ***S. typhimurium* ATCC 14028** |
| ***Verbascum sinuatum*** | 16 | 16 | 16 |
| ***Withainia somnifera*** | 16 | 16 | 16 |
| ***Ephedra aphylla*** | 4 | 16 | 16 |
| ***Ephedra foeminea*** | 4 | 16 | 16 |

### 3.2 Anti-biofilm activity of selected extracts.

The most promising extracts were selected to verify their anti-biofilm properties prior to the analyses of their chemical composition. To this purpose, plant extracts characterized by the lowest $MIC_{100}$ values were selected to investigate their anti-biofilm properties. In particular, *H. maris, R. chalepensis,* and *C. hyalolepis* aqueous extracts, *V. sinuatum, W. somnifera,* and *E. aphylla* methanolic extracts, as well as *V. sinuatum* ,in addition to *E. foeminea* ethanolic extracts were selected. Bacterial strains under test were incubated with increasing concentrations of selected extracts and, at the end of the incubation, crystal violet assays were performed to evaluate plant extracts' effects on biofilm formation [13] (**Figures 2, 3, and 4**). A significant inhibition (about 50-60%) of biofilm formation was observed at sub-$MIC_{100}$ concentrations in the case of aqueous plant extracts on both Gram-negative strains *E. coli* ATCC 25922 (blue lines) and *S.*

*typhimurium* ATCC 14028 (black lines in **Figure 2**). Similar effects on biofilm formation were also observed when *E. coli* ATCC 25922 and *S. typhimurium* ATCC 14028 strains were treated with ethanolic or methanolic extracts (**Figures 3 and 4**). No significant inhibition of biofilm formation, instead, was observed in the case of the Gram-positive *S. aureus* ATCC 29213 bacterial strain (red lines) treated with all the different extract types (**Figures 2, 3 and 4**). The only exception was represented by *W. somnifera* methanolic extract that was found to determine about 80% inhibition of biofilm formation (**Figure 3b**).

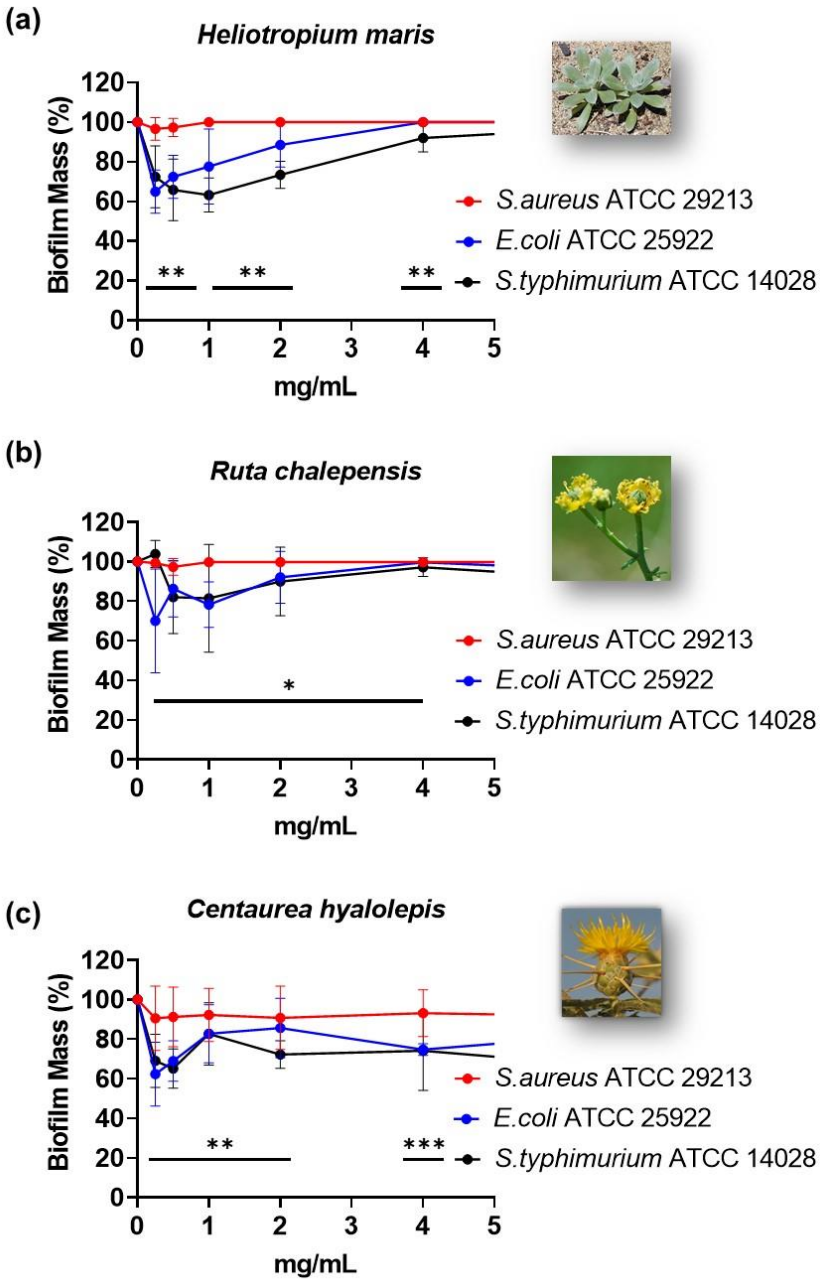


**Figure 2.** Anti-biofilm activity of aqueous extracts obtained from *H. maris* (a), *R. chalepensis* (b), *and C. hyalolepis* (c) on *S. aureus* ATCC 29213 (red lines), *E. coli* ATCC 25922 (blue lines) and *S. typhimurium* ATCC 14028 (black lines) strains. The effects of increasing concentrations of extracts were evaluated on biofilm formation. Biofilm was stained with crystal violet and measurements were carried out at 630 nm. Data represents the mean (±standard deviation, SD) of at least three independent experiments, each one was carried out with triplicate determinations.

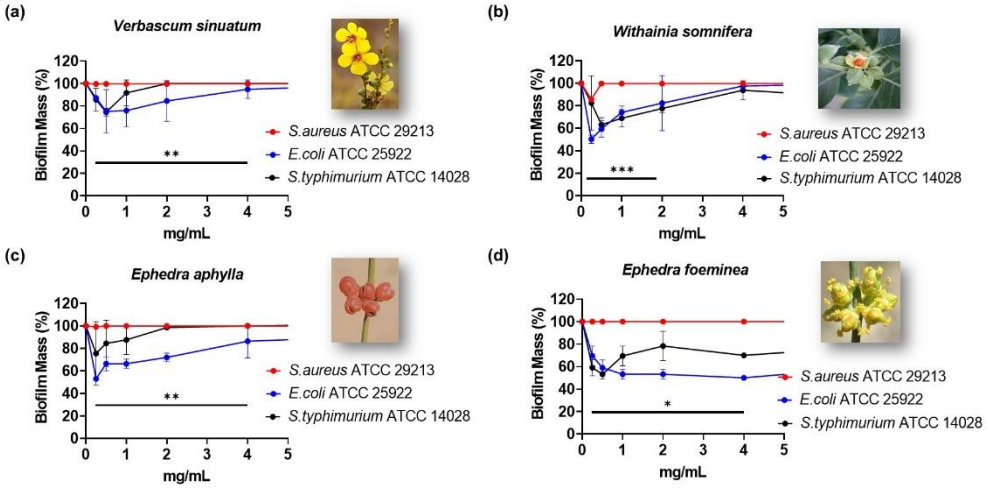


**Figure 3.** Anti-biofilm activity of methanolic extracts obtained from *V. sinuatum* (a), *W. somnifera* (b), *E. aphylla* (c) and *E. foeminea* (d) on *S. aureus* ATCC 29213 (red lines), *E. coli* ATCC 25922 (blue lines) and *S. typhimurium* ATCC 14028 (black lines) strains. The effects of increasing concentrations of extracts were evaluated on biofilm formation. Biofilm was stained with crystal violet and measurements were carried out at 630 nm. Data represents the mean (±standard deviation, SD) of at least three independent experiments, each one was carried out with triplicate determinations.

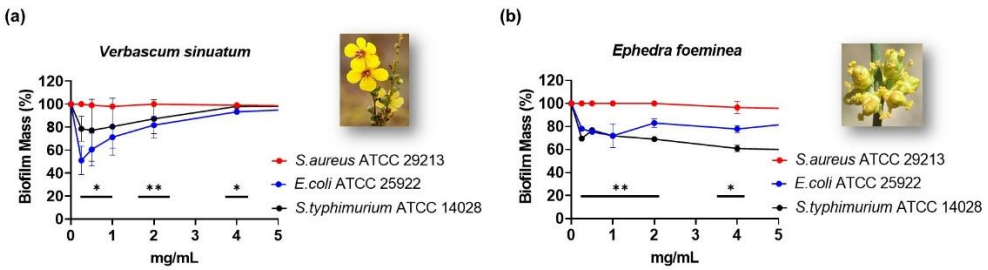


**Figure 4.** Anti-biofilm activity of ethanolic extracts obtained from *V. sinuatum* (a) and *E. foeminea* (b) on *S. aureus* ATCC 29213 (red lines), *E. coli* ATCC 25922 (blue lines) and *S. typhimurium* ATCC 14028 (black lines) strains. The effects of increasing concentrations of extract were evaluated on biofilm formation. Biofilm was stained with crystal violet and measurements were carried out at 630 nm. Data represents the mean (±standard deviation, SD) of at least three independent experiments; each one was carried out with triplicate determinations.

## 4. Discussion

It is well established in the literature that plants are endowed with broad-spectrum antibacterial and anti-biofilm activities [17]. This is due to their content of metabolites falling into several chemical categories, *i.e.*, tannins, phenols, alkaloids, flavonoids, peptides, essential oils, and terpenoids, etc. [2,3]. However, this content is influenced by the plant physiological state, geographical distribution as well as by the season of cultivation, it is affirmed that several factors play a critical role in determining the effectiveness of plant extracts in fighting microbes [11]. Here, it was demonstrated that several plant extracts are active against Gram-positive and Gram-negative bacteria, with $MIC_{100}$ values ranging from 2 to 33 mg/mL depending on the type of extract. It was found and widely reported that solvents used to prepare extracts strongly influence the chemical nature of extracted components and, as a consequence, the degree of detected activity [18-20].

For example, *E. foeminea* water extract was found to be less effective against *S. aureus* ATCC 29213 ($MIC_{100}$ = 33 mg/mL) with respect to extracts obtained in methanol and ethanol for which had $MIC_{100}$ values of 4 mg/mL and 2 mg/mL, respectively. Starting from these interesting and promising results, efforts have been devoted to the identification of the compounds responsible for the antimicrobial properties, in order to verify their future applicability in biotechnological fields, such as pharmaceutical, cosmeceutical, agricultural, and food fields [3][20]. Since the ability of bacteria to form biofilm is considered as a powerful virulence factor enhancing their resistance to antibiotics as well as their ability to escape host immune defenses [21,22], the capability of plant extracts to exert anti-biofilm properties has been also evaluated.

Performing crystal violet assays, demonstrated that the crude water extracts of *C. hyalolepis* and *W. somnifera* exhibited anti-biofilm activity (about 60% formation inhibition) against *E. coli* ATCC 25922 and *S. typhimurium* ATCC 14028 [24, 25]. Similarly, the ethanolic and methanolic crude extracts of *V. sinuatum, W. somnifera, E. foeminea*, and *E. aphylla* were found to be responsible for 50% inhibition of biofilm formation when tested against *E. coli* ATCC 25922 and *S. typhimurium* ATCC 14028 bacterial strains [24][26,27]. None of the extracts was found to exert anti-biofilm properties on *S. aureus* ATCC 29213 independently from the extraction procedure used. This was probably associated to specific properties of the bacterial membrane and the cell wall found in analyzed strains, which were particularly resistant.

Regarding the possible mechanisms, underlying extracts anti-biofilm properties, it should be highlighted that crude extracts are a mixture of various compounds varying in their content. The availability of iron or the acidity are crucial factors to turn on the quorum sensing (QS), a key step in the biofilm formation process [29]. Therefore, it was difficult, at this stage, to explain the crude extracts activity due to the different factors that could influence the achieved results. It was crucial to fractionate the main chemical constituents of the active extract composition by using chemical and biological analyses.

# 5. References


[1] Svoboda, K.; Brooker, J. D.; Zrustova, J. Antibacterial and Antioxidant Properties of Essential Oils: Their Potential Applications in the Food Industries. *Acta Horticulturae*, **2006** (709), 35–44. 10.17660/ActaHortic.2006.709.4

[2] Valle Jr, D.; Andrade, L.; Puzon J. I.; Cabrera, J. J. M.; Rivera, W. L. Antibacterial activities of ethanol extracts of Philippine medicinal plants against multidrug-resistant bacteria. *Asian pacific journal of tropical biomedicine*.**2015**, 5(7):532-540.https://doi.org/10.1016/j.apjtb.2015.04.005

[3] Savoia, D. Plant-derived antimicrobial compounds: alternatives to antibiotics. *Future Microbiology* **2012**, 7, 979. https://doi.org/10.2217/fmb.12.68

[4] Cowan, M.M. Plant product as antimicrobial agents. *Clin. Microbiol. Rev.* **1999**, 12, 564–582. https://doi.org/10.1128/CMR.12.4.564

[5] Garcia, A.; Bocanegra-Garcia, V.; Palma-Nicolas, J.P.; Rivera, G. Recent advances in antitubercular natural products. *Eur. J. Med. Chem.* **2012**, *49*, 1–23.https://doi.org/10.1016/j.ejmech.2011.12.029

[6] Kurek, A.; Grudniak, A.M.; Kraczkiewicz, D.A.; Wolska, K.I. New antibacterial therapeutics and strategies. *Pol. J. Microbiol.* **2011**, 60, 3–12

[7] Fowler, Z.L.; Baron, C.M.; Panepinto, J.C.; Koffas, M.A. Melanization of flavonoids by fungal and bacterial laccases. *Yeas*t. **2011**, 28, 181–188. https://doi.org/10.1002/yea.1829

[8] Iwasa K.; Moriyasu M.; Yamori T.; Turuo T.; Lee D. U.; Wiegrebe W. In vitro cytotoxicity of the protoberberine-type alkaloids. *Journal of natural products*,**2001**, *64*(7), 896-898. https://doi.org/10.1021/np000554f

[9] Yi, Z. B.; Yu, Y.; Liang, Y. Z.; Zeng, B. Evaluation of the antimicrobial mode of berberine by LC/ESI-MS combined with principal component analysis. *Journal of pharmaceutical and biomedical analysis*, **2007**,*44* (1), 301-304. https://doi.org/10.1016/j.jpba.2007.02.018

[10] WHO. WHO traditional medicine strategy. **2002**, Geneva.

[11] Sahib, N.G.; Anwar, F.; Gilani, A.H.; Hamid, A.A.; Saari, N.; Alkharfy, K.M. Coriander *Coriandrum sativum* L.: a potential source of high-value components for functional foods and nutraceuticals – a review. *Phytother.* **2013**, *27*, 1439-1456. https://doi.org/10.1002/ptr.4897

[12] Wiegand, I.; Hilpert, K.; Hancock, R. Agar and broth dilution methods to determine the minimal inhibitory concentration (MIC) of antimicrobial substances. *Nat Protoc* **2008** *3*, 163–175 https://doi.org/10.1038/nprot.2007.521

[13] Gaglione, R.; Dell'Olmo, E.; Bosso, A.; Chino, M.; Pane, K.; Ascione ,F.; Itri, F.; Caserta, S.; Amoresano, A.; Lombardi, A.; Haagsman, H.P. ; Piccoli, R.; Pizzo, E.; Veldhuizen, E.J.A.; Notomista, E.; Arciello, A. Novel human bioactive peptides identified in apolipoprotein B: evaluation of their therapeutic potential, Biochemical Pharmacology. **2017** *130*, 34-50 https://doi.org/10.1016/j.bcp.2017.01.009

[14] Ashraf, M. U.; Muhammad, G.; Hussain, M. A.; Bukhari, S. N. *Cydonia oblonga* M., a medicinal plant rich in phytonutrients for pharmaceuticals. *Frontiers in pharmacology*,**2016**, *7*, 163. https://doi.org/10.3389/fphar.2016.00163

[15] Farhadi, F.; Khameneh, B.; Iranshahi, M.; Iranshahy, M. Antibacterial activity of flavonoids and their structure–activity relationship: An update review. *Phytotherapy Research*,2019, *33*(1), 13-40. https://doi.org/10.1002/ptr.6208

[16] Singariya, P.; Mourya, K. K.; Kumar,P. A. D. M. A. Comparative Microcidal Activity of *Withania somnifera* and *Cenchrus setigerus* against the Pathogenic Micro-organisms. *Int J Pharmacy Pharm Sci*, **2011**,*3*(5), 511-555.

[17] Guzzo, F.; Scognamiglio, M.; Fiorentino, A.; Buommino, E.; D'Abrosca B. Plant derived natural products against *Pseudomonas aeruginosa* and *Staphylococcus aureus*: Antibiofilm activity and molecular mechanisms. *Molecules*, **2020**, *25*(21), 5024. 10.3390/molecules25215024

[18] Ksouri, R.; Megdiche, W.; Falleh, H.; Trabelsi, N.; Boulaaba, M.; Smaoui, A.; Abdelly, C. Influence of biological, environmental and technical factors on phenolic content and antioxidant activities of Tunisian halophytes. *Comptes Rendus Biologies*,**2008**, *331*(11), 865-873. https://doi.org/10.1016/j.crvi.2008.07.024

[19] Lefebvre, T.; Destandau, E.; Lesellier, E. Selective extraction of bioactive compounds from plants using recent extraction techniques: A review. *Journal of Chromatography A*, **2021**,*1635*, 461770. https://doi.org/10.1016/j.chroma.2020.461770

[20] Ni, Z. J.; Wang, X.; Shen, Y.; Thakur, K.; Han, J.; Zhang, J. G.; Hu, F.; Wei, Z. J. Recent updates on the chemistry, bioactivities, mode of action, and industrial applications of plant essential oils. *Trends in Food Science & Technology***, 2021**,*110*, 78-89.https://doi.org/10.1016/j.tifs.2021.01.070

[21] Lei, S.; Hu, Y.; Yuan, C.; Sun, R.; Wang, J.; Zhang, Y.; Zhang, Y.; Lu, D.; Fu, L.; Jiang, F. Discovery of Sortase A covalent in-hibitors with benzofuranene cyanide structures as potential antibacterial agents against *Staphylococcus aureus*. *European Journal of Medicinal Chemistry* **2022**, 229. https://doi.org/10.1016/j.ejmech.2021.114032

[22] Roy, R.; Tiwari,M.; Donelli, G.; Tiwari,, V. Strategies for combating bacterial biofilms: A focus on anti-biofilm agents and their mechanisms of action. *Virulence*, 2018,*9*(1), 522-554. https://doi.org/10.1080/21505594.2017.1313372

[23] Akbarian, M.; Chen, S. H.; Kianpour, M.; Farjadian, F.; Tayebi, L.; Uversky, V. N. A review on biofilms and the currently available antibiofilm approaches: Matrix-destabilizing hydrolases and anti-bacterial peptides as promising candidates for the food industries. *International Journal of Biological Macromolecules*.**2022**, Volume 219, Pages 1163-1179. https://doi.org/10.1016/j.ijbiomac.2022.08.192

[24] Saleem, S.; Muhammad, G.; Hussain, M. A.; Altaf, M.; Bukhari, S. N. A. (*Withania somnifera* L.: Insights into the phytochemical profile, therapeutic potential, clinical trials, and future prospective. *Iranian Journal of Basic Medical Sciences,**2020**,* 23(*12*), 1501. 10.22038/IJBMS.2020.44254.10378

[25] Chemsa , A. E.; Zellagui, A.; Öztürk, M.; Ebru, E. R. O. L.; Ceylan, O.; Duru , M. E. The chemical composition of *Centaurea furfuracea* Coss. and Dur. essential oil with antioxidant, anticholinesterase and antibiofilm activities. *Journal of ongoing chemical research*, **2018**; 3(2), 54-63.

[26] Sen-Utsukarci, B.; Dosler, S. I. B. E. L.; Taskin, T.; Abudayyak, M.; Ozhan, G.; Mat A. An evaluation of antioxidant, antimicrobial, antibiofilm and

cytotoxic activities of five *Verbascum* species in Turkey. *Farmacia*,**2018**, *66*, 1014-1020. HTTP://DOI.ORG/10.31925/FARMACIA.2018.6.14

[27] Dbeibia, A.; Taheur, F. B.; Altammar, K. A.; Haddaji, N.; Mahdhi, A.; Amri, Z.; Mzoughi, R.; Jabeur, C. Control of *Staphylococcus aureus* methicillin resistant isolated from auricular infections using aqueous and methanolic extracts of *Ephedra alata*. *Saudi Journal of Biological Sciences*,**2022**, *29*(2), 1021-1028. https://doi.org/10.1016/j.sjbs.2021.09.071

[28] Singariya, P.; Mourya, K. K.; Kumar, P. (2012). Antimicrobial Activity of the Crude Extracts of *Withania somnifera* and *Cenchrus setigerus* In-vitro. *Pharmacognosy journal*, **2012,** *4*(27), 60-65. https://doi.org/10.5530/pj.2012.27.10

[29] Beigomi, M.; Biabangard, A.; Rohani, R. Evaluation of antimicrobial effects of Rosemary and *Withania somnifera* methanol extract prepared by ultrasound waveform on *Escherichia coli* biofilm isolated from urinary tract infection. *Micro Environer*,**2021**, *1*(2), 17-25. https://doi.org/10.54458/mev.v1i01.6670

# CHAPTER 3

# Bio-guided Purification and Identification of *Centaurea hyalolepis* Active Metabolites

Shurooq Ismail

Department of Chemical Sciences, PhD in Biotechnology

University of Naples Federico II

# Bio-guided Purification and Identification of *Centaurea hyalolepis* Active Metabolites

## 1. Introduction

*Centaurea hyalolepis* is a plant that belongs to the well-known *Asteraceae*, also named Compositae family [1]. It is one of the biggest plant families comprising more than 1,620 genera and 23,600 species of herbs, shrubs and trees [1,2]. The genus *Centaurea* comprises about 500 species that are predominately distributed around the Mediterranean area and in West Asia [3]. The phytochemical constituents of plants represent a precious reservoir of novel, diverse and potent drugs [4]. For this reason, researchers devoted their efforts to the investigation of wild plants endowed with beneficial medical properties. In particular, *Centaurea* species were widely used as a remedy for several health related issues, such as diarrhea, urinary tract infections, diuretic problems, diabetes, inflammation, bacterial infections, dandruff, and others [4-7].

Phytochemical analyses revealed that *Centaurea* plant species contain several metabolites, such as sesquiterpene lactones (STLs), essential oils, flavonoids, alkaloids, and lignans [8,9]. It is worth noting, that STLs and flavonoids are the predominant metabolites of *Centaurea* [10], and they are probably responsible for most of the reported biological activities of *Centaurea* crude extracts [9]. Recently, STLs were widely analyzed for their biological properties, and found to be endowed with antibacterial, antifungal, anti-inflammatory, anti-cancer and anti-oxidative properties [11]. This elicited a great interest that led to the purification and isolation of STLs from Asteraceae family members known to be very rich in STLs [12]. It was demonstrated the unique bioactivity of STLs is correlated to their molecular structure characterized by the presence of α,β-unsaturated carbonyl structures with α-methylene or γ-lactone rings aside by the basic 15-carbon backbone structure [13,14]. This molecular structure of STLs might allow covalent interactions with sulfhydryl groups of enzymes or other nucleophile biological molecules [13-15].

In this chapter, it was demonstrated that *C. hyalolepis* crude extract obtained in dichloromethane ($CH_2Cl_2$) was endowed with significant antimicrobial properties towards a panel of Gram-positive and Gram-negative bacterial strains by broth microdilution assays to evaluate Minimal Inhibitory Concentration (MIC) values. Considering this observation, a bio-guided fractionation of *C. hyalolepis* total extract

was performed by multiple steps of thin layer chromatography and column chromatography. The fractions with antimicrobial properties were further processed at each step. Nuclear magnetic resonance (NMR) spectroscopy and mass spectrometry (MS) analyses were performed to identify the chemical structure of the isolated metabolites as well.

## 2. Methods

**2.1 Materials.** Optical rotations were measured on a Jasco P-1010 digital polarimeter; $^{1}H$ and $^{13}C$ NMR spectra were recorded at 400 and 100 MHz, respectively, in $CDCl_3$ and $CD_3OD$ on a Bruker spectrometer. The same solvent was used as an internal standard. DEPT, COSY-45, HSQC, HMBC, and NOESY experiments [16] were performed using Bruker microprograms. Electrospray ionization mass spectra (ESIMS) were performed using the LC/MS TOF system AGILENT 6230B (Agilent Technologies, Milan, Italy), HPLC 1260 Infinity. Column chromatography (CC) was performed on silica gel (Merck, Kieselgel 60, 0.063−0.200 mm). Analytical and preparative TLC were performed on silica gel plates (Kieselgel 60, $F_{254}$, 0.25 and 0.5 mm respectively) or on reverse phase ($KC_{18}$ $F_{254}$, 0.20 mm) plates and the compounds were visualized by exposure to UV light and/or iodine vapors and/or by spraying with 10% $H_2SO_4$ in MeOH. Then with 5% phosphomolybdic acid in EtOH, followed by heating at 110 °C for 10 min. CC silica gel were from Merck, Kieselgel 60, 0.063–0.200 mm [17]. All the reagents and the solvents were purchased from Sigma-Merck (Milan, Italy), unless specified otherwise.

**2.2 Plant Collection and Identification.** The leaves of *C. hyalolepis* were collected from their natural habitat in West-Bank, Palestine, during March 2021. Identification of the plant was carried out by the plant taxonomist Dr. Ghadeer Omar from the Department of Biology and Biotechnology at An-Najah National University in Palestine. Representative plant specimens of the studied plant were collected, pressed until drying, chemically poisoned to prevent bacterial and fungal infections, then mounted on herbarium sheets and provided with voucher number (ANUH1625) to be deposited at An-Najah National University herbarium. The collected leaves of *C. hyalolepis* were then washed with water to remove soil and dust particles and dried. Exposure to light was avoided to prevent possible loss of effective metabolites. The dried leaves were then powdered using a blender prior to the extraction process.

**2.3 Extract Preparation and Purification**. Plant material (728 g) was extracted (1×2,500 mL) by $H_2O$/MeOH (1/1,*v/v*) under stirred conditions at room temperature for 48 h. The suspension was then centrifuged at 7,000 rpm for 40 min) and the supernatant was extracted by hexane (3×1,000 mL) and successively with $CH_2Cl_2$ (3×1,000 mL). Methanol was then removed under reduced pressure by using EtOAc (3×600 mL). Bio-guided purification was subsequently performed by testing

each sample towards six bacterial strains both at time 0 and after each purification step. The portion (3.5 g) of $CH_2Cl_2$ organic extract showing antibacterial activity was further purified by CC and eluted in $CHCl_3$/*i*-PrOH (9/1,*v/v),* thus obtaining 6 homogeneous fractions **(Figure 1)** whose antibacterial activity was tested against a Gram-positive *E. faecalis* ATCC 29212 and a Gram-negative *S. typhimurium* ATCC 14028 bacterial strain. The residues of fractions (CH.4 and CH.5) were combined in one fraction named CH.6 as they shared the same profile on TLC and showed similar antibacterial activity. Fraction CH.6 was further purified by CC and TLC, as shown in **Figure 1.** CC was performed by analyzing 568 mg of CH.6 and elution was carried out in $CHCl_3$/MeOH (9/1,*v/v*). The third fraction obtained (CH.6.3) was further purified by CC and eluted in $CH_2Cl_2$/*i*-PrOH (9/1,*v/v*). Eluted fraction was found to contain a sesquiterpene lactone identified as cnicin (**compound 1**, 53.75 mg). The second obtained fraction (CH.6.2) was purified by CC and eluted in $CH_2Cl_2$/*i*-PrOH (9/1,*v/v*) to obtain a pure sesquiterpene lactone identified as 11β,13-dihydrosalonitenolide (**compound 2**, 44.36 mg). Fraction CH.3 (341.69 mg) was found to be endowed with antibacterial activity, and was firstly purified by CC and elution in $CH_2Cl_2$/MeOH (95/5,*v/v*) followed by reverse-CC and elution in acetonitrile/$H_2O$ (4/6,*v/v*), thus obtaining a sesquiterpene lactone namely salonitenolide (**compound 3**, 81.08 mg).

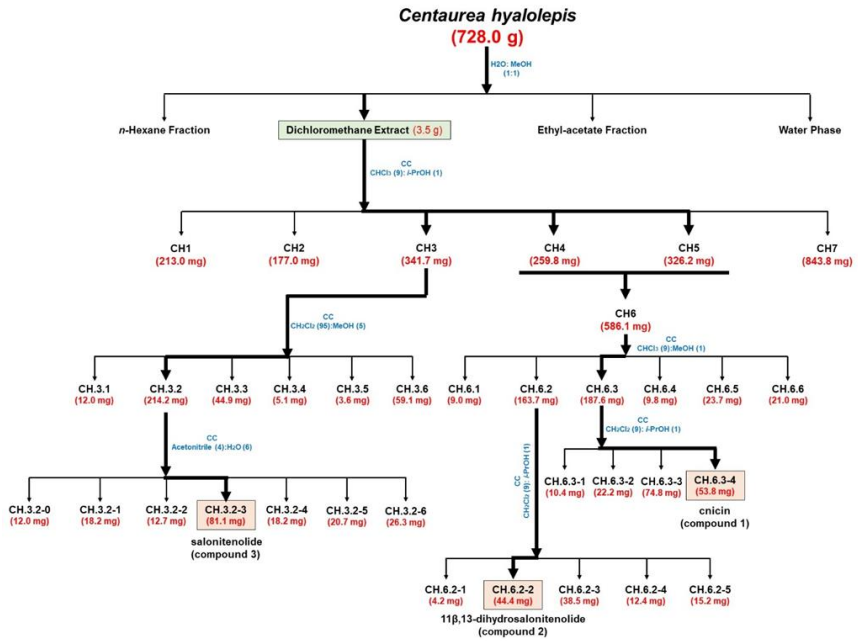


**Figure 1.** Schematic overview of the bio-guided fractionation of the extracts obtained in $CH_2Cl_2$ from *C. hyalolepis* leaves.

**2.4 Adsorption Chromatography Technique.** Chromatography is the separation of a mixture of components based on their differential interactions with two chemical or physical phases: a mobile phase and a stationary phase [18,19]. Chromatographic separations are usually performed for the determination of the composition of a sample. The isolation of an individual compound from a mixture could be achieved by the adsorption chromatography in which the adsorbent is either packed in an open tube (column chromatography) or shaped in the form of a sheet (thin-layer chromatography, TLC) [20]. As it is illustrated in **(Figure 2)** [21]**.**

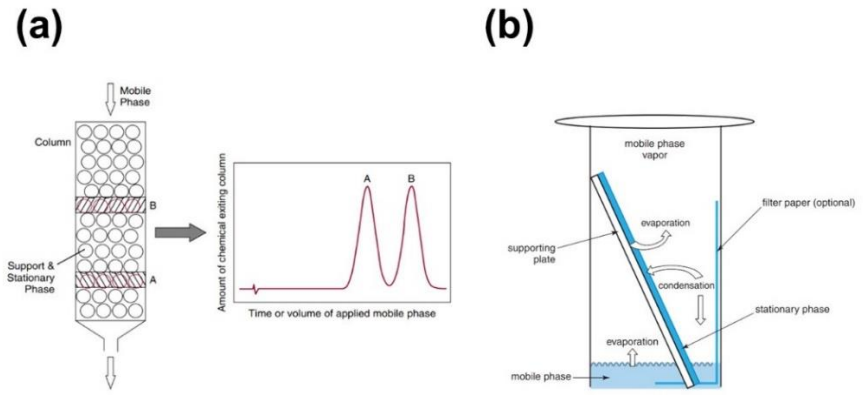


**Figure 2. (a)** Schematic representation of the employed chromatographic system and separation of 2 analytes indicated as A and B. **(b)** Schematic representation of a chamber for conventional TLC. From Hage, 2018.

A suitable solvent based on the mixture composition is selected to elute from the adsorbent. Plant extracts as well as purified fraction's mixtures were separated to isolate and identify several compounds by using silica gel as a solid phase. Furthermore, solvent combinations based on the extract content were setup specifically for each extract. Relaying on the amount of extract achieved (mg) either column chromatography (CC) or preparative thin layer chromatography (TLC) were applied to achieve the purified compounds. It is specified in the provided purification schemes for all purified fractions at each step of the purification process which solvent combinations were used as well as the chromatographic method applied.

**2.5 Bacterial Strains and Growth Conditions.** Six bacterial strains were used to evaluate the antibacterial and anti-biofilm properties of the plant extracts and of the plant-derived compounds. *Staphylococcus aureus* ATCC 29213, methicillin-resistant *Staphylococcus aureus*

(MRSA WKZ-2), *Enterococcus faecalis* ATCC 29212*, Acinetobacter baumannii* ATCC 17878*, Escherichia coli* ATCC 25922 and *Salmonella typhimurium* ATCC 14028. American type culture collection (ATCC) numbers represent the standard strain numbers assigned to these microorganisms. Bacterial strains were grown in Muller Hinton Broth (MHB; Becton Dickinson Difco, Franklin Lakes, NJ, USA) and on Tryptic Soy Agar (TSA; Oxoid Ltd., Hampshire, UK). In all experiments, bacteria were inoculated and grown overnight in MHB at 37 °C. The next day, bacteria were transferred to a fresh MHB tube and grown to mid-logarithmic phase.

**2.6 Antimicrobial Activity Assays.** To test extracts antimicrobial activity, bacterial cells were diluted to $2x10^6$ CFU/mL in Nutrient Broth (NB; Difco, Becton Dickinson, Franklin Lakes, NJ, USA) along with increasing amounts of each tested extract or compound. In each case, starting from a stock solution, two-fold serial dilutions were prepared according to broth microdilution method [22]. $MIC_{100}$ values were determined as the lowest extract or compound concentration responsible for no visible bacterial growth after overnight incubation.

**2.7 Statistical analyses**. Statistical analyses were performed by using a Student's t-test. Significant differences were indicated as *P < 0.05, **P < 0.01 or ***P < 0.001. Graphs were performed with the GraphPad Prism 8 software.

# 3. Results

## 3.1 Bio-guided fractionation of *C. hyalolepis* extracts followed by isolation and identification of bioactive metabolites.

To isolate the compounds responsible for *C. hyalolepis* antibacterial and/or anti-biofilm properties, total extracts were subjected to purification steps as described in the Materials and Methods Section and schematically reported in **Figure 1**. The extract obtained in $CH_2Cl_2$ was subjected to combined steps of CC and TLC. The experimental strategy allowed obtaining 3 pure metabolites belonging to the sesquiterpene lactone group of plant metabolites **(Figure 3)**.

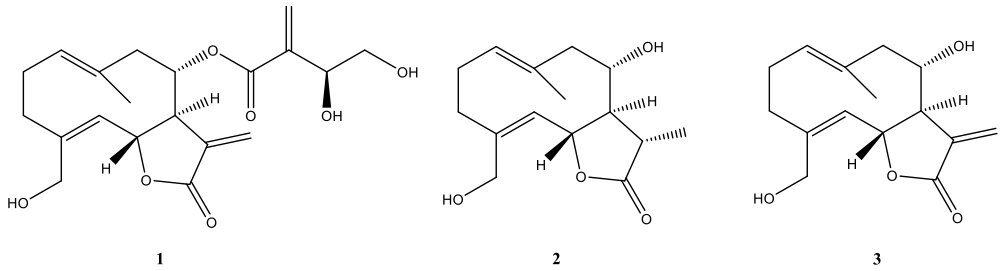


**Figure 3.** Chemical structures of isolated compounds **1**-**3**.

The first compound corresponding to fraction CH.6.3-4 was identified as **cnicin** (**compound 1)**, which was reported for the first time in 1960 by Miloś Suchý [23]. In fact, its $^1$H NMR spectrum **(Figure 4)** was comparable to that reported in the literature when cnicin was isolated from *C. malacitana* [24]. Furthermore, the specific optical rotation value $[\alpha]_D$ = +152.4º(c 0.5, MeOH), was found to be very similar to that reported in literature $[\alpha]_D$ = +169.6º(c 0.1, MeOH) [25].

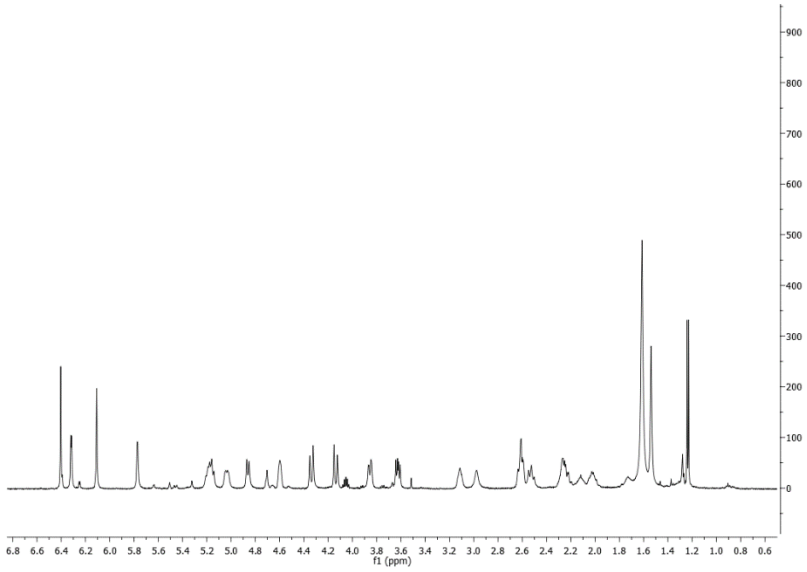


**Figure 4**. $^{1}$H NMR spectrum of **cnicin** (**compound 1**) recorded in $CDCl_3$ at 500 MHz.

On the other hand, compound corresponding to fraction CH.6.2-2 was identified as **11β,13-dihydrosalonitenolide** (**compound 2**), which was isolated for the first time from the extract obtained from the aerial parts of *C. calcitrapa* together with cnicin and other germacranolides [26]. Its $^{1}$H NMR spectrum **(Figure 5)** was found to be comparable to that reported by Marco and others in 1992 [26]. The absolute configuration was confirmed by measuring the specific optical rotation value$[\alpha]_D$ = +81º(c 0.5, $CHCl_3$), that was found to be comparable to that reported in the literature $[\alpha]_D$ = +98º(c 5, $CHCl_3$) [26].

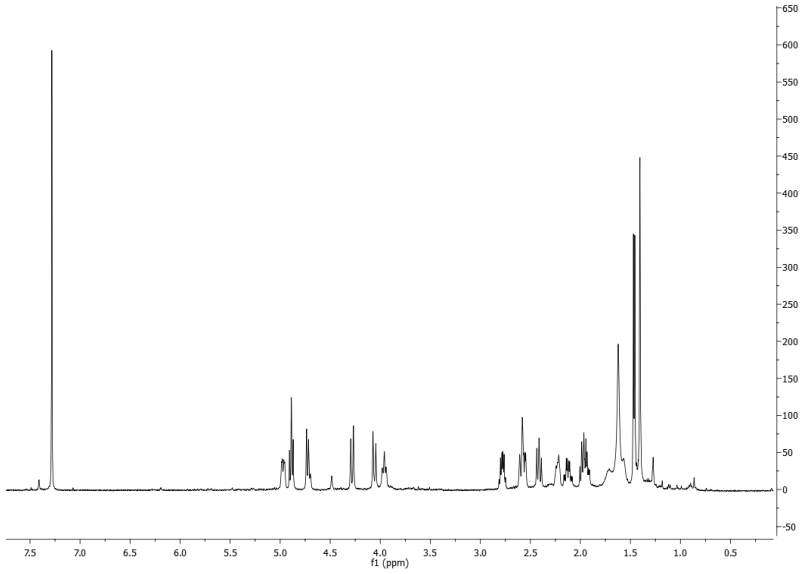


**Figure 5**. $^{1}$H NMR spectrum of **11β,13-dihydrosalonitenolide** recorded in $CDCl_3$ at 500 MHz.

Finally, compound corresponding to fraction CH.3.2-3 was identified as **salonitenolide** (**compound 3**) which was isolated for the first time from *C. salonitana* in 1965 [27]. Its $^{1}$H NMR spectrum **(Figure 6)** was found to be comparable to that reported in the literature when it was isolated from *C. malacitana* [28]. Moreover, the absolute configuration was confirmed by measuring the specific optical rotation value $[\alpha]_D$ = +152.4º(c 0.35, MeOH), which was found to be comparable to that reported in the literature $[\alpha]_D$ = +199.4º(c 0.04, MeOH) [29].

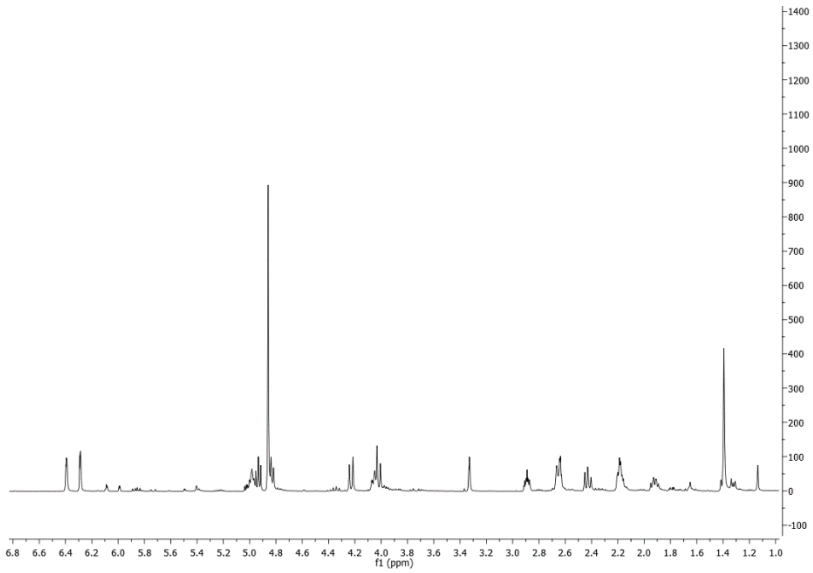


**Figure 6**. $^{1}$H NMR spectrum of **Salonitenolide** recorded in $CD_3OD$ at 500 MHz.

## 3.2 Antimicrobial activity of total extracts from *C. hyalolepis.*

*Centaurea* genera species were used in folk medicine for thousands of years by different nations to cure various illnesses including diabetes, diarrhea, eye infections, respiratory diseases, gallstones, rheumatic problems, inflammation states, and bacterial infections [4, 5]. The crude leaf extract from *C. hyalolepis* was obtained in different solvents, such as hexane, dichloromethane ($CH_2Cl_2$) , ethyl-acetate (EtOAc) and water, and tested on a panel of Gram-positive (*S. aureus ATCC* 29213*, S. aureus* MRSA WKZ-2*, E. faecalis ATCC* 29212) and Gram-negative (*A. baumannii* ATCC 17878*, E. coli* ATCC 25922 and *S. typhimurium* ATCC 14028) pathogens. The antimicrobial activity was evaluated by using the broth microdilution assay [30] to determine the minimal inhibitory concentration (MIC) values, which are reported in **Table 1**.

The dichloromethane ($CH_2Cl_2$) extract exhibited the best antibacterial activity ($MIC_{100}$ values ranging from 0.25 to 2 mg/mL) against all the tested bacterial strains. Indeed, both Gram-positive and Gram-negative tested strains were found to be susceptible to *C. hyalolepis* $CH_2Cl_2$ extract. For this reason, dichloromethane ($CH_2Cl_2$) extract was selected for further purification steps performed to identify the plant metabolites responsible for the observed antibacterial activity (**Table 1**).

**Table 1**. $MIC_{100}$ values (mg/mL) determined for *C. hyalolepis* extracts obtained in water, hexane, dichloromethane ($CH_2Cl_2$), and ethyl acetate (EtOAc). Reported data refer to three biological replicates.

| | $MIC_{100}$ (mg/mL) | | | |
|---|---|---|---|---|
| **Bacterial strains** | **Hexane Extract** | **$CH_2Cl_2$ Extract** | **EtOAc Extract** | **Residual water phase** |
| *S. aureus* ATCC 29213 | 1 | 0.25 | 1 | > 2 |
| *S. aureus* MRSA WKZ-2 | 1 | 0.5 | 1 | > 2 |
| *E. faecalis* ATCC 29212 | 2 | 2 | 1 | > 2 |
| *E. coli* ATCC 25922 | 2 | 1 | 1 | > 2 |
| *S. typhimurium* ATCC 14028 | 1 | 1 | 1 | > 2 |
| *A. baumannii* ATCC 17878 | 2 | 0.25 | 0.5 | > 2 |

$CH_2Cl_2$ extract was subjected to several purification steps as reported in **Figure 1**. At each step, purified fractions were tested on the Gram-positive *E. faecalis* ATCC 29212 and on the Gram-negative *A. baumannii* ATCC 17878. Obtained results were reported in **Table 2.**

**Table 2**. $MIC_{100}$ values (mg/mL) determined for fractions obtained upon purification of $CH_2Cl_2$ *C. hyalolepis* total extract. Reported data refer to three biological replicates.

| | $MIC_{100}$ (mg/mL) | |
|---|---|---|
| **$CH_2Cl_2$ Fractions** | ***E. faecalis* ATCC 29212** | ***S. typhimurium* ATCC 14028** |
| **CH.1** | 0.125 | 0.125 |
| **CH.2** | 1 | 1 |
| **CH.3** | 0.125 | 0.0312 |
| **CH.4** | 0.125 | 0.0625 |
| **CH.5** | 0.25 | 0.0312 |
| **CH.7** | 1 | 1 |

*E. faecalis ATCC* 29212 and *S. typhimurium* ATCC 14028 bacterial strains were selected since they were found to be more resistant than other strains to $CH_2Cl_2$ extract antibacterial activity with $MIC_{100}$ values ranging from 1-2 mg/mL (**Table 1**). It has to be highlighted that fractions obtained upon the chromatographic step were found to be more active than the total $CH_2Cl_2$ extract, being effective on both *E. faecalis* ATCC 29212 and *S. typhimurium* ATCC 14028 bacterial strains with $MIC_{100}$ values comprised between 0.0312 and 1mg/mL (**Table 2**). Following the first chromatographic step, fractions

CH.4 and CH.5 were combined in one fraction named CH.6 since they were found to have similar antimicrobial activity and to share the same TLC profile. Based on the detected antimicrobial properties, fractions CH.3 and CH.6 were selected to be subjected to further purification steps.

### 3.3 Antibacterial activity of isolated compounds cnicin, 11β,13-dihydrosalonitenolide and salonitenolide.

To verify whether the isolated compounds were responsible for the antimicrobial properties detected in the case of the organic $CH_2Cl_2$ extract, antibacterial activity assays were performed by determining the minimal inhibitory concentration (MIC), as well as, the minimal bactericidal concentration (MBC). This was achieved by testing increasing concentrations of each isolated compound on *S. aureus* ATCC 29213, *S. aureus* MRSA WKZ-2, *E. faecalis* ATCC 29212, *A. baumannii* ATCC 17878, *E. coli* ATCC 25922 and *S. typhimurium* ATCC 14028. As shown in **Figures 7-9**, cnicin (compound **1**) was found to be the most active compound against all the tested bacterial strains. Indeed, it has to be highlighted that cnicin is a sesquiterpene lactone commonly present in *Centaurea* species and well-known for its antibacterial activity [4][31]. Indeed, this was supported here, cnicin was found to be particularly active against the Gram-negative bacterial strains; *E. coli* ATCC 25922 and *S. typhimurium* ATCC 14028 to which $MIC_{100}$ values detected were 0.125 mg/mL (**Figure 7**).

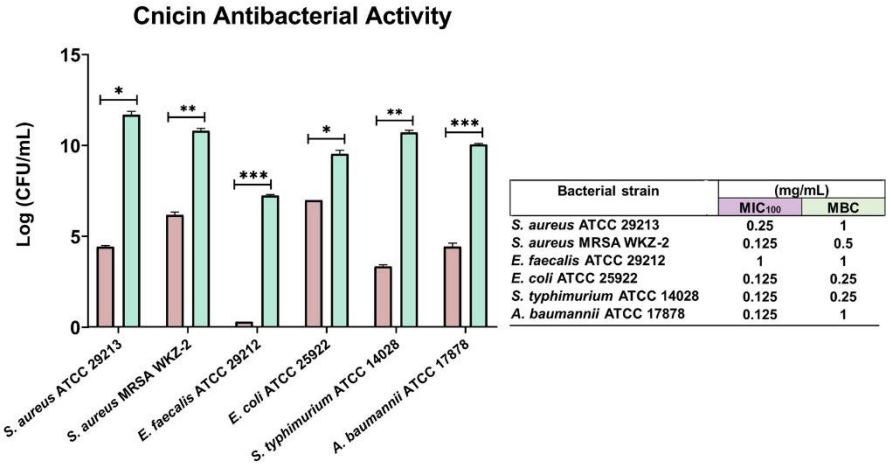


| Bacterial strain | (mg/mL) | |
|---|---|---|
| | $MIC_{100}$ | MBC |
| *S. aureus* ATCC 29213 | 0.25 | 1 |
| *S. aureus* MRSA WKZ-2 | 0.125 | 0.5 |
| *E. faecalis* ATCC 29212 | 1 | 1 |
| *E. coli* ATCC 25922 | 0.125 | 0.25 |
| *S. typhimurium* ATCC 14028 | 0.125 | 0.25 |
| *A. baumannii* ATCC 17878 | 0.125 | 1 |

**Figure 7.** Minimal Inhibitory Concentration $MIC_{100}$ (mg/mL) and Minimal Bactericidal Concentration MBC (mg/mL) values determined for the compound **1** cnicin against a panel of Gram-positive and Gram-negative bacterial strains. Data represents the mean (±standard deviation, SD) of at least three independent experiments.

Furthermore, compound **3** was found to be effective on all the tested strains even with higher $MIC_{100}$ values detected with respect to those detected with cnicin (**Figure 8**). Compound **2**, 11β,13-dihydrosalonitenolide, showed the lowest antibacterial activity with $MIC_{100}$ values ranging from 0.5 to 7.5 mg/mL. These values were found to be significantly higher than those detected for the crude $CH_2Cl_2$ extract ($MIC_{100}$ values ranging from 0.25 to 2 mg/mL as reported in **Table 1**). Comparing MIC and MBC values, cnicin was found to be the most active compound (**Figures 7-9**). It has also to be noted that *E. faecalis* ATCC 29212 bacterial strain was found to be the most resistant strain to the antimicrobial activity of tested compounds **1**-**3** (**Figure 9**).

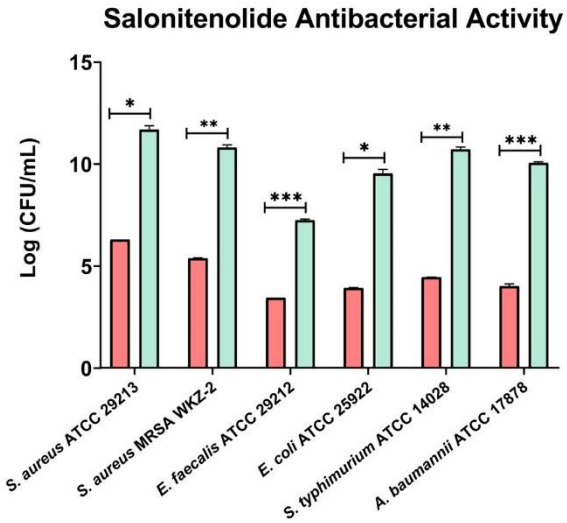


| Bacterial strain | (mg/mL) | |
|---|---|---|
| | $MIC_{100}$ | MBC |
| *S. aureus* ATCC 29213 | 0.25 | 1 |
| *S. aureus* MRSA WKZ-2 | 0.25 | <1 |
| *E. faecalis* ATCC 29212 | 1* | <1 |
| *E. coli* ATCC 25922 | 1 | <1 |
| *S. typhimurium* ATCC 14028 | 1 | 1 |
| *A. baumannii* ATCC 17878 | 1 | <1 |

(*$MIC_{99}$)

**Figure 8.** Minimal Inhibitory Concentration $MIC_{100}$ (mg/mL) and Minimal Bactericidal Concentration MBC (mg/mL) values determined for compound **3** salonitenolide against a panel of Gram-positive and Gram-negative bacterial strains. Data represents the mean (±standard deviation, SD) of at least three independent experiments.

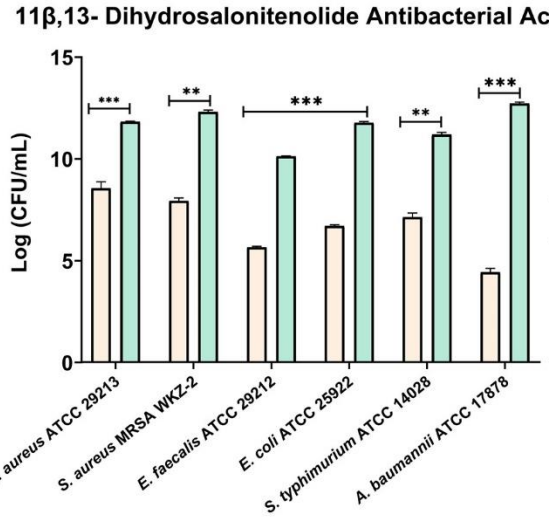


| Bacterial strain | (mg/mL) | |
|---|---|---|
| | $MIC_{100}$ | MBC |
| *S. aureus* ATCC 29213 | 0. 5 | 7.5 |
| *S. aureus* MRSA WKZ-2 | 0.625 | 7.5 |
| *E. faecalis* ATCC 29212 | 7.5 | <7.5 |
| *E. coli* ATCC 25922 | 1.25 | 2.5 |
| *S. typhimurium* ATCC 14028 | 0.937 | 7.5 |
| *A. baumannii* ATCC 17878 | 0.5 | 2.5 |

**Figure 9.** Minimal Inhibitory Concentration $MIC_{100}$ (mg/mL) and Minimal Bactericidal Concentration MBC (mg/mL) values determined for compound **2** 11β,13-dihydrosalonitenolide against a panel of Gram-positive and Gram-negative bacterial strains. Data represents the mean (±standard deviation, SD) of at least three independent experiments.

## 4. Discussion

A bio-guided purification of *C. hyalolepis* organic extract obtained in $CH_2Cl_2$ was performed to identify bioactive metabolites responsible for its antimicrobial properties. Through the purification process, fractions with antimicrobial activity were analyzed and revealed the presence of three sesquiterpene lactones (STLs) identified as cnicin, 11β,13-dihydrosalonitenolide, and salonitenolide (**1**-**3**) in **Figure 3**.

*C. hyalolepis* belongs to the well-known Asteraceae, also named as Compositae family [1]. *Centaurea* plant species were reported to be very rich in STLs and flavonoids metabolites [10]. Cnicin (compound **1**), one of the compounds identified, was isolated for the first time in 1960 from *Cnicus benedictus* [23], a plant that grows in the Mediterranean regions and used for thousands of years to cure liver diseases, anorexia, indigestion problems, ulcers, and swollen fingers [31]. Cnicin was then isolated from several plants [1][23][26][29][31] and analyzed over years to evaluate its beneficial pharmaceutical properties [24][34,35][39-42]. 11β,13-dihydrosalonitenolide (Compound **2**), was isolated for the first time from the aerial parts of *C. calcitrapa* together with cnicin [26]. Furthermore, it was isolated from the aerial parts of *C. alba*, *C. spinosa* and *C. pullata* [42-44]. Salonitenolide (compound **3**) was isolated for the first time from *C. salonitana* in 1965 [27], and then from *Ambrosia artemisiifolia* [45], *C. malacitana* [28], and *C. melitensis* [46] together with other sesquiterpene lactones, such as cnicin. STLs represent important bioactive compounds of several medicinal plants that exert anti-inflammatory, anti-diabetic, anti-malarial, anti-proliferative, anti-parasitic, and antibacterial properties [47].

The isolated cnicin and salonitenolide were found to be endowed with antibacterial activity against the tested Gram-positive and Gram-negative bacterial strains ($MIC_{100}$ = 0.25 -1 mg/mL). 11β,13-dihydrosalonitenolide (compound **2**), was found to have a lower antibacterial activity ($MIC_{100}$ = 0.5 -1.25 mg/mL) in comparison with the other two isolated compounds. Among the tested bacterial strains, *E. faecalis* ATCC 29212 was found to be the most resistant to the antimicrobial properties of these metabolites. Although, compounds **1**-**3** belong to the class of sesquiterpene lactones, key differences in structural features might be responsible for the detected variations in their antibacterial efficacy (**Figure 3**). Moreover, several factors were reported to influence STLs antibacterial properties, such as the compound structure, concentration in solution, hydrophobicity,

geometric orientation, the specific bacterial strain tested, and the chemical environment [48]. Comparing the antimicrobial activity of the purified compounds with that of the crude extract from *C. hyalolepis*, it appears that the isolated pure compounds were endowed with stronger antibacterial properties. The difference in metabolites antimicrobial activity might be correlated to several factors, such as compounds solubility, pH, iron concentration or antagonistic effects exerted by several metabolites acting in a mixture [38].

Taking into account that cnicin is the strongest antibacterial compound among the three isolated ones; it is plausible that it contributes almost to the antibacterial properties of the whole extract. Cnicin is a STL that belongs to the germacranolide group of terpenes [31], characterized by an exocyclic α-methylene group in addition to γ-butyrolactone ring [31]. It was demonstrated that this α-methylene group is responsible for the antimicrobial activity of sesquiterpene lactones in general and of cnicin in particular [32,33]. It is worth noting that cnicin might react through Michael addition mechanism with nucleophilic groups present in the surrounding target molecules, a molecular event that might be the basis of cnicin's antimicrobial activity [11]. Therefore, the absence of this structural feature in 11β,13-dihydrosalonitenolide (**2**) might be responsible for the significant lowering of the antimicrobial activity of this compound with respect to that of cnicin under the tested experimental conditions. In the related literature, it was reported that cnicin interacts with proteins found in bacterial membranes, thus causing cell lysis and death [33]. Cnicin also acts by blocking bacterial cell wall synthesis through the irreversible inhibition of MurA, which is an enzyme responsible for the catalysis of the first step of the synthesis of peptidoglycans [36]. The effects of cnicin on biofilms is by interfering with quorum-sensing (QS), a key step leading to biofilms formation [37].

Moreover, a challenging aspect in purifying plant natural compounds is the abundancy of the active metabolites, which are usually changing, according to the surrounding abiotic factors, geographical location and the physiological conditions of the collected plants. Furthermore, one more factor that must be taken into consideration is the solvent used during the extraction process. The approach applied here considered this factor by using different solvents ranging in their polarity from the most nonpolar one *i.e.* hexane to the most polar one *i.e.* water. In conclusion, this is the first report describing a detailed purification of *C. hyalolepis* crude extract to discover metabolites responsible for its antibacterial activity. However, it is

recommended to conduct more investigations in the future on *C. hyalolepis* metabolites for a better understanding of their potential pharmacological and biological properties such as, anti-biofilm, anti-inflammatory, anticancer, and antioxidant activities.

# 5. References


[1] Ayad, R.; Akkal, S. Chapter 12 - Phytochemistry and biological activities of Algerian Centaurea and related Genera, Editor(s): Atta-ur-Rahman, *Studies in Natural Products Chemistry, Elsevier*, **2019** 63, Pages 357-414,ISSN 1572-5995,ISBN 9780128179017 https://doi.org/10.1016/B978-0-12-817901-7.00012-5.

[2] Flora of Israel. Available online at http://flora.huji.ac.il/browse asp. Danin A. Accessed on December 10, **2018**.

[3] Djeddi, S.; Argyropoulou, C.; Skaltsa, H. Secondary metabolites from *Centaurea grisebachii* ssp grisebachii , *Biochemical systematics and ecology*,**2008** ,Volume 36 , 336-339, https://doi.org/10.1016/j.bse.2007.11.001

[4] Tiwana, G.; Fua, J.; Lu, L.; Cheesman, M. J.; Cock, I. E. A Review of the Traditional Uses, Medicinal Properties and Phytochemistry of *Centaurea benedicta* L. *Pharmacognosy Journal*, **2021**,*13,3,*798-812. 10.5530/pj.2021.13.102

[5] Chemsa, A. E.; Zellagui, A.; Öztürk, M.; Ebru, E. R. O. L.; Ceylan, O.; Duru, M. E. The chemical composition of *Centaurea furfuracea* Coss. and Dur. essential oil with antioxidant, anticholinesterase and antibiofilm activities. *Journal of ongoing chemical research*, **2018**; *3*(2), 54-63.

[6] Zengin, G.; Cakmak, Y. S.; Guler, G. O.; Aktumsek, A. In vitro antioxidant capacities and fatty acid compositions of three *Centaurea* species collected from Central Anatolia region of Turkey. *Food and Chemical Toxicology*, **2010**, *48*(10), 2638-2641 https://doi.org/10.1016/j.fct.2010.06.033

[7] Csupor, D.; Blazsó, G.; Balogh, Á.; Hohmann, J. The traditional Hungarian medicinal plant *Centaurea sadleriana* Janka accelerates wound healing in rats. *Journal of ethnopharmacology*, **2010**, *127*(1), 193-195. https://doi.org/10.1016/j.jep.2009.09.049

[8] Shoeb, M.; Celik , S.; Jaspars, M.; Kumarasamy, Y.; MacManus, S. M.; Nahar, L.;Thoo-Lin, P.K.; Sarker, S. D. Isolation, structure elucidation and bioactivity of schischkiniin, a unique indole alkaloid from the seeds of *Centaurea schischkinii*. *Tetrahedron*,**2005**, *61*(38),9001-9006. https://doi.org/10.1016/j.tet.2005.07.047

[9] Khammar, A.; Djeddi, S. Pharmacological and biological properties of some *Centaurea* species. *Eur J Sci Res*,**2012**, 84(3), 398-416.

[10] Ismail, S.; Hammouda, F.; Rimpler, H.; Abdallah, S. Flavonoids and Sesquiterpene Lactones, Constituents of *Centaurea alexandrina. Planta Medica,* **1986***, 52(6), 527–527.* 10.1055/s-2007-969314

[11] Matos, M.S.; Anastácio, J.D.; Nunes, dos Santos, C. Sesquiterpene Lactones: Promising Natural Compounds to Fight Inflammation. *Pharmaceutics*, **2021**, *13*, 991 https://doi.org/10.3390/ pharmaceutics13070991

[12] Chaturvedi, D.; Dwivedi, P.K. Recent Developments on the Antidiabetic Sesquiterpene Lactones and Their Semisynthetic Analogues. Discovery and Development of Antidiabetic Agents from Natural Products: Natural Product Drug Discovery*. Elsevier*. **2016**, 185-208.10.1016/B978-0-12-809450-1.00006-5.

[13] Picman, A. K. Biological activities of sesquiterpene lactones. *Biochemical systematics and Ecology*,**1986**, *14*(3), 255-281. https://doi.org/10.1016/0305-1978(86)90101-8

[14] Kupchan, S. M.; Fessler, D. C.; Eakin, M. A.; Giacobbe, T. J. Reactions of alpha methylene lactone tumor inhibitors with model biological nucleophiles. *Science*,**1970**, *168*(3929),376-378. 10.1126/science.168.3929.376

[15] Schmidt, T. J. Toxic activities of sesquiterpene lactones: structural and biochemical aspects. *Curr Org Chem*, **1999** *3*(6), 577-608.

[16] Berger, S.; Braun, S. 200 and more NMR experiments (pp. 305-307). *Weinheim: Wiley-Vch* **2004**.

[17] Masi, M.; Di Lecce, R.; Tuzi, A.; Teodoro, Linaldeddu, B.; Montecchio, L.; Maddau, L.; Evidente, A. Hyfraxinic acid, a phytotoxic tetrasubstituted octanoic Acid, produced by the ash (*Fraxinus excelsior L.*) pathogen *Hymenoscyphus fraxineus* together with viridiol and some of its analogues. *Journal of agricultural and food chemistry* **2019** 67.49 : 13617-13623. 10.1021/acs.jafc.9b06055

[18] Ettre, LS. Nomenclature for chromatography. *Pure Appl Chem* **1993**;*65*:819e72, http://dx.doi.org/10.1351/pac199365040819

[19] Miller, J. M. Chromatography: concepts and contrasts. John Wiley & Sons,**2005**.

[20] Speight, J.G.; El-Gendy, N. Chapter 1 – Petroleum Composition and Properties, Editor(s): James G. Speight, Nour Shafik El-Gendy, Introduction to Petroleum Biotechnology,*Gulf Professional Publishing*, **2018**, Pages 1-39,ISBN 9780128051511. https://doi.org/10.1016/B978-0-12-805151-1.00001-1.

[21] Hage, D.S. Chapter 1 - Chromatography, Editor(s): Nader Rifai, Andrea Rita Horvath, Carl T. Wittwer, Principles and *Applications of Clinical Mass Spectrometry,Elsevier*, **2018**, Pages 1-32, ISBN 9780128160633, https://doi.org/10.1016/B978-0-12-816063-3.00001-3.

[22] Gaglione, R.; Dell'Olmo, E.; Bosso, A.; Chino, M.; Pane, K.; Ascione, F.; Itri, F.; Caserta, S.; Amoresano, A.; Lombardi, A.; Haagsman, H.P. ; Piccoli, R.; Pizzo, E.; Veldhuizen, E.J.A.; Notomista, E.; Arciello, A. Novel human bioactive peptides identified in apolipoprotein B: evaluation of their therapeutic potential, Biochemical Pharmacology.**2017** *130*, 34-50 https://doi.org/10.1016/j.bcp.2017.01.009

[23] Suchý, M.; Benešová, V.; Herout; V.; Šorm, F. On Terpenes, CXIX. The structure of cnicin, a sesquiterpene lactone from *Cnicus benedictus* L. *Chemische Berichte* ,**1960** *93* (11), 2449-2456. https://doi.org/10.1002/cber.19600931103

[24] Rustaiyan, A.; Niknejad, A.; Aynehchi, Y. Chemical constituents of *Centaurea brugueriana*. *Planta medica,***1982**; *44*(03), 185-186. 10.1055/s-2007-971441

[25] Kurita, M.; Tanigawa, M.; Narita, S.; Usuki, T. Synthetic study of cnicin: Synthesis of the side chain and its esterification. Tetrahedron Letters,**2016**, 57(52), 5899-5901. https://doi.org/10.1016/j.tetlet.2016.11.067

[26] Marco, J. A.; Sanz, J. F.; Sancenon, F.; Susanna, A.; Rustaiyan, A.; Saberi, M. Sesquiterpene lactones and lignans from *Centaurea* species. *Phytochemistry*, **1992**. *31*(10), 3527-3530. https://doi.org/10.1016/0031-9422(92)83721-A

[27] Suchý, M.; Herout, V.; Šorm, F. On terpenes. CLXXIV. The structure of salonitolide, a sesquiterpenic lactone of germacrane type from *Centaurea salonitana* VIS. *Collect. Czech. Chem. Commun.* **1965**, *30*,2863-2864 https://doi.org/10.1135/cccc19652863

[28] Barrero, A. F.; Sánchez, J. F.; Arana, E. Germacranolides from *Santolina rosmarinifolia* subsp. canescens. *Phytochemistry*, **1988**. *27*(12), 3969-3970.https://doi.org/10.1016/0031-9422(88)83058-9

[29] Adekenov, S. M.; Buděšínský, M.; Abdikalikov, M. A.; Turdybekov, C. M.; Šaman, D.; Błoszyk, E.; Drożdż, B.; Holub, M. Sesquiterpenic lactones of the *Inula caspica* BLUME species. *Collection ofCzechoslovak chemical communications*, **1990**. *55*(6), 1568-1579. https://doi.org/10.1135/cccc19901568

[30] Wiegand, I.; Hilpert, K.; Hancock, R. Agar and broth dilution methods to determine the minimal inhibitory concentration (MIC) of antimicrobial substances. *Nat Protoc* **2008 3**, 163–175 https://doi.org/10.1038/nprot.2007.521

[31] Berger, S.; Sicker, D. *Classics in spectroscopy: isolation and structure elucidation of natural products*. John Wiley & Sons,**2009** ,443-458.

[32] Adekenov,S. M. Sesquiterpene lactones from plants of the family *Asteraceae* in the Kazakhstan flora and their biological activity. *Chemistry of Natural Compounds*,**1995**, *31*(1), 21-25. https://doi.org/10.1007/BF01167564

[33] Dimkić, I., Petrović, M., Gavrilović, M. et al. New perspectives of purple starthistle (*Centaurea calcitrapa*) leaf extracts: phytochemical analysis, cytotoxicity and antimicrobial activity. *AMB Expr*, **2020**, *10*, 183 . https://doi.org/10.1186/s13568-020-01120-

[34] Mezache, N.; Bendjeddou, D.; Satta, D.; Mekkiou, R.; Benayache, S.; Benayache, F. Secondary metabolites from *Centaurea lippi. Chem Nat Compd.* **2010**, *46*, 801–802. 10.1007/s10600-010-9748-5.

[35] Belkacem, S.; Belbache, H.; Boubekri, C.; Mosset, P.; Rached-Mosbah, O.; Marchioni, E.; Benayache, S.; Benayache, F. Chemical constituents from *Centaurea parviflora* Desf. *RJPBCS.* **2014**, *5*, 1275-1279. Available online: http://rjpbcs.com/.../[132].pdf

[36] Bachelier, A.; Mayer, R.; Klein, CD. Sesquiterpene lactones are potent and irreversible inhibitors of the antibacterial target enzyme MurA. *Bioorg Med Chem Lett*. **2006**; *16*(21):5605-5609. https://doi.org/10.1016/j.bmcl.2006.08.021

[37] Hentzer ,M.; Riedel, K.; Rasmussen, TB.; Heydorn, A.; Andersen, JB.; Parsek, MR.; Rice, SA.; Eberl, L.; Molin, S.; Høiby, N.; Kjelleberg, S. Inhibition of quorum sensing in *Pseudomonas aeruginosa* biofilm bacteria by a halogenated furanone compound. *Microbiology*. **2002**;148(1):87-102. https://doi.org/10.1099/00221287-148-1-87

[38] Beigomi, M.; Biabangard, A.; Rohani, R. Evaluation of antimicrobial effects of Rosemary and *Withania somnifera* methanol extract prepared by ultrasound waveform on *Escherichia coli* biofilm isolated from urinary tract infection. *Micro Environer*, **2021**. *1*(2), 17-25. https://doi.org/10.54458/mev.v1i01.6670

[39] Lakhal, H.; Boudiar, T.; Kabouche, A.; Kabouche, Z.; Touzani, R.; Bruneau, C. New sesquiterpene lactone and other constituents from *Centaurea sulphurea* (Asteraceae). *Nat. Prod. Commun.* **2010**, *5*, 10.1177/1934578X1000500603 .

[40] Kitouni, R.; Benayache, F.; Benayache, S. Flavonoids of the exudate of *Centaurea calcitrapa*. *Chem. Nat. Compd.* **2015**, *51*, 762-763. 10.1007/s10600-015-1404-7.
[41] Grafakou, M.E.; Djeddi, S.; Tarek, H.; Skaltsa, H. Secondary metabolites from the aerial parts of *Centaurea papposa* (Coss.) Greuter. *Biochem. Syst. Ecol.* **2018**, *76*, 15-22. 10.1016/j.bse.2017.11.005.
[42] Fernández, I.; Pedro, J.; Polo, E. Sesquiterpene lactones from *Centaurea alba* and *C. conifera*. *Phytochemistry.* **1995**, *38*, 655-657. 10.1016/0031-9422 (94)00688-P.
[43] Saroglou, V.; Karioti, A.; Demetzos, C.; Dimas, K.; Skaltsa, H. Sesquiterpene Lactones from *Centaurea spinosa* and their antibacterial and cytotoxic activities*. J.Nat. Prod.* **2005**, *68*, 1404-1407. 10.1021/np058042u.
[44] Djeddi, S.; Karioti, A.; Sokovic, M.; Koukoulitsa, C.; Skaltsa, H. A novel sesquiterpene lactone from *Centaurea pullata*: Structure elucidation, antimicrobial activity, and prediction of pharmacokinetic properties. *Bioor. Med Chem.* **2008**, *16*, 3725-3731. 10.1016/j.bmc.2008.01.056
[45] Porter, T.H.; Mabry, T.J.; Yoshioka, H.; Fischer, N.H. The isolation and structure determination of artemisiifolin, a new germacranolide from *Ambrosia artemisiifolia* L. (compositae). *Phytochemistry.***1970**, *9*, 199–204. 10.1016/s0031-9422(00)86630-3.
[46] Ayad, R.; Ababsa, Z. E.; Belfadel, F. Z.; Akkal, S.; León, F.; Brouard, I.; Medjroubi, K. Phytochemical and biological activity of Algerian *Centaurea melitensis. Int. J. Med. Arom. Plants* **2012**, *2*, 151-154.
[47] Salazar-Gómez, A.; Ontiveros-Rodríguez, J.C.; Pablo-Pérez, S.S.; Vargas-Díaz, M.E.; Garduño-Siciliano, L. The potential role of sesquiterpene lactones isolated from medicinal plants in the treatment of the metabolic syndrome - A review. *S. Afr. J. Bot.* **2020**, *135*, 240–251. 10.1016/j.sajb.2020.08.020.
[48] Schmidt, T.J.; Heilmann, J. Quantitative structure-cytotoxicity relationships of sesquiterpene lactones derived from partial charge (Q)-based fractional Accessible Surface Area Descriptors (Q_frASAs). *QSAR.* **2002**, *21*, 276-287. 10.1002/1521-3838(200208)21:3<276::AID-QSAR276>3.0.CO;2-S.

# CHAPTER 4

# Bio-guided Purification and Identification of Active Metabolites From *Ephedra foeminea*

Shurooq Ismail
Department of Chemical Sciences, PhD in Biotechnology
University of Naples Federico II

# Bio-guided Purification and Identification of Active Metabolites from *Ephedra foeminea*

## 1. Introduction

Humans have always used plants as a natural source for food, animal feeds and as a medical option to treat several diseases [1]. Indeed, conventional medicinal plants were reported to contain compounds with antimicrobial, antifungal, anti-inflammatory, antiviral, and anticancer properties [2]. Among compounds responsible for these interesting and promising bioactivities, an important role is played by essential oils and other secondary metabolites, including alkaloids, terpenoids, tannins and flavonoids [2,3]. Several plants' secondary metabolites were found to have antimicrobial properties exerted through different mechanisms of action, such as the ability to form complexes with extracellular and soluble proteins, thus sequestering them, or with membrane proteins of targeted microbes, thus determining a perturbation of membrane organization. Some secondary metabolites were also reported to cause membrane disruption and bacterial enzymes inhibition [4-7]. The abundance and bioactivities of these compounds may greatly vary depending on plant species and environmental conditions. Traditional herbal medicine is gaining great attention in developing countries due to the strong demand for natural compounds able to exert therapeutic effects in the absence of harmful side effects. However, it has to be highlighted that only a small percentage (1-10%) of available plant species is used by humans [8,9]. Furthermore, in many cases, chemical composition of used plants has not been deeply characterized [3].

Plants belonging to *Ephedra* genera falling in the Ephedraceae family represent a group of perennial gymnosperms distributed in aired and semiarid regions all over the world [10-13]. Palestine is characterized by the presence of a wide variety of vegetation. Probably because of this, the practice of complementary and alternative medicine is very common [14] even if it is not clear whether these practices are supported by plants effective pharmacological properties or if they are merely based on folklore [15]. In this scenario, researchers focused their efforts to search for novel effective drugs and to identify them starting from still unexplored folk medicinal wild plants [16]. *Ephedra* plants are widely grown also in Palestine; the presence of five species was recorded, such as *E. foeminea*, *E. alata*, *E. aphyla*, *E. ciliata* and *E. fragilis* [17]. Alanda (*Ephedra foeminea* or *Ephedra campylopoda*) is the Arabic name for a low stalky Eurasian shrub from the *Ephedraceae*

family, present in northern Palestine and across the southeastern Mediterranean. In Oriental Arab medicine, it is used to treat agitation and skin rash. Moreover, the aerial parts of various *Ephedra* species were proved to contain active alkaloids, such as phenylpropylamino, alkaloids, ephedrine, and pseudoephedrine [18]. The phytochemical analysis of the aqueous, methanolic and ethanolic extracts of *E. foeminea* revealed the presence of different phytoconstituents. It was revealed that the methanolic extract contains (i) high levels of phenols, carbohydrates, sterols/steroids, flavones and lignin; (ii) moderate levels of tannins, quinones, amino acids, cardiac glycosides, and phlobatannins; (iii) low levels of resins, terpenoids, flavonoids, coumarins, reducing sugars, and anthocyanins; and (iv) the absence of alkaloids, saponins, anthraquinones, and fixed oils and lipids [19]. It is reported as well in other *Ephedra* species the high content of alkaloids namely ephedrine and pseudoephedrine, which are known process several pharmaceutical properties, which are able to increase the heartbeat rate, the blood pressure, to promote bronchodilatation and to affect the central nervous system [20].

Because of their diverse content of compounds, plants from *Ephedra* genera were widely used throughout the history of humankind. They were employed as an ointment to improve wound healing or to treat bronchial asthma, chills, colds, coughs, edema, fever, allergies, syphilis, and gonorrhea [21]. *Ephedra* extracts were even used as food supplement to enhance performance and weight loss until 2004 when they were banned by Food and Drug Administration (FDA) because of several death events due to negative effects on cardiac and cardiovascular systems [22]. In a more recent study, the ethanolic extract of *E. foeminea* was found to exert anticancer properties [23]. However, while the alkaloid content of *Ephedra* species was widely descripted, only a few papers focused on the non-alkaloid content. Based on this, it appears promising to investigate the biological activities of these still unexplored secondary metabolites that might represent a source of novel compounds with interesting bioactivities.

Recently, the fast spread of multidrug resistant (MDR) microorganisms requires the urgent development of effective alternatives to conventional antibiotics [3]. In this context, plant-derived compounds might represent an interesting starting point for the future design of compounds and therapeutic strategies effective against MDR bacterial infections. To develop a combinatorial therapeutic strategy effective against MDR bacterial infections, synergistic effects between plant-derived bioactive compounds and antibiotics were reported by

several studies [24-28]. Among the available alternatives to conventional antibiotics, antimicrobial peptides (AMPs) attracted considerable attention, since they are naturally occurring peptides found in all organisms, including bacteria, fungi, plants, mammals, and human beings. They are key components of the innate immune system and were found to exert broad-spectrum antimicrobial activity, by being effective against Gram-positive bacteria, Gram-negative bacteria, fungi, parasites and even against enveloped viruses [29-31]. In recent years, a precious bioinformatics tool was developed by Pane *et al*. [32] to identify putative antimicrobial peptides (AMPs) within the sequences of human precursor proteins and to quantitatively predict their antimicrobial activity [32]. By using this approach, hundreds of potential HDPs were identified in human secreted proteins.

Promising effective AMPs were also identified in human apolipoprotein B. ApoB-derived peptides, 38 and 26 residues long, have been named r(P)ApoB$_L$ and r(P)ApoB$_S$, respectively. P refers to the presence of a Pro residue at the N-terminus of each peptide released upon acidic hydrolysis of an Asp-Pro bond, whereas L and S refer to a longer or a shorter version of the produced peptide. Peptides have been recombinantly produced in *E. coli* by using a cost-effective production procedure [33]. Produced peptides were found to be endowed with broad-spectrum antimicrobial activity, while being neither toxic nor hemolytic towards human and murine eukaryotic cells [33]. Furthermore, both ApoB-derived peptides were found to synergistically act in combination with conventional antibiotics or EDTA, thus opening interesting perspectives to their applicability in pharmaceutical and cosmeceutical fields [33]. ApoB-derived peptides were also found to exert significant anti-biofilm activity, being able to prevent biofilm formation, attachment and even to disrupt pre-existing biofilms. Significant anti-biofilm effects were also detected against bacterial strains not sensitive to peptides direct antimicrobial activity, such as methicillin resistant *S. aureus* [33]. Peptides were found as well to be effective in a mouse model of skin infection and to exert antifungal properties [34].

In this chapter, a bio-guided purification of *E. foeminea* extracts was performed to isolate bioactive compounds that were identified by nuclear magnetic resonance (NMR) spectroscopy and mass spectrometry (MS) analyses. Following this experimental strategy; a novel potent glycosylated falvonoide namely kaempferol-3-*O*-α-L-(2″,4″-di-*E*-*p*-coumaroyl)-rhamnopyranoside, particularly showed excpetional antibacterial and antibiofilm activities against *S.*

*aureus* bacterial strains. These intersting findings were followed by predicting the potential bacterial receptors to which the isolated compound might be interacted using molecular docing analyses. Futhermore, the the cytotoxic acitivity, as well as, the potential synergestitic effects were evaluted along with ApoB-derived antimicrobial peptides using check board assays to determine the fractional inhibitory concentrantion (FIC) index.

## 2. Methods

**2.1 Materials.** All the reagents were purchased from Sigma-Merck (Milan, Italy), unless specified otherwise. Optical rotations were measured on a Jasco P-1010 digital polarimeter (Tokyo, Japan); $^{1}H$ and $^{13}C$ nuclear magnetic resonance (NMR) spectra were recorded at 400 and 100 MHz, respectively, in $CDCl_3$, acetone-d6 and $CD_3OD$ on a Bruker spectrometer (Billerica, MA, USA). The same solvents were used as internal standards. DEPT, COSY-45, HSQC, HMBC, and NOESY experiments [35] were performed using Bruker microproGrams. Electrospray ionization mass spectra (ESIMS) were performed using the LC/MS TOF system AGILENT 6230B (Agilent Technologies, Milan, Italy). Analytical and preparative thin layer chromatography (TLC) were performed on silica gel plates (Kieselgel 60, F254, 0.25 and 0.5 mm respectively) or on reverse phase (Kieselgel 60 RP-18 F254, 0.20 mm). Plates and the compounds were visualized by exposure to UV light and/or iodine vapors and/or by spraying firstly with 10% $H_2SO_4$ in MeOH, and then with 5% phosphomolybdic acid in EtOH, followed by heating at 110°C for 10 min. Column chromatography (CC) was performed using silica gels (Merck, Kieselgel 60, 0.063-0.200 mm).

### 2.2 *Ephedra foeminea* Plant Collection and Identification.

The aerial parts of *E. foeminea* were collected from their natural habitat in West- Bank, Palestine during September 2020. Identification of the plant was carried out at the Department of Biology and Biotechnology, An-Najah National University in Palestine. Representative plant specimens were collected, pressed until drying, then chemically poisoned to prevent bacterial and fungal infections, and finally mounted on herbarium sheets, and provided with voucher number (ANUH1895). Subsequently they were deposited at An-Najah National University herbarium. *E. foeminea* collected aerial parts were washed with water, to remove soil and dust particles, and then dried. Exposure to light was avoided to prevent possible loss of effective metabolites. The dried aerial parts were finely powdered using a blender, in order to make them ready for subsequent extraction processes.

## 2.3 Plant Extract Preparation and Purification.

Plant material (700g) was extracted (1×2,000 mL) by ethanol/$H_2O$ (7/3, *v*/*v*) under stirring conditions at room temperature for 48 h. Afterwards, the sample was centrifuged at 7,000 rpm for 40 min. 10 mL of the supernatant were concentrated under reduced pressure, in order to evaporate the ethanol, and lyophilized to obtain 120 mg of ethanol extract. The rest of the supernatant was firstly extracted by hexane (3×800 mL), then with $CH_2Cl_2$ (3×800 mL), and, after removing ethanol under reduced pressure, with EtOAc (3×700 mL). Each kind of extract and the residual water phase were then tested for antimicrobial properties on 6 bacterial strains. Since hexane organic extract (280 g) displayed interesting antibacterial activity, it was purified by column chromatography (CC) and eluted with $CHCl_3$/*i*-PrOH (95/5, *v*/*v*), thus obtaining 8 homogeneous fractions (H1-H8). Among them, fraction H2 was found to retain antibiotic activity and was further purified by using different steps of CC and TLC (**Figure 1**). Briefly, H2 fraction (113.8 mg) was purified by CC and eluted with ethyl acetate/ hexane (40/60, *v*/*v*). The first obtained fraction (H2.1 in **Figure 1**) was further purified by two steps of TLC and eluted with $CHCl_3$/*i*-PrOH (98/2, *v*/*v*), to obtain 4 homogeneous fractions. Among these, fraction H2.1.C (10.42 mg) was further purified to obtain a pure oil identified as carvacrol (**compound 1**, 4.7 mg) and a pure amorphous solid identified as thymol (**compound 2**, 1.7 mg).

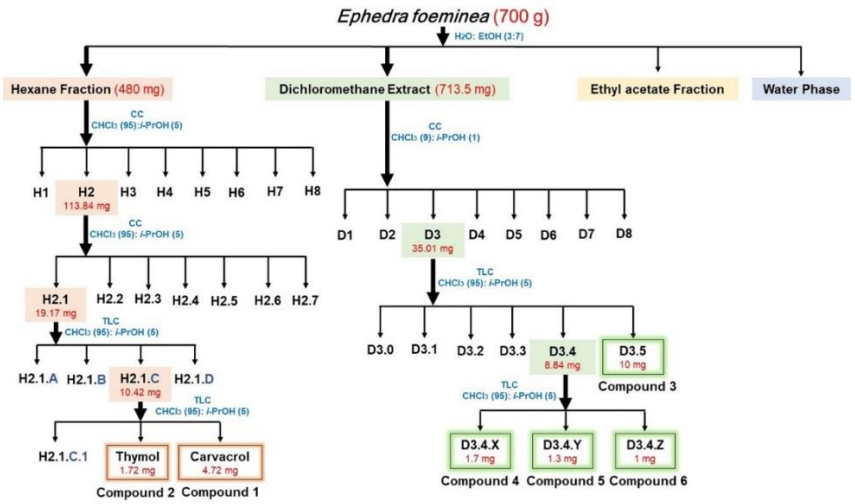


**Figure 1**. Schematic representation of the bio-guided fractionation of extracts obtained from *E. foeminea* aerial parts.

Organic extract obtained in $CH_2Cl_2$ (713.5 mg) was found to retain interesting antimicrobial properties and was purified by CC and eluted with $CH_2Cl_2$/*i*-PrOH (9/1,*v/v*), thus obtaining 8 homogeneous fractions (D1-D8) (**Figure 1**). Among them, fraction D3 (35.01 mg) was found to retain antibiotic activity and was further purified by using two steps of TLC (**Figure 1**). Briefly, fraction D3 was purified by TLC and eluted in $CHCl_3$/*i*-PrOH (9/1,*v/v*), thus obtaining 6 homogeneous fractions (**Figure 1**). Fraction D3.5 (10.06 mg) in **Figure 1** was found to be a pure yellow powder identified as kaempferol-3-*O*-*α*-L-(2”,4”-di-*E*-*p*-coumaroyl)-rhamnopyranoside (**compound 3**, 10.06 mg). Fraction D3.4 (8.84 mg) in **Figure 1** was further purified by TLC to obtain 3 pure amorphous solids, fractions D3.4.X, D3.4.Y and D3.4.Z in **Figure 1**. Fractions were analyzed by NMR and mass spectrometry and identified as kaempferol-3-*O*-*α*-L-(2”-*E*-*p*-coumaroyl,4”-*Z*-*p*-coumaroyl)-rhamnopyranoside (**compound 4**, 1.65 mg), kaempferol-3-*O*-*α*-L-(2”-*Z*-*p*-coumaroyl,4”-*E*-*p*-coumaroyl)- rhamnopyranoside (**compound 5**, 1.56 mg), and kaempferol-3-*O*-*α*-L-(2”,4”-di-*Z*-*p*-coumaroyl)-rhamnopyranoside (**compound 6**, 0.88 mg), respectively.

## 2.4 Bacterial Strains and Growth Conditions.

Six bacterial strains were used in the present study, *i.e., S. aureus* ATCC 29213, methicillin-resistant *S. aureus* MRSA WKZ-2, *E. faecalis* ATCC 29212, *A. baumannii* ATCC 17878, *E. coli* ATCC 25922 and *S. typhimurium* ATCC 14028. All bacterial strains were grown in Muller Hinton Broth (MHB; Becton Dickinson Difco, Franklin Lakes, NJ/ USA) and on Tryptic Soy Agar (TSA; Oxoid Ltd., Hampshire, UK). In all the experiments, bacteria were inoculated and grown overnight in MHB at 37 °C. The next day, bacteria were transferred to a fresh MHB tube and grown to mid-logarithmic phase.

## 2.5 Antimicrobial Activity.

The antimicrobial activity of *E. foeminea* extracts and its derived compounds were tested towards 6 bacterial strains, *i.e., S. aureus* ATCC 29213, methicillin-resistant *S. aureus* (MRSA WKZ-2), *E. faecalis* ATCC 29212, *A. baumannii* ATCC 17878, *E. coli* ATCC 25922 and *S. typhimurium* ATCC 14028 by using broth microdilution method [33][36]. Bacteria were grown to mid-logarithmic phase in MHB at 37°C and then diluted to $2x10^6$ CFU/mL in Nutrient Broth (NB, Difco, Becton Dickinson, Franklin 12 Lakes, NJ). To perform the assay, bacterial

samples were mixed (1:1,*v/v*) with two-fold serial dilutions of the compound under test and incubated for 20 h at 37°C. Following the incubation, each sample was diluted and plated on TSA, in order to count the number of colonies. All the experiments were carried out in three independent replicates. $MIC_{100}$ values were determined as the lowest compound concentration responsible for no visible bacterial growth after over-night incubation.

### 2.6 r(p)ApoB$_L^{Pro}$ Peptide Production.

Expression and isolation of the recombinant peptide r(p)ApoB$_L^{Pro}$ was carried out as previously described [33] with the only exception of the final gel-filtration step, that was added to remove salts used along the purification process and that tend to attach to the peptides [37].

### 2.7 Checkerboard Assay and determination of Fractional Inhibitory Concentration (FIC) Index.

Combinations of recombinant r(p)ApoB$_L^{Pro}$ peptide and the isolated compound kaempferol-3-O-α-L-(2″,4″-di-*E*-*p*-coumaroyl)-rhamnopyranoside (compound **3**) were tested on *S. aureus* ATCC 29213, *S. aureus* MRSA WKZ-2, *E. coli* ATCC 25922, and *A. baumannii* ATCC 17878 to evaluate if they act in synergism. Fractional Inhibitory Concentration (FIC) indexes were calculated by using the conventional "checkboard" assay. To achieve this purpose, two-fold serial dilutions of r(p)ApoB$_L^{Pro}$ peptide were tested in combination with two-fold serial dilutions of compound **3**. The FIC indexes were calculated based on equation (1).

$$\mathrm{FIC} = \mathrm{FIC\ (A)} + \mathrm{FIC\ (B)} \quad (1)$$

$$\mathrm{FIC\ (A)} = \frac{MIC_{100}\ of\ drug\ A\ in\ combination}{MIC_{100}\ of\ drug\ A\ alone} \quad (2)$$

$$\mathrm{FIC\ (B)} = \frac{MIC_{100}\ of\ drug\ B\ in\ combination}{MIC_{100}\ of\ drug\ B\ alone} \quad (3)$$

FIC indexes ≤ 0.5 were classified as synergism, FIC indexes between 0.5 and 1 were associated with additive effects, whereas FIC indexes between 1 and 4 were classified as indifferent effects [33].

## 2.8 Anti-biofilm Activity Assays.

To evaluate anti-biofilm effects, bacteria inocula were grown over-night at 37°C, then diluted to $1\times10^8$ CFU/mL in 0.5X MHB containing increasing concentrations of the compound under test. The samples were then incubated at 37°C for 24h, in order to test the effects on biofilm formation. In the case of crystal violet assay, bacterial biofilm was washed 3 times with phosphate buffer (PBS 1X) and then incubated with the dye (0.04%) for 20 min at room temperature. Following the incubation, samples were washed with PBS and then the dye bound to cells was dissolved in 33% acetic acid. Spectrophotometric measurements were then carried out at a wavelength of 630 nm by using a microtiter plate reader (FLUOstar Omega, BMG LABTECH, and Germany) [33][38]. Confocal laser scanning microscopy (CLSM) analyses in static conditions were carried out by using Thermo Scientific™ Nunc™ Lab-Tek™ Chambered Cover glass systems (Thermo Fisher Scientific, Waltham, MA, USA). The viability of the cells within the biofilm structure was evaluated by sample staining with LIVE/DEAD® Bacterial Viability kit (Molecular Probes Thermo Fisher Scientific, Waltham, MA, USA). Staining was performed accordingly to manufacturer instructions. Biofilm images were collected by using a confocal laser scanning microscope (Zeiss LSM 710, Zeiss, Germany) and a 63X objective oil-immersion system. Biofilm architecture was analyzed by using the Zen Lite 2.3 software package. Each experiment was performed in triplicate and all the images were taken under identical conditions [39].

## 2.9 Eukaryotic Cell Cultures and Biocompatibility Evaluation.

Immortalized human keratinocytes (HaCaT) and human dermal fibroblasts (HDF) were cultured in high-glucose Dulbecco's modified Eagle's medium (DMEM) supplemented with 10% fetal bovine serum (FBS), 1% antibiotics (Pen/strep) and 1% L-glutamine and grown at 37 °C in a humidified atmosphere containing 5% $CO_2$. To evaluate the biocompatibility of kaempferol-3-*O*-*α*-L-(2",4"-di-*E*-*p*-coumaroyl)-rhamnopyranoside, cells were seeded into 96-well plates at a density of $3\times10^3$ cells/well in 100 µL of complete DMEM 24h prior to the treatment. They were then incubated in the presence of increasing compound concentrations (0.5-5 $\mu g.mL^{-1}$) for 72h. Following the treatment, cell culture supernatants were replaced with 0.5 mg/mL MTT

(3-(4,5-dimethylthiazol-2-yl)-2,5-diphenyltetrazolium bromide) reagent dissolved in DMEM medium without red phenol (100 µL/well). After 4h of incubation at 37°C, the resulting insoluble formazan salts were solubilized in 0.01 N HCl in anhydrous isopropanol and quantified by measuring the absorbance at λ = 570 nm using an automatic plate reader spectrophotometer (Synergy™ H4 Hybrid Microplate Reader, BioTek Instruments, Inc., Winooski, Vermont, USA), as previously described. Cell survival was expressed as the mean of the percentage values compared to control untreated cells.

**2.10 Molecular Docking Analyses.**

The chemical structure of kaempferol-3-*O*-*α*-L-(2″,4″-di-*E*-*p*-coumaroyl)-rhamnopyranoside was prepared and used as a ligand in molecular docking analyses with the main aim to predict the ligand's binding affinity and possible chemical interactions with 2 putative interactors present in *S. aureus* cells, *i.e.*, sortase A (PDB ID-1T2P) and tyrosyl tRNA synthetase (TyRS) (PDB ID- 1JIL). To do this, the crystallographic 3D structures of the target enzymes were retrieved from protein data bank. The Autodock tool 1.5.6 was used to optimize the structures of the putative receptor and of the ligand. This was performed upon removal of water molecules and heteroatoms, and addition of polar hydrogens and Kollman charges. Molecular docking was performed by using CB Dock web server that represents an implementation of the popular docking proGram Autodock Vina [40]. The docked complexes were visualized to identify putative receptor-ligand interactions by using Discovery Studio (DS) Visualizer 2020 (Biovia, San Diego, USA). The binding affinity of the compound under test towards the targets was estimated based on intermolecular interactions and bonds' lengths (**Table 8**).

**2.11 Statistical Analyses.** Statistical analyses were performed by using Student's t-Test. Significant differences were indicated as *($P < 0.05$), **($P < 0.01$), ***($P < 0.001$) or **** ($P < 0.0001$). Graphs were obtained by using GraphPad Prism 8 software.

# 3. Results

## 3.1 Antimicrobial and anti-biofilm activity of *E. foeminea* extracts.

*E. foeminea* ethanolic extract was firstly investigated for its antibacterial activity towards three Gram-positive (*S. aureus* ATCC 29213, *S. aureus* MRSA WKZ-2, *E. faecalis* ATCC 29212) and three Gram-negative (*A. baumannii* ATCC 17878, *E. coli* ATCC 25922 and *S. typhimurium* ATCC 14028) bacterial strains. The ethanolic extract was found to exert strong antimicrobial properties towards 3 out of 6 bacterial strains tested, with $MIC_{100}$ values ranging between 1.25 to 2.5 mg/mL **(Table 1).**

**Table 1.** $MIC_{100}$ values (mg/mL) determined for *E. foeminea* ethanolic, hexane, dichloromethane and ethyl acetate extracts tested on a panel of Gram-positive and Gram-negative bacterial strains. (-) indicates not tested samples. Reported data refer to three biological replicates.

| | **$MIC_{100}$ (mg/mL)** | | | |
|---|---|---|---|---|
| **Gram-positive strains** | **Ethanol** | **Hexane** | **$CH_2Cl_2$** | **EtOAc** |
| *S. aureus* ATCC 29213 | 2.5 | 0.625 | 1.25 | 2.5 |
| *S. aureus* MRSA WKZ-2 | 10 | - | - | - |
| *E. faecalis* ATCC 29212 | 10 | - | - | - |
| **Gram-negative strains** | | | | |
| *E. coli* ATCC 25922 | 1.25 | 2.5 | 2.5 | 2.5 |
| *S. typhimurium* ATCC 14028 | 2.5 | 1.25 | 2.5 | 2.5 |
| *A. baumannii* ATCC 17878 | 5 | - | - | - |

Considering its effectiveness on both Gram-negative and Gram-positive bacterial strains, ethanolic extract was found to have a broad-spectrum antimicrobial activity **(Table 1)**. Interestingly, significant antimicrobial effects were also detected on *S. aureus* MRSA WKZ-2, *E. faecalis* ATCC 29212, and *A. baumannii* ATCC 17878 bacterial strains, even if higher doses of the extract ($MIC_{100}$ values comprised between 5 and 10 mg/mL) were required to obtain the same effects recorded on the other tested strains **(Table 1)**. To identify compounds responsible for detected effects, further extraction procedures were sequentially performed as detailed in Materials and Methods Section. In particular, three solvents characterized by a different polarity, namely (i) hexane, (ii) dichloromethane, and (iii) ethyl acetate were used. The antibacterial activity of each obtained fraction was investigated on the same bacterial strains described above and it was found that hexane,

dichloromethane, and ethyl acetate extracts were able to exert antimicrobial activity on 3 out of 6 bacterial strains tested with $MIC_{100}$ values comprised between 0.625 and 2.5 mg/mL **(Table 1)**.

The results mentioned above suggested that the extracts retained a significant broad-spectrum antimicrobial activity by being effective on both Gram-negative and Gram-positive bacterial strains **(Table 1)**. In the case of water phase, no significant antimicrobial activity was detected on any of the tested strains. Based on this, it can be hypothesized that most of the compounds responsible for the antibacterial activity were extracted using the organic solvents. The anti-biofilm properties of the extracts were also evaluated by performing crystal violet assays. Interestingly, ethanolic, hexane, dichloromethane, and ethyl acetate extracts were found to exert anti-biofilm properties, by affecting the biofilm formation in the case of *S. typhimurium* ATCC 14028 **(Figure 2a).** No significant anti-biofilm properties were detected for the water phase **(Figure 2a)**. Ethanolic extract was also tested on *S. aureus* MRSA WKZ-2, *E. faecalis* ATCC 29212 and *A. baumannii* ATCC 17878 and was found to be effective on these strains with a significant inhibition of biofilm formation (about 50-70% inhibition) in the case of *A. baumannii* ATCC 17878 and *S. aureus* MRSA WKZ-2 **(Figure 2b).**

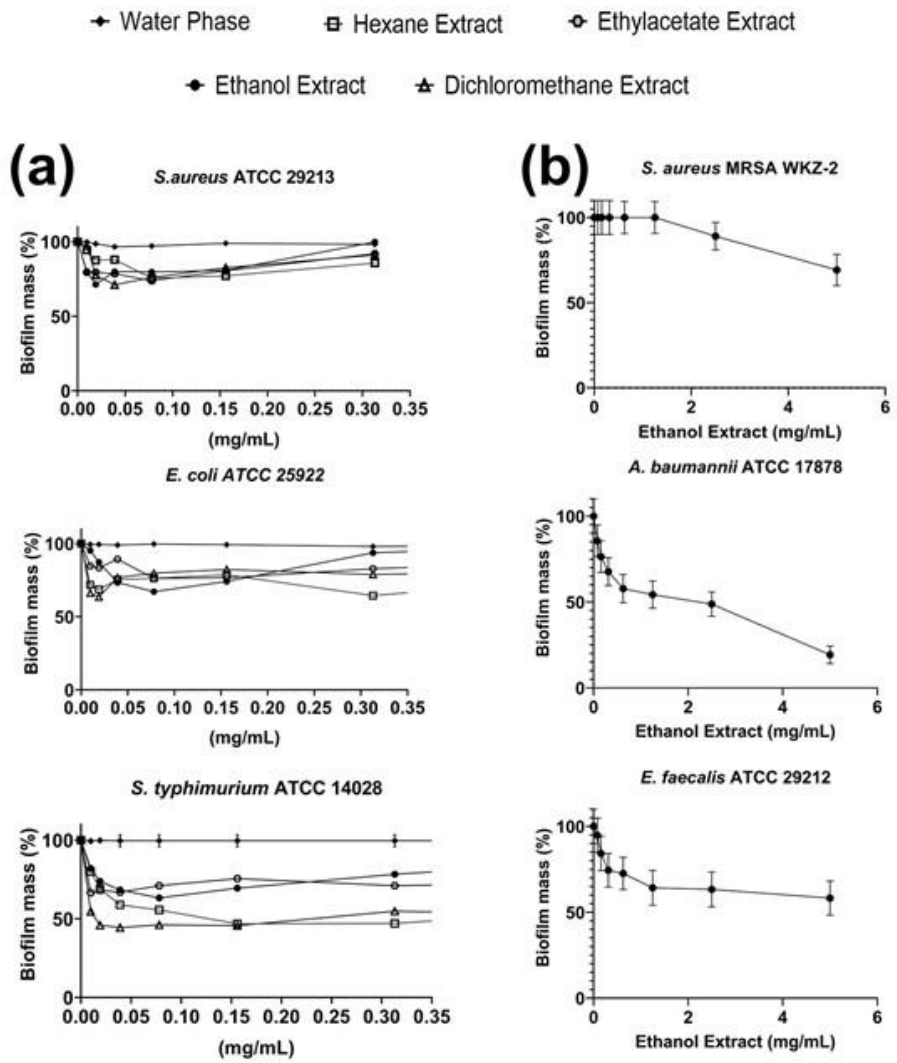


**Figure 2.** Anti-biofilm activity of *E. foeminea* plant extracts on *S. aureus* ATCC 29213, *S. aureus* MRSA WKZ-2, *E. faecalis* ATCC 29212, *A. baumannii* ATCC 17878, *E. coli* ATCC 25922, and *S. typhimurium* ATCC 14028. (a) Extracts obtained in ethanol, hexane, dichloromethane, ethyl acetate, or water phase were tested against *S. aureus* ATCC 29213, *E. coli* ATCC 25922, and *S. typhimurium* ATCC 14028. (b) Ethanolic extract was tested against *A. baumannii* ATCC 17878, *E. faecalis* ATCC 29212, and *S. aureus* MRSA WKZ-2. The effects of increasing concentrations of each extract were evaluated on biofilm formation. At the end of the incubations, biofilm samples were stained with crystal violet and measured at 630 nm. Data represent the mean (±standard deviation, SD) of at least three independent experiments, each one carried out with triplicate determinations.

### 3.2 Bio-guided fractionation of plant extracts followed by isolation and identification of active compounds

To isolate the bioactive compounds exerted antibacterial and/or anti-biofilm activities, the most promising extracts (hexane and dichloromethane extracts) obtained from *E. foeminea* were subjected to sequential purification steps by TLC or CC as reported in the Materials and Methods Section and in **(Figure 1)**. Fractions obtained upon extraction in hexane and two sequential steps of CC were found to be endowed with antimicrobial activity **(Table 2)**.

**Table 2**. $MIC_{100}$ values (mg/mL) determined for fractions obtained upon extraction in hexane and two sequential steps of column chromatography.

| | **$MIC_{100}$ (mg/mL) of fractions extracted in hexane** | | | | | | |
|---|---|---|---|---|---|---|---|
| **Bacterial strains** | **1** | **2** | **3** | **4** | **5** | **6** | **7** |
| *S. aureus* ATCC 29213 | 2.5 | 2.5 | 2.5 | 0.313 | 0.313 | 2.5 | 1.25 |
| *E. coli* ATCC 25922 | 2.5 | 2.5 | 2.5 | 2.5 | 2.5 | 2.5 | 2.5 |
| *S. typhimurium* ATCC 14028 | 2.5 | 2.5 | 2.5 | 2.5 | 2.5 | 2.5 | 2.5 |

Two main compounds were isolated from hexane extract and identified as carvacrol (compound **1**, 4.72 mg), and as thymol (compound **2**, 1.72 mg) (**Figure 3**) comparing their spectroscopic data ($^1$H NMR and ESI MS) with those reported in the literature (**Appendix A2. Figures S1 and S2**). It is noteworthy, that no data in the literature exist about the presence of these two compounds in *E. foeminea* [21].

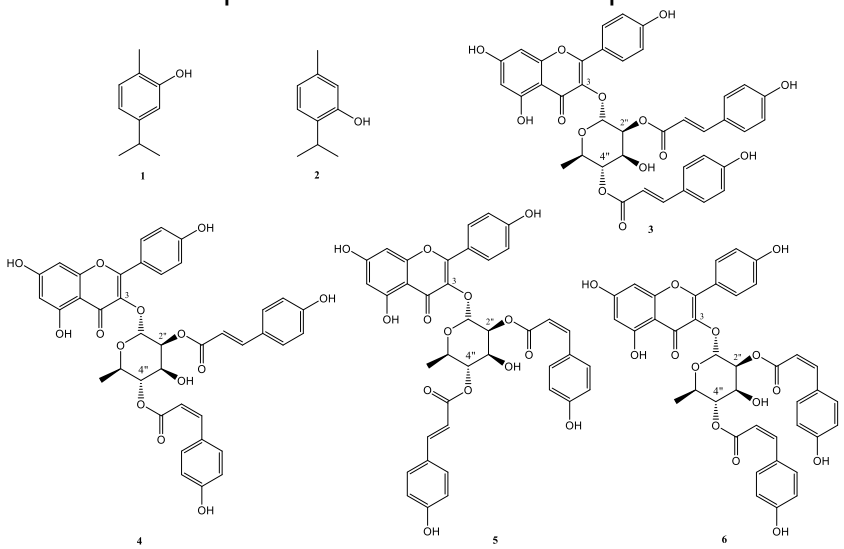

**Figure 3.** Chemical structures of isolated compounds **1-6.**

The active compounds from $CH_2Cl_2$ extract were fractionated by combined CC and TLC on direct and reverse phase to obtain four pure metabolites as reported in detail in the Materials and Methods Section. The first investigation of their $^1$H NMR spectra showed the signals of flavonol glycosides. In particular, $^1$H NMR spectrum of compound **3** was recorded in acetone-$d_6$ [41] and in $CD_3OD$ [42] (**Appendix A2. Figures S3-S13**). In acetone-$d_6$, two broad signals at δ 6.28 (H-6) and 6.48 (H-8) were detected and the two doublets $A_2X_2$ aromatic system protons at δ 7.13 (H-3',5') and 7.91 (H-2',6'), $J$ = 8.7 Hz, typical of a kaempferol residue. The presence of the anomeric proton at δ 5.83 (H-1'', brs), the methane protons at δ 5.62 (H-2, brs), 4.20 (H-3, dd, $J$ = 9.7 and 3.0 Hz), 4.98 (H-4, t, $J$ = 9.7 Hz), 3.39 (dd, $J$ = 9.7 and 6.1 Hz), and the secondary methyl group at δ 0.86 (H-6, d, $J$ = 6.1 Hz) suggested the presence of an α-rhamnopyranoside moiety substituted in position H-2'' and H-4'' by two *p*-coumaroyl residues as observed from their typical signals. In particular, the signals of the double bonds H-2''' and H-3''' at δ 6.44 and 7.68 ($J$ = 16.0 Hz) and H-2'''' and H-3'''' at δ 6.31 and 7.56 ($J$ = 16.1 Hz) revealed the presence of two *E*-configured double bounds. COSY spectrum (**Appendix A2. Figures S7-S8**) confirmed the connections around the rhamnopyranoside and the positions of the *p*-coumaroyl residues at H-2'' and H-4''of the sugar residue for the downfield shifts showed by these protons. By extensive study of 2D $^{13}$C NMR spectra (HSQC and HMBC), the chemical shifts were assigned to all the carbons and protons (**Appendix A2. Figures S10-S13**). By this way, compound **3** has been identified as kaempferol-3-*O*-α-L-(2",4"-di-*E*-*p*-coumaroyl)-rhamnopyranoside as previously reported [41-44]. The identification was also supported by the data collected by ESI MS spectrum which showed the protonated $[M + H]^+$ ion at *m/z* 725.

Compounds **4**-**6** showed similar 1D and 2D $^1$H and $^{13}$C NMR spectra indicating that they differ from compound **3** for the configuration of the double bonds on the two *p*-coumaroyl residues (**Appendix A2. Figures S14-S24**). In particular, the $^1$H NMR spectrum of compound **4** differed from that of compound **3** for the signals of the double bonds H-2''' and H-3''' at δ 6.45 and 7.70 ($J$ = 15.9 Hz) and H-2'''' and H-3'''' at δ 5.78 and 6.92 ($J$ = 10.0 Hz), thus suggesting the presence of *trans*- and *cis*-*p*-coumaroyl moieties. Compound **4** was identified as kaempferol-3-*O*-α-L-(2"-*E*-*p*-coumaroyl,4"-*Z*-*p*-coumaroyl)-rhamnopyranoside as previously reported [45]. The $^1$H NMR spectrum of compound **5** differed from that of compound **3** for the signals of the double bonds H-2''' and H-3''' at δ 5.88 and 6.93 ($J$ = 11.8 Hz) and H-2'''' and H-3'''' at δ 6.33 and 7.59 ($J$ = 16.0 Hz), thus suggesting the

presence of *trans*- and *cis*-*p*-coumaroyl moieties. Therefore, compound **5** was identified as kaempferol-3-*O*-α-L-(2”-*Z*-*p*-coumaroyl,4”-*E*-*p*-coumaroyl)-rhamnopyranoside as previously reported [43]. Compound **6** was, instead, identified as kaempferol-3-*O*-α-L-(2”,4”-di-*Z*-*p*-coumaroyl)-rhamnopyranoside. In fact, its $^{1}$H NMR spectrum differed from that of compound **3** for the signals of the double bonds H-2’’’ and H-3’’’ at δ 5.77 and 6.87 (*J* = 12.0 Hz) and H-2’’’’ and H-3’’’’ at δ 5.89 and 6.92 (*J* = 12.0 Hz). By extensive use of 1D and 2D $^{1}$H and $^{13}$C NMR spectra, the chemical shifts were assigned to all the carbons and protons of compounds **4**-**6** (**Appendix A2. Figures S14-S24**).

### 3.3 Evaluation of the antimicrobial activity of isolated compounds (1-6).

Assays were performed by testing increasing concentrations of each isolated compound on *S. aureus* ATCC 29213, *S. aureus* MRSA WKZ-2, *E. faecalis* ATCC 29212, *A. baumannii* ATCC 17878, *E. coli* ATCC 25922, and *S. typhimurium* ATCC 14028. As shown in **Table 3**.

**Table 3**. $MIC_{100}$ values (µg/mL) determined for carvacrol and thymol purified from *E. foeminea* hexane extract.

| | **$MIC_{100}$ (µg/mL)** | |
|---|---|---|
| **Gram-positive strains** | **Carvacrol** | **Thymol** |
| *S. aureus* ATCC 29213 | 100 | 600 |
| *S. aureus* MRSA WKZ-2 | 50 | 2,400 |
| *E. faecalis* ATCC 29212 | 100 | 1,200 |
| **Gram-negative Strains** | | |
| *E. coli* ATCC 25922 | 200 | 600 |
| *S. typhimurium* ATCC 14028 | 100 | 300 |
| *A. baumannii* ATCC 17878 | 100 | 1,200 |

Carvacrol was found to be active on all the strains tested. The strongest effects were observed on *S. aureus* ATCC 29213 and *S. aureus* MRSA WKZ-2, with $MIC_{100}$ values of 100 and 50 µg/mL, respectively (**Table 3**). *E. coli* bacterial strain was found to be the least sensitive to carvacrol antimicrobial activity, with $MIC_{100}$ value of 200 µg/mL (**Table 3**). In the case of thymol, higher $MIC_{100}$ values were detected with respect to carvacrol on the same tested bacterial strains, meanwhile *S. typhimurium* ATCC 14028 was found to be the most susceptible bacterial strain ($MIC_{100}$ = 300 µg/mL) and *S. aureus* MRSA

WKZ-2 was found to be the least sensitive to thymol antimicrobial effects ($MIC_{100}$ = 2,400 µg/mL) (**Table 3**).

The antimicrobial activity was also tested for the other isolated compound **3** on *S. aureus* ATCC 29213, *S. aureus* MRSA WKZ-2, *E. faecalis* ATCC 29212, *E. coli* ATCC 25922, *S. typhimurium* ATCC 14028, and *A. baumannii* ATCC 17878. A very strong antimicrobial activity towards Gram-positive *S. aureus* ATCC 29213 and *S. aureus* MRSA WKZ-2 was found. $MIC_{100}$ values were found to be as low as 0.49 µg/mL in the case of both bacterial strains (**Table 4**).

**Table 4.** $MIC_{100}$ values (µg/mL) determined for compound **3** purified from *E. foeminea* dichloromethane extract.

| | **$MIC_{100}$ (µg/mL)** | |
|---|---|---|
| **Gram-positive strains** | **Compound 3** | **Gentamycin** |
| *S. aureus* ATCC 29213 | 0.49 | ≤ 1 |
| *S. aureus* MRSA WKZ-2 | 0.49 | ≤ 1 |
| *E. faecalis* ATCC 29212 | 500 | ≤ 8 |
| **Gram-negative strains** | | |
| *E. coli* ATCC 25922 | 250 | ≤ 4 |
| *S. typhimurium* ATCC 14028 | 1,000 | ≤ 15 |
| *A. baumannii* ATCC 17878 | 1,000 | ≤ 2 |

Higher $MIC_{100}$ values were detected in the case of the other bacterial strains tested with values comprised between 250 and 1,000 µg/mL (**Table 4 and Table 5**). It is worth noting that compound **3** was the only isomer to be endowed with this strong antimicrobial activity on *S. aureus* strains. Indeed, the other tested isomers (compounds **4**-**6**) were found to exert antimicrobial properties with $MIC_{100}$ values higher than 1,000 µg/mL when tested on *S. aureus* MRSA WKZ-2 (**Table 5**).

**Table 5.** $MIC_{100}$ values (µg/mL) determined for the compounds **3-6** purified from *E. foeminea* dichloromethane extract.

| | **$MIC_{100}$ (µg/mL)** | |
|---|---|---|
| | ***S. aureus* MRSA WKZ-2** | ***A. baumannii* ATCC 17878** |
| kaempferol-3-*O*-α-L-(2",4"-di-*E*-*p*-coumaroyl)-rhamnopyranoside | 0.49 | 1,000 |
| kaempferol-3-*O*-α-L-(2"-*Z*-*p*-coumaryl,4"-di-*E*-*p*-coumaryl rhamnopyranoside | >1,000 $MIC_{95}$ = 1,000 | 1,000 |
| kaempferol-3-*O*-α-L-(2"-*E*- *p*-coumaryl,4"-di-*Z*-*p*-coumaryl)-rhamnopyranoside | >1,000 $MIC_{98}$ = 1,000 | 1,000 |
| kaempferol-3-*O*-α-L-(2",4"-di-*Z*-*p*-coumaryl)-rhamnopyranoside | >1,000 $MIC_{98}$ = 1,000 | 1,000 |

### 3.4 Evaluation of the anti-biofilm activity of compound 3.

The anti-biofilm properties of the purified compound **3** were also evaluated by performing crystal violet assays on *S. aureus* ATCC 29213, *S. aureus* MRSA WKZ-2, *E. faecalis* ATCC 29212, *A. baumannii* ATCC 17878, *E. coli* ATCC 25922, and *S. typhimurium* ATCC 14028 bacterial strains incubated with increasing concentrations of the isolated compound. In all the cases, a significant inhibition (about 30-80%) of biofilm formation was observed, with the strongest effects obtained in the case of *A. baumannii* ATCC 17878 and *S. aureus* MRSA WKZ-2 bacterial strains (**Figure 4**). It is noteworthy, that significant effects on biofilm formation were obtained at concentrations significantly lower than $MIC_{100}$ values detected on the same bacterial strains. To deepen on compound **3** anti-biofilm activity, Confocal Laser Scanning Microscopy (CLSM) analyses were also performed. Firstly, *E. foeminea* crude ethanolic extract was analyzed for its effects on the formation of *S. aureus* MRSA WKZ-2, and *A. baumannii* ATCC 17878 biofilms. As it was observed in **Figure 5**, significant effects on biofilm architecture and thickness were evaluated upon treatment of both bacterial strains with the ethanolic extract for 24h. When pure compound **3** was analyzed on the same bacterial strains, significant effects on biofilm architecture and thickness were also evaluated (**Figure 6**). Furthermore, when the pure compound **3** was tested on *A.*

*baumannii* ATCC 17878 biofilm, changes in the biofilm morphology were found to be associated with a strong aggregation of bacterial cells that appeared to form groove-like structures (**Figure 6a**). Furthermore, filamentous structures (**Figure 6b**) were observed; they indicated an interference with cell division, which is probably due to a septation block, as previously reported for different anti-biofilm compounds [46].

A significant decrease of cell density also appeared clear upon treatment with the pure compound (**Figure 6**), which was an indication of a high percentage of cell death. When the anti-biofilm activity of the isomers, *i.e.*, compounds **4-6**, was analyzed, different results were obtained. Moreover, CLSM analyses were performed to test isomers effects on *S. aureus* MRSA WKZ-2, and *A. baumannii* ATCC 17878 biofilm formation. In the case of compound **5**, a slight effect on biofilm thickness was evaluated on *A. baumannii* ATCC 17878 upon 24h of incubation (**Figure 7**), whereas no significant effects were detected on *S. aureus* MRSA WKZ-2 (**Figure 8**). A similar result was obtained also in the case of the isomer compound **4** (**Figure 7**), whereas no significant effects on both bacterial strains were detected in the case of isomer compound **6** (**Figure 9**).

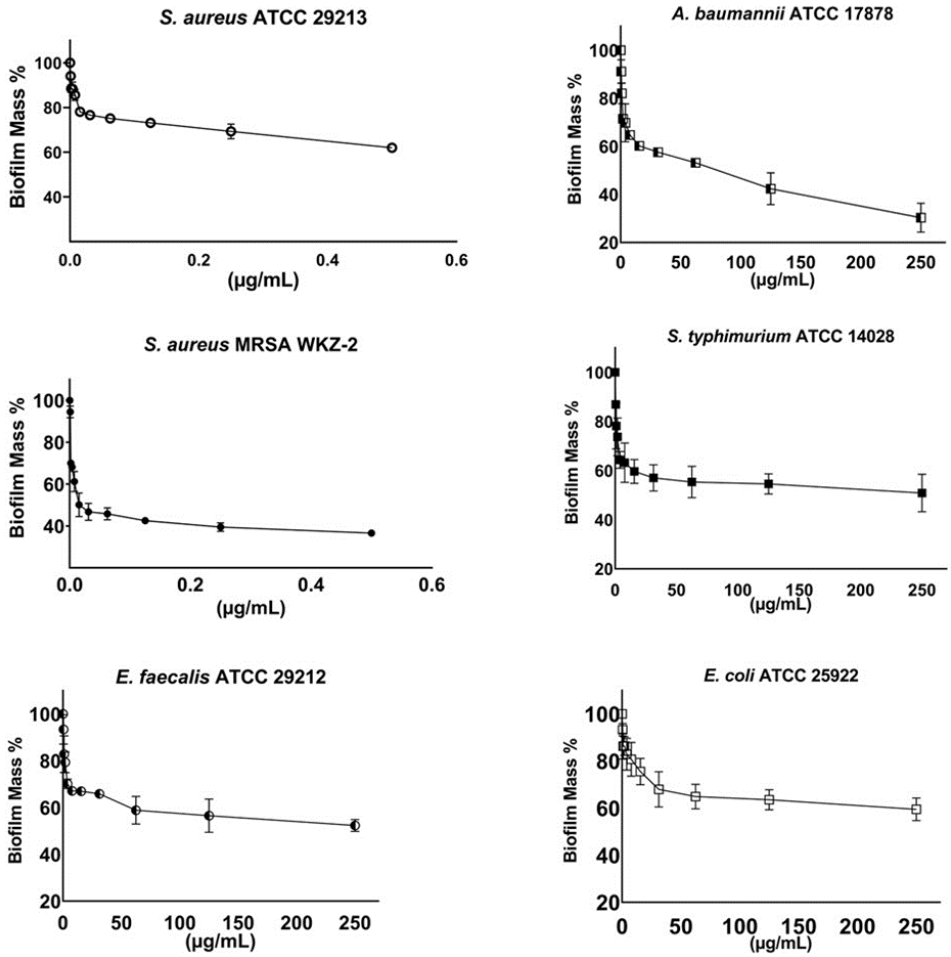


**Figure 4.** Anti-biofilm activity of kaempferol-3-*O*-α-L-(2",4"-di-*E*-*p*-coumaroyl)-rhamnopyranoside (compound **3**) was evaluated by crystal violet assays on *S. aureus* ATCC 29213, *S. aureus* MRSA WKZ-2, *E. faecalis* ATCC 29212, *A. baumannii* ATCC 17878, *S. typhimurium* ATCC 14028, and *E. coli* ATCC 25922. The effects of increasing concentrations of the compound were evaluated on biofilm formation. Biofilms were stained with crystal violet and samples were analyzed by using a plate reader to measure absorbance at 630 nm. Data represents the mean (±standard deviation, SD) of at least three independent experiments, each one carried out with triplicate determinations.

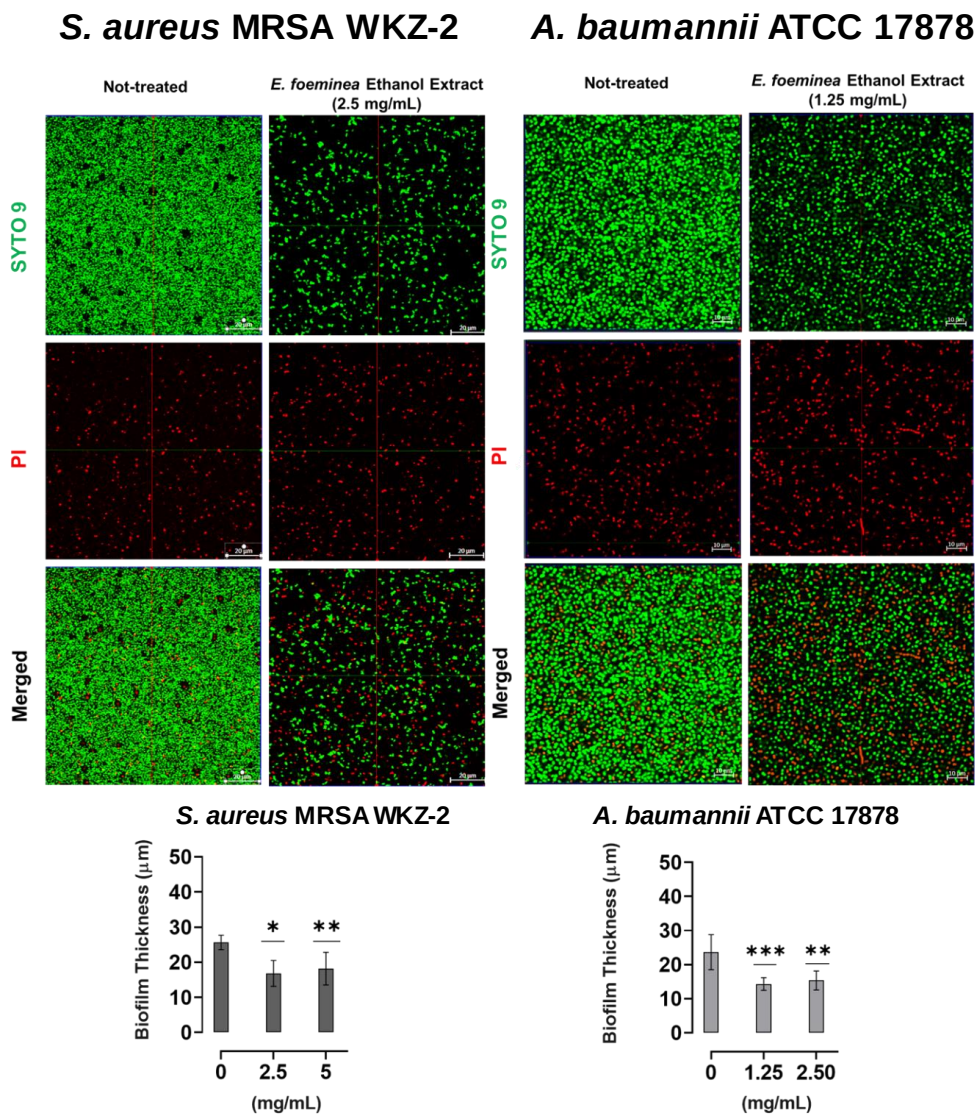


**Figure 5.** Anti-biofilm activity of *E. foeminea* ethanolic extract. Effects of *E. foeminea* ethanolic extract were evaluated on biofilm formation in the case of *S. aureus* MRSA WKZ-2, and *A. baumannii* ATCC 17878 by CLSM. Biofilm cells were stained with LIVE/DEAD BacLight bacterial viability kit (Molecular Probes, Eugene, OR) containing a 1:1 mol/mol ratio of SYTO-9 (green fluorescence, all cells) and propidium iodide (PI; red fluorescence, dead cells). The biofilm images were obtained by confocal z-stack using Zen Lite 2.3 software. All the images were taken under identical conditions. Significant differences were indicated as (*P< 0.05), (**P< 0.001) or (***P< 0.0001) for treated samples *versus* control ones. Each experiment was carried out in triplicate.

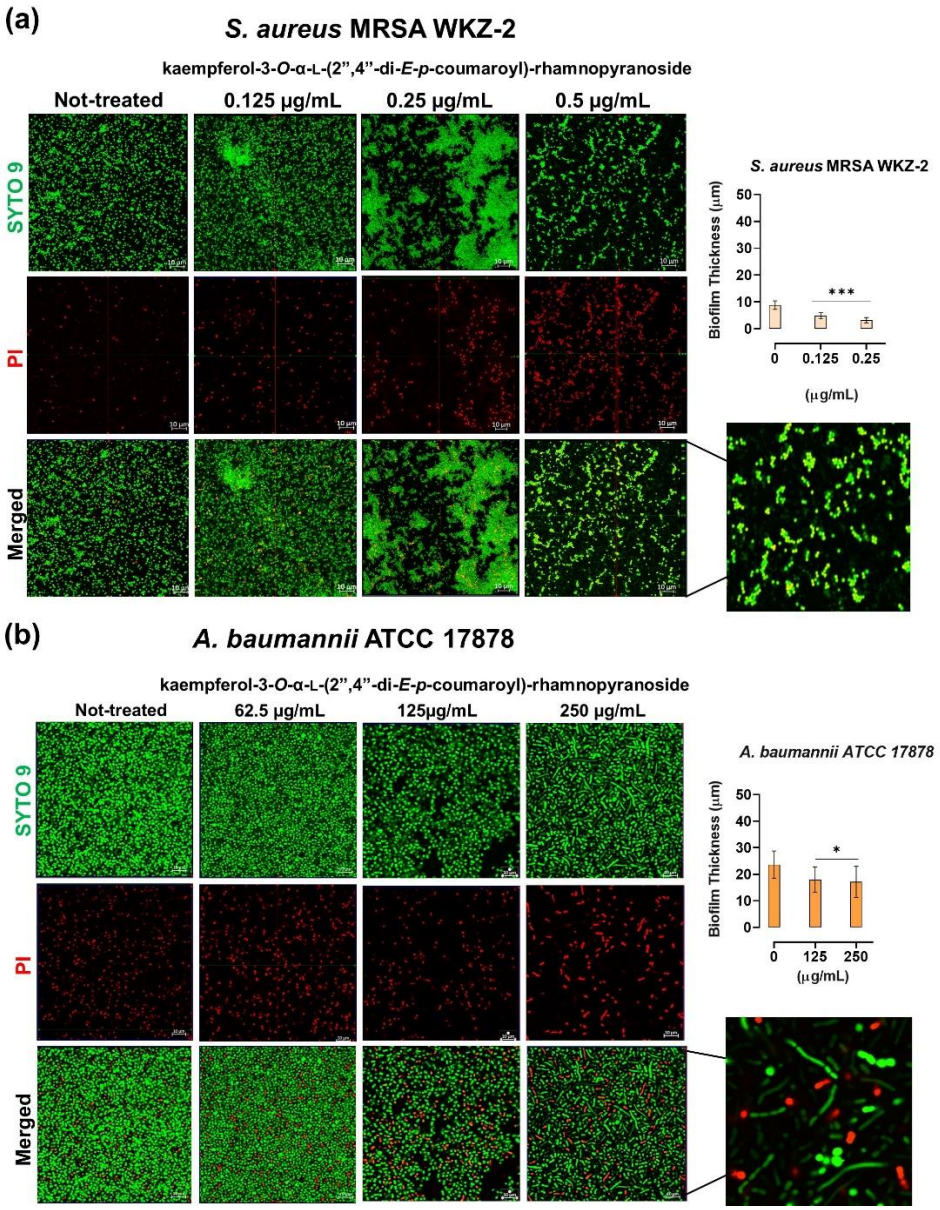


**Figure 6**. Anti-biofilm activity of purified kaempferol-3-*O*-α-L-(2",4"-di-*E*-*p*-coumaroyl)-rhamnopyranoside (compound **3**). Effects of compound **3** were evaluated on biofilm formation in the case of *S. aureus* MRSA WKZ-2 (a), and *A. baumannii* ATCC 17878 (b) by CLSM. Biofilm cells were stained with LIVE/DEAD BacLight bacterial viability kit (Molecular Probes, Eugene, OR) containing a 1:1 mol/mol ratio of SYTO-9 (green fluorescence, all cells) and propidium iodide (PI; red fluorescence, dead cells). Biofilm images were obtained by confocal z-stack using Zen Lite 2.3 software. All the images were taken under identical conditions. Significant differences were indicated as (*P< 0.05) or (***P< 0.0001) for treated samples *versus* control ones. Each experiment was carried out in triplicate.

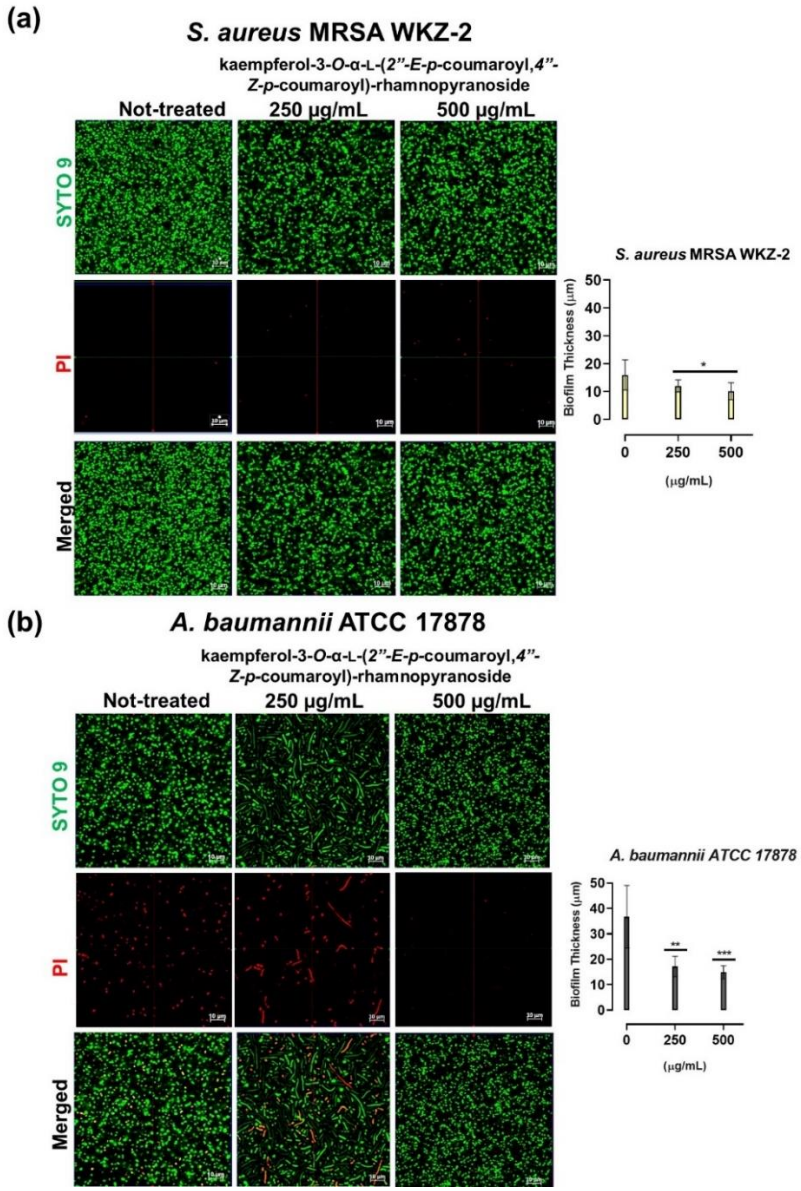


**Figure 7.** Anti-biofilm activity of purified kaempferol-3-*O*-α-L-(*2''-E-p*-coumaroyl,*4''-Z-p*-coumaroyl)- rhamnopyranoside (compound **4**). Effects of compound **4** were evaluated on biofilm formation in the case of *S. aureus* MRSA WKZ-2 (a), and *A. baumannii* ATCC 17878 (b) by CLSM. Biofilm cells were stained with LIVE/DEAD BacLight bacterial viability kit (Molecular Probes, Eugene, OR) containing a 1:1 mol/mol ratio of SYTO-9 (green fluorescence, all cells) and propidium iodide (PI; red fluorescence, dead cells). The biofilm images were obtained by confocal z-stack using Zen Lite 2.3 software. All the images were taken under identical conditions. Significant differences were indicated as (*P< 0.05), (**P< 0.001) or (***P< 0.0001) for treated *versus* control ones. Each experiment was carried out in triplicate.

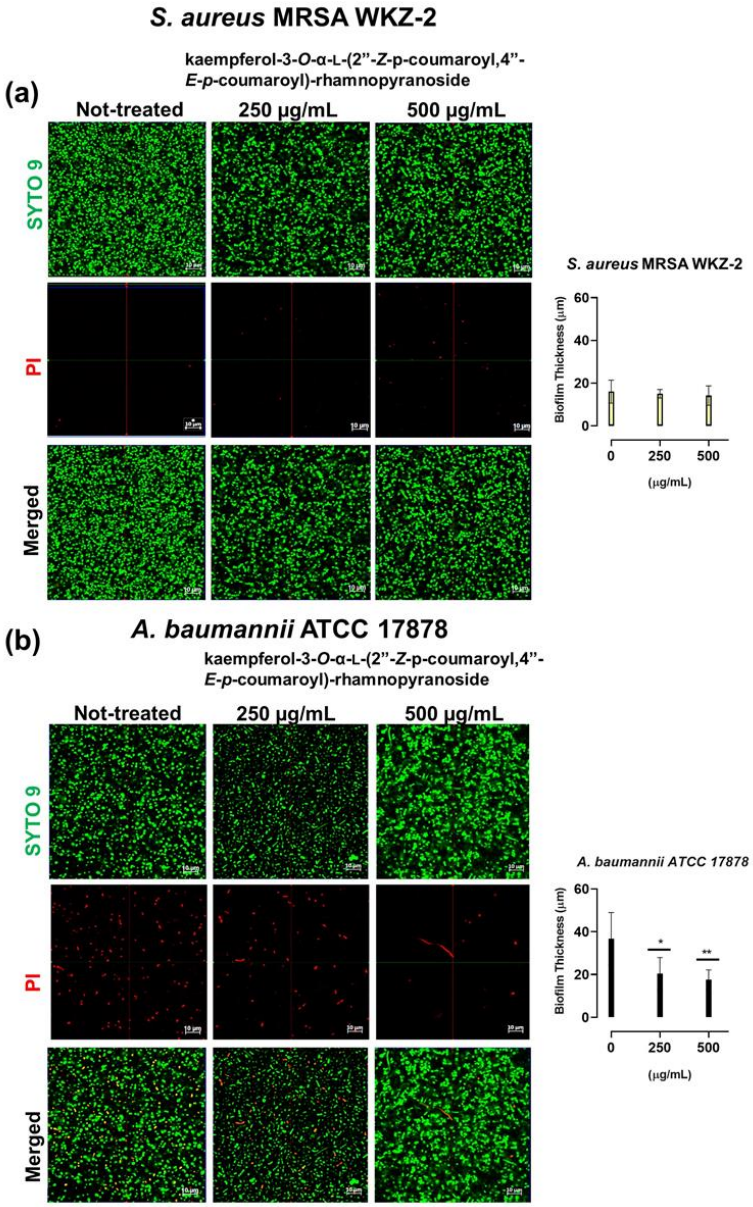


**Figure 8**. Anti-biofilm activity of purified kaempferol-3-*O*-α-L-(*2''-Z-p*-coumaroyl,*4''-E-p*-coumaroyl)-rhamnopyranoside (compound **5**). Effects of compound **5** were evaluated on biofilm formation in the case of *S. aureus* MRSA WKZ-2 (a), and *A. baumannii* ATCC 17878 (b). Biofilm cells were stained with LIVE/DEAD BacLight bacterial viability kit (Molecular Probes, Eugene, OR) containing a 1:1 mol/mol ratio of SYTO-9 (green fluorescence, all cells) and propidium iodide (PI; red fluorescence, dead cells). The biofilm images were obtained by confocal z-stack using Zen Lite 2.3 software. All the images were taken under identical conditions. Significant differences were indicated as (*P< 0.05) or (**P< 0.001) for treated samples *versus* control ones. Each experiment was carried out in triplicate.

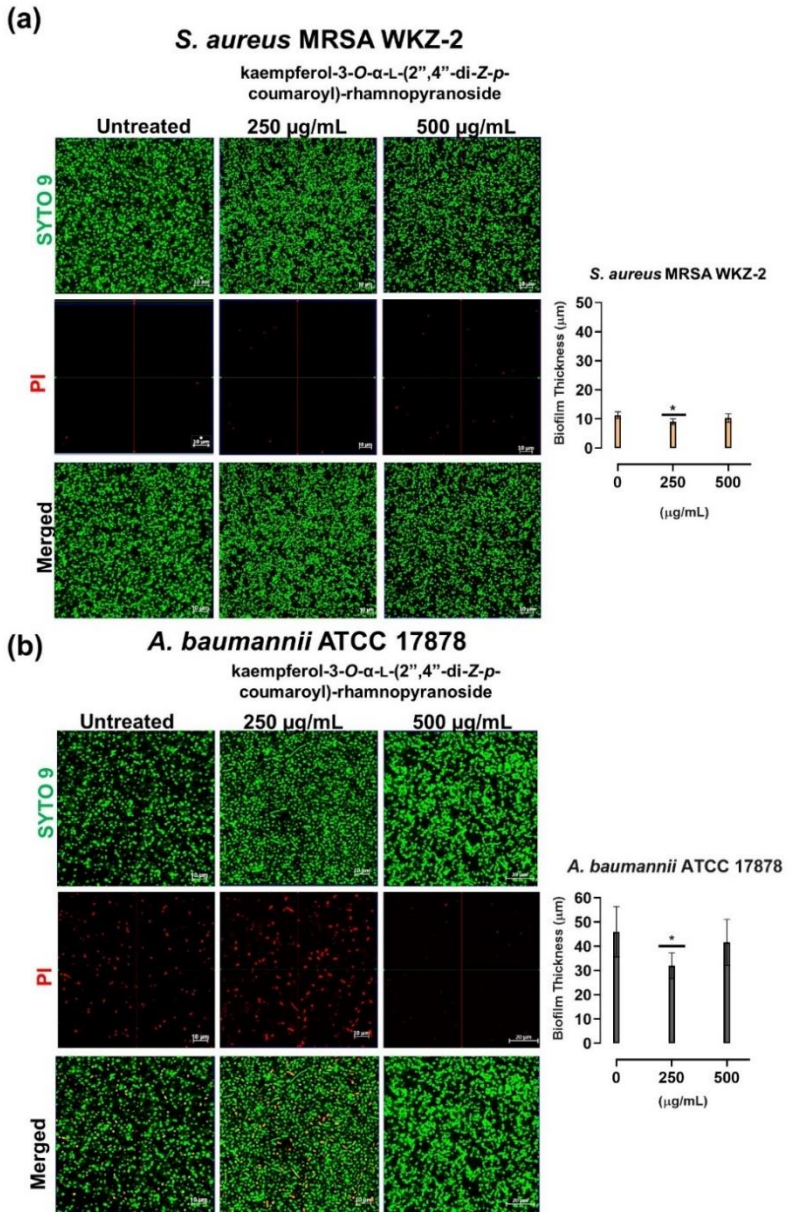


**Figure 9.** Anti-biofilm activity of purified kaempferol-3-*O*-α-L-(2",4"-di-*Z*-*p*-coumaroyl)-rhamnopyranoside (compound **6**). Effects of compound **6** were evaluated on biofilm formation in the case of *S. aureus* MRSA WKZ-2 (a), and *A. baumannii* ATCC 17878 (b) by CLSM. Biofilm cells were stained with LIVE/DEAD BacLight bacterial viability kit (Molecular Probes, Eugene, OR) containing a 1:1 mol/mol ratio of SYTO-9 (green fluorescence, all cells) and propidium iodide (PI; red fluorescence, dead cells). The biofilm images were obtained by confocal z-stack using Zen Lite 2.3 software. All the images were taken under identical conditions. Significant differences were indicated as (*P< 0.05) for treated samples *versus* control ones. Each experiment was carried out in triplicate.

### 3.5 Evaluation of synergistic effects between kaempferol-3-*O*-*α*-L-(2",4"-di-*E*-*p*-coumaroyl)-rhamnopyranoside and ApoB-derived peptides.

Starting from the interesting antimicrobial and anti-biofilm activities of both kaempferol-3-*O*-*α*-L-(2",4"-di-*E*-*p*-coumaroyl)-rhamnopyranoside (compound **3**) (**Table 5**) and ApoB-derived peptides [33], the exploitation of synergistic effects between these two elements was performed. To proceed with this, conventional checkboard assays were set-up [47]. Hence, two-dimensional arrays of serial concentrations of the tested compounds were used as the basis to calculate fractional inhibitory concentration (FIC) indexes [47], in order to verify whether paired combinations of compounds could exert inhibitory effects that are more than the sum of their effects alone [66]. It has been reported that FIC indexes ≤ 0.5 are an indication of synergism, whereas FIC indexes between 0.5 and 1.0 are associated with additive effects. Indifferent effects are, instead, associated to FIC indexes between 1.0 and 4.0, whereas FIC indexes >4.0 are indicative of antagonistic effects [48]. To perform these experiments, the antimicrobial properties of compound **3** and of r(P)ApoB$_L^{Pro}$ peptide were firstly evaluated separately against a panel of Gram-positive and Gram-negative bacteria (**Table 6**).

**Table 6.** MIC$_{100}$ values (μM) determined for r(p)ApoB$_L^{Pro}$ and kaempferol-3-O-*α*-L-(2",4"-di-*E*-*p*-coumaroyl)- rhamnopyranoside tested on a panel of Gram-positive and Gram-negative bacterial strains. Reported data refer to three biological replicates.

| | **MIC$_{100}$ (μM)** | |
|---|---|---|
| | r(p)ApoB$_L^{Pro}$ | kaempferol-3-O-*α*-L-(2",4"-di-*E*-*p*-coumaroyl)- rhamnopyranoside |
| *S. aureus* ATCC 29213 | 40 | 0.68 |
| *S. aureus* (MRSA WKZ-2) | 40 | 0.68 |
| *E. coli* ATCC 25922 | 5 | 1350 |
| *A. baumannii* ATCC 17878 | 2.5 | 1350 |

Then combinations of the 2 compounds were tested on the selected bacterial strains. Determined FIC indexes were all indicative of additive effects (**Table 7**). Notably, no FIC indexes higher than 1.0 were measured. The best results were obtained in the case of *S. aureus* MRSA WKZ-2 and *A. baumannii* ATCC 17878 bacterial strains with FIC indexes of 0.63 and 0.77, respectively. Detected additive effects require further investigation in the future and pose the bases for the future development of combinatorial therapeutic approaches able to counteract multidrug resistant infections [33].

**Table 7.** Combination therapy analyses. Fractional inhibitory concentration (FIC) indexes determined for r(p)ApoB$_{L}^{Pro}$ peptide tested in combination with kaempferol-3-O-*α*-L-(2",4"-di-*E*-*p*-coumaroyl)- rhamnopyranoside on Gram-positive and Gram-negative bacterial strains. Indexes were obtained from a minimum of three independent experiments, each one carried out with triplicate determinations.

| | **∑FIC Index** |
|---|---|
| *S. aureus* ATCC 29213 | 1 |
| *S. aureus* (MRSA WKZ-2) | 0.63 |
| *E. coli* ATCC 25922 | 1 |
| *A. baumannii* ATCC 17878 | 0.77 |

### 3.6 Prediction of the target of kaempferol-3-*O*-*α*-L-(2",4"-di-*E*-*p*-coumaroyl)-rhamnopyranoside antimicrobial and anti-biofilm activity by molecular docking

Among the well-known proteins responsible for bacterial biofilm adhesion, formation, and aggregation, Sortase A (Srt A) [49] attracted our attention. This enzyme catalyzes the covalent linkage of the cell wall proteins (CWA) to the peptidoglycan [49]. Indeed, the inactivation of its enzymatic activity was reported to interfere with the ability of bacterial cells to cause infections because of the failure of fibronectin proteins attachment to the cell wall [50]. For this reason, Srt A protein attracted the attention of researchers as an interesting target for the development of antimicrobial and anti-biofilm drugs [51]. Another interesting target is represented by aminoacyl–tRNA synthases (aaRSs) [52] playing a key role in the translation of nucleic acid sequences into a polypeptide sequence [53]. Indeed, the inhibition of these enzymes is associated to a blockage of bacterial cells growth due to the interference with protein synthesis [52]. Furthermore, it has to be highlighted that significant differences in the topology of ATP binding domain have been reported between human and bacterial aaRS, probably due to the different functions that these enzymes play in human cells [54], thus enhancing the possibility to selectively target bacterial aaRSs enzymes [52].

Based on this, a preliminary evaluation of the putative molecular bases of compound **3** antimicrobial and anti-biofilm properties was performed by selecting Sortase A (Srt A) protein and aminoacyl–tRNA synthases (aaRSs) as targets in molecular docking analyses. The tested compound **3** demonstrated substantial binding to both selected targets. The binding free energy, in the case of the complex with tyrosyl tRNA synthetase, was computed to be higher (-9.5 kcal/mol) than that determined in the case of sortase A (-8.3 kcal/mol). In the case of all

the analyzed complexes, the binding of the ligand to the active site of the proteins was found to be mediated by hydrogen bonding, hydrophobic and various van der Waal's force interactions (**Table 8, Figure 10 a-d**). Furthermore, for the complex with tyrosyl tRNA synthetase, the binding was found to be supported by a carbon-hydrogen bond and several hydrophobic interactions. Indeed, the tested ligand was found to be bonded to several amino acid residues, such as Gly 38, Ala 43, His 47, His 50 and Leu 223 (**Table 8**). The maximum number of interactions was observed in the case of His 47 residue. It is noteworthy that residues His 47 and His 50 have been reported as suitable targets of specific inhibitors of the enzyme tyrosyl tRNA synthetase [54]. In the case of the complex with Sortase-A, various non-covalent forces were described including conventional hydrogen bonding, carbon-hydrogen bonding and hydrophobic interactions. Amino acids Ala 92, Ala 104, Val 168, Thr 180, Val 193, Arg 197 and Ile 199 were predicted to mediate the interaction between the test ligand and the Sortase-A enzyme (**Table 8**).

**Table 8.** Details of the intermolecular interactions between the tested ligand and *S. aureus* target enzymes tyrosyl tRNA synthetase and sortase A.

| **Interaction between antimicrobial compound and tyrosyl tRNA synthetase** | | | **Interaction between antimicrobial compound and sortase A** | | |
|---|---|---|---|---|---|
| **Interacting amino acid** | **Type of interaction** | **Bond length (Å)** | **Interacting amino acid** | **Type of interaction** | **Bond length (Å)** |
| His 50 | Carbon-hydrogen bond | 3.57 | Val 168 | Hydrogen bond | 2.21 |
| His 47 | Pi-Sigma | 3.92 | Arg 197 | Hydrogen bond | 2.35 |
| His 47 | Pi-Pi T shaped | 5.02 | Ala 92 | Hydrogen bond | 2.66 |
| His 47 | Pi-Pi T shaped | 4.96 | Val 168 | Hydrogen bond | 2.70 |
| Gly 38 | Amide Pi Stacked | 3.52 | Thr 180 | Hydrogen bond | 2.49 |
| Ala 43 | Pi -Alkyl | 5.00 | Val 193 | Pi-Sigma | 3.79 |
| Leu 223 | Pi -Alkyl | 5.37 | Ala 92 | Pi-alkyl | 5.11 |
| | | | Ala 104 | Pi-Alkyl | 5.07 |
| | | | Val 168 | Pi-Alkyl | 4.65 |
| | | | Ile 199 | Pi-Alkyl | 4.54 |

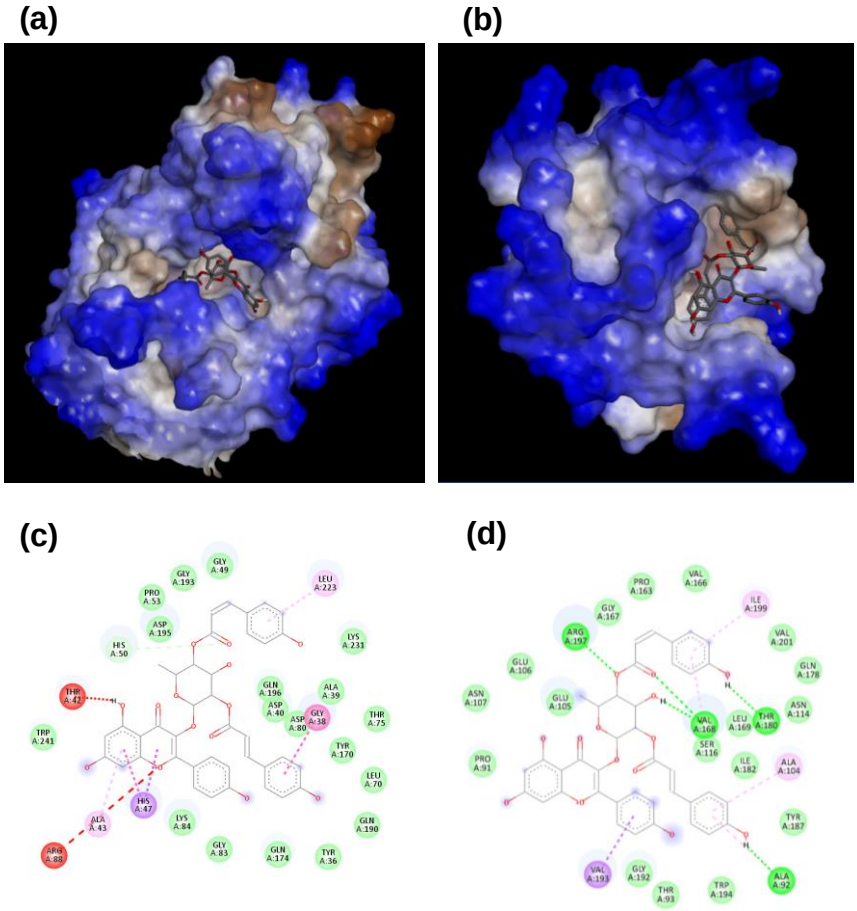


**Figure 10.** 3D orientation of kaempferol-3-*O*-α-L-(2”,4”-di-*E*-*p*-coumaroyl)-rhamnopyranoside (compound **3**) (shown in stick) at the active pocket of tyrosyl tRNA synthetase (a) and sortase A (b); 2D representation of intermolecular interactions between the antimicrobial compound and enzyme targets tyrosyl tRNA synthetase (c) and sortase A (d).

It is noteworthy, that residue Arg 197 represents a suitable target of an inactivating drug, since it was reported to play a crucial role in the active site of Sortase-A enzyme [51]. It has to be highlighted that non-covalent forces generally mediate the biological activity of effective drugs are of great importance in the design and development of novel drugs. Hydrogen bonds generally deliver structural strength and stability to protein-ligand complexes, whereas hydrophobic forces play a crucial role in amplifying ligands’ binding affinity towards the surface of the target in a physiological environment [55,56]. Van der Waal’s interactions, being weak electrostatic forces, play an important role in stabilizing the three-dimensional structure of protein-ligand complexes [57]. Based on reported findings, it can be hypothesized that the strong

antibacterial activity of kaempferol-3-*O*-α-L-(2”,4”-di-*E*-*p*-coumaroyl)-rhamnopyranoside against *S. aureus* bacterial cells might be mediated by its binding to these two selected enzymes (tyrosyl tRNA synthetase and Sortase-A) and to the consequent blockage of key residues present in the active site determining the inhibition of their enzymatic activity.

### 3.7 Analysis of kaempferol-3-*O*-*α*-L-(2”,4”-di-*E*-*p*-coumaroyl)-rhamnopyranoside biocompatibility

To verify whether compound **3** satisfies the requirements to be employed in the future as a bioactive molecule in biomedical field, biocompatibility analyses on eukaryotic cells were performed. To this purpose, immortalized human keratinocytes (HaCaT) and human dermal fibroblasts (HDF) were incubated with increasing concentrations (from 0.5 μg/mL to 5 μg/mL) of the compound under test for 72h. As shown in **Figure 11a and b**, no significant toxic effects were detected under the experimental conditions tested, thus indicating that the identified compound is selectively toxic towards prokaryotic cells. A slight toxicity was detected only in the case of HDF cells at the highest concentrations tested (**Figure 11b**).

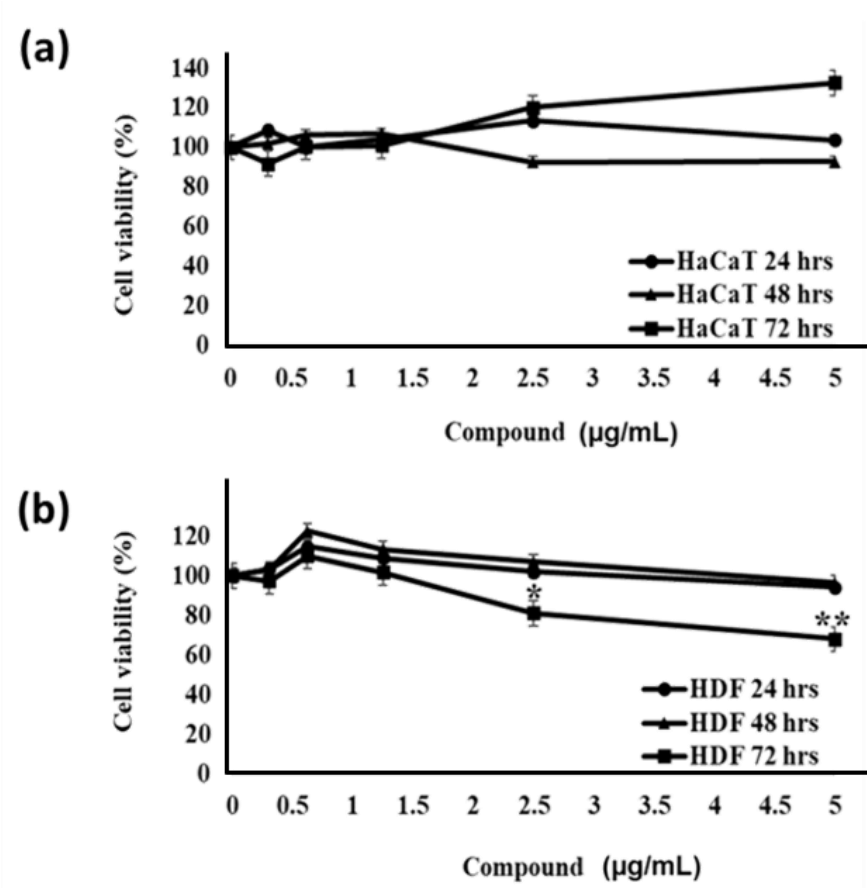


**Figure11**. Effects of kaempferol-3-*O*-α-L-(2",4"-di-*E*-*p*-coumaroyl)-rhamnopyranoside (compound **3**) on the viability of HaCat (a) and HDF cells (b). Cell viability was expressed as the percentage of MTT reduction with respect to control cells tested under the same conditions but in the absence of the compound under test. The experimental data represent the average of three independent experiments, each one was carried out with triplicate determinations. Significant differences were indicated as (*P< 0.05) or (**P< 0.001) for treated samples *versus* control ones. Each experiment was carried out in triplicate.

## 4. Discussion

A bio-guided purification of *E. foeminea* extracts was carried out to isolate compounds with antimicrobial and anti-biofilm properties. Six compounds were isolated and identified as carvacrol, thymol and four glycosylated kaempferol, *i.e.*, kaempferol-3-*O*-α-L-(2”,4”-di-*E*-*p*-coumaroyl)-rhamnopyranoside,kaempferol-3-*O*-α-L-(2”-*E*-*p*-coumaroyl,4”-*Z*-*p*-coumaroyl)-rhamnopyranoside, kaempferol-3-*O*-α-L-(2”-*Z*-*p*-coumaroyl,4”-*E*-*p*-coumaroyl)-rhamnopyranoside,and kaempferol-3-*O*-α-L-(2”,4”-di-*Z*-*p*-coumaroyl)-rhamnopyranoside (compounds **1**-**6** in **Figure 3**). These metabolites were identified for the first time in *E. foeminea* organic extracts and compounds **1**-**3** were found to be endowed with strong antimicrobial properties and promising anti-biofilm activity.

Carvacrol and thymol were largely investigated and are known for their medical properties. They were also employed as food preservatives and food additives because of their well-known antimicrobial activity [58] probably due to their physiochemical properties, such as hydrophobicity, partition coefficient and ability to form H-bonds with interacting target molecules [59]. Carvacrol is an aromatic monoterpene generally present in aromatic plants as thyme and oregano, and thymol is an isomer of carvacrol. Carvacrol has been reported to exert significant antimicrobial properties when tested on a wide range of bacterial strains, such as *E. coli*, *S. aureus*, *L. monocytogenes*, and *S. typhimurium* [60-63]. Molecular mechanisms underlying carvacrol antimicrobial activity imply bacterial membrane disruption due to an alteration of its fluidity, integrity, and functionality [58,59]. Carvacrol was also reported to cause depletion of intracellular ATP due to an alteration of intracellular pH value consequent to an interference with protons influx [58,59]. In the literature, further mechanisms were also described to explain carvacrol effects on the viability of bacterial cells, such as the induction of reactive oxygen species (ROS) and the inhibition of efflux pumps [58,59]. Due to its hydrophobicity, carvacrol was also reported to penetrate the hydrophobic environment of bacterial biofilm matrix, to interact with bacterial membranes and to interfere with their ability to form biofilms by altering bacterial cells motility and by reducing cells’ ability to adhere to substrates [58,59]. Carvacrol anti-biofilm activity was also described to be mediated by its ability to interfere with signaling pathways of

quorum sensing (QS) by blocking the genes expression that are specificly involved [58,59]. Based on these observations, it is plausible that carvacrol might be, at least in part, responsible for the antimicrobial and anti-biofilm activity observed by testing *E. foeminea* hexane extract (**Table 1 and Figure 5**).

It is worthy to note that, in *E. foeminea* dichloromethane extract, four glycosylated isomers of kaempferol (compounds **3**-**6** in **Figure 3**) were identified for the first time. Compound **3** was isolated for the first time from *Pentachondra pumila* collected in New Zealand [41] and from unripe fruits of *Ocotea vellosiana* [64]. Subsequently, it was isolated from several sources, such as the leaves of *Laurus nobilis* [42], the buds of *Mammea longifolia* [43], the leaves of *Eriobotrya japonica* [65], the leaves of *Cinnamomun kotoense* [45], the aerial parts of *Epimedium sagittatum*, and the leaves of *Machilus philippinens* [66]. Compound **4** was isolated for the first time from the aerial parts of *Epimedium sagittatum* together with compounds **3** and **5** and other related compounds [44]. Regarding compound **5**, it was isolated for the first time together with compound **3** from the leaves of *Cinnamomun kotoense*, and a mixture of both compounds was found to be able to suppress peripheral blood mononuclear cell (PBMC) production induced by phytohemagglutinin (PHA) [45]. Finally, compound **6** was isolated for the first time from several sources together with other isomers, such as from the leaves of *Laurus nobilis* [42] together with compound **3**, the leaves of *Machilus philippinens* together with compound **4** [66] and the leaves of *Eriobotrya japonica* together with compound **3** [65].

Interestingly, despite the presence of other isomers, compound **3** was found to be the only isomer to be endowed with robust antimicrobial activity towards *S. aureus* strains sensitive or resistant to conventional antibiotics (**Table 4**). In the past, strong antimicrobial properties were reported for compounds **3** and **4** isolated from *Laurus nobilis* against methicillin-resistant *S. aureus* strains and against vancomycin-resistant *Enterococci* [67]. Considering the strong antibacterial activity of compound **3** (**Table 4**) with respect to that showed by its isomers (compounds **4**-**6** in **Table 5**), it is plausible that stereochemistry of the double bonds of the *p*-coumaroyl residues is a key structural feature associated with the antibiotic activity. In particular,

the *E,E* stereochemistry of the double bonds of the *p*-coumaroyl residues seems to be fundamental (**Table 4**).

Considering the promising antimicrobial activity of compound **3** among the identified compounds, molecular docking studies were also performed, aiming to predict the suitable molecular targets of compound **3** to explain its antimicrobial activity. Obtained results suggested that the antibacterial activity of the tested compound **3** against *S. aureus* strains might be correlated to the inhibition of sortase A and/or tyrosyl tRNA synthetase. Sortase A (Srt A) is one of the well-known proteins responsible for biofilm adhesion, formation, and aggregation [49]. This enzyme catalyses the formation of covalent bonds between cell wall proteins (CWA) and peptidoglycan molecules of bacterial cell wall [49]. It was reported that, in the presence of inactivating mutations of Srt A, bacterial cells are no longer able to cause infections because of the failure of the attachment of fibronectin proteins to the cell wall [50]. This makes Srt A a suitable target for the development of novel and effective antimicrobial and anti-biofilm drugs [51].

Aminoacyl–tRNA synthases (aaRSs) also represent good candidates as targets of antimicrobial strategies [52]. Indeed, their inhibition is associated to a blockage of cell growth due to an interference with protein synthesis processes [52]. Furthermore, differences in the topology of the ATP binding domain between human and bacterial enzymes are at the basis of the possibility to selectively target bacterial enzymes [54]. As a matter of fact, this is in agreement with the data obtained by treating human eukaryotic cells with compound **3**, while it exerted toxic effects on *S. aureus* bacterial cells, it was found to be harmless towards immortalized human keratinocytes (HaCaT) and human dermal fibroblasts (HDF) at concentrations effective on bacterial cells (**Figure 11**). Interestingly, it was also demonstrated that compound **3** is able to exert additive effects when tested in combination with a human ApoB-derived antimicrobial peptide. However, one of the main challenges during this work was the low isolated amount of the purified compound **3**, which was at a certain point an obstacle in the performance of further experiments. It is highly recommended to chemically synthesize compound **3** which will be a challenging task due to the stereochemistry of the double bonds which are responsible for compound **3** potent activity to investigate its

applicability. Altogether, obtained data open interesting perspectives to the future applicability of identified compound **3** in several fields to counteract bacterial infections.

# 5. References


[1] Svoboda, K.; Brooker, J.D.; Zrustova J. Antibacterial and Antioxident Properties of Essential Oils: Their Potential Applications in the Food Industries. *Acta Horticulturae* **2006**, *709*, 35–44. https://doi.org/10.17660/ActaHortic.2006.709.4

[2] Valle Jr, D.L.; Andrade, J.I.; Puzon, J.J.M.; Cabrera, E.C.; Rivera, W.L. Antibacterial activities of ethanol extracts of Philippine medicinal plants against multidrug-resistant bacteria. *Asian pacific journal of tropical biomedicine* **2015**, *5*, 532-540. https://doi.org/10.1016/j.apjtb.2015.04.005

[3] Savoia, D. Plant-derived antimicrobial compounds: alternatives to antibiotics. *Future Microbiology* **2012**, *7*, 979. https://doi.org/10.2217/fmb.12.68

[4] Cowan, M.M. Plant product as antimicrobial agents. *Clin. Microbiol*. *Rev.* **1999,** *12*, 564–582.https://doi.org/10.1128/CMR.12.4.564

[5] Garcia, A.; Bocanegra-Garcia, V.; Palma-Nicolas, J.P.; Rivera, G. Recent advances in antitubercular natural products. *Eur. J. Med. Chem.* 2012, *49*, 1–23.https://doi.org/10.1016/j.ejmech.2011.12.029

[6] Kurek, A.; Grudniak, A.M.; Kraczkiewicz, D.A.; Wolska, K.I. New antibacterial therapeutics and strategies. *Pol. J. Microbiol.* **2011**, *60*, 3–12

[7] Fowler, Z.L.; Baron, C.M.; Panepinto, J.C.; Koffas, M.A. Melanization of flavonoids by fungal and bacterial laccases. *Yeast* **2011**, *28*, 181–188. https://doi.org/10.1002/yea.1829

[8] WHO. WHO traditional medicine strategy. **2002**, Geneva.

[9] Sahib, N.G.; Anwar, F.; Gilani, A.H.; Hamid, A.A.; Saari, N.; Alkharfy, K.M. Coriander *Coriandrum sativum* L.: a potential source of high-value components for functional foods and nutraceuticals – a review. *Phytother.* **2013**, *27*, 1439-1456. https://doi.org/10.1002/ptr.4897

[10] O'Dowd, N.A.; McCauley, G.; Wilson, JA.N.; Parnell, T.A.K.; Kavanaugh, D. In vitro culture, micropropagation and the production of ephedrine and other alkaloids. In *Biotechnology in Agriculture and Forestry*, Bajaj YPS. Ed., Springer, Berlin, 1998; p. 41 https://doi.org/10.1007/978-3-642-58833-4_10

[11] Pirbalouti, A.G.; Azizi, S.; Amirmohammadi, M.; Craker, L. Healing effect of hydro-alcoholic extract of *Ephedra pachyclada* Boiss. in experimentally gastric ulcer in rat. *Acta Pol Pharm*. **2013**, *70*, 1003-1009

[12] Hollander, J.L.; Vander Wall, S.B.; Baguley, J.G. Evolution of seed dispersal in North American *Ephedra*. *Evol. Ecol*. **2010**, *24*, 333–345. https://doi.org/10.1007/s10682-009-9309-1

[13] Ickert-Bond, S.M.; Rydin, C.; Renner, S.S. A fossil-calibrated relaxed clock for *Ephedra* indicates an Oligocene age for the divergence of Asian and New World clades and Miocene dispersal into South America. *Journal of Systematics and Evolution* **2009**, *47*, 444-456. https://doi.org/10.1111/j.1759-6831.2009.00053.x

[14] Sawalha, A. F. Complementary and alternative medicine (CAM) in Palestine: use and safety implications. *The Journal of Alternative and Complementary Medicine* **2007**, *13*, 263-270. https://doi.org/10.1089/acm.2006.6280

[15] Abou-Elkhair, E.; Fadda, H.; Abu-Mohsen, U. Antibacterial activity and Phytochemical analysis of some medicinal plants from Gaza Strip-Palestine. *Journal of Al-Azhar University-Gaza* **2010**, *12*, 45-54.

[16] Ickert-Bond, S.M.; Renner, S.S. The Gnetales: Recent insights on their morphology, reproductive biology, chromosome numbers, biogeography, and divergence times. *J. Syst. Evol*. **2016**, *54*, 1–16. https://doi.org/10.1111/jse.12190

[17] Flora of Israel. Available online at http://flora.huji.ac.il/browse asp. Danin A. Accessed on December 10, **2018**.

[18] Yeung, E.C. Embryogeny of Pbaseolus: The role of the suspensor. *Z. Pflanzenphysiol*. **1980**, *96*, 17-28

[19] Kallassy, H.; Fayyad-Kazan, M.; Makki, R.; Yolla, E.M.; Rammal, H.; Leger, D.Y.; Badran B. Chemical composition and antioxidant, anti-inflammatory, and antiproliferative activities of Lebanese *Ephedra Campylopoda* plant. *Medical science monitor basic research* **2017**, *23*, 313. https://doi.org/10.12659/MSMBR.905056

[20] Ibragic, S.; Sofic, E. Chemical composition of various *Ephedra* species. *Bosnian Journal of Basic Medical Sciences* **2015**, *15*, 21-27. https://doi.org/10.17305/bjbms.2015.539

[21] González-Juárez, D.E.; Escobedo-Moratilla, A.; Flores, J.; Hidalgo-Figueroa, S.; Martínez-Tagüeña, N.; Morales-Jiménez, J.; Muñiz-Ramírez, A.; Pastor-Palacios, G.; Pérez-Miranda, S.; Ramírez-Hernández, A.; Trujillo, J.; Bautista, E. A Review of the *Ephedra* genus: Distribution, Ecology, Ethnobotany, Phytochemistry and Pharmacological Properties. *Molecules* **2020**, *25*, 3283. https://doi.org/10.3390/molecules25143283

[22] Mills, S.; Bone, K. *The Essential Guide to Herbal Safety,* Elsevier Inc, St. Louis, MO, **2004**.

[23] Mendelovich, M.; Shoshan, M.; Fridlender, M.; Mazuz, M.; Namder, D.; Nallathambi, R.; Selvaraj, G.; Kumari, P.; Ion, A.; Wininger, S.; Nasser, A.; Samara, M.; Sharvit, Y.; Kapulnik, Y.; Dudai, N.; Koltai, H. Effect of *Ephedra foeminea* active compounds on cell viability and actin structures in cancer cell lines. *J. Med. Plants Res*. **2017**, *11,* 690–702. https://doi.org/10.5897/JMPR2017.6471

[24] Moon, S. E.; Kim, H. Y.; Cha, J. D. Synergistic effect between clove oil and its major compounds and antibiotics against oral bacteria. *Archives of oral biology*,**2011**, *56*(9), 907-916. https://doi.org/10.1016/j.archoralbio.2011.02.005

[25] Adwan, G.; Abu-Shanab, B.; Adwan, K. Antibacterial activities of some plant extracts alone and in combination with different antimicrobials against multidrug–resistant *Pseudomonas aeruginosa* strains. *Asian Pacific journal of tropical medicine*, **2010**, *3*(4), 266-269. https://doi.org/10.1016/S1995-7645(10)60064-8

[26] Hemaiswarya, S.; Doble, M. Synergistic interaction of phenylpropanoids with antibiotics against bacteria. *Journal of Medical Microbiology*,**2010**, *59*(12), 1469-1476. https://doi.org/10.1099/jmm.0.022426-0

[27] Mahboubi, M.; Bidgoli, F. G. Anti-staphylococcal activity of Zataria multiflora essential oil and its synergy with vancomycin. *Phytomedicine*, **2010**,*17*(7), 548-550. https://doi.org/10.1016/j.phymed.2009.11.004

[28] Rakholiya, K.;Chanda, S. In vitro interaction of certain antimicrobial agents in combination with plant extracts against some pathogenic bacterial strains. *Asian Pacific Journal of Tropical Biomedicine*, **2012**, *2*(3), S1466-S1470. https://doi.org/10.1016/S2221-1691(12)60439-0

[29] Hancock, R. E. Cationic antimicrobial peptides: towards clinical applications. *Expert opinion on investigational drugs*,**2000**, *9*(8), 1723-1729.https://doi.org/10.1517/13543784.9.8.1723

[30] Gordon, Y. J.; Romanowski, E. G.; McDermott, A. M. A review of antimicrobial peptides and their therapeutic potential as anti-infective drugs. *Current eye research*,**2005**, *30*(7), 505-515. https://doi.org/10.1080/02713680590968637

[31] Kosikowska, P.; Lesner, A. Antimicrobial peptides (AMPs) as drug candidates: a patent review (2003–2015). *Expert opinion on therapeutic patents*,**2016**, *26*(6), 689-702. https://doi.org/10.1080/13543776.2016.1176149

[32] Pane, K.; Durante, L.; Crescenzi, O.; Cafaro, V.; Pizzo, E.; Varcamonti, M.; Notomista, E. Antimicrobial potency of cationic antimicrobial peptides can be predicted from their amino acid composition: Application to the detection of "cryptic" antimicrobial peptides. *Journal of Theoretical Biology*. **2017**, 419, 254–265. https://doi.org/10.1016/j.jtbi.2017.02.012

[33] Gaglione, R.; Dell'Olmo, E.; Bosso, A.; Chino, M.; Pane, K.; Ascione, F.; Itri, F.; Caserta, S.; Amoresano, A.; Lombardi, A.; Haagsman, H.P.; Piccoli, R.; Pizzo, E.; Veldhuizen, E.J.A.; Notomista, E.; Arciello, A. Novel human bioactive peptides identified in apolipoprotein B: evaluation of their therapeutic potential. *Biochemical Pharmacology* **2017**, *130*, 34-50. https://doi.org/10.1016/j.bcp.2017.01.009

[34] Dell'Olmo, E.; Gaglione, R.; Cesaro, A.; Cafaro, V.; Teertstra, W. R.; de Cock, H.; Notomista, E; Haagsman H.P. ; Veldhuizen E.J.A.; Arciello, A. Host defence peptides identified in human apolipoprotein B as promising antifungal agents. *Applied microbiology and biotechnology*,**2021** *105*(5), 1953-1964.https://doi.org/10.1007/s00253-021-11114-3

[35] Berger, S.; Braun, S. 200 and more NMR experiments. Weinheim: Wiley-Vch, **2004**; pp. 305-307.

[36] Pizzo, E.; Pane, K.; Bosso, A.; Landi, N.; Ragucci, S.; Russo, R.; Gaglione, R.; Torres, M.D.T.; de la Fuente-Nunez, C.; Arciello, A.; Di Donato, A.; Notomista, E.; Di Maro, A. Novel bioactive peptides from PD-L1/2, a type 1 ribosome inactivating protein from Phytolacca dioica L. Evaluation of their antimicrobial properties and anti-biofilm activities. *Biochim Biophys Acta Biomembr.* **2018**, *1860*, 1425-1435. https://doi.org/10.1016/j.bbamem.2018.04.010

[37] Gaglione, R.; Pane, K.; Dell'Olmo, E.; Cafaro, V.; Pizzo, E.; Olivieri, G.; Notomista, E.; Arciello, A. Cost-effective production of recombinant peptides in *Escherichia coli*. *New biotechnology*. **2019,** *51*, 39-48. https://doi.org/10.1016/j.nbt.2019.02.004

[38] Monti, D.M.; Guglielmi, F.; Monti, M.; Cozzolino, F.; Torrassa, S.; Relini, A.; Pucci, P.; Arciello, A.; Piccoli, R. Effects of a lipid environment on the fibrillogenic pathway of the N-terminal polypeptide of human apolipoprotein A-I, responsible for in vivo amyloid fibril formation. *Eur Biophys J*. **2010**, *39,* 1289-1299. https://doi.org/10.1007/s00249-010-0582-2.

[39] Gaglione, R.; Cesaro, A.; Dell'Olmo, E.; Di Girolamo, R.; Tartaglione, L.; Pizzo, E.; Arciello, A. Cryptides Identified in Human Apolipoprotein B as New Weapons to Fight Antibiotic Resistance in Cystic Fibrosis Disease*. Int J Mol Sci* **2020**, 21, 2049. https://doi.org/10.3390/ijms21062049

[40] Liu, Y.; Grimm, M.; Dai, Wt.; Hou, M.C.; Xiao, Z.X.; Cao, Y. CB-Dock: a web server for cavity detection-guided protein–ligand blind docking. *Acta*

*Pharmacol Sin* **2020**, *41*, 138–144. https://doi.org/10.1038/s41401-019-0228-6

[41] Bloor, S.J. An antimicrobial kaempferol-diacyl-rhamnoside from Pentachondra pumila. *Phytochemistry* **1995**, *38*, 1033-1035. https://doi.org/10.1016/0031-9422(94)00661-C

[42] Fiorini, C.; David, B.; Fourasté, I.; Vercauteren, J. Acylated kaempferol glycosides from Laurus nobilis leaves. *Phytochemistry* **1998**, *47*, 821-824. https://doi.org/10.1016/S0031-9422(97)00563-3

[43] Rao, J.M.L.; Yada, H.; Ono, H.; Yoshida, M. Acylated and non-acylated flavonol monoglycosides from the Indian minor spice nagkesar (*Mammea longifolia*). *Journal of agricultural and food chemistry* **2002**, *50*, 3143-3146. https://doi.org/10.1021/jf011461m

[44] Wang, G.J.; Tsai, T.H.; Lin, L.C. Prenylflavonol, acylated flavonol glycosides and related compounds from *Epimedium sagittatum*. *Phytochemistry* **2007**, *68*, 2455-2464. https://doi.org/10.1016/j.phytochem.2007.05.035

[45] Kuo, Y.C.; Lu, C.K.; Huang, L.W.; Kuo, Y.H.; Chang, C.; Hsu, F.L.; Lee, T.H. Inhibitory effects of acylated kaempferol glycosides from the leaves of *Cinnamomum kotoense* on the proliferation of human peripheral blood mononuclear cells. *Planta medica* **2005**, *71*, 412-415. https://doi.org/10.1055/s-2005-864134

[46] Gaglione, R.; Cesaro, A.; Dell'Olmo, E.; Della Ventura, B.; Casillo, A.; Di Girolamo, R.; Velotta, R.; Notomista, E.; Veldhuizen, E.J.A.; Corsaro, M.M.; De Rosa, C.; Arciello A. Effects of human antimicrobial cryptides identified in apolipoprotein B depend on specific features of bacterial strains. *Scientific Reports* **2019**, *9*, 6728. https://doi.org/10.1038/s41598-019-43063-3

[47] Longo, F., Vuotto, C., & Donelli, G.. Biofilm formation in Acinetobacter baumannii. *New Microbiol*, **2014**,*37*(2), 119-127. http://www.ncbi.nlm.nih.gov/pubmed/24858639.

[48] Meletiadis, J.; Pournaras, S.; Roilides, E.; Walsh, T. J. Defining fractional inhibitory concentration index cutoffs for additive interactions based on self-drug additive combinations, Monte Carlo simulation analysis, and in vitro-in vivo correlation data for antifungal drug combinations against *Aspergillus fumigatus*. *Antimicrobial agents and chemotherapy*,**2010**, *54*(2), 602–609. https://doi.org/10.1128/AAC.00999-09

[49] Mazmanian, S.K.; Liu, G.; Ton-That, H.; Schneewind, O. *Staphylococcus aureus* sortase, an enzyme that anchors surface proteins to the cell wall. *Science* **1999**, 285, 760-763. https://doi.org/10.1126/science.285.5428.760

[50] Weiss, W.J.; Lenoy, E.; Murphy, T.; Tardio, L.; Burgio, P.; Projan, S.J.; Schneewind, O.; Alksne, L. Effect of srtA and srtB gene expression on the virulence of *Staphylococcus aureus* in animal models of infection. *J Antimicrob Chemother* **2004**, *53*, 480–486. https://doi.org/10.1093/jac/dkh078

[51] Lei, S.; Hu, Y.; Yuan, C.; Sun, R.; Wang, J.; Zhang, Y.; Zhang, Y.; Lu, D.; Fu, L.; Jiang, F. Discovery of Sortase A covalent inhibitors with benzofuranene cyanide structures as potential antibacterial agents against *Staphylococcus aureus*. *European Journal of Medicinal Chemistry* **2022**, *229*. doi: https://doi.org/10.1016/j.ejmech.2021.114032

[52] Xiao, Z.P.; Wei, W.; Wang, P.F. ; Shi, W.K.; Zhu, N.; Xie, M.Q.; Sun, Y.W.; Li, L.X.; Xie, Y.X.; Zhu, L.S.; Tang, N.; Ouyang, H.; Li, X.H.; Wang, G.C.; Zhu, H.L. Synthesis and evaluation of new tyrosyl-tRNA synthetase inhibitors as antibacterial agents based on a N2-(arylacetyl) glycinanilide

scaffold. *European Journal of Medicinal Chemistry* **2015**, *102*, 631-638. https://doi.org/10.1016/j.ejmech.2015.08.025

[53] Lapointe, J. Mechanism and evolution of multidomain aminoacyl-tRNA synthetases revealed by their inhibition by analogues of a reaction intermediate, and by properties of truncated forms. *Journal of Biomedical Science and Engineering* **2013**, *6*, 943-946. https://doi.org/10.4236/jbise.2013.610115.

[54] Giegé, R.; Springer, M. Aminoacyl-tRNA Synthetases in the Bacterial World. *EcoSal Plus* **2016**, *7*. https://doi.org/10.1128/ecosalplus.ESP-0002-2016

[55] Padhi, S.; Masi, M.; Chourasia, R.; Rajashekar, Y.; Rai, A.K.; Evidente, A. ADMET profile and virtual screening of plant and microbial natural metabolites as SARS-CoV-2 S1 glycoprotein receptor binding domain and main protease inhibitors. *European Journal of Pharmacology* **2020**, *890*, 2021. https://doi.org/10.1016/j.ejphar.2020.173648

[56] Talukdar, R.; Padhi, S.; Rai, A.K.; Masi, M.; Evidente, A.; Jha, D.K.; Cimmino, A.; Tayung, K. Isolation and Characterization of an Endophytic Fungus *Colletotrichum coccodes* Producing Tyrosol from Houttuynia cordata Thunb. Using ITS2 RNA Secondary Structure and Molecular Docking Study. *Frontiers in Bioengineering and Biotechnology* **2021**, *9*. https://doi.org/10.3389/fbioe.2021.650247.

[57] Righetti, P.G.; Boschetti, E. Low-Abundance Protein Access by Combinatorial Peptide Libraries. In *Low-Abundance Proteome Discovery*, Elsevier, 2013; pp. 79-157, https://doi.org/10.1016/B978-0-12-401734-4.00004-X

[58] Zhang, D.; Gan, R.; Ge, Y.; Yang, Q.; Ge, J.; Li, H.; Corke, H. Research Progress on the Antibacterial Mechanisms of Carvacrol: A Mini Review. *Bioactive Compounds in Health and Disease* **2018**, *1*, 71-81. https://doi.org/10.31989/bchd.v1i6.551

[59] Marinelli, L.; Di Stefano, A.; Cacciatore, I. Carvacrol and its derivatives as antibacterial agents. *Phytochem Rev* **2018**, *17*, 903–921, https://doi.org/10.1007/s11101-018-9569-x

[60] Stratakos, A.C.; Sima, F.; Ward, P.; Linton, M.; Kelly, C.; Pinkerton, L.; Stef, L.; Pet, I.; Corcionivoschi, N. The in vitro effect of carvacrol, a food additive, on the NB pathogenicity of O157 and non-O157 Shiga-toxin producing *Escherichia coli*. Food Control; **2017**, Food Control, 84, 290-296.doi: https://doi.org/10.1016/j.foodcont.2017.08.014

[61] Engel, J.B.; Heckler, C.; Tondo, E.C.; Daroit, D.J.; da Silva Malheirosm P. Antimicrobial activity of free and liposome-encapsulated thymol and carvacrol against *Salmonella* and *Staphylococcus aureus* adhered to stainless steel. *International journal of food microbiology* **2017**, *252*, 18-23. https://doi.org/10.1016/j.ijfoodmicro.2017.04.003

[62] Carvalho, R.I.; Medeiros, A.S.D.J.; Chaves, M.; Souza, E.L.D.; Magnani, M. Lipids, pH, and their interaction affect the inhibitory effects of carvacrol against *Salmonella typhimurium* PT4 and Escherichia coli O157:H7. *Front Microbiol* **2017**, *8*. https://doi.org/10.3389/fmicb.2017.02701

[63] Chung, D.; Cho, T.J.; Rhee, M.S. Citrus fruit extracts with carvacrol and thymol eliminated 7-log acid-adapted *Escherichia coli* O157:H7, *Salmonella typhimurium*, and Listeria monocytogenes: A potential of effective natural antibacterial agents. *Food Res Int* **2018**, *107*, 578. https://doi.org/10.1016/j.foodres.2018.03.011

[64] Garcez, W.S.; Yoshida, M.; Gottlieb, O.R. Benzylisoquinoline alkaloids and flavonols from Ocotea vellosiana. *Phytochemistry* **1995**, *39*, 815-816. https://doi.org/10.1016/0031-9422(94)00961-R

[65] Kawahara, N.; Satake, M.; Goda, Y. A new acylated flavonol glycoside from the leaves of *Eriobotrya japonica*. *Chemical and pharmaceutical bulletin* **2002**. *50*, 1619-1620. https://doi.org/10.1248/cpb.50.1619

[66] Lee, S.S.; Lin, H.C.; Chen, C.K. Acylated flavonol monorhamnosides, α-glucosidase inhibitors, from *Machilus philippinensis*. *Phytochemistry.* **2008**, *69*, 2347-2353. https://doi.org/10.1016/j.phytochem.2008.06.006

[67] Otsuka, N.; Liu, M.H.; Shiota, S.; Ogawa, W.; Kuroda, T.; Hatano, T.; Tsuchiya, T. Anti-methicillin resistant *Staphylococcus aureus* (MRSA) compounds isolated from *Laurus nobilis*. *Biological and Pharmaceutical Bulletin* **2008**, *31*, 1794-1797. https://doi.org/10.1248/bpb.31.1794

# CHAPTER 5

# Development of Cellulose Films Functionalized with Bioactive Plant-Derived Compounds

Shurooq Ismail

Department of Chemical Sciences, PhD in Biotechnology

University of Naples Federico II

# Development of Cellulose Films Functionalized with Bioactive Plant-Derived Compounds

## 1. Introduction

Active packaging refers to a packaging system that is used to extend the shelf-life, freshness and safety of packaged food [1]. Active packaging systems could be divided into two major categories: (i) those absorbing undesired moisture, carbon dioxide, oxygen, ethylene, or unpleasant odors, and (ii) those releasing active compounds, such as antimicrobials or antioxidants [2]. In traditional manufacturing systems, active compounds are added to the bulk of the processed or fresh food. It is worthy to note, that most of food spoilage or contaminations involve the surface and not the bulk of the food. Hence, it appears more efficient to add antimicrobial compounds on the surface of the packaged food also considering that the direct addition of active compounds to the bulk of the food might cause a loss or a decrease of their activity due to direct interactions with food components [2]. It was estimated that about 1.3 billion tons of food resources are wasted every year all over around the world [3]. In this scenario, a fundamental aspect is represented by food spoilage that might be prevented by effective packaging systems representing a barrier protecting food samples from physical, environmental or biological damages that might occur during transportation or storage [2][4,5]. Several biodegradable polymers were exploited in packaging industry [6-8] **(Figure 1).**

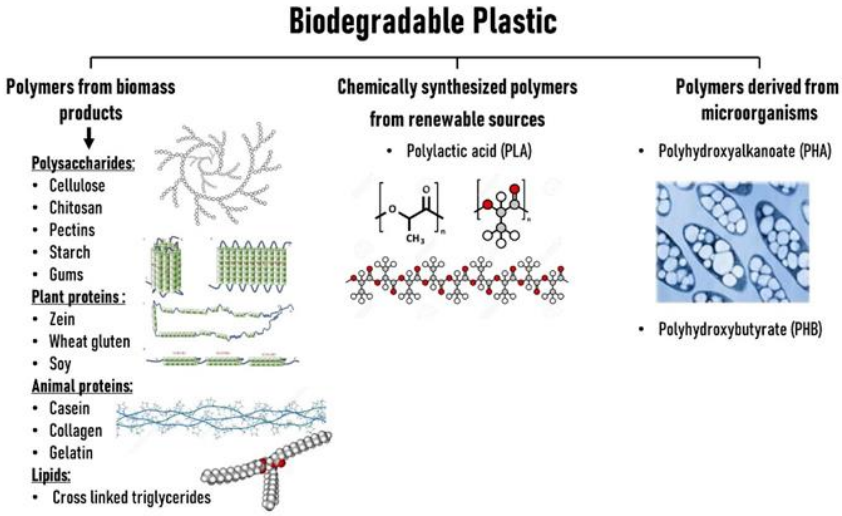


**Figure 1.** Biodegradable plastic polymers employed in food packaging industry (Adapted from Romão *et al.,* 2022 **and** Rehman *et al.*, 2020).

Among available alternatives, cellulose is a promising polymer employed in food packaging industry. It is obtained from plant cell walls, and it is highly available, inexpensive, renewable, biodegradable, environmentally sustainable and above of all biocompatible and safe to be used in food biotechnological applications [9,10]. Moreover, unique mechanical properties and high thermal resistance had characterized cellulose and its derivatives. They are also provide an impermeable physical isolation from ultraviolet rays and other environmental factors [10,11].

In recent years, cellulose and its derivatives were loaded with several antimicrobials and antioxidants, in order to enhance the quality and to prolong the shelf-life of packaged food samples [12]. Hydroxyethyl cellulose (HEC) is a non-ionic hydrophilic cellulose obtained upon the substitution of hydroxyl groups with hydroxyethyl groups [13]. It is widely used in cosmetics, cleaning solutions, and other household products as a thickening agent [6]. Furthermore, it was reported that carboxymethyl cellulose (CMC) was cross-linked with HEC by using citric acid to produce CMC-HEC films able to remove heavy metals from wastewater [14]. In biomedical field, HEC hydrogels were found to be suitable as wound dressing material [15]. In food field, several studies proved the applicability of HEC films to develop active packaging systems [16-18].

Cyclodextrins (CDs) are cyclic, non-reducing oligosaccharides produced by enzymatically modified starch [19]. They can be identified to 3 main classes of CDs derivatives: α-CD, β-CD, and γ-CD characterized by 6, 7 or 8 glucose units, respectively **(Figure 2)** [19-21]. CDs were described as a suitable system to deliver drugs in several biomedical, cosmeceutical, and food technology applications [19,20]. Regarding their applicability in food field, CDs attracted researchers' attention by beening recognized as safe (GRAS) [22]. Furthermore, they were found not to alter the packaged food quality, taste, and color [19].

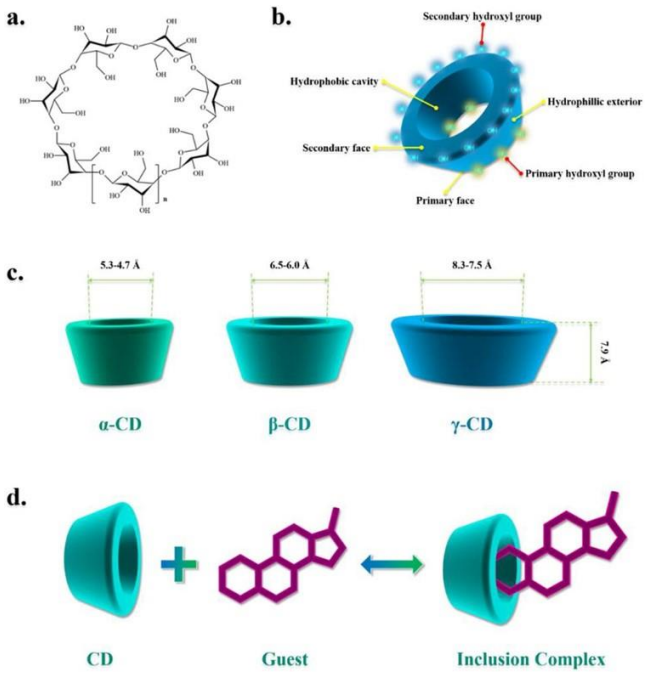


**Figure 2.** Cyclodextrins (CDs) general structures (**a**) the monomer unit with units, (**b**) Digital structure of CDs (**c**) the structures of α-, β-, and γ-CDs. (**d**) Digital representation of inclusion complex formation. Reused from Liu Y. *et al.,* 2022.

This chapter was dedicated to develop a model of food packaging system. Films were obtained by cross-linking hydroxyethyl cellulose (HEC) with citric acid in addition to HPβCD to encapsulate hydrophobic compounds. Once prepared, films were functionalized with the model compound, quercetin, which is known for its antioxidant and antimicrobial properties [23-25], as well as, the novel identified compound from *E. foeminea* plant namely kaempferol-3-*O*-α-L-(2”,4”-di-*E*-*p*-coumaroyl)-rhamnopyranoside that was functionalized to the prepared films. Moreover, the films physical and biological properties were evaluated and reported in the following sections.

## 2. Methods

**2.1 Materials.** All the reagents were purchased from Sigma-Merck (Milan, Italy), unless specified otherwise. Hydroxyethyl cellulose (HEC; Natrosol$^{TM}$ 250 HX) was purchased from Ashland Industries Europe GmbH, Switzerland**.** Citric acid 1-hydrate ($C_6H_8O_7.H_2O$; MW = 210.14 g/mol) and glycerol QP ($C_3H_8O_3$; MW = 92.10 g/mol) were purchased from PRS Panreac, Barcelona, Spain. Quercetin (Q4951-10G; $C_{15}H_{10}O_7$; MW = 302.24 g/mol) was obtained from Sigma-Merck. 2-Hydroxypropyl Beta Cyclodextrin (HPβCD; Kleptose® HP oral grade; high average molar substitution = 0.85; MW 1480.7 g/mol) was purchased from Roquette® (France). Absolute ethanol was obtained from VWR Chemicals, France.

**2.2 Preparation of films of Hydroxyethyl Cellulose (HEC) containing 2-Hydroxypropyl Beta Cyclodextrin (HEC-HPβCD).** HEC-HPβCD films were prepared by dissolving HEC powder in boiling distillated water (2%,*w/v*) under vigorous stirring obtained by using a VWR/VOS 60 homogenizer. After about 2h, completely dissolved HEC powder was mixed with HPβCD (0.5 %, *w/v*), and the plasticizing agent glycerol was incorporated into the mixture (0.1 %,*v/v*). The cross-linking agent citric acid was finally added (10 %,*w/w*) at room temperature under continuous stirring of (150 rpm). After 6h, the homogenous solution was poured into a ceramic mold (12 cm diameter) and incubated at 37°C for 16h to allow water evaporation upon temperature increase up to 80°C to dry the films 8h. Cross-linking was achieved by incubating the film at 110°C for 1h. The film was then stored at room temperature until usage. HEC films without HPβCD were prepared by using the same procedure with the only exception of HPβCD powder addition.

**2.3 Calibration curves prepared to evaluate loading and release from films.** Calibration curves were prepared based on absorbance measurements ($\lambda_{max}$) by using UV- visible spectrophotometer with 1.0 cm matching quartz cell. To do this, 125 µg/mL of quercetin were scanned from 190 nm to 800 nm against a mixture of ethanol and water (50:50,*v/v*) as a blank. Wavelength range was selected around wavelength maximum ($\lambda_{max}$ = 374 nm). The calibration curve was constructed by plotting absorbance *versus* concentration values (40-1.25 µg/mL; **Figure 3**). Calibration curves were constructed by performing a linear regression analysis.

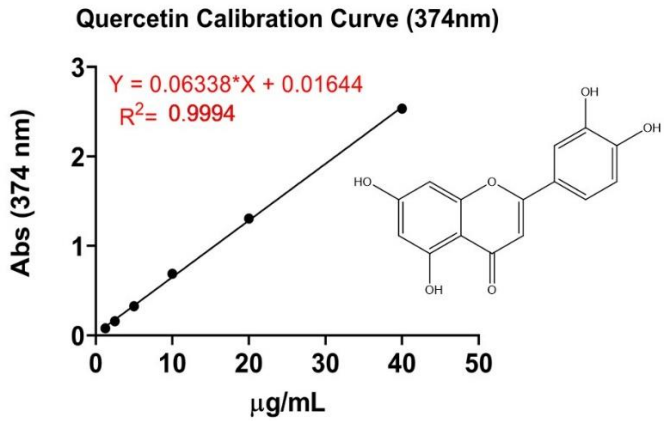


**Figure 3.** Calibration curve obtained for pure quercetin. Data represents the mean (±standard deviation, SD) of at least three independent experiments.

The same procedure was employed for kaempferol-3-*O*-α-L-(2",4"-di-*E*-*p*-coumaroyl)-rhamnopyranoside. The absorbance of this compound (100 µg/mL) was scanned from 190 nm to 800 nm against a mixture of ethanol and water (50:50,*v/v*) as a blank. Wavelength range was selected around wavelength maximum ($\lambda_{max}$ = 316 nm). The calibration curve was constructed by plotting absorbance values at $\lambda_{max}$ *versus* concentration values (24 – 0.38 µg/mL; **Figure 4**). Calibration curves were constructed by performing a linear regression analysis.

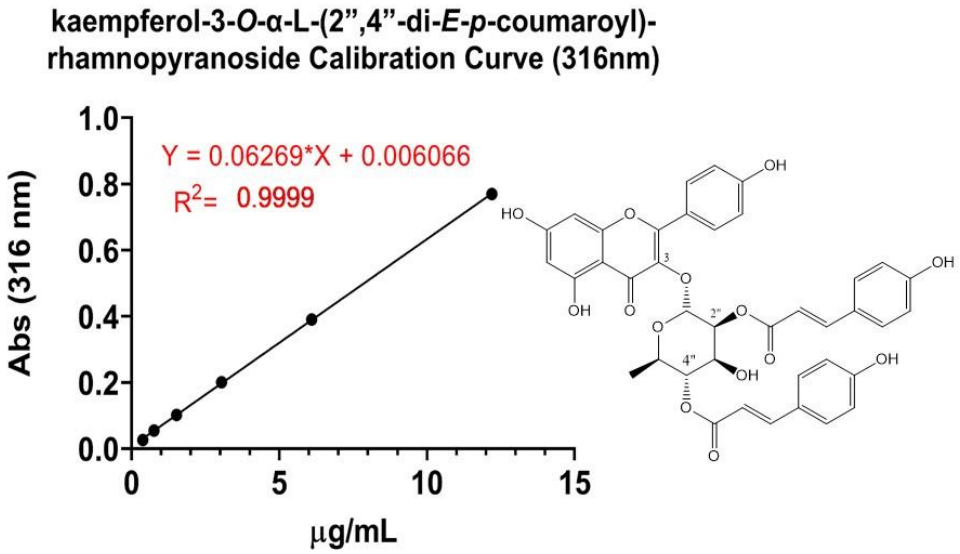


**Figure 4.** Calibration curve of kaempferol-3-*O*-α-L-(2",4"-di-*E*-*p*-coumaroyl)-rhamnopyranoside. Data represents the mean (±standard deviation, SD) of at least three independent experiments.

**2.4 Quercetin Loading and Release Experiments.** HEC and HEC-HPβCD films (1cm$^2$ area) were placed in separate vials in the presence of 5 mL of quercetin (5,000 µg/mL) in an ethanol: water (50:50,*v/v*) solution. Films were then placed at 37°C under stirring (180 rpm) in the dark. The absorbance of quercetin solution employed for film loading was monitored at 374 nm (UV–Vis spectrophotometer Agilent 8534, Waldbronn, Germany). In this way, the amount of loaded quercetin was evaluated by subtracting the amount of quercetin remaining in the solution (determined by using previously prepared calibration curves) from the total initial amount [26]. Release experiments were carried out by placing quercetin-loaded films (previously rinsed with Ethanol 50 %) in Falcon® tubes containing 10mL of ethanol 50% [27]. The tubes were incubated at 37°C under stirring (180 rpm) in the dark. Samples were taken every hour in the first 8h of incubation, and their absorbance values were measured at 374 nm (Agilent 8534, Waldbronn, Germany). Loading analyses were performed for 96h. Quercetin amount was determined based on calibration curves prepared as described above **(Figure 3)**.

**2.5 Isolated kaempferol-3-*O*-α-L-(2",4"-di-*E*-*p*-coumaroyl)-rhamnopyranoside Loading and Release Experiments.** HEC and HEC-HPβCD films (1cm$^2$ area) were placed in separate wells of a 24-multiwell plate in the presence of 0.5 mL of kaempferol-3-*O*-α-L-(2",4"-di-*E*-*p*-coumaroyl)-rhamnopyranoside (500 µg/mL) in a solution of ethanol: water (50:50,*v/v*) solution. Films were then placed at 37°C under stirring (180 rpm). The absorbance of kaempferol-3-*O*-α-L-(2",4"-di-*E*-*p*-coumaroyl)-rhamnopyranoside solution employed for film loading was monitored at $\lambda_{max}$ 316 nm (UV–Vis spectrophotometer Agilent 8534, Waldbronn, Germany) for 96h. The amount of loaded kaempferol-3-*O*-α-L-(2",4"-di-*E*-*p*-coumaroyl)-rhamnopyranoside was calculated by subtracting the amount of the compound remaining in the solution after 96h from the total initial amount. Amount of kaempferol-3-*O*-α-L-(2",4"-di-*E*-*p*-coumaroyl)-rhamnopyranoside was determined on the basis of absorbance values by using calibration curves prepared as described above **(Figure 4)** [28]. Release experiments were carried out by placing kaempferol-3-*O*-α-L-(2",4"-di-*E*-*p*-coumaroyl)-rhamnopyranoside-loaded films (previously rinsed with Ethanol 50 %) in Falcon® tubes containing 10 mL of ethanol 50% as a food stimulant [27]. The tubes were then incubated at 37°C under stirring (180 rpm). Aliquots were taken from the solution every hour in the first 8h of the experiment, and their absorbance values were determined at 316 nm. Analyses were carried out for 192h. Also in this case, kaempferol-3-*O*-

α-L-(2”,4”-di-*E*-*p*-coumaroyl)-rhamnopyranoside amount was determined on the basis of calibration curves prepared as described above **(Figure 4)**.

**2.6 Water uptake.** HEC and HEC-HPβCD films (1 $cm^2$) were dried for 1 day at 37°C, weighed, and placed into Falcon® tubes in the presence of 5 mL of quercetin (5,000μg/mL), as well as in water and in a solution containing 50% ethanol at room temperature. Three replicates were tested each hour during the first 8h and then every 24h for 4 days. Every time, films' surfaces were carefully wiped with an absorbent paper, to remove the excess water, and then weighed. The increase in weight, corresponding to the water uptake, was determined by using the equation below (1) where $W_0$ and $W_t$ represent the weight of dried film and of swollen film at time t, respectively.

$$\text{Water uptake } (\%) = \frac{Wt - W0}{W0} \times 100 \qquad (1)$$

**2.7 Fourier-Transform Infrared (FT-IR) spectroscopy analyses.** IR spectra were recorded at room temperature by using an infrared spectrometer (FTIR Shimadzu-IR Prestige 21, Shimadzu Corporation, Kanda-Nishikicho, Tokyo, Japan) with a total attenuated internal reflection (ATR). All the spectra were obtained with resolution of 4 $cm^{-1}$ (32 scans) in the range of 4000-400 $cm^{-1}$.

**2.8 Mechanical Properties.** Tensile properties of the films and Young's modulus were investigated by using a TA.XT Plus Texture Analyzer, Stable Micro Systems, Ltd., Surrey, UK and a load cell of 30 kg. Each film sample was prepared with the dimensions of 10 mm X 35 mm and placed between grip heads of the testing machine at room temperature. Stress–strain plots were recorded at a crosshead speed of 0.1 mm/s with triplicated determinations. Young's modulus was calculated from the slope of the linear portion of the stress *versus* strain curves while the percentage of elongation at break (% E) was determined by using the equation below (2).

$$\text{Elongation break } (\%) = \frac{L(\text{at break})}{L0} \times 100 \qquad (2)$$

**2.9 Bacterial strains and growth conditions.** Six bacterial strains were used to evaluate the antibacterial properties of quercetin, *i.e.*, *S. aureus* ATCC 29213, methicillin-resistant *S. aureus* MRSA WKZ-2, *E. faecalis* ATCC 29212*, A. baumannii* ATCC 17878*, E. coli* ATCC 25922 and *S. typhimurium* ATCC 14028. American type culture collection (ATCC) numbers represent the standard strain numbers assigned to these microorganisms. Bacterial strains were grown in Muller Hinton

Broth (MHB; Becton Dickinson Difco, Franklin Lakes, NJ/USA) and on Tryptic Soy Agar (TSA; Oxoid Ltd., Hampshire, UK). In all the experiments, bacteria were inoculated and grown overnight in MHB at 37°C.

**2.10 Quercetin antimicrobial activity.** The antimicrobial activity of quercetin was tested against six bacterial strains. Bacterial cells were diluted to $2x10^6$ CFU/mL in Nutrient Broth (NB; Difco, Becton Dickinson, Franklin Lakes, NJ) along with increasing amounts of quercetin. Broth microdilution method was employed [29]. $MIC_{100}$ values were determined as the lowest concentration of quercetin responsible for no visible bacterial growth after overnight incubation.

**2.11 Antimicrobial activity of loaded films.** The antimicrobial activity of HEC and HEC-HPβCD films loaded with quercetin or kaempferol-3-*O*-α-L-(2",4"-di-*E*-*p*-coumaroyl)-rhamnopyranoside was evaluated by using as control unloaded films that were extensively washed by using sterile milli-Q water to remove the excess of acetic acid used as a cross-linker during films preparation. Both loaded and unloaded films were sterilized by UV treatment for 20 min. afterwards, bacterial solutions were prepared starting from a single colony that was transferred into 5 mL of MHB and grown at 37°C to mid-log phase. Then, bacterial suspensions were diluted using 0.5X NB to reach a density of 1,000 CFU/$cm^2$. The bacterial suspension (0.5 mL) was then placed upon each film and incubated at 37°C for 3-4h. Following incubation, bacterial supernatants were transferred from each well to a sterile Eppendorf tube, diluted and plated to evaluate the planktonic cells growth. The remaining films were rinsed with 1 mL of sterile 0.9% NaCl, in order to remove the non-adherent bacteria. Films were then washed and transferred into a sterile Eppendorf tube containing 1 mL of 0.5X NB. Adherent bacterial cells were detached by vortexing for 1-5 min. Upon dilution, 100 µL of each sample were transferred on TSA plates as duplicates. Plates were incubated at 37°C for 16h and colonies were counted to evaluate the antibacterial activity of the loaded films.

**2.12 Statistical analyses.** Statistical analyses were performed by using Student's t-test. Significant differences were indicated as * $P < 0.05$, ** $P < 0.01$ or *** $P < 0.001$. Graphs were performed by using GraphPad Prism 8 software.

# 3. Results

## 3.1 Structural characterization of HEC and HEC-HPβCD films loaded with quercetin.

Average thickness of HEC and HEC-HPβCD films was found to be approximately 0.0785 ± 0.0045 mm **(Table 1)**.

**Table 1**: Mechanical properties of HEC and HEC-HPβCD films containing or not quercetin. Data represent the mean (±standard deviation, SD) of at least three independent experiments.

| Film | Film Thickness (mm) | Young's Modulus (MPa) | Elongation Break (%) |
|---|---|---|---|
| **HEC** | 0.087 ± 0.012 | 13.37 ± 0.75 | 140.15 ± 8.04 |
| **HEC-HPβCD** | 0.077 ± 0.006 | 10.42 ± 0.72 | 158.48 ± 5.34 |
| **Quercetin-HEC** | 0.06 ± 0.000 | 2.19 ± 0.61 | 192.52 ± 26.07 |
| **Quercetin-HEC-HPβCD** | 0.09 ± 0.000 | 0.27 ± 0.06 | 213.59 ± 6.48 |

Both HEC and HEC-HPβCD films were prepared by esterification cross-linking mechanism [30]. Citric acid (10% w/w) was used as a non-toxic cross-linking agent. The optimal temperature value to obtain stable transparent films as shown in **Figure 5** was set at 110°C.

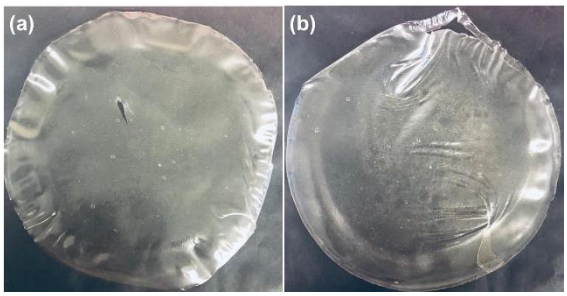


**Figure 5.** Appearance of casted HEC films (**a**) and of HEC-HPβCD films (**b**).

To evaluate the films water uptake potentials, changes in film weight over time upon immersion in water or ethanol (50%) at room temperature. In all the cases, both kinds of films were found to reach complete swelling (saturation state) within 30 min immersion (**Figure 6 and b**). The swelling rate was found to be slightly higher in the case of HEC-HPβCD films (60%) **(Figure 6b)** with respect to HEC films (40%)

**(Figure 6a)**. This might be due to the hydrophilic nature of HPβCD whose presence might confer higher hydration capacity [31].

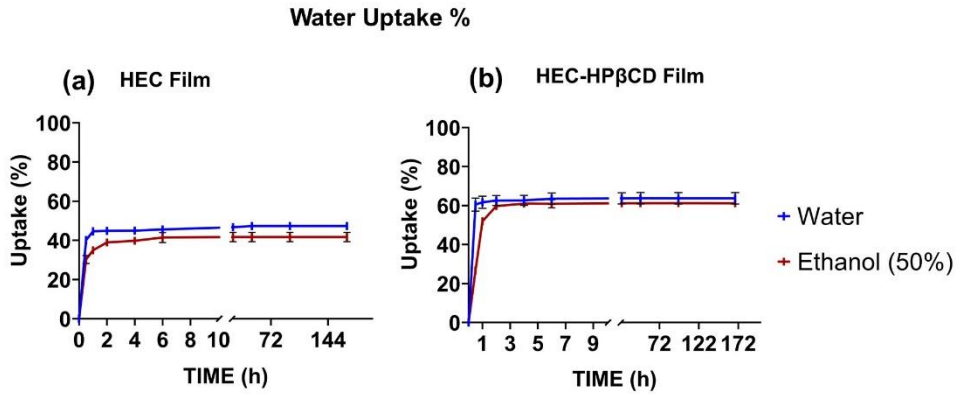


**Figure 6.** Water uptake ability of HEC (**a**) and HEC-HPβCD films (**b**) in absolute water or in water containing 50% ethanol. Data represents the mean (±standard deviation, SD) of at least three independent determinations.

Since one of the most important features of films employed in food packaging applications is their strength, Young's modulus and elongation break were recorded at room temperature **(Table 1)** as described in the Materials and Methods Section. No significant differences were detected between HEC and HEC-HPβCD films. In the presence of quercetin, instead, a higher strength and stretch ability before break was detected probably due to the interaction between loaded drug and HEC polymer [32]. ATR–FTIR analyses of produced films were also performed **(Figure 7 and 8)**. When HEC and HEC-HPβCD films loaded with quercetin were analyzed, it was observed the presence of novel peaks between 1456.24 - 1398.39 $cm^{-1}$ not present when the spectra of quercetin alone or of the films alone were analyzed (**Figure 7 and 8**), a clear indication of the effective incorporation of quercetin compound in the prepared films. Furthermore, it should be highlighted that, when films spectra were analyzed, a peak at 1687.71 $cm^{-1}$ was observed **(Figure 7 and 8)**, indicative of C=O ester bonds due to the cross-linking mediated by citric acid.

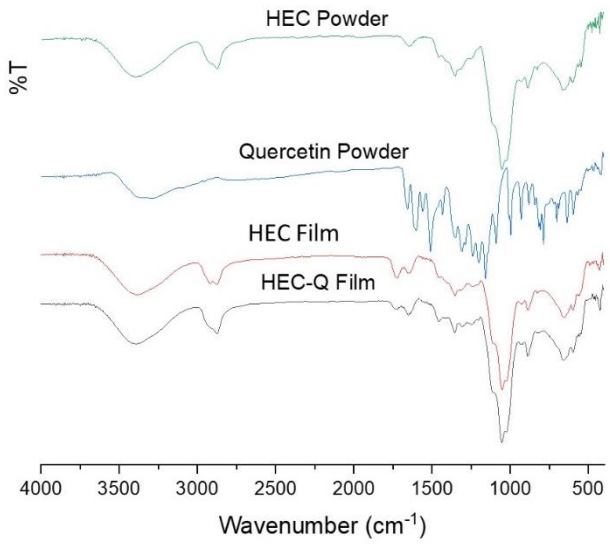


**Figure 7.** ATR–FTIR spectra of quercetin, HEC powder, HEC film and HEC films loaded with quercetin.

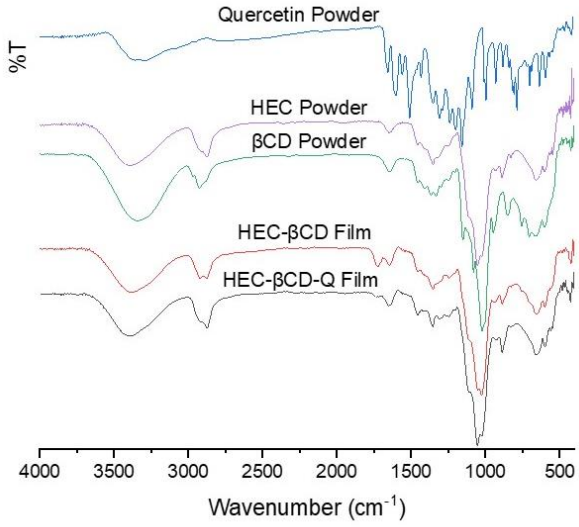


**Figure 8.** ATR–FTIR spectra of quercetin, HEC powder, HPβCD powder, HEC-HPβCD films and HEC-HPβCD films loaded with quercetin.

## 3.2 Analysis of quercetin loading and release from HEC and HEC-HPβCD films.

The effective loading of quercetin in prepared films was evaluated as described in details in the Materials and Methods Section. As shown in **Figure 9**, a fast loading of quercetin was observed in the

case of both films in the first 24 h of incubation **(Figure 9)**. It was also found that about 60% of initial quercetin was loaded in the case of HEC-HPβCD films, whereas only 40% of initial quercetin was loaded in the case of HEC films (**Figure 9**). This different behavior might be due to the presence of hydrophilic HPβCD, which was able to entrap a higher amount of quercetin compound. However, it has to be highlighted that, once loaded, quercetin was not significantly released from films (**Figure 10**) probably because of the formation of electrostatic interactions between the carboxyl groups of the films and the loaded quercetin [27][30].

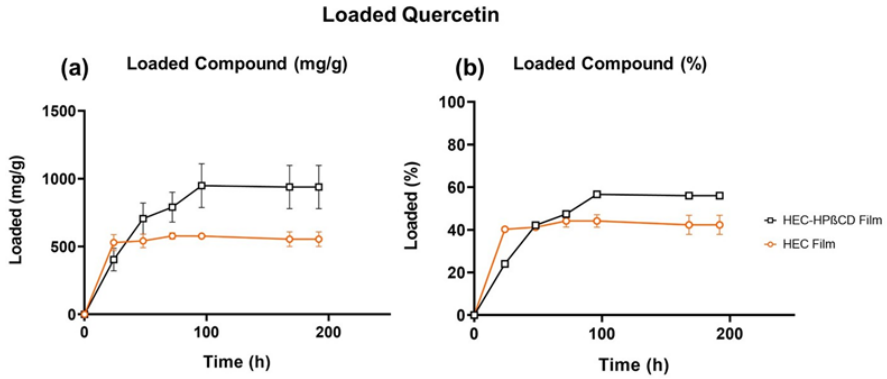


**Figure 9.** Cumulative loading of quercetin into both HEC and HEC-HPβCD films reported as mg of quercetin *per* g of the film (**a**) or as percentage values (**b**). Loading was recorded for seven days. The test was carried out in quadruplicate.

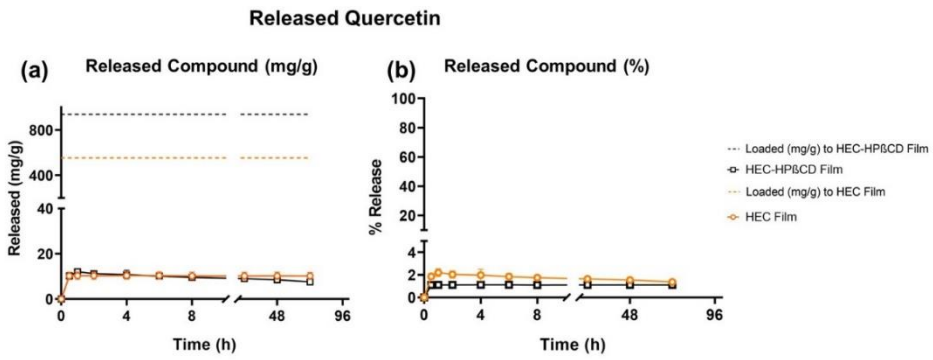


**Figure 10.** Cumulative release of quercetin from both HEC and HEC-HPβCD films reported as mg of quercetin per g of the film (**a**) or as percentage values (**b**). Release was recorded for three days. The test was carried out in quadruplicate.

### 3.3 Analysis of kaempferol-3-*O*-α-L-(2",4"-di-*E*-*p*-coumaroyl)-rhamnopyranoside loading and release from HEC and HEC-HPβCD films.

Once the model films were set-up using quercetin, the same kinds of films were prepared by loading kaempferol-3-*O*-α-L-(2",4"-di-*E*-*p*-coumaroyl)-rhamnopyranoside as described in the Materials and Methods Section. As shown in **Figure 11**, about 40% of kaempferol-3-*O*-α-L-(2",4"-di-*E*-*p*-coumaroyl)-rhamnopyranoside was loaded in the case of both HEC and HEC-HPβCD films after 96h incubation. Release experiments were also performed as described in the Materials and Methods Section. As shown in **Figure 12**, about 40% release was detected in the case of HEC films and about 60% release was detected in the case of HEC-HPβCD films. Detected differences in the release rate might be due to the presence of hydrophilic HPβCD, which was probably responsible for the higher swell-ability of HEC-HPβCD films, with a consequent higher diffusion rate [30].

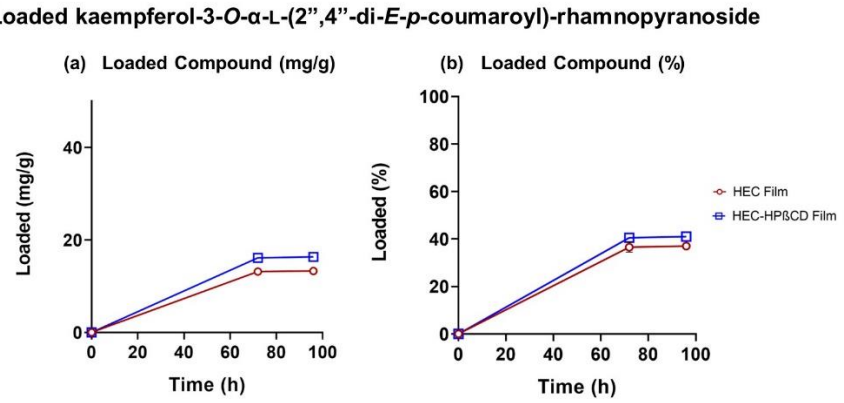


**Figure 11.** Cumulative loading of kaempferol-3-*O*-α-L-(2",4"-di-*E*-*p*-coumaroyl)-rhamnopyranoside into both HEC and HEC-HPβCD films reported as mg of compound *per* g of film (**a**) or as percentage values (**b**). Loading was recorded for 96 h. The test was carried out in duplicate.

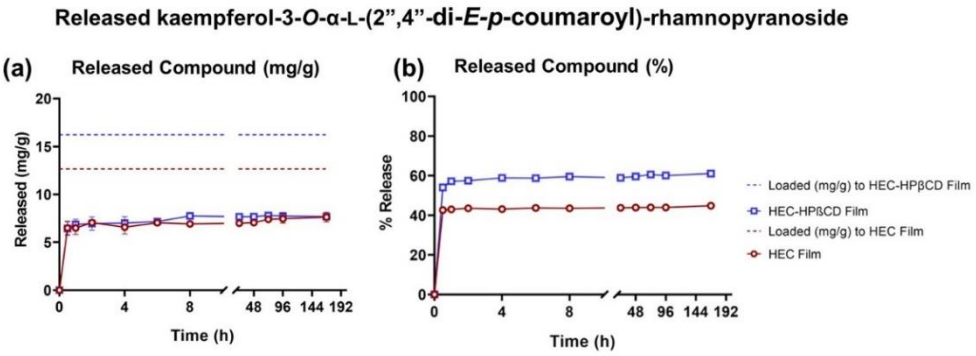


**Figure 12.** Cumulative release of kaempferol-3-*O*-α-L-(2",4"-di-*E*-*p*-coumaroyl)-rhamnopyranoside from both HEC and HEC-HPβCD films reported as mg of compound per g of films (**a**) or as percentage values (**b**). Release was recorded for 192 h. The test was carried out in duplicate.

## 3.4 Evaluation of the antimicrobial activity of quercetin loaded films.

Prior to the evaluation of the antimicrobial properties the quercetin-loaded films, the antibacterial activity of quercetin alone was evaluated on a panel of Gram-positive and Gram-negative bacterial strains: *S. aureus* ATCC 29213, *S. aureus* MRSA WKZ-2, *E. faecalis* ATCC 29212, *A. baumannii* ATCC 17878, *E. coli* ATCC 25922, and *S. typhimurium* ATCC 14028. As shown in **Figure 13**, a strong activity against *A. baumannii* ATCC 17878 bacterial strain was observed ($MIC_{100}$ = 1.08 mg/mL). Although the antimicrobial activity of quercetin was extensively described, it was also reported that its main disadvantage is its hydrophobicity that is limiting its applicability in *in vitro* and *in vivo* assays [33].

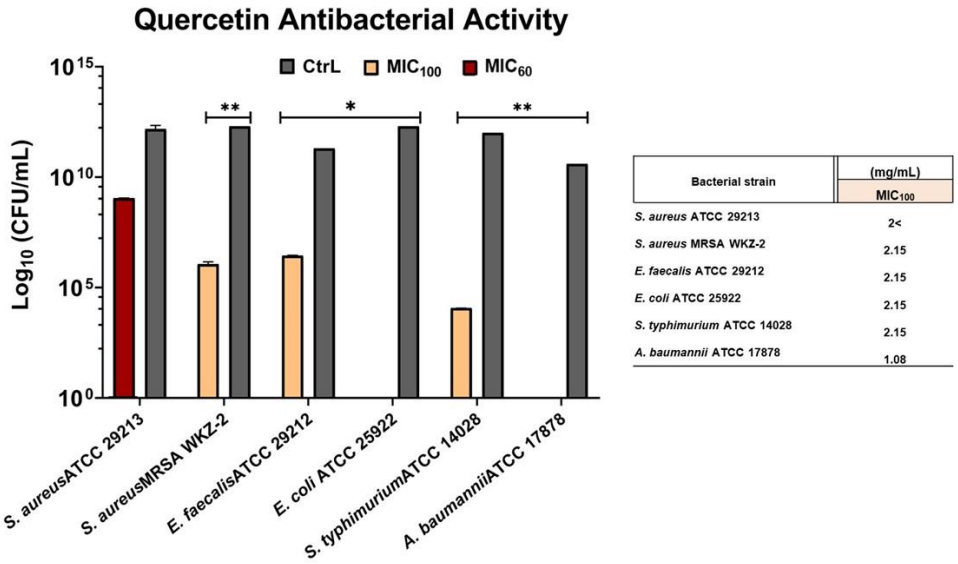


| Bacterial strain | (mg/mL) MIC100 |
|---|---|
| *S. aureus* ATCC 29213 | 2< |
| *S. aureus* MRSA WKZ-2 | 2.15 |
| *E. faecalis* ATCC 29212 | 2.15 |
| *E. coli* ATCC 25922 | 2.15 |
| *S. typhimurium* ATCC 14028 | 2.15 |
| *A. baumannii* ATCC 17878 | 1.08 |

**Figure 13.** Minimal Inhibitory Concentration $MIC_{100}$ (mg/mL) values determined for quercetin tested against *S. aureus* MRSA WKZ-2, *E. faecalis* ATCC 29212, *A. baumannii* ATCC 17878, *E. coli* ATCC 25922, and *S. typhimurium* ATCC 14028 bacterial strains. Data represents the mean (±standard deviation, SD) of three independent experiments.

The antimicrobial activity of HEC and HEC-HPβCD films loaded with quercetin was also analyzed against *A. baumannii* ATCC 17878 bacterial strain. Accordingly, due to the low quercetin release rate detected in previous experiments, no significant antimicrobial properties were detected **(Figure 14)**.

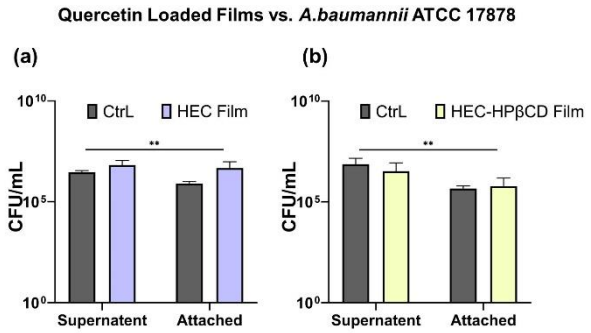


**Figure 14.** Antimicrobial activity of quercetin loaded HEC (**a**) or HEC-HPβCD films (**b**) against *A. baumannii* ATCC 17878 bacterial strain. Data represents the mean (±standard deviation, SD) of three independent experiments.

### 3.5 Evaluation of the antimicrobial activity of kaempferol-3-*O*-α-L-(2",4"-di-*E*-*p*-coumaroyl)-rhamnopyranoside loaded films.

The antimicrobial activity of HEC and HEC-HPβCD films loaded with kaempferol-3-*O*-α-L-(2",4"-di-*E*-*p*-coumaroyl)-rhamnopyranoside was analyzed against *S. aureus* ATCC 29213 bacterial strain, selected on the basis of its high susceptibility to kaempferol-3-*O*-α-L-(2",4"-di-*E*-*p*-coumaroyl)-rhamnopyranoside ($MIC_{100}$ = 0.5 μg/mL). A slight significant antimicrobial effect was detected only in the case of functionalized HEC-HPβCD films **(Figure 15b).**

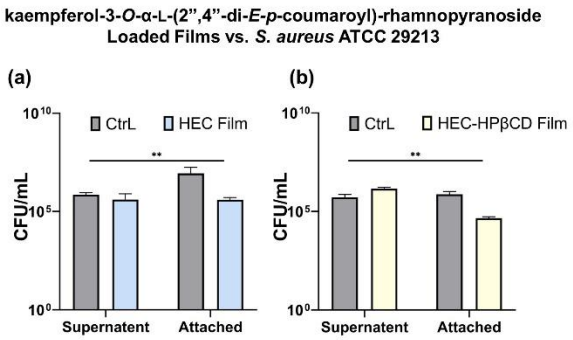


**Figure 15.** Antimicrobial activity of kaempferol-3-*O*-α-L-(2",4"-di-*E*-*p*-coumaroyl)-rhamnopyranoside loaded HEC (**a**) or HEC-HPβCD films (**b**) against *S. aureus* ATCC 29213 bacterial strain. Data represents the mean (±standard deviation, SD) of three independent experiments.

## 4. Discussion

In the last years, extensive research was devoted to the development of active food packaging systems that are biodegradable, safe and effective in improving the shelf-life or the freshness of packaged food products. Among available alternatives to produce edible films, cellulose was selected as it is a natural, abundant, and biocompatible polymer found to be suitable for food packaging applications [10]. Indeed, cellulose derived hydrogels (HEC) are considered as good delivery systems for hydrophilic compounds due to their polar properties [31]. The inclusion of cyclodextrins (CDs) into cellulose films was reported as an effective strategy to deliver hydrophobic and water insoluble compounds as well [31].

In the present Thesis, plant-derived kaempferol-3-*O*-α-L-(2",4"-di-*E*-*p*-coumaroyl)-rhamnopyranoside was loaded into HEC films in the absence or in the presence of βCDs (HPβCD) by using citric acid as the cross-linking agent at relatively high temperatures 110ºC **(Figure 5).** The effective formation of cross-links was verified by FT-IR analyses **(Figure 7 and 8).** It is important to notice that, in addition to cross-linking, the presence of citric acid has been reported to provide additional binding sites for the delivered compounds through the formation of ionic or hydrogen bonds. Involvement of the available free carboxyl and hydroxyl groups on the cross-linking agent enhanced the delivery of the functionalized compounds [31].

Both HEC and HEC-HPβCD films exhibited high swelling rates, probably due to the hydrophilic nature of HEC and to its high content in hydroxyl groups **(Figure 6)** [31]. A significant release of kaempferol-3-*O*-α-L-(2",4"-di-*E*-*p*-coumaroyl)-rhamnopyranoside from both HEC and HEC-HPβCD films was observed upon loading **(Figure 12b)** and a slight antimicrobial activity was detected in the case of functionalized HEC-HPβCD films.

Taking in to account these preliminary promising results; further investigations should be performed in the future by loading a higher amount of kaempferol-3-*O*-*α*-L-(2",4"-di-*E*-*p*-coumaroyl)-rhamnopyranoside into the selected films. Moreover, deep evaluation of the functionalized films' structural and mechanical properties, as well as, their antimicrobial and anti-biofilm activities is highly recommended, in order to verify films applicability in the food field as an effective active packaging system.

# 5. References


[1] Dainelli, D.; Gontard, N.; Spyropoulos, D.; Zondervan-van, den Beuken, E.; Tobback, P. Active and intelligent food packaging: legal aspects and safety concerns. *Trends in Food Science & Technology*,**2008**, *19*,S103-S112. https://doi.org/10.1016/j.tifs.2008.09.011

[2] Yildirim, S.; Röcker, B.; Pettersen, M. K.; Nilsen-Nygaard, J.; Ayhan, Z.; Rutkaite, R.; Radusin, T.; Suminska, P.; Marcos, B. ; Coma, V. Active packaging applications for food. *Comprehensive Reviews in Food Science and Food Safety*, **2018,** *17*(1), 165-199.https://doi.org/10.1111/1541-4337.12322

[3] Ishangulyyev, R.; Kim, S.; Lee, S. H. Understanding food loss and waste—why are we losing and wasting food?. *Foods*, **2019** *8*(8), 297. https://doi.org/10.3390/foods8080297

[4] Youssef, A.M.; Assem, F.M.; Abdel-Aziz, M.E.; Elaaser, M.; Ibrahim, O.A.; Mahmoud, M.; Abd El-Salam, M.H. Development of bionanocomposite materials and its use in coating of Ras cheese. *Food Chem*. **2019**, 270, 467–475. https://doi.org/10.1016/j.foodchem.2018.07.114

[5] Al-Tayyar, N.A.; Youssef, A.M.; Al-Hindi, R. Antimicrobial food packaging based on sustainable Bio-based materials for reducing foodborne Pathogens: A review. *Food Chem*. **2020**, 310, 125915. https://doi.org/10.1016/j.foodchem.2019.125915

[6] Romão, S.; Bettencourt, A.; Ribeiro, I. A. Novel Features of Cellulose-Based Films as Sustainable Alternatives for Food Packaging. *Polymers*,**2022**, *14*(22), 4968. https://doi.org/10.3390/polym14224968

[7] Huang, K.; Wang, Y. Recent applications of regenerated cellulose films and hydrogels in food packaging. *Current Opinion in Food Science*, **2022,** *43*, 7-17. https://doi.org/10.1016/j.cofs.2021.09.003

[8] Rehman, A.; Jafari, S. M.; Aadil, R. M.; Assadpour, E.; Randhawa, M. A.; Mahmood, S. Development of active food packaging via incorporation of biopolymeric nanocarriers containing essential oils. *Trends in Food Science & Technology*,**2020**, *101*, 106-121. https://doi.org/10.1016/j.tifs.2020.05.001

[9] Singh, P.; Magalhães, S.; Alves, L.; Antunes, F.; Miguel, M.; Lindman, B.; Medronho, B. Cellulose-based edible films for probiotic entrapment. *Food Hydrocoll*. **2018**, *88*, 68–74.https://doi.org/10.1016/j.foodhyd.2018.08.057

[10] He, X.; Lu, W.; Sun, C.; Khalesi, H.; Mata, A.; Andaleeb, R.; Fang, Y. Cellulose and cellulose derivatives: Different colloidal states and food-related applications. *Carbohydrate Polymers*. **2020**, 255, 117334. https://doi.org/10.1016/j.carbpol.2020.117334

[11] Liu, Y.; Ahmed, S.; Sameen, D. E.; Wang, Y.; Lu, R.; Dai, J.; Li, S; Qin, W. A review of cellulose and its derivatives in biopolymer-based for food packaging application. *Trends in Food Science & Technology*,**2021**, *112*, 532-546. https://doi.org/10.1016/j.tifs.2021.04.016

[12] David, G.; Gontard, N.; Angellier-Coussy, H. Mitigating the impact of cellulose particles on the performance of biopolyester-based composites by gas-phase esterification. *Polymers*,**2019**, *11*(2), 200. https://doi.org/10.3390/polym11020200

[13] Noreen, A.; Zia, K. M.; Tabasum, S.; Khalid, S.; Shareef, R. A review on grafting of hydroxyethylcellulose for versatile applications. *International journal of biological macromolecules*,**2020** *150*, 289-303. https://doi.org/10.1016/j.ijbiomac.2020.01.265

[14] Ayouch, I.; Kassem, I.; Kassab, Z.; Barrak, I.; Barhoun, A.; Jacquemin, J.; Draoui, K.; El Achaby, M. Crosslinked carboxymethyl cellulose-hydroxyethyl cellulose hydrogel films for adsorption of cadmium and methylene blue from aqueous solutions. *Surfaces and Interfaces,* **2021,** *24, 101124.* https://doi.org/10.1016/j.surfin.2021.101124

[15] El Fawal, G.F.; Abu-Serie, M.M.; Hassan, M.A.; Elnouby, M.S. Hydroxyethyl cellulose hydrogel for wound dressing: Fabrication, characterization and in vitro evaluation. *International journal of biological macromolecules*, **2018**,*111*, 649-659. https://doi.org/10.1016/j.ijbiomac.2018.01.040

[16] Liu, C.; Jin, T.; Liu, W.; Hao, W.; Yan, L.; Zheng, L. Effects of hydroxyethyl cellulose and sodium alginate edible coating containing asparagus waste extract on postharvest quality of strawberry fruit. *LWT,* **2021**, 148, 111770. https://doi.org/10.1016/j.lwt.2021.111770

[17] El Fawal, G.; Hong, H.; Song, X.; Wu, J.; Sun, M.; He, C.; Mo, X.; Jiang, Y.; Wang, H. Fabrication of antimicrobial films based on hydroxyethylcellulose and ZnO for food packaging application. *Food Packaging and Shelf Life*, **2020**, *23*, 100462. https://doi.org/10.1016/j.fpsl.2020.100462

[18] Rukmanikrishnan, B.; Ramalingam, S.; Kim, S.S.; Lee, J. Rheological and anti-microbial study of silica and silver nanoparticles-reinforced k-carrageenan/hydroxyethyl cellulose composites for food packaging applications.*Cellulose*,**2021**, *28*(9), 5577-5590.https://doi.org/10.1007/s10570-021-03873-z

[19] Liu, Y.; Sameen, D. E.; Ahmed, S.; Wang, Y.; Lu, R.; Dai, J.; Li, S.; Qin, W. Recent advances in cyclodextrin-based films for food packaging. *Food Chemistry*, *370*,**2022**, 131026. https://doi.org/10.1016/j.foodchem.2021.131026

[20] Poulson, B. G.; Alsulami, Q. A.; Sharfalddin, A.; El Agammy, E. F.; Mouffouk, F.; Emwas, A. H.; Jaremko, L.; Jaremko, M. (2021). Cyclodextrins: Structural, chemical, and physical properties, and applications. *Polysaccharides*,**2022**, *3*(1), 1-31. https://doi.org/10.3390/polysaccharides3010001

[21] Loftsson, T.; Brewster, M. E. Pharmaceutical applications of cyclodextrins. 1. Drug solubilization and stabilization. *Journal of pharmaceutical sciences*,**1996**, *85*(10), 1017-1025.https://doi.org/10.1021/js950534b

[22] Cai, R.; Yuan, Y.; Cui, L.; Wang, Z.; Yue, T. Cyclodextrin-assisted extraction of phenolic compounds: Current research and future prospects. *Trends in Food Science & Technology*,**2018**, *79*, 19-27. https://doi.org/10.1016/j.tifs.2018.06.015

[23] Božič, M.; Gorgieva, S.; Kokol, V. Homogeneous and heterogeneous methods for laccase-mediated functionalization of chitosan by tannic acid and quercetin. *Carbohydrate polymers*,**2012**, *89*(3), 854-864. https://doi.org/10.1016/j.carbpol.2012.04.021

[24] Jantarat, C.; Attakitmongkol, K.; Nichsapa, S.; Sirathanarun, P.; Srivaro, S. Molecularly imprinted bacterial cellulose for sustained-release delivery of

quercetin. *Journal of Biomaterials Science, Polymer Edition*,**2020**, *31*(15), 1961-1976.10.1080/09205063.2020.1787602

[25] Nguyen, T. L. A.; Bhattacharya, D. Antimicrobial Activity of Quercetin: An Approach to Its Mechanistic Principle. *Molecules*,**2022**, *27*(8), 2494. https://doi.org/10.3390/molecules27082494

[26] Vivero-Lopez, M.; Xu, X.; Muras, A.; Otero, A.; Concheiro, A.; Gaisford, S.; Basit, A.W.; Alvarez-Lorenzo, C.; Goyanes, A. Anti-biofilm multi drug-loaded 3D printed hearing aids. *Materials Science and Engineering: C*, **2021**, *119*, 111606.https://doi.org/10.1016/j.msec.2020.111606

[27] Baner, A.; Bieber, W.; Figge, K.; Franz, R.; Piringer, O. Alternative fatty food simulants for migration testing of polymeric food contact materials. *Food Additives & Contaminants*,**1992**, 9(2), 137-148. https://doi.org/10.1080/02652039209374056

[28] Lin, S. Y.; Chen, K. S.; Run-Chu, L. Design and evaluation of drug-loaded wound dressing having thermos responsive, adhesive, absorptive and easy peeling properties. *Biomaterials*,**2001**, 22(22), 2999-3004. https://doi.org/10.1016/S0142-9612(01)00046-1

[29] Gaglione, R.; Dell'Olmo, E.; Bosso, A.; Chino, M.; Pane, K.; Ascione F.; Itri F.; Caserta, S.; Amoresano, A.; Lombardi, A.; Haagsman, H.P. ; Piccoli, R.; Pizzo, E.; Veldhuizen, E.J.A.; Notomista, E.; Arciello, A. Novel human bioactive peptides identified in apolipoprotein B: evaluation of their therapeutic potential, *Biochemical Pharmacology*. **2017***, 130*, 34-50 https://doi.org/10.1016/j.bcp.2017.01.009

[30] Ghorpade, V.S.; Yadav, A.V.; Dias, R.J.; Mali, K.K. Fabrication of citric acid cross linked β-cyclodextrin / hydroxyethylcellulose hydrogel films for controlled delivery of poorly soluble drugs. *Journal of Applied Polymer Science*,**2018**, *135*(27), 46452.https://doi.org/10.1002/app.46452

[31] Ghorpade, V. S.; Yadav, A. V.; Dias, R. J. Citric acid crosslinked β-cyclodextrin/carboxymethylcellulose hydrogel films for controlled delivery of poorly soluble drugs. *Carbohydrate Polymers*,**2017**, *164*, 339-348. https://doi.org/10.1016/j.carbpol.2017.02.005

[32] Zulkifli, F. H.; Hussain, F. S. J.; Harun, W. S. W.; Yusoff, M. M. Highly porous of hydroxyethyl cellulose biocomposite scaffolds for tissue engineering. *International journal of biological macromolecules*,**2019**, *122*, 562-571.https://doi.org/10.1016/j.ijbiomac.2018.10.156

[33] Nguyen, T. L. A.; Bhattacharya, D. Antimicrobial Activity of Quercetin: An Approach to Its Mechanistic Principle. *Molecules*,**2022**, *27*(8), 2494. https://doi.org/10.3390/molecules27082494

# CHAPTER 6

# General Discussion and Concluding Remarks

Shurooq Ismail

Department of Chemical Sciences, PhD in Biotechnology

University of Naples Federico II

## General Discussion and Concluding Remarks

The discovery of penicillin by Sir Alexander Fleming in 1928 changed the course of medicine, leading to the introduction of antibiotics that greatly reduced the number of deaths from infections. However, the brilliance of antibiotics has turned out to be their weakness. As more antibiotics were being used to treat infections, the bacteria started to adapt to survive in the presence of these drugs, thus making them less effective. Without mitigation, antibiotic resistance will become a global threat within the next few decades. Certainly, if antibiotics are used at the current rate and bacterial resistance continues to develop making people more susceptible to life threatening diseases, people's life expectancy will be significantly reduced. "Super bugs" multidrug resistant (MDR) microbes were extensively described, thus revealing the current antimicrobial resistance (AMR) crisis [1]. The universal threat to human health imposed by AMR and the uncontrolled spread of MDR microbes is serious. If this issue is not resolved, the antibiotics used with great effectiveness in the past may no longer provide the required protection against bacterial infections [2]. It was reported that, in the absence of effective strategies, the increase in drug resistance could be responsible for the death of 10 million people *per* year by year 2050 [3]. Furthermore, AMR were found to influence not only human health but also other vital sectors, such as agriculture, veterinary, economy, and food industry. According to the alerts of World Health Organization (WHO), food contaminations are a serious public health threat with about 600 million people worldwide getting sick from eating contaminated food each year [4]. It was also reported that most food-borne bacteria are able to form biofilms, causing a consequent increase of their potency and resistance to antibiotics [5]. In this scenario, the development of effective alternatives to antibiotics, which are able to overcome AMR phenomenon, appears to be urgent.

Secondary metabolites of animals, plants, bacteria, algae, and fungi were extensively investigated for their antimicrobial properties [2]. Particularly, about 200,000 secondary plant metabolites were identified. Among these, 170,000 were found to possess distinctive chemical structures [6]. Alkaloids, terpenoids, and polyphenols are the plant secondary metabolites that are more frequently found to exert special antimicrobial properties [7]. The majority of antimicrobial agents can be divided into four major groups: (i) those interfering with the formation of cell walls, (ii) those inhibiting the synthesis of proteins, (iii) those interfering with the synthesis of nucleic acids, and (iv) those inhibiting a specific metabolic pathway [8]. Beyond plant-derived natural

compounds, antimicrobial peptides (AMPs) as well, attracted considerable attention as effective alternatives to antibiotics, by being endowed with a broad range of biological properties [9,10]. AMPs represent several advantages over conventional antibiotics, such as (i) the lower probability to induce resistance development, (ii) a broad-spectrum antimicrobial and anti-biofilm activity, and (iii) the ability to modulate host immune response [11]. Based on this, one of the main aims of the present thesis was to identify novel and effective antimicrobial plant-derived compounds and to evaluate their ability to act in synergism with selected AMPs, in order to set-up novel combinatorial therapeutic approaches which are able to counteract AMR.

**In chapter 2,** several plant extracts were screened for their antimicrobial and anti-biofilm properties. This screening represents a preliminary step to identify plants containing metabolites effective as antimicrobials. Several plant extracts were found to be active against Gram-positive and Gram-negative bacteria, with $MIC_{100}$ values ranging from 2 to 33 mg/mL. Among the screened plants, *E. foeminea* and *C. hyalolepis* extracts were found to exert the strongest antimicrobial properties. In the literature, the antimicrobial activity of the crude plant extracts was generally attributed to the presence of tannins, phenols, alkaloids, flavonoids, peptides, essential oils, and terpenoids [12,13]. It worthy to note that several factors play a crucial role in determining the antimicrobial efficacy of plant extracts, such as plant physiological state, geographical dispersion, and the season of cultivation [14]. Furthermore, it was widely reported that solvents used to prepare extracts have a strong influence on the chemical nature of obtained extracts and consequently, on their biological properties [15-19]. It is worthy to note, that generally a plant-derived compound is considered as antimicrobial with a MIC value in the range of 100-1,000 µg/mL unlike compounds isolated from fungi or bacteria that should possess a MIC value comprised between 0.01 and 10 µg/mL [20].

The ability of plant extracts to exert anti-biofilm properties was also investigated, considering that bacterial biofilms are powerful virulence factors conferring to bacterial ability to escape antibiotics and the human immune defense [18,19]. The crude extracts of *C. hyalolepis* and *E. foeminea* were found to exhibit anti-biofilm activity (50-60% inhibition of biofilm formation) against *E. coli* ATCC 25922 and *S. typhimurium* ATCC 14028 bacterial strains, whereas *S. aureus* ATCC 29213 strain was found to be resistant to their anti-biofilm properties. Detected anti-biofilm activity might be due to the concomitant presence

of several compounds in plant extracts and to the presence of iron as well as to the extracts acidity, all factors that might influence the quorum sensing (QS); a key step in the biofilm formation process [21]. Starting from the obtained promising results, efforts were devoted to the identification of the compounds responsible for the detected antimicrobial properties.

**In chapter 3,** a bio-guided purification of $CH_2CL_2$ extract of *C. hyalolepis* was performed. The isolated compounds were identified and found to be as three sesquiterpene lactones (STLs) namely cnicin, 11β,13-dihydrosalonitenolide, and salonitenolide. To the best of our knowledge, this is the first report describing a detailed purification of *C. hyalolepis* crude extract to discover active metabolites responsible for the bioactivities of the crude extract. *C. hyalolepis* which belongs to the well-known Asteraceae, also named as Compositae family [22]. *Centaurea* plant species contain several metabolites with STLs and flavonoids which are the predominant metabolites [23]. The isolated cnicin and salonitenolide were found to be endowed with antimicrobial activity ($MIC_{100}$ = 0.25 -1mg/mL) against the tested Gram-positive and Gram-negative strains (*S. aureus* ATCC 29213, *S. aureus* MRSA WKZ-2, *E. faecalis* ATCC 29212, *A. baumannii* ATCC 17878, *E. coli* ATCC 25922, and *S. typhimurium* ATCC 14028). In the case of 11β,13-dihydrosalonitenolide, instead, a lower activity ($MIC_{100}$ = 0.5 -1.25 mg/mL) was detected against the same tested bacterial strains with *E. faecalis* ATCC 29212 bacterial strain that was found to be resistant to these compounds.

Based on the literature, differences among compounds antimicrobial activity might be explained based on differences in structural elements [24]. Indeed, several factors might influence STLs antimicrobial properties, such as compound structure, its concentration, hydrophobicity, geometric orientation, the tested bacterial strain, and the chemical environment [24,25]. Cnicin is a STL characterized by an exocyclic α-methylene group in addition to γ-butyrolacton ring [26]. It was demonstrated this α-methylene group is responsible for the antimicrobial activity of sesquiterpene lactones in general and of cnicin in particular [27]. It is worth noting that cnicin might react through a Michael addition mechanism with nucleophilic groups present in surrounding target molecules, a molecular event that might be at the basis of cnicin antimicrobial activity [24]. Based on this, the absence of this structural feature in 11β,13-dihydrosalonitenolide (**2**) might be responsible for the significantly lower antimicrobial activity of this compound with respect to that of cnicin under the experimental

conditions tested. Cnicin antimicrobial mechanism of action is well reported in the literature. It is known to interact with bacterial membrane proteins and consequently cause cell lysis and death [28]. It is also able to block bacterial cell wall synthesis by irreversibly inhibiting MurA, an enzyme responsible for the catalysis of the first step of peptidoglycan synthesis [29]. It was also reported that cnicin is able to stop biofilm formation by inhibiting quorum-sensing (QS) [30]. The identified compounds might possess multiple biological properties, such as anti-biofilm, anti-inflammatory, anticancer, and antioxidant activity, that should be investigated furtherly in the future.

**In chapter 4,** a bio-guided purification of *E. foeminea* crude extracts was carried out to isolate compounds with antimicrobial and anti-biofilm properties. Six compounds were isolated and identified as carvacrol (compound **1**), thymol (compound **2**) and four glycosylated kaempefrol, *i.e.*, kaempferol-3-*O*-α-L-(2”,4”-di-*E*-*p*-coumaroyl)-rhamnopyranoside,kaempferol-3-*O*-α-L-(2”-*E*-*p*-coumaroyl,4”-*Z*-*p*-coumaroyl)-rhamnopyranoside, kaempferol-3-*O*-α-L-(2”-*Z*-*p*-coumaroyl,4”-*E*-*p*-coumaroyl)-rhamnopyranoside, and kaempferol-3-*O*-α-L-(2”,4”-di-*Z*-*p*-coumaroyl)-rhamnopyranoside (compounds **3-6**). These metabolites were identified for the first time from *E. foeminea* organic extracts. Additionally, compounds **1**-**3** were found to exert strong antimicrobial properties and promising anti-biofilm activity.

According to Lai and Roy (2004), the hydroxyl (-OH) group of phenolic compounds plays a key role in determining compounds antimicrobial activity since it could interact with bacteria’s cell membranes and induce the leakage of cell components [31]. Furthermore, the position of the (-OH) group was reported to have a strong impact on compounds antimicrobial effectiveness [32]. Carvacrol and thymol are well-known antimicrobial essential oils largely employed as food preservatives and food additives [33]. Molecular mechanisms underlying carvacrol antimicrobial activity imply bacterial membrane disruption due to an alteration of its fluidity, integrity, and functionality [33,34]. Moreover, it could cause a depletion of intracellular ATP, an induction of reactive oxygen species (ROS), and the inhibition of efflux pumps [33,34]. Carvacrol is able to inhibit biofilm formation by interference with signaling pathways of quorum sensing (QS) by blocking the expression of specific involved genes. Carvacrol might also induce biofilm matrix disruption by interfering with bacterial cells motility and its ability to adhere to substrates [33,34]. Based on this, carvacrol might be, at least in part, responsible for *E. foeminea* hexane extract antimicrobial and anti-biofilm properties.

Interestingly, for the first time it was identified in *E. foeminea* dichloromethane extract four glycosylated isomers of kaempefrol (compounds **3**-**6** in). Compound **3** was already isolated from other plants, such as *Pentachondra pumila* [35], *Ocotea vellosiana* [36], *Laurus nobilis* [37], *Mammea longifolia* [38], *Eriobotrya japonica* [39], *Cinnamomun kotoense* [40], *Epimedium sagittatum*, and *Machilus philippinens* [41]. Based on evidence reported in the literature, geometric orientation of compounds **3-6** might have a remarkable effect on their antibacterial and anti-biofilm properties. Compound **3** was the only isomer that was found to be endowed with robust antimicrobial properties against *S. aureus* strains sensitive or resistant to conventional antibiotics. In the literature, strong antimicrobial properties were reported for compounds **3** and **4** that were isolated from *Laurus nobilis* against methicillin-resistant *S. aureus* strains and against vancomycin-resistant *Enterococci* [42]. Considering the strong antibacterial activity of compound **3** with respect to that detected for compounds **4**-**6**, it is plausible that the stereochemistry of the double bonds of the *p*-coumaroyl residues is a key structural feature associated to the antibiotic activity. In particular, the *E,E* stereochemistry of the double bonds of the *p*-coumaroyl residues appears to play a key role in conferring antimicrobial properties. Indeed, the influence of the number and position of the double bonds on the antimicrobial potency of plant-derived compounds was reported by Gochev *et al.,* 2010 [43].

The possible molecular targets of compound **3** antimicrobial activity were speculated based on the molecular docking experiments. Based on the obtained results, it can be assumed that compound **3** antibacterial activity might be correlated to the inhibition of sortase A and/or tyrosyl tRNA synthetase. Sortase A (Srt A) is a well-known protein responsible for biofilm adhesion, formation, and aggregation [44]. Furtherly, to support this activity, in the presence of inactivating mutations of Srt A, bacterial cells were no longer able to cause infections, because of the failure of the attachment of fibronectin proteins to the cell wall [45]. Hence, Srt A represents a suitable target for the development of novel and effective antimicrobial and anti-biofilm drugs [18]. Aminoacyl–tRNA synthases (aaRSs) inhibition is associated to a blockage of cell growth due to an interference with protein synthesis processes [46]. Hence, also this class of enzymes represents a suitable target for antimicrobial strategies. It is noteworthy, that compound **3**, while exerting toxic effects on *S. aureus* bacterial cells, was found to be harmless towards immortalized human keratinocytes (HaCaT) and human dermal fibroblasts (HDF) at concentrations effective on bacterial

cells under the tested experimental conditions. Compound **3** cytocompitabilty adds an important tassel to its future applicability in biomedical or food industry fields to counteract bacterial infections.

In the last few years, several studies exploited combinatorial therapeutic approaches, based on the concomitant employment of AMPs and conventional antibiotics, as suitable tools to counteract antimicrobial resistance [11]. recently, our research group demonstrated that ApoB-derived peptides synergistically act in combination with conventional antibiotics or EDTA, and are able to enhance the effectiveness of traditional antibiotics against common skin pathogens [9,10][47]. Interestingly, in the present Thesis, it was demonstrated that ApoB-derived peptides are able to potentiate the activity of compound **3** towards Gram-positive and Gram-negative tested bacteria. In particular, r(P)ApoB$_{L}^{Pro}$ peptide showed additive effects when tested in combination with compound **3** against *S. aureus* MRSA WKZ-2 and *A. baumannii* ATCC 17878 bacterial strains. The achieved result is a promising one; it might allow the future development of combinatorial therapeutic approaches characterized by lowering the concentration of the single antimicrobial agents, thus minimizing the undesired selection of resistance phenotypes [47]. Altogether, obtained results indicated that compound **3** is a powerful antimicrobial agent, in particular against *S. aureus* MRSA WKZ-2, which could be employed in future therapeutic strategies to counteract the AMR worrying phenomenon.

**In chapter 5,** attempts to deliver Kaempferol-3-*O*-α-L-(2”,4”-di-*E*-*p*-coumaroyl)-rhamnopyranoside through biodegradable films were conducted. In particular, an active food packaging system was developed by using cellulose, a natural, abundant and biocompatible polymer [48]. Cellulose derived hydrogels (*i.e.*, HEC) are considered as a good delivery system for hydrophilic compounds in active packaging due to their polar properties. To make this system able to deliver also hydrophobic and water insoluble compounds, cyclodextrins were incorporated due to their ability to enclose this kind of compounds in their cavities [49]. Kaempferol-3-*O*-α-L-(2”,4”-di-*E*-*p*-coumaroyl)-rhamnopyranoside was loaded into HEC films in the absence or in the presence of cyclodextrins by using citric acid as a cross-linker at relatively high temperatures 110ºC**.** Obtained films were characterized by Fourier transform infrared spectroscopy (FT-IR) that confirmed the formation of cross-links in the produced films. Both kinds of films were found to be characterized by high swelling rates, probably due to the hydrophilic nature of HEC characterized by a high content in hydroxyl

groups [49]. Obtained films were then successfully loaded with Kaempferol-3-*O*-α-L-(2”,4”-di-*E*-*p*coumaroyl)-rhamnopyranoside (500 μg/mL) that was found to be effectively released (60% release) under the experimental conditions tested. According to this, functionalized films were also found to be endowed with significant antimicrobial properties, thus opening interesting perspectives to future studies aimed at evaluating their applicability in food packaging.

In conclusion, plants represent a rich and variable source of compounds endowed with a broad spectrum of biological activates. Plant-derived compounds' structural diversity is tremendous, and a slight structural modification in the orientation or number or position of functional groups might have a strong impact on the strength of the conferred antimicrobial properties. In the future, biological activities of the isolated compounds will be further investigated, to deeply evaluate their applicability in several biotechnological and pharmaceutical fields. Moreover, considerable efforts will be devoted to the evaluation of synergistic effects between plant-derived compounds and AMPs and/or conventional antibiotics, in order to set-up suitable combinatorial therapeutic approaches able to counteract MDR phenotype.

# References


[1] Blanco, P.; Hernando-Amado, S.; Reales-Calderon, J. A.; Corona, F.; Lira, F.; Alcalde-Rico, M.; Bernardini, A.; Sanchez, M. B.; Martinez, J. L. Bacterial multidrug efflux pumps: much more than antibiotic resistance determinants. *Microorganisms*,**2016,** *4*(1), 14. https://doi.org/10.3390/microorganisms4010014

[2] Álvarez-Martínez, F. J.; Barrajón-Catalán, E.; Micol, V. Tackling antibiotic resistance with compounds of natural origin: A comprehensive review. *Biomedicines*, **2020**, *8*(10), 405. https://doi.org/10.3390/biomedicines8100405

[3] O'Neill, J. Tackling drug-resistant infections globally: final report and recommendations. Copyright: Government of the United Kingdom **2016**. https://apo.org.au/sites/default/files/resource-files/2016-05/apo nid63983.pdf

[4] World Health Organization (WHO), *Food Safety*, World Health Organization (WHO), Geneva, Switzerland, **2022**, https://www.who.int/news-room/fact-sheets/detail/food-safety

[5] Mah, T. F. C.; O'Toole, G. A. Mechanisms of biofilm resistance to antimicrobial agents. *Trends in microbiology*,**2001,** *9*(1), 34-39. https://doi.org/10.1016/S0966-842X(00)01913-2

[6] Harvey, A.; Edrada-Ebel, R.; Quinn, R. The re-emergence of natural products for drug discovery in the genomics era. *Nat Rev Drug Discov* ,**2015**,14, 111–129. https://doi.org/10.1038/nrd4510

[7] Radulovic, N. S.; Blagojevic, P. D.; Stojanovic-Radic, Z. Z.; Stojanovic, N. M. Antimicrobial plant metabolites: structural diversity and mechanism of action. *Current medicinal chemistry*,**2013**, *20*(7), 932-952. https://doi.org/10.2174/092986713805219136

[8] Tenover, F. C. Mechanisms of antimicrobial resistance in bacteria. *The American journal of medicine*,**2006,** *119*(6), S3-S10. https://doi.org/10.1016/j.amjmed.2006.03.011

[9] Dell'Olmo, E.; Gaglione, R.; Cesaro, A.; Cafaro, V.; Teertstra, W. R.; de Cock, H.; Notomista, E; Haagsman H.P. ; Veldhuizen E.J.A.; Arciello, A. Host defence peptides identified in human apolipoprotein B as promising antifungal agents. *Applied microbiology and biotechnology*,**2021** *105*(5), 1953-1964.https://doi.org/10.1007/s00253-021-11114-3

[10] Cesaro, A.; Torres, M. D.; Gaglione, R.; Dell'Olmo, E.; Di Girolamo, R.; Bosso, A.; Pizzo,E.; Haagsman,H. P.; Veldhuizen,E. J. A.; Fuente-Nunez, C.; Arciello, A. Synthetic Antibiotic Derived from Sequences Encrypted in a Protein from Human Plasma. *ACS nano*,**2022**, *16*(2), 1880-1895. https://doi.org/10.1021/acsnano.1c04496

[11] Magana, M.; Pushpanathan, M.; Santos, A. L.; Leanse, L.; Fernandez, M.; Ioannidis, A; Giulianotti, M.A.; Apidianakis, Y.; Bradfute, S.; Andrew, L.; *et al.*; Tegos, G. P. The value of antimicrobial peptides in the age of resistance. *The Lancet Infectious Diseases*,**2020,** *20*(9), e216-e230. https://doi.org/10.1016/S1473-3099(20)30327-3

[12] Valle Jr, D.; Andrade L.; Puzon J. I.; Cabrera J. J. M.; Rivera W. L. Antibacterial activities of ethanol extracts of Philippine medicinal plants against multidrug-resistant bacteria. *Asian pacific journal of tropical biomedicine*,**2015**,5(7):532-540. https://doi.org/10.1016/j.apjtb.2015.04.005

[13] Savoia, D. Plant-derived antimicrobial compounds: alternatives to antibiotics. *Future Microbiology*,**2012**, 7, 979. https://doi.org/10.2217/fmb.12.68

[14] Sahib, N.G.; Anwar, F.; Gilani, A.H.; Hamid, A.A.; Saari, N.; Alkharfy, K.M. Coriander *Coriandrum sativum L*.: a potential source of high-value components for functional foods and nutraceuticals – a review. *Phytother.* **2013**, *27*, 1439-1456. https://doi.org/10.1002/ptr.4897

[15] Ksouri R.; Megdiche W.; Falleh H.; Trabelsi N.; Boulaaba M.; Smaoui A.; Abdelly C. Influence of biological, environmental and technical factors on phenolic content and antioxidant activities of Tunisian halophytes. *Comptes RendusBiologies*,**2008**, *331*(11),865-873. https://doi.org/10.1016/j.crvi.2008.07.024

[16] Lefebvre T.; Destandau E.; Lesellier E. Selective extraction of bioactive compounds from plants using recent extraction techniques: A review. *Journal of Chromatography A*, **2021**,*1635*,461770. https://doi.org/10.1016/j.chroma.2020.461770

[17] Ni Z. J.; Wang X.; Shen Y.; Thakur K.; Han J.; Zhang J. G.; Hu F.; Wei Z. J. Recent updates on the chemistry, bioactivities, mode of action, and industrial applications of plant essential oils. *Trends in Food Science & Technology***, 2021**,*110*, 78-89. https://doi.org/10.1016/j.tifs.2021.01.070

[18] Lei, S.; Hu, Y.; Yuan, C.; Sun, R.; Wang, J.; Zhang, Y.; Zhang, Y.; Lu, D.; Fu, L.; Jiang, F. Discovery of Sortase A covalent in-hibitors with benzofuranene cyanide structures as potential antibacterial agents against *Staphylococcus aureus*. *European Journal of Medicinal Chemistry* **2022**, 229. https://doi.org/10.1016/j.ejmech.2021.114032

[19] Roy R.; Tiwari, M.; Donelli G.; Tiwari V. Strategies for combating bacterial biofilms: A focus on anti-biofilm agents and their mechanisms of action. *Virulence*, **2018**,*9*(1),522-554. https://doi.org/10.1080/21505594.2017.1313372

[20] Tegos, G.; Stermitz, F. R.; Lomovskaya, O.; Lewis, K. Multidrug pump inhibitors uncover remarkable activity of plant antimicrobials. *Antimicrobial agents and chemotherapy*,**2002,** *46*(10), 3133–3141.https://doi.org/10.1128/AAC.46.10.3133-3141.2002

[21] Beigomi M.; Biabangard A.; Rohani R. Evaluation of antimicrobial effects of Rosemary and *Withania somnifera* methanol extract prepared by ultrasound waveform on Escherichia coli biofilm isolated from urinary tract infection. *Micro Environer*,**2021**, *1*(2), 17-25. https://doi.org/10.54458/mev.v1i01.6670

[22] Ayad R.; Akkal S. Chapter 12 - Phytochemistry and biological activities of Algerian Centaurea and related Genera, Editor(s): Atta-ur-Rahman, *Studies in Natural Products Chemistry, Elsevier*, **2019** *63*, Pages 357-414,ISSN 1572-5995,ISBN 9780128179017 https://doi.org/10.1016/B978-0-12-817901-7.00012-5.

[23] Ismail S.; Hammouda F.; Rimpler H.; Abdallah S. Flavonoids and Sesquiterpene Lactones, Constituents of *Centaurea alexandrina. Planta Medica,* **1986***, 52(6), 527–527.* 10.1055/s-2007-969314

[24] Matos, M. S.; Anastácio, J. D.; Nunes dos Santos, C. Sesquiterpene lactones: Promising natural compounds to fight inflammation. *Pharmaceutics*, **2021** *13*(7), 991. https://doi.org/10.3390/pharmaceutics13070991

[25] Schmidt, T. J.; Heilmann, J. Quantitative Structure-Cytotoxicity Relationships of Sesquiterpene Lactones derived from partial charge (Q) - based fractional Accessible Surface Area Descriptors (Q_frASAs). *Quantitative Structure-Activity Relationships*,**2002** *21*(3), 276-287.https://doi.org/10.1002/1521-3838(200208)21:3<276::AID-QSAR276>3.0.CO;2-S

[26] Adekenov S. M. Sesquiterpene lactones from plants of the family Asteraceae in the Kazakhstan flora and their biological activity. *Chemistry of Natural Compounds*,**1995**, *31*(1), 21-25. https://doi.org/10.1007/BF01167564

[27] Dimkić, I., Petrović, M., Gavrilović, M. et al. New perspectives of purple starthistle (*Centaurea calcitrapa*) leaf extracts: phytochemical analysis, cytotoxicity and antimicrobial activity. *AMB Expr*, **2020**, *10*, 183 . https://doi.org/10.1186/s13568-020-01120-

[28] Van Wyk, B. E.; Wink M. *Medicinal plants of the world*. CABI. **2018.**

[29] Bachelier, A.; Mayer R.; Klein CD. Sesquiterpene lactones are potent and irreversible inhibitors of the antibacterial target enzyme MurA. *Bioorg Med Chem Lett*. **2006**; *16*(21):5605-5609. https://doi.org/10.1016/j.bmcl.2006.08.021

[30] Hentzer, M.; Riedel, K.; Rasmussen TB.; Heydorn A.; Andersen JB.; Parsek MR.; Rice SA.; Eberl L.; Molin S.; Høiby N.; Kjelleberg S. Inhibition of quorum sensing in *Pseudomonas aeruginosa* biofilm bacteria by a halogenated furanone compound. *Microbiology*, **2002**;148(1):87-102. https://doi.org/10.1099/00221287-148-1-87

[31] Lai, P. K.; Roy, J. Antimicrobial and chemopreventive properties of herbs and spices. *Current medicinal chemistry*,**2004**, *11*(11), 1451-1460. https://doi.org/10.2174/0929867043365107

[32] Dorman, H. D.; Deans, S. G. Antimicrobial agents from plants: antibacterial activity of plant volatile oils. *Journal of applied microbiology*, **2000**,*88*(2), 308-316.https://doi.org/10.1046/j.1365-2672.2000.00969.x

[33] Zhang, D.; Gan, R.; Ge, Y.; Yang, Q.; Ge, J.; Li, H.; Corke, H. Research Progress on the Antibacterial Mechanisms of Carvacrol: A Mini Review. *Bioactive Compounds in Health and Disease* **2018**, *1*, 71-81. https://doi.org/10.31989/bchd.v1i6.551

[34] Marinelli, L.; Di Stefano, A.; Cacciatore, I. Carvacrol and its derivatives as antibacterial agents. *Phytochem Rev* **2018**, *17*, 903–921, https://doi.org/10.1007/s11101-018-9569-x

[35] Bloor, S.J. An antimicrobial kaempferol-diacyl-rhamnoside from *Pentachondra pumila*. *Phytochemistry* **1995**, *38*, 1033-1035. https://doi.org/10.1016/0031-9422(94)00661-C

[36] Garcez, W.S.; Yoshida, M.; Gottlieb, O.R. Benzylisoquinoline alkaloids and flavonols from *Ocotea vellosiana*. *Phytochemistry* **1995**, *39*, 815-816. https://doi.org/10.1016/0031-9422(94)00961-R

[37] Fiorini, C.; David, B.; Fourasté, I.; Vercauteren, J. Acylated kaempferol glycosides from *Laurus nobilis* leaves. *Phytochemistry* **1998**, *47*, 821-824. doi: https://doi.org/10.1016/S0031-9422(97)00563-3

[38] Rao, J.M.L.; Yada, H.; Ono, H.; Yoshida, M. Acylated and non-acylated flavonol monoglycosides from the Indian minor spice nagkesar (*Mammea longifolia*). *Journal of agricultural and food chemistry* **2002**, *50*, 3143-3146. https://doi.org/10.1021/jf011461m

[39] Kawahara, N.; Satake, M.; Goda, Y. A new acylated flavonol glycoside from the leaves of *Eriobotrya japonica*. *Chemical and pharmaceutical bulletin* **2002**, *50*, 1619-1620. https://doi.org/10.1248/cpb.50.1619

[40] Kuo, Y.C.; Lu, C.K.; Huang, L.W.; Kuo, Y.H.; Chang, C.; Hsu, F.L.; Lee, T.H. Inhibitory effects of acylated kaempferol glycosides from the leaves of *Cinnamomum kotoense* on the proliferation of human peripheral blood mononuclear cells. *Planta medica* **2005**, *71*, 412-415. https://doi.org/10.1055/s-2005-864134

[41] Lee, S.S.; Lin, H.C.; Chen, C.K. Acylated flavonol monorhamnosides, α-glucosidase inhibitors, from *Machilus philippinensis*. *Phytochemistry* **2008**, *69*, 2347-2353. https://doi.org/10.1016/j.phytochem.2008.06.006

[42] Otsuka, N.; Liu, M.H.; Shiota, S.; Ogawa, W.; Kuroda, T.; Hatano, T.; Tsuchiya, T. Anti-methicillin resistant *Staphylococcus aureus* (MRSA) compounds isolated from *Laurus nobilis*. *Biological and Pharmaceutical Bulletin* **2008**, *31*, 1794-1797. https://doi.org/10.1248/bpb.31.1794

[43] 43 Gochev, V.; Dobreva, A.; Girova, T.; Stoyanova, A. Antimicrobial activity of essential oil from *Rosa alba*. *Biotechnology & Biotechnological Equipment*. **2010** *24*(sup1), 512-515. https://doi.org/10.1080/13102818.2010.10817892

[44] Mazmanian, S.K.; Liu, G.; Ton-That, H.; Schneewind, O. *Staphylococcus aureus* sortase, an enzyme that anchors surface proteins to the cell wall. *Science* **1999**, 285, 760-763. https://doi.org/10.1126/science.285.5428.760

[45] Weiss, W.J.; Lenoy, E.; Murphy, T.; Tardio, L.; Burgio, P.; Projan, S.J.; Schneewind, O.; Alksne, L. Effect of srtA and srtB gene expression on the virulence of *Staphylococcus aureus* in animal models of infection. *J Antimicrob Chemother* **2004**, *53*, 480–486. https://doi.org/10.1093/jac/dkh078

[46] Xiao, Z.P.; Wei, W.; Wang, P.F. ; Shi, W.K.; Zhu, N.; Xie, M.Q.; Sun, Y.W.; Li, L.X.; Xie, Y.X.; Zhu, L.S.; Tang, N.; Ouyang, H.; Li, X.H.; Wang, G.C.; Zhu, H.L. Synthesis and evaluation of new tyrosyl-tRNA synthetase inhibitors as antibacterial agents based on a N2-(arylacetyl) glycinanilide scaffold. *European Journal of Medicinal Chemistry* **2015**, *102*, 631-638. https://doi.org/10.1016/j.ejmech.2015.08.025

[47] Gaglione, R.; Dell'Olmo, E.; Bosso, A.; Chino, M.; Pane, K.; Ascione, F.; Itri, F.; Caserta, S.; Amoresano, A.; Lombardi, A.; Haagsman, H.P.; Piccoli, R.; Pizzo, E.; Veldhuizen, E.J.A.; Notomista, E.; Arciello, A. Novel human bioactive peptides identified in apolipoprotein B: evaluation of their therapeutic potential. *Biochemical Pharmacology* **2017**, *130*, 34-50. https://doi.org/10.1016/j.bcp.2017.01.009

[48] He X.; Lu W.; Sun C.; Khalesi H.; Mata A.; Andaleeb R.; Fang Y. Cellulose and cellulose derivatives: Different colloidal states and food-related applications. *Carbohydrate Polymers*. **2020**, 255, 117334. https://doi.org/10.1016/j.carbpol.2020.117334

[49] Ghorpade, V. S.; Yadav, A. V.; Dias, R. J. Citric acid crosslinked β-cyclodextrin/carboxymethylcellulose hydrogel films for controlled delivery of poorly soluble drugs. *Carbohydrate Polymers*.**2017**, *164*, 339-348. https://doi.org/10.1016/j.carbpol.2017.02.005

# APPENDICES

## A1. Abbreviations:

**AMR:** Antimicrobial Resistance; **MDR**: Multi-Drug-Resistant; **AMPs**: Antimicrobial Peptides; **HDPs**: Host Defence Peptides; **ApoB**: Apolipoprotein B; **ATCC** American Type Culture Collection; **MRSA**: Methicillin-Resistant *Staphylococcus aureus*; **MIC**: Minimal Inhibitory Concentration; **MBC**: Minimal Bacterocidal Concentration **TSA**: Tryptic Soy Agar; **MHB**: Muller Hinton Broth; **NB**: Nutrient Broth; **SD**: Standard Deviation; **Ecg**:Epicatechin Gallate; **FIC**: Fractional Inhibitory Concentration; **PBS**: Phosphate-Buffered Saline; **CFU**: Colony Forming Unit; **CLSM**: Confocal Laser Scanning Microscopy; **MTT**: 3-(4,5-Dimethylthiazol-2-yl)- 2,5- Diphenyltetrazolium Bromide; **HaCaT**: Immortalized Human Keratinocytes; **DMEM**: Dulbecco's Modified Eagle's Medium; **FBS**: Fetal Bovine Serum; **HDF**: Human Dermal Fibroblasts; **CC**: Coulmn Chromatography; **TLC**:Thin Layer Chromatography; **NMR**:Nuculear Magnatic Resonance; **MS**: Mass Spectroscopy;**PLA**: Polylacatic Acid; **HEC:**Hydroxyethyl Cellulose**;CMC:** Carboxymethyl Cellulose **; CD:** Cyclodextrins**; HPβCD:** 2-Hydroxypropyl-β-cyclodextrin**; STLs :**Sesquiterpene Lactones; **GSH:** Glutathione**; FDA:** Food and Drug Administration; **WHO**: World Health Organization; **GRAS:** Generally Recognized As Safe; **FT-IR:** Fourier-transform Infrared Spectroscopy; **EPs**: Efflux Pumps; **DMSO**: Dimethyl Sulfoxide; **TyRs** :Tyrozol tRNA Synthathase; **Srt A**: Sortase A; **$CDCl_3$:** Deuterated Chloroform**; LPS:** Lipopolysaccharides; **$CD_3OD$:** Deuterated Methanol; **COSY-45:** $^1H$-$^1H$ Correlation Spectroscopy; **NOESY:** Nuclear Overhauser Effect Spectroscopy; **MPa:** Mega Pascal; **HPLC:** High Performance Liquid Chromatography; **EtOAc:** Ethyl Acetate; **iPrOH**: Isopropyl Alcohol; **EDTA:** Ethylene Diaminetetra Acetic Acid; **PBMC**: Peripheral Blood Mononuclear Cells; **PHA:** Phytohemagglutinin; **CWA**: Cell Wall Proteins; **ROS**: Reactive Oxygen Species.

## A2. List of Supplementary Figures

**Figure S1**. $^{1}$H NMR spectrum of carvacrol, **compound 1** ($CDCl_3$, 400 MHz).

**Figure S2**. $^{1}$H NMR spectrum of thymol, **compound 2** ($CDCl_3$, 400 MHz).

**Figure S3**. $^{1}$H NMR spectrum of kaempferol-3-*O*-α-L-(2",4"-di-*E*-*p*-coumaroyl)-rhamnopyranoside **compound 3** (MeOD, 400 MHz).

**Figure S4**. $^{1}$H NMR spectrum of kaempferol-3-*O*-α-L-(2",4"-di-*E*-*p*-coumaroyl)-rhamnopyranoside **compound 3** (MeOD, 400 MHz) in the range 8.1 to 5.4 ppm.

**Figure S5**. $^{1}$H NMR spectrum of kaempferol-3-*O*-α-L-(2",4"-di-*E*-*p*-coumaroyl)-rhamnopyranoside **compound 3** (acetone-$d_6$, 400 MHz).

**Figure S6**. $^{1}$H NMR spectrum of kaempferol-3-*O*-α-L-(2",4"-di-*E*-*p*-coumaroyl)-rhamnopyranoside **compound 3** (acetone-$d_6$, 400 MHz) in the range 8.0 to 5.5 ppm.

**Figure S7**. COSY spectrum of kaempferol-3-*O*-α-L-(2",4"-di-*E*-*p*-coumaroyl)-rhamnopyranoside, **compound 3** (acetone-$d_6$, 400 MHz).

**Figure S8**. COSY spectrum of kaempferol-3-*O*-α-L-(2",4"-di-*E*-*p*-coumaroyl)-rhamnopyranoside **compound 3** (acetone-$d_6$, 400 MHz) in the range 8.0 to 5.6 ppm.

**Figure S9**. NOESY spectrum of kaempferol-3-*O*-α-L-(2",4"-di-*E*-*p*-coumaroyl)-rhamnopyranoside **compound 3** (acetone-$d_6$, 400 MHz).

**Figure S10**. $^{13}$C NMR spectrum of kaempferol-3-*O*-α-L-(2",4"-di-*E*-*p*-coumaroyl)-rhamnopyranoside **compound 3** (acetone-$d_6$, 400 MHz).

**Figure S11**. HSQC spectrum of kaempferol-3-*O*-α-L-(2",4"-di-*E*-*p*-coumaroyl)-rhamnopyranoside **compound 3** (acetone-$d_6$, 400 MHz).

**Figure S12**. HMBC spectrum of kaempferol-3-*O*-α-L-(2",4"-di-*E*-*p*-coumaroyl)-rhamnopyranoside, **compound 3** (acetone-$d_6$, 400 MHz).

**Figure S13**. ESI MS spectrum of kaempferol-3-*O*-α-L-(2",4"-di-*E*-*p*-coumaroyl)-rhamnopyranoside **compound 3** recorded in positive modality.

**Figure S14**. $^{1}$H NMR spectrum of kaempferol-3-*O*-α-L-(2"-*E*-*p*-coumaroyl,4"-*Z*-*p*-coumaroyl)-rhamnopyranoside **compound 4** (MeOD, 400 MHz).

**Figure S15**. $^{1}$H NMR spectrum of kaempferol-3-*O*-α-L-(2"-*E*-*p*-coumaroyl,4"-*Z*-*p*-coumaroyl)-rhamnopyranoside **compound 4** (MeOD, 400 MHz) in the range 8.0 to 5.3 ppm.

**Figure S16**. COSY spectrum of kaempferol-3-*O*-α-L-(2"-*E*-*p*-coumaroyl,4"-*Z*-*p*-coumaroyl)-rhamnopyranoside **compound 4** (acetone-$d_6$, 400 MHz).

**Figure S17**. $^{1}$H NMR spectrum of kaempferol-3-*O*-α-L-(2"-*E*-*p*-coumaroyl,4"-*Z*-*p*-coumaroyl)-rhamnopyranoside **compound 4** (acetone-$d_6$, 400 MHz).

**Figure S18**. $^{1}$H NMR spectrum of kaempferol-3-*O*-α-L-(2"-*E*-*p*-coumaroyl,4"-*Z*-*p*-coumaroyl)-rhamnopyranoside **compound 4** (acetone-$d_6$, 400 MHz) in the range 8.0 to 5.4 ppm.

**Figure S19**. $^{1}$H NMR spectrum of kaempferol-3-*O*-α-L-(2”-*Z*-*p*-coumaroyl,4”-*E*-*p*-coumaroyl)-rhamnopyranoside **compound 5** (MeOD, 400 MHz).

**Figure S20**. $^{1}$H NMR spectrum of kaempferol-3-*O*-α-L-(2”-*Z*-*p*-coumaroyl,4”-*E*-*p*-coumaroyl)-rhamnopyranoside **compound 5** (MeOD, 400 MHz) in the range 8.0 to 5.4 ppm.

**Figure S21**. $^{1}$H NMR spectrum of kaempferol-3-*O*-α-L-(2”,4”-di-*Z*-*p*-coumaroyl)-rhamnopyranoside **compound 6** (MeOD, 400 MHz).

**Figure S22**. $^{1}$H NMR spectrum of kaempferol-3-*O*-α-L-(2”,4”-di-*Z*-*p*-coumaroyl)-rhamnopyranoside **compound 6** (MeOD, 400 MHz) in the range 7.9 to 5.5 ppm.

**Figure S23**. $^{1}$H NMR spectrum of kaempferol-3-*O*-α-L-(2”,4”-di-*Z*-*p*-coumaroyl)-rhamnopyranoside **compound 6** (acetone-$d_6$, 400 MHz).

**Figure S24**. $^{1}$H NMR spectrum of kaempferol-3-*O*-α-L-(2”,4”-di-*Z*-*p*-coumaroyl)-rhamnopyranoside **compound 6** (acetone-$d_6$, 400 MHz) in the range 8.0 to 5.4 ppm.

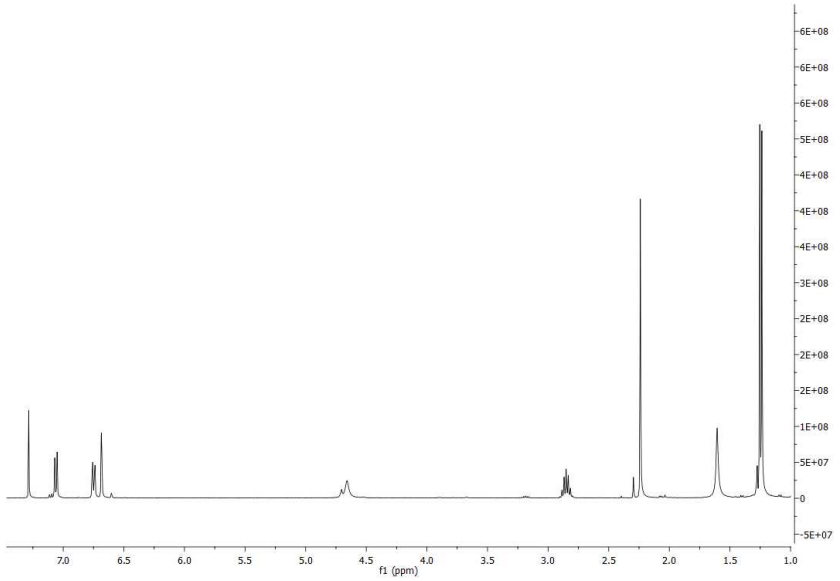


**Figure S1**. $^{1}H$ NMR spectrum of carvacrol **compound 1** ($CDCl_3$, 400 MHz).

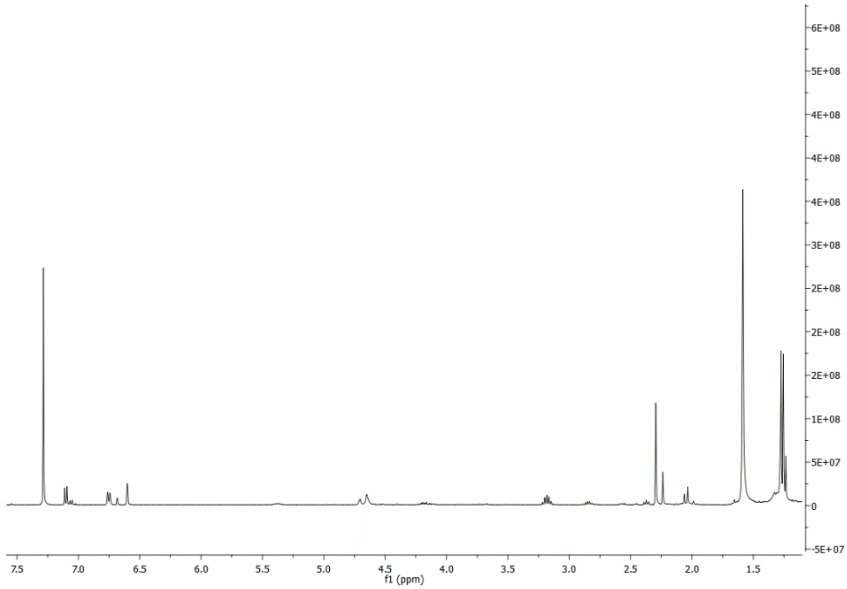


**Figure S2**. $^{1}H$ NMR spectrum of thymol **compound 2** ($CDCl_3$, 400 MHz).

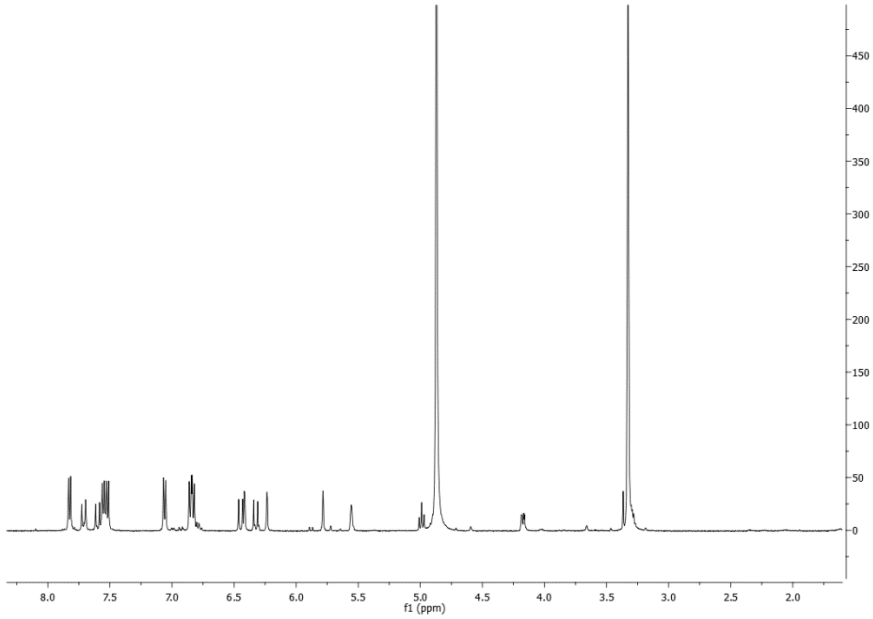


**Figure S3**. $^{1}$H NMR spectrum of kaempferol-3-*O*-α-L-(2”,4”-di-*E*-*p*-coumaroyl)-rhamnopyranoside **compound 3** (MeOD, 400 MHz).

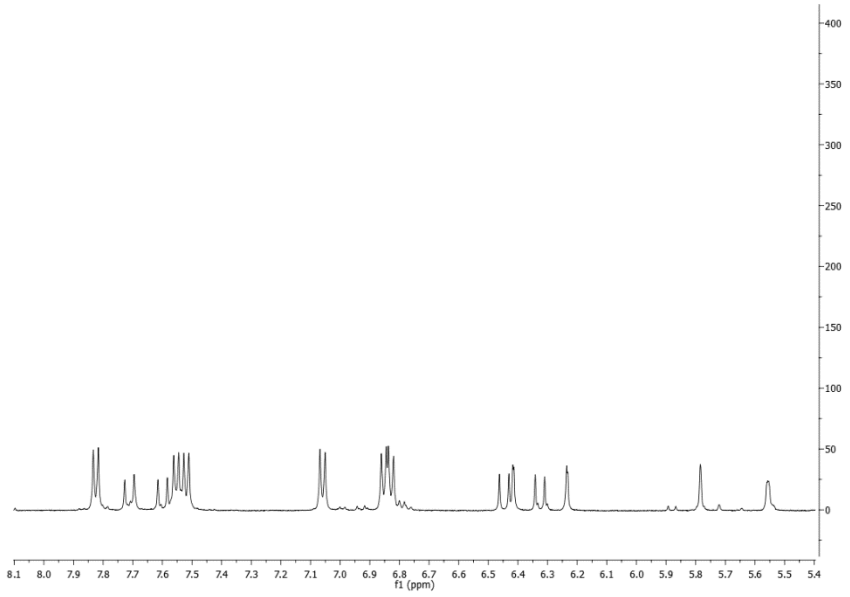


**Figure S4**. $^{1}$H NMR spectrum of kaempferol-3-*O*-α-L-(2”,4”-di-*E*-*p*-coumaroyl)-rhamnopyranoside **compound 3** (MeOD, 400 MHz) in the range 8.1 to 5.4 ppm.

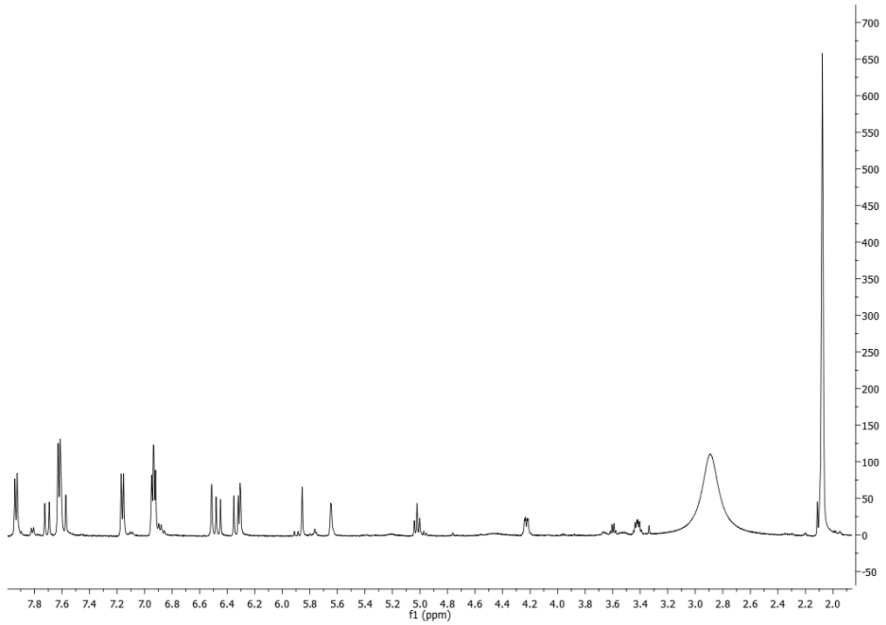


**Figure S5**. $^{1}$H NMR spectrum of kaempferol-3-*O*-α-L-(2”,4”-di-*E*-*p*-coumaroyl)-rhamnopyranoside **compound 3** (acetone-$d_6$, 400 MHz).

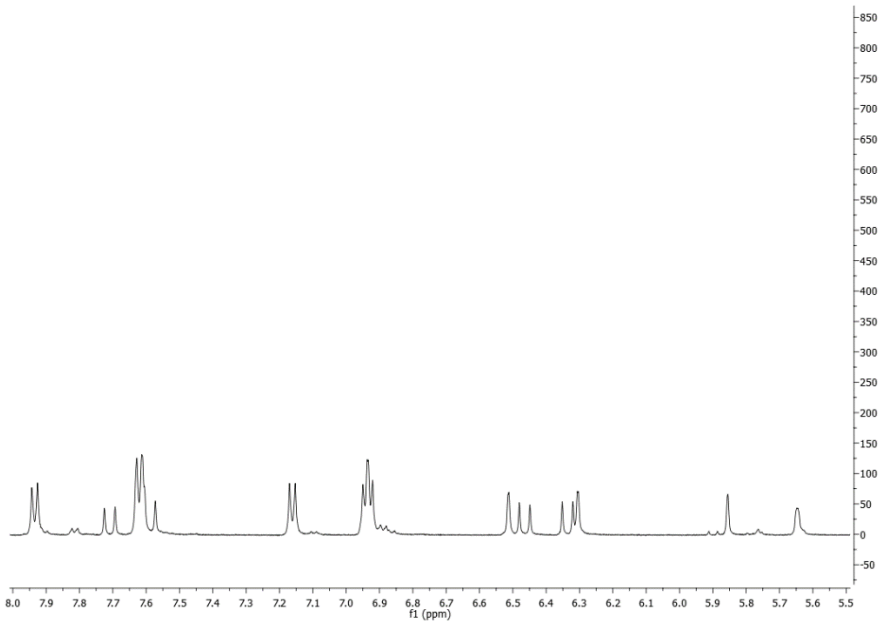


**Figure S6**. $^{1}$H NMR spectrum of kaempferol-3-*O*-α-L-(2”,4”-di-*E*-*p*-coumaroyl)-rhamnopyranoside **compound 3** (acetone-$d_6$, 400 MHz) in the range 8.0 to 5.5 ppm

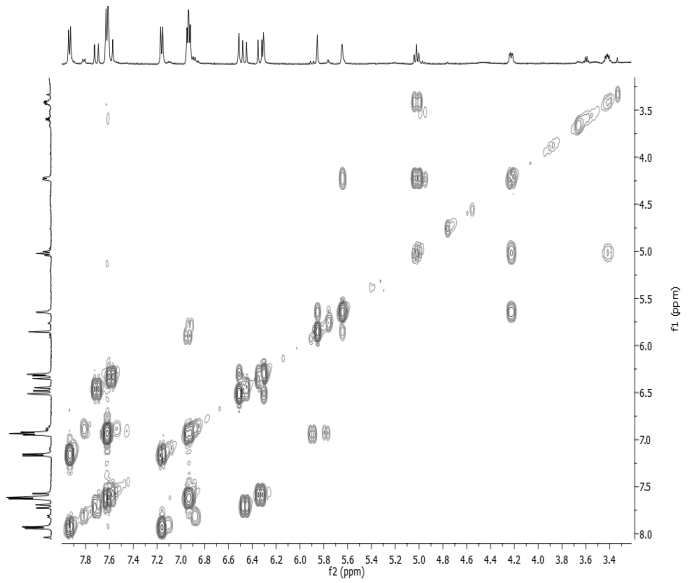


**Figure S7**. COSY spectrum of kaempferol-3-*O*-α-L-(2”,4”-di-*E*-*p*-coumaroyl)-rhamnopyranoside **compound 3** (acetone-$d_6$, 400 MHz).

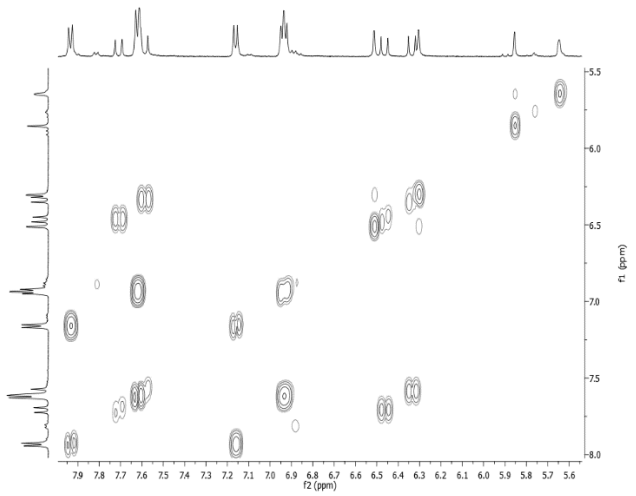


**Figure S8**. COSY spectrum of kaempferol-3-*O*-α-L-(2”,4”-di-*E*-*p*-coumaroyl)-rhamnopyranoside **compound 3** (acetone-$d_6$, 400 MHz) in the range 8.0 to 5.6 ppm.

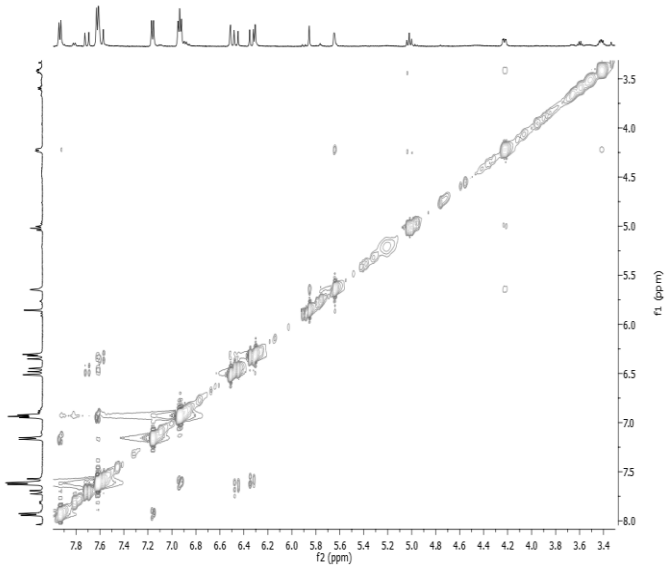


**Figure S9**. NOESY spectrum of kaempferol-3-*O*-α-L-(2”,4”-di-*E*-*p*-coumaroyl)-rhamnopyranoside **compound 3** (acetone-$d_6$, 400 MHz).

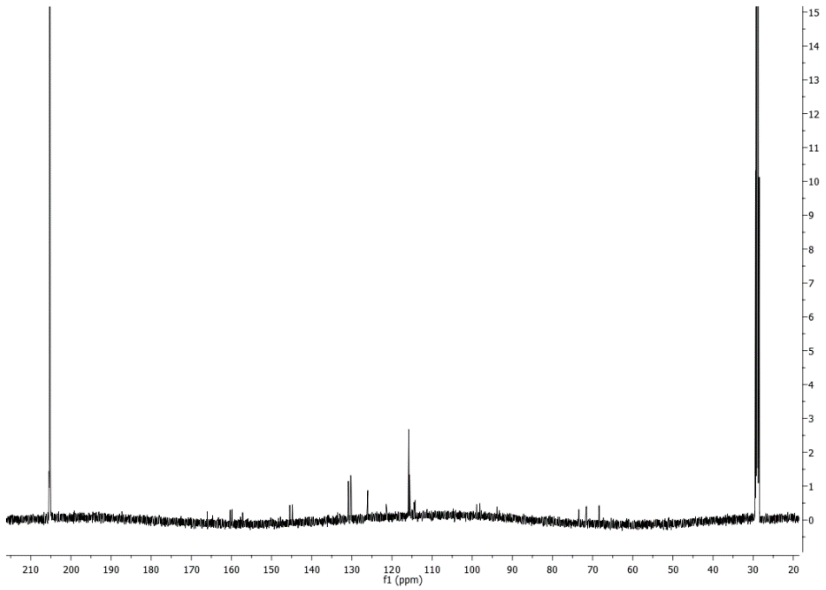


**Figure S10**. $^{13}$C NMR spectrum of kaempferol-3-*O*-α-L-(2”,4”-di-*E*-*p*-coumaroyl)-rhamnopyranoside **compound 3** (acetone-$d_6$, 400 MHz).

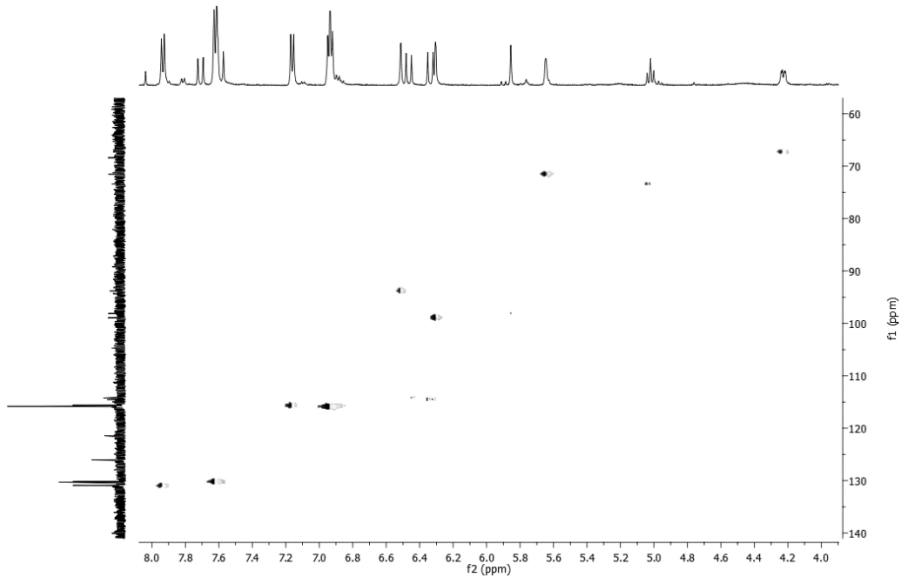


**Figure S11**. HSQC spectrum of kaempferol-3-*O*-α-L-(2”,4”-di-*E*-*p*-coumaroyl)-rhamnopyranoside **compound 3** (acetone-$d_6$, 400 MHz).

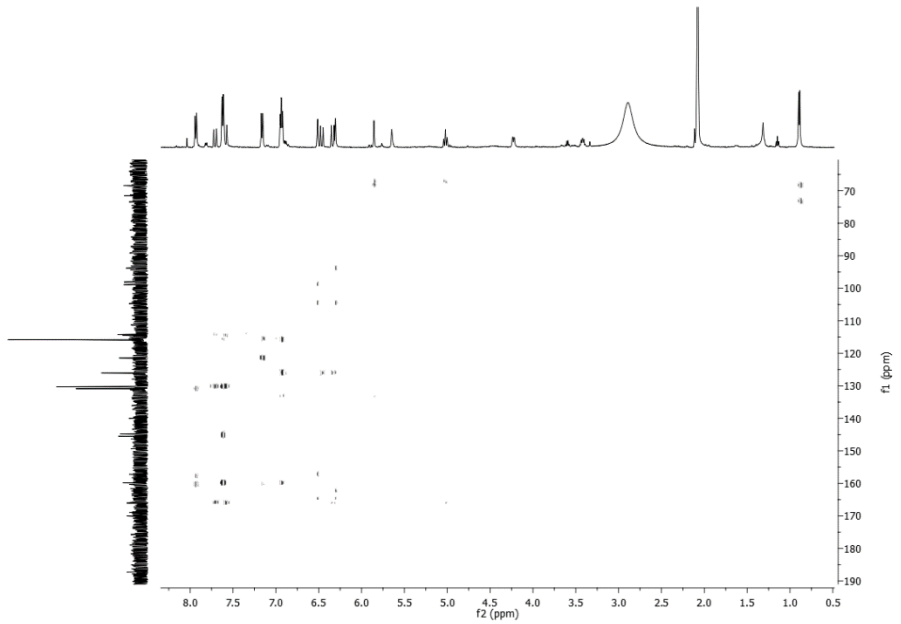


**Figure S12**. HMBC spectrum of kaempferol-3-*O*-α-L-(2”,4”-di-*E*-*p*-coumaroyl)-rhamnopyranoside **compound 3** (acetone-$d_6$, 400 MHz).

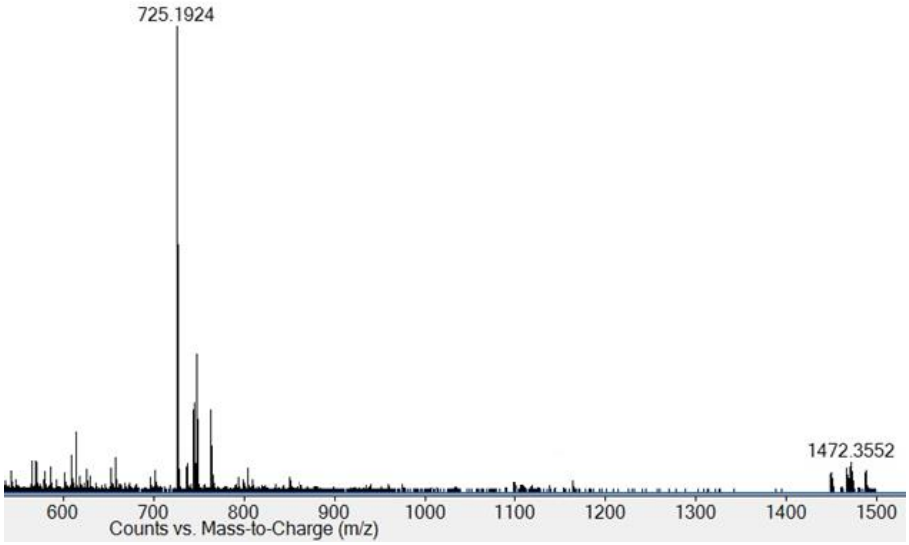


**Figure S13**. ESI MS spectrum of kaempferol-3-*O*-α-L-(2”,4”-di-*E*-*p*-coumaroyl)-rhamnopyranoside **compound 3** recorded in positive modality.

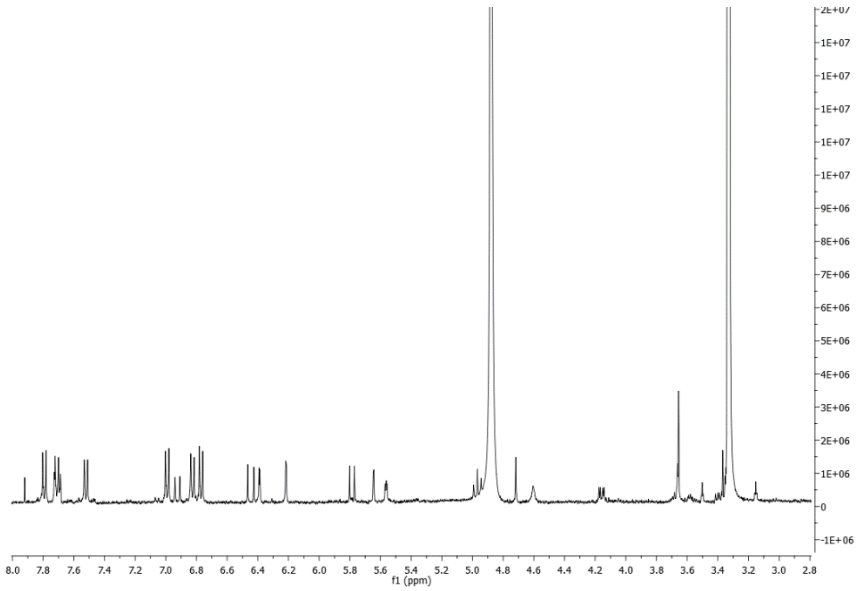


**Figure S14**. $^{1}$H NMR spectrum of kaempferol-3-*O*-α-L-(2”-*E*-*p*-coumaroyl,4”-*Z*-*p*-coumaroyl)-rhamnopyranoside **compound 4** (MeOD, 400 MHz).

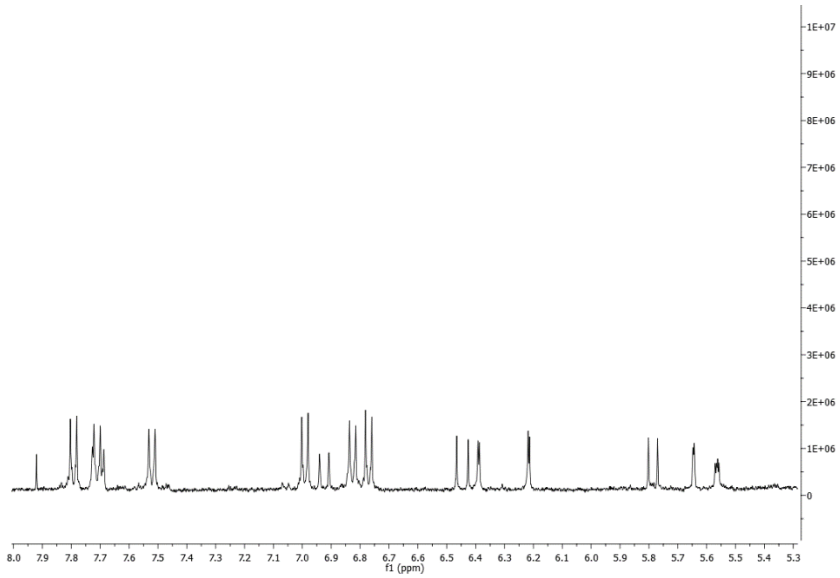


**Figure S15**. $^{1}$H NMR spectrum of kaempferol-3-*O*-α-L-(2”-*E*-*p*-coumaroyl,4”-*Z*-*p*-coumaroyl)-rhamnopyranoside **compound 4** (MeOD, 400 MHz) in the range 8.0 to 5.3 ppm.

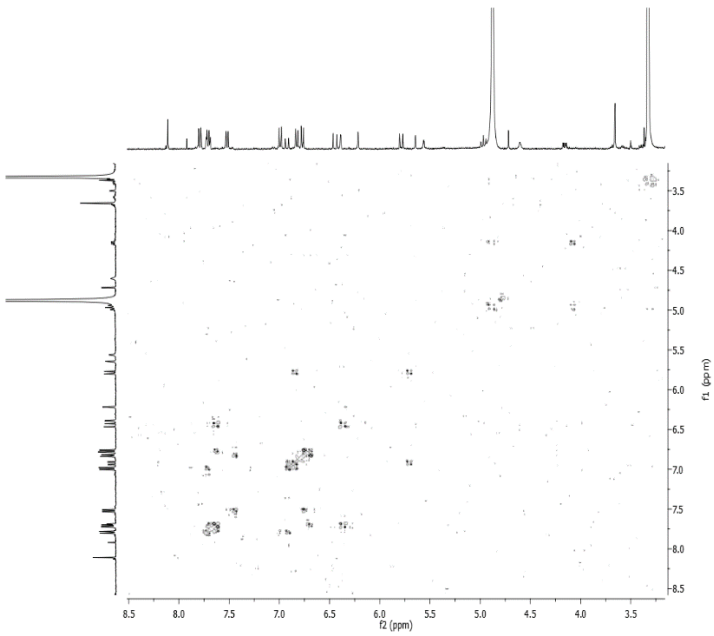


**Figure S16**. COSY spectrum of kaempferol-3-*O*-α-L-(2”-*E*-*p*-coumaroyl,4”-*Z*-*p*-coumaroyl)-rhamnopyranoside **compound 4** (acetone-$d_6$, 400 MHz).

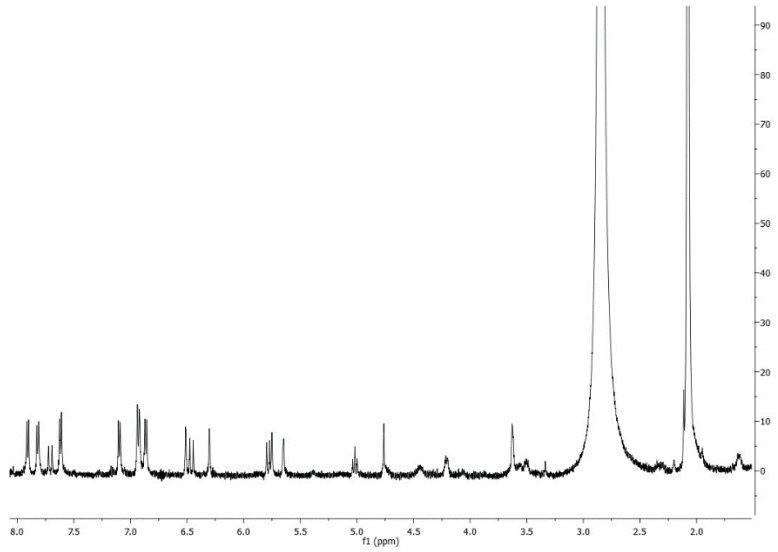


**Figure S17**. $^{1}$H NMR spectrum of kaempferol-3-*O*-α-L-(2”-*E*-*p*-coumaroyl,4”-*Z*-*p*-coumaroyl)-rhamnopyranoside **compound 4** (acetone-$d_6$, 400 MHz).

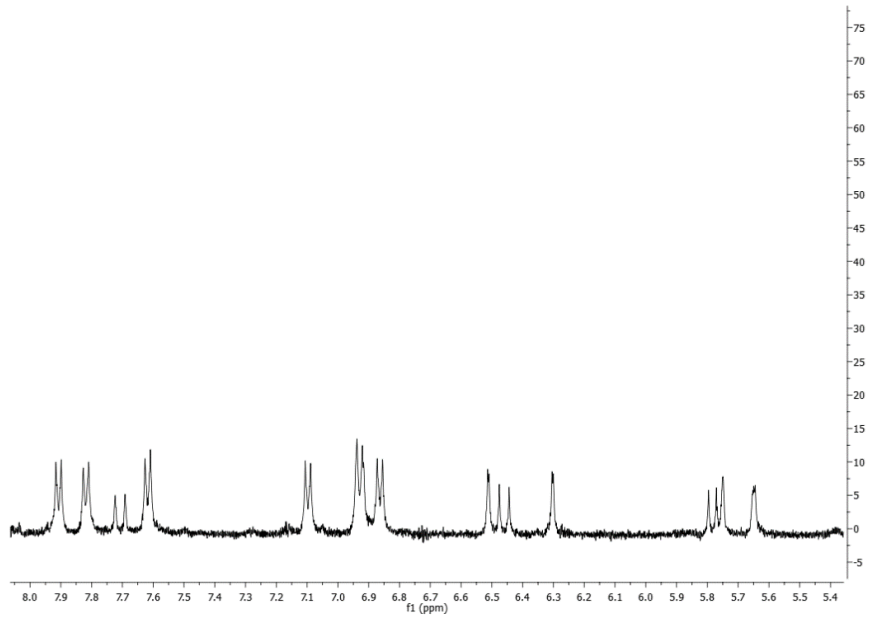


**Figure S18**. $^{1}$H NMR spectrum of kaempferol-3-*O*-α-L-(2”-*E*-*p*-coumaroyl,4”-*Z*-*p*-coumaroyl)-rhamnopyranoside **compound 4** (acetone-$d_6$, 400 MHz) in the range 8.0 to 5.4 ppm.

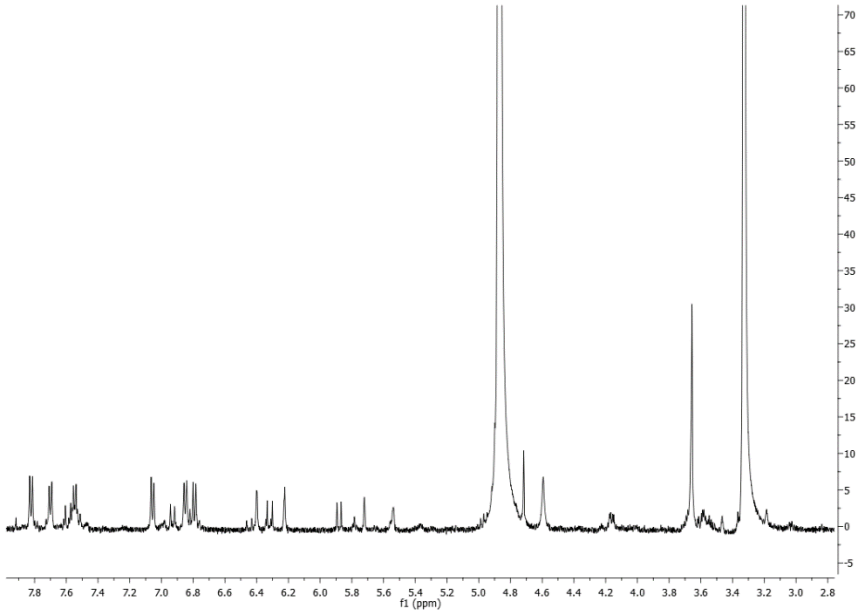


**Figure S19**. $^{1}$H NMR spectrum of kaempferol-3-*O*-α-L-(2”-*Z*-*p*-coumaroyl,4”-*E*-*p*-coumaroyl)-rhamnopyranoside **compound 5** (MeOD, 400 MHz).

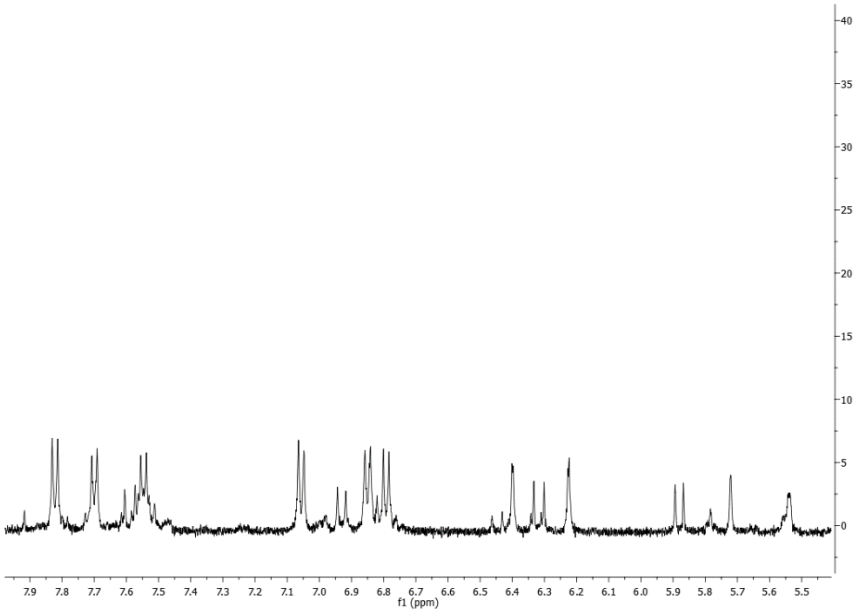


**Figure S20**. $^{1}$H NMR spectrum of kaempferol-3-*O*-α-L-(2”-*Z*-*p*-coumaroyl,4”-*E*-*p*-coumaroyl)-rhamnopyranoside **compound 5** (MeOD, 400 MHz) in the range 8.0 to 5.4 ppm.

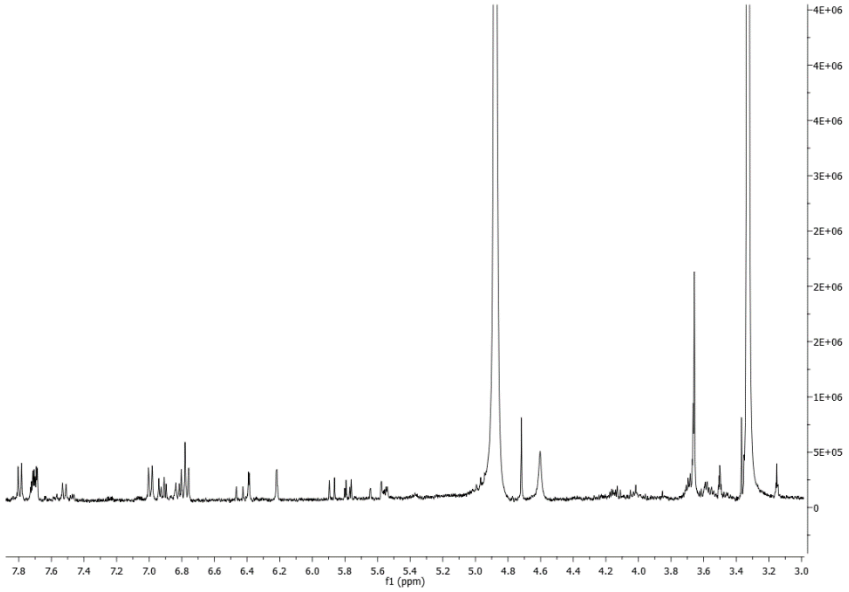


**Figure S21**. $^{1}$H NMR spectrum of kaempferol-3-*O*-α-L-(2”,4”-di-*Z*-*p*-coumaroyl)-rhamnopyranoside, **compound 6** (MeOD, 400 MHz).

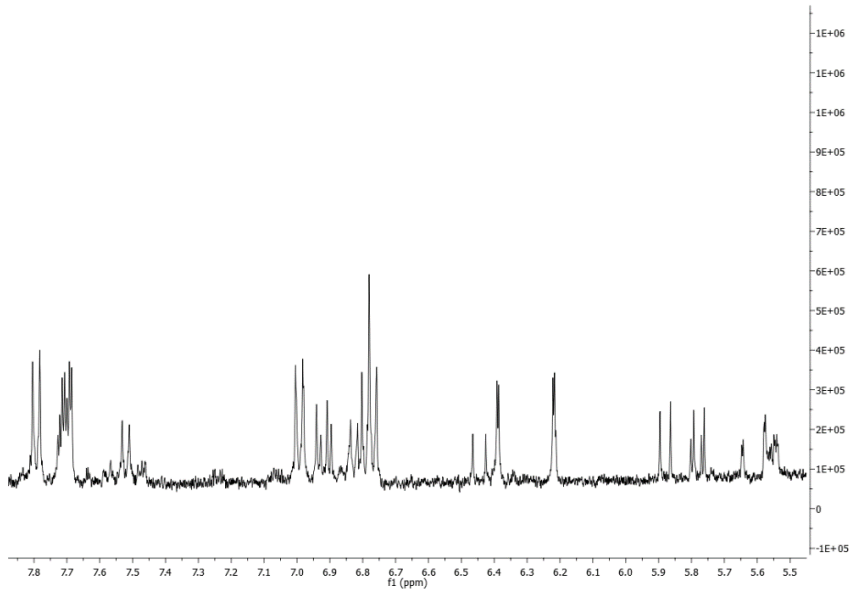


**Figure S22**. $^{1}$H NMR spectrum of kaempferol-3-*O*-α-L-(2”,4”-di-*Z*-*p*-coumaroyl)-rhamnopyranoside **compound 6** (MeOD, 400 MHz) in the range 7.9 to 5.5 ppm.

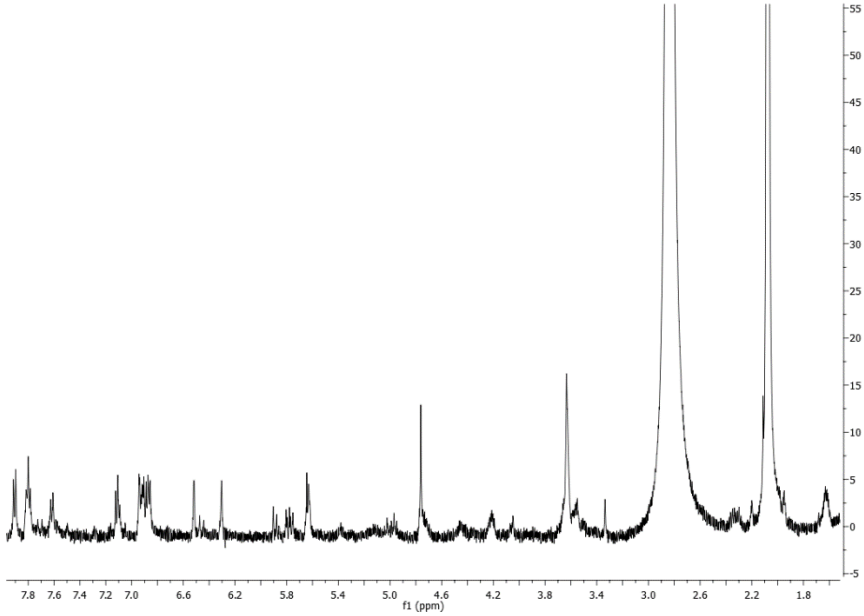


**Figure S23**. $^{1}$H NMR spectrum of kaempferol-3-*O*-α-L-(2”,4”-di-*Z*-*p*-coumaroyl)-rhamnopyranoside **compound 6** (acetone-$d_6$, 400 MHz).

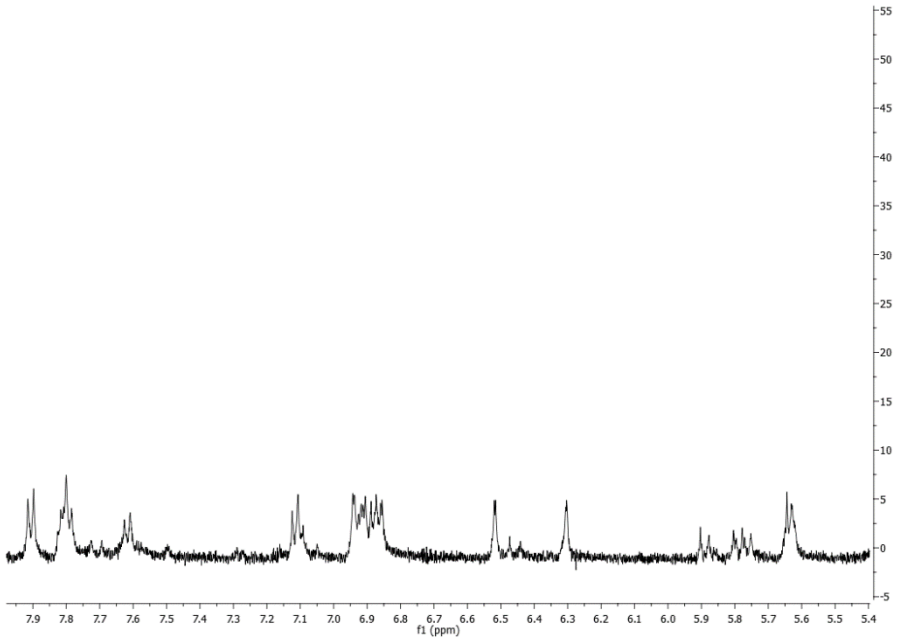


**Figure S24**. $^{1}$H NMR spectrum of kaempferol-3-*O*-α-L-(2”,4”-di-*Z*-*p*-coumaroyl)-rhamnopyranoside **compound 6** (acetone-$d_6$, 400 MHz) in the range 8.0 to 5.4 ppm.

## A3. List of Publications and Communications

1. **Shurooq M. Ismail***, Ghaleb M. Adwan, and Naser R. Jarrar. **Evaluation of Antimicrobial and Genotoxic Activity of *Ephedra foeminea* Ethanolic and Aqueous Extracts on *Escherichia coli***. *Jordan Journal of Biological Sciences*, 2020, Volume 13, Number 1,March 2020, ISSN 1995-6673, Pages 123 – 126.

2. **Shurooq Ismail**, Rosa Gaglione, Marco Masi, Srichandan Padhi, Amit K. Rai, Ghadeer Omar, Alessio Cimmino, Angela Arciello. ***Ephedra foeminea* as a Novel Source of Antimicrobial and Anti-Biofilm Compounds to Fight Multidrug Resistance Phenotype.** *Int. J. Mol. Sci.* **2023***, 24*(4),3284; **https://doi.org/10.3390/ijms24043284.**

3. Eliana Dell'Olmo , Katia Pane , Martina Schibeci , Angela Cesaro ,Maria De Luca ,**Shurooq Ismail** ,Rosa Gaglione, Angela Arciello. **Host defence peptides identified in human apolipoprotein B as natural food biopreservatives: evaluation of their biosafety and digestibility.** (2023, *Peptide Science*, Accepted).

## A4. List of Communications

**Shurooq Ismail,** Rosa Gaglione, Marco Masi, Srichandan Padhi, Ghadeer Omar, Alessio Cimmino, Angela Arciello. ***Ephedra foeminea* Plant as a Novel Source of Bioactive Compounds Endowed with Antimicrobial and Anti-biofilm Properties** (Oral presentation, The National Meeting "Sezione SIB Campania 2022" 26 October 2016, Naples, Italy.)

## A5. Experiences in Foreign Labraratories

Visiting period at the Department of Pharmacology, Pharmacy and Pharmaceutical Technology, Faculty of Pharmacy of the University of Santiago de Compostela, Spain, from April 1st 2022 to October 1st 2022. The work was carried out in the lab of Professor Dr. Carmen Alvarez-Lorenzo.

**“In the name of Almighty God, The Most Gracious, The Most Merciful, Alhamdulillah, praise be to ALLAH.”**

**Firstly, I would like to thank the Almighty God for His Blessing in the completion of this thesis. Allah, who had given me the strength and the encouragement throughout all the challenging moments of accomplishing this thesis. I am deeply grateful for His love, mercy, and grace. Then, praise is addressed to Prophet Muhammad, peace be upon him, who has guided us to the better life of today.”**

## A6. Acknowledgements

First, I would like to express my deepest and sincere appreciation to my supervisor **Prof. Angela Arciello** for giving me the chance to join her scientific group in the Department of Chemical Sciences at the University of Naples Federico II. Thanks for her precious, continuous guidance and support throughout the course of my study. Her wide knowledge and logical way of thinking have been of great value for me. Thanks for her dedicated supervision, constant encouragement towards the completion of this thesis and for her contribution to my personal and professional growth.

Then, I would like to express the deepest appreciation for **Prof. Alessio Cimmino**, for his continued collaboration and valuable feedback. More thanks to him for giving me the chance to join his team and introducing me to the world of organic chemistry. He has provided me with insightful comments on my research that have been a substantial aid to accomplish this thesis.

I extend my gratitude to **Prof. Dr. Carmen Alvarez-Lorenzo**, for hosting me for six months in the Faculty of Pharmacy at the University of Santiago de Compostela, Spain. Her careful instructions, novel inspirations, and constructive advices enabled me to improve this thesis.

I am also grateful to my external tutor **Prof. César de la Fuente**, from the Departments of Bioengineering & Chemical and Biomolecular Engineering, University of Pennsylvania, USA. I truly appreciated your advices and guidance during the course of my Phd study.

I would like also to express my sincere gratitude to **Dr. Rosa Gaglione** for the continuous support during my PhD study, for her patience, motivation, enthusiasm, and immense knowledge. I would like also to express my sincere appreciation to **Dr. Paola Imbimbo** and **Dr. Marco Masi**, for their support, encouragement and friendship. Their willingness to give guidance, advice and support was a great help to me.

I would like also to express my deepest appreciation to **Prof. Marco Moracci**; the PhD program coordinator for his cooperation and support. Thanks also are extended to the **PhD board committee** for their kind cooperation during the course of my study.

My sincere thanks to my colleagues, **Angelica**, **Maria**, **Martina**, **Gennaro**, **Davide, Enrica**, **Luigi,** for whom I have a great regard and respect. During this work, I had the pleasure to collaborate with many colleagues in the group of Prof. Cimmino; **Dr. Jesus Garcia**, **Gabriele** and **Maria** to whom I wish to extend my warmest thanks and best regards. Thanks also are extended to all members of the group of Prof. Dr. Carmen in Spain. Endless love and gratitude goes to my dearest friends, **Rita**, **Diana**, **Mariana**, **Maria**, **Inês** and **Caroline**; all of you made my time aboard full of fun and unforgettable adventures and memories. Special thanks go to my beloved friends, **Rafah**, **Ibtihaj,** and **Asma**, who exerted no chance to support and encourage me.

This endeavor would not have been possible without the approval of my home university, which gave me this precious opportunity to proceed in my PhD studies. Therefore, thanks also go to all administrative and scientific boards of **An-Najah National University**. I would like to express special thanks to my colleagues in the Department of Biotechnology. Deep thanks to **Dr. Maen Ishtaiwi** and **Dr. Mohammed Sabbah**, who encouraged me to start my PhD studies in Naples.

I owe my loving thanks to my supportive and encouraging parents, **Muhammad** and **Afaf.** Thanks to them not only for being by my side throughout my PhD study course, but also for their endless sacrifices, care and love. I am grateful for you both forever. My special gratitude goes to my beloved sisters **Noor**, **Rawan**, **Duá, Nidá, Aya** and **Tasneem** as well as to my dearest brother **Abdullah**. Without your support and love, I will not have achieved my goals. I would like also to extend my sincere gratitude and great respect to my Uncle **Dr. Walid Masoud** who followed up my health status and provided me with valuable medical advices. I finally extend my thanks to all members of my extended family and friends in and outside Palestine.

## A7. Published Papers

JJBS

*Volume 13, Number 1,March 2020*
*ISSN 1995-6673*
*Pages 123 - 126*

**Jordan Journal of Biological Sciences** **Short Communication**

# Evaluation of Antimicrobial and Genotoxic Activity of *Ephedra foeminea* Ethanolic and Aqueous Extracts on *Escherichia coli*

Shurooq M. Ismail*, Ghaleb M. Adwan, and Naser R. Jarrar

*Department of Biology and Biotechnology, An-Najah National University,P.O. Box (7)-Nablus, Palestine*

*Received February 21, 2019; Revised April 23, 2019; Accepted May 7, 2019*

**Abstract**

This study was conducted to evaluate the antimicrobial activity and the genotoxic effects of ethanolic and aqueous extracts of aerial parts of *Ephedra foeminea* (*E. foeminea*) plant on *Escherichia coli* (*E. coli* ATCC 25922). Antimicrobial activity was investigated using microbroth dilution method, while the genotoxic effect was determined using enterobacterial repetitive intergenic consensus (ERIC)-PCR. MIC value of both ethanolic and aqueous extracts of *E. foeminea* plant was found to be 50 mg/ml. Genotoxic effects of both extracts, showed an alteration in (ERIC)-PCR profiles of *E. coli* strain treated with extracts compared to untreated control. These alterations included a decreased intensity or absence of some amplified fragments. Such findings strongly indicate the genotoxic effects of both ethanolic and aqueous extracts from *E. foeminea* plant on *E. coli*. The findings draw attention to the unsafe, use of *E. foeminea* plant in folkloric medicine and point out the capability of using *E. foeminea* to treat bacterial infections. Future studies are required to know the exact molecules as well as the mechanisms responsible for the genotoxicity of this plant. *In vivo* genotoxicity studies are recommend for assessment of the safety of using *E. foeminea* plant for therapeutic purposes.

**Keywords:** *Ephedra foeminea*, Genotoxicity potential, Plant extracts, Antimicrobial activity.

## 1. Introduction

The family Ephedraceae consists of only one genus called *Ephedra* L. It has a group of approximately fifty species of perennials, evergreen, and dioecious sub-shrubs species growing up to four feet tall, with slender and joined stems. In general, species of this genus adapted to grow wild in arid and semiarid conditions and disseminated mainly in the moderate zones of Asia, Europe and North America (O'Dowd *et al*., 1998; Pirbalouti *et al*., 2013). Approximately 25 species of *Ephedra* are found in the drier regions of the Old World covering the area westwards from Central Asia across southwest Asia and into North Africa and Mediterranean Europe (Caveney *et al*., 2001). In the New World, about 24 species of *Ephedra* are found ranging from the southwestern United States to the central plateau of Mexico, and in South America occur in an area from Ecuador to Patagonia (Caveney et al., 2001). *Ephedra* grows widely in Palestine. In the flora Palestina, 5 species of *Ephedra* has been reported, included *E. foeminea*, *E. alata*, *E. aphyla*, *E. ciliata* and *E. fragilis* (Danin, 2018).

Approximately, all commercial applications of *Ephedra* extracts derived from the ephedrine alkaloids found in the stems in many Eurasian *Ephedra* species. These extracts are used in traditional medicine to treat several diseases such as bronchial asthma, coughs, chills, allergies, colds, edema, headaches, fever, flu and gastric disorders. In addition, *Ephedra* shows anticancer and antimicrobial activities (Parsaeimehr *et al*., 2010; Pirbalouti *et al*., 2013; Dehkordi *at al*., 2015; Dosari *et al*., 2016; Al-Rimawi *et al*., 2017; Mendelovich *et al*., 2017). Besides, it was shown that hydro-alcoholic extract of *E. pachyclada* was effective in experimentally healing rat ulcers (Pirbalouti *et al*., 2013).

*Ephedra* possesses a high antioxidant potential since it has been considered as a source of different phenolic compounds, as well as, a natural source of alkaloids such as ephedrine, pseudoephedrine, and other related compounds. (Eberhardt *et al*., 2000; Parsaeimehr *et al*. 2010; Amakura *et al*., 2013; Dehkordi *et al*., Ibragic and Sofić 2015; Al-Rimawi *et al*., 2017). The studies conducted on the cytotoxicity of *Ephedra* showed that ephedrine derivatives and ground ma-huang extracts were more cytotoxic than those of the whole herb extracts. A study on Neuro-2a cell line showed the cell line was more sensitive to the cytotoxicity (Lee *et al*., 2000). Ethanolic leaf extract and fruit juice of *E. foeminea* reduced viability of cancer cells *in vitro*, whereas the aqueous extract reduced the cytotoxicity in all cell lines (Mendelovich *et al*., 2017). Since there is no scientific report to date about the genetoxicity of *E. foeminea* on prokaryotes, the current study was performed to determine the antimicrobial effect of ethanolic and aqueous extracts from *E. foeminea* plant growing wild in Palestine as well as evaluate the genotoxic effect of these extracts on *E. coli* strain using enterobacterial repetitive intergenic consensus (ERIC)-PCR.

* Corresponding author e-mail: shurooq.ismail@najah.edu.

## 2. Materials and Methods

### *2.1. Plant collection and identification*

The aerial parts of *E. foeminea* were collected from a natural habitat in Tulkarm province, West Bank-Palestine, during September, 2018. Identification of the plant was carried out by the plant taxonomist Dr. Ghadeer Omar, Department of Biology and Biotechnology, An-Najah National University, Palestine.

The collected aerial parts of *E. foeminea* were washed with water to remove soil and dust particles then dried. Exposure to light was avoided to prevent possible loss of effective ingredients. The dried aerial parts were powdered finely using a blender to make them ready for ethanolic and aqueous extract preparation.

### *2.2. Plant extract preparation*

#### *2.2.1. Ethanolic extract*

Approximately 50 g of dried aerial parts powder were mixed thoroughly using magnetic stirrer in 200 mL of 80% ethanol. The ethanol-aerial parts mixture was incubated on a shaker at room temperature for 48h. The mixture was filtered using muslin cloth to remove large insoluble particles. After that, the mixture was centrifuged at 5,000 rpm for 15 min at 4°C to remove fine particles. Then, the supernatant extract was dried and concentrated by using rotary evaporator at 50°C. The obtained dried plant extract powder was stored in refrigerator at 4°C. Before starting the experiments, this material was dissolved in 10% Dimethyl Sulfoxide (DMSO) to obtain a concentration of 200 mg/mLand stored at 4ºC for further assays.

#### *2.2.2. Aqueous extract*

Aqueous aerial parts extract was prepared by mixing approximately 50 g of dried aerial parts powder thoroughly using magnetic stirrer in 200 ml of cold (room temperature) sterile distilled water. The water-aerial parts mixture was incubated on a shaker at room temperature for 48h. The mixture was filtered using muslin cloth to remove large insoluble particles. After that, the mixture was centrifuged at 5,000 rpm for 15 min at 4°C to remove fine particles. Then the supernatant extract was dried and concentrated by freeze dryer (lyophilizer). The obtained dried plant extract powder was stored in refrigerator at 4°C. Before starting the experiments, this dried plant extract powder was dissolved in a sterile distilled water to obtain a concentration of 200 mg/mL and stored at 4ºC for further assays.

### *2.3. Determination of MIC for plant extracts by broth microdilution method*

MIC of plant extracts was determined by the broth microdilution method in sterile 96- wells microtiter plates according to the CLSI instructions (CLSI, 2017). The plant extract (200 mg/mL of 10% DMSO) and 10% DMSO (negative control) were two fold-serially diluted in nutrient broth directly in the wells of the plates in a final volume of 100µL. After that, a bacterial inoculum size of $10^4$ CFU/mL was added to each well. Negative control wells containing either 100µL nutrient broth only, or 100µL DMSO with bacterial inoculum, or plant extracts and nutrient broth without bacteria were included in this experiment. Each plant extract was run in duplicate. The microtiter plate was then covered and incubated at 37°C for 24h. The MIC was taken as the minimum concentration of the dilutions that inhibited the growth of the test microorganism. MIC was determined by visual inspection.

### *2.4. Evaluation of the genotoxic potential of Ephedra foeminea aerial extracts on E. coli*

Few colonies from a 24 hour old *E. coli* strain growth culture plated on EMB agar medium were sub-cultured under sterile conditions into a bottle containing 20-mL of nutrient broth, then incubated at 37°C for 1 hour with continuous shaking. After that, aseptically, 1 mL of one hour old *E. coli* culture was added to each of eight sterile bottles each containing 25 mL broth medium. These bottles were incubated at 37°C for 1 hour with continuous shaking. Then three different concentrations of ethanolic extract (3.5 mg/mL, 1.75 mg/mL and 0.875 mg/mL of 10% DMSO), and other three different concentrations of aqueous extract (3.5 mg/mL, 1.75 mg/mL and 0.875 mg/mL of distilled water) were added into six bottles of the *E. coli* broth culture. The other two bottles were considered as a negative or untreated control by adding a specific volume of 10% DMSO and distilled water into each bottle.

Genome of *E. coli* was prepared for enterobacterial repetitive intergenic consensus (ERIC) PCR according to the method described previously (Adwan *et al*., 2013). Three mL samples were taken from the *E. coli* growth culture after 2 hours, 6 hours, and 24 hours, centrifuged for five minutes at 14,000 rpm where the supernatant of each sample was discarded. Then, each bacterial sample pellet was re-suspended in 0.8 mL of Tris-EDTA (10 mM Tris-HCl, 1 mM EDTA [pH 8]), centrifuged for five minutes at 14,000 rpm; after that, the supernatant was discarded. The pellet of each bacterial sample was re-suspended in a 300 µL of sterile distilled water and boiled for 15 minutes. Then the mixture was incubated in ice for 10 minutes. The samples were pelleted by centrifugation at 14,000 rpm for five minutes, and each sample supernatant was transferred into a new Eppendorf tube. The DNA concentration for each sample was determined by using nanodrop spectrophotometer (GenovaNano, Jenway) and the DNA samples were stored at -20ºC for ERIC-PCR analysis. The ERIC-PCR was performed using Primer ERIC1: 5`-ATG TAA GCT CCT GGG GAT TCA C-3` and Primer ERIC2: 5-AAG TAA GTG ACT GGG GTG AGC G-3`. Each PCR reaction mix (25 µL) was composed of 10 mM PCR buffer pH 8.3; 3 mM $MgCl_2$; 0.4 mM of each dNTP; 0.8 µM primer; 1.5U of Taq DNA polymerase and fixed amount of DNA template (60 ng). Then, DNA amplification was carried out using the thermal cycler (Mastercycler personal, Eppendorf, Germany) according to the following thermal conditions: initial denaturation for 3 min at 94 ºC; followed by 40 cycles of denaturation at 94 ºC for 50 s, annealing at 50 ºC for 1 min and extension at 72 ºC for 1 min, followed by a final extension step at 72ºC for 5 min. The PCR products were analyzed by electrophoresis through 1.8% agarose gel. The ERIC-PCR profile was visualized using UV trans-illuminator and photographed. Changes in ERIC-PCR banding pattern profiles following plant extracts treatments, including variations in band intensity as well as gain or loss of bands, were taken into consideration (Lalrotluanga *et al*., 2011; Atienzar *et al*., 2002).

## 3. Results

Results of this study showed that both aqueous and ethanolic aerial parts extracts of *E. foeminea* had an antibacterial activity. The MIC value of both aqueous and ethanolic aerial parts extracts of *E. foeminea* on *E. coli* strain were found to be 50 mg/ml.

DNA genome which was extracted from each *E. coli* strain which was treated with different concentrations of both aqueous and ethanolic aerial parts extracts of *E. foeminea* at various time intervals. Changes in extracted DNA genome from *E. coli* strain were evaluated and compared with untreated controls at the same time intervals.

The effect of aqueous aerial parts extract on genome of *E. coli* strain was evaluated by using ERIC-PCR. ERIC-PCR profile showed that a band with an amplicon length of about 800-bp was less intense in *E. coli* strain treated with 3.5 mg/mL and 1.75 mg/mL (Figure 1A, lanes 1 and 2) of aqueous aerial parts extract for 2h. Besides, this band disappeared in *E. coli* strain treated with 0.875 mg/ml of the same extract (Figure 1A, lane 3), in comparison with the same band appeared in un-treated control. Moreover, all bands disappeared after 6h in the *E. coli* strain treated with 3.5 mg/mL aqueous aerial parts extract (Figure 1A, lane 4). The band with an amplicon length of about 800-bp was less intense in *E. coli* strain treated with 1.75 mg/mL (Figure 1A, lane 5) disappeared in *E. coli* strain treated with 0.875 mg/mL of the same extract for 6h (Figure 1A, lane 6), in comparison with the same band appeared in the un-treated control. The band with an amplicon length of about 800-bp disappeared in *E. coli* strain treated with 3.5 mg/ml, 1.75 mg/mL and 0.875 mg/mL aqueous aerial parts extract for 24h (Figure 1A, lanes 7,8 and 9). Moreover, the band with an amplicon length of about 300-bp was less intense (Figure 1A, lanes 7, 8 and 9) in comparison with the same band appeared in un-treated control. It was observed that in lane number four most bands disappeared when treated with aqueous aerial parts extract of *E. foeminea* of 3.5 mg/mL concentration. ERIC-PCR profiles for *E. coli* strain untreated and treated with different concentrations of aqueous aerial parts extract of *E. foeminea* at the different time intervals are shown in Figure 1A.

Comparing the ERIC-PCR profile of untreated control samples with the profile of the *E. coli* treated with ethanolic aerial parts extract showed decreasing of intensity or loss of some bands from the profile. ERIC-PCR profile showed that a band with an amplicon length of about 800-bp was less intense in *E. coli* strain treated with 3.5 mg/mL (Figure 1B, lane 2 and 5) and disappeared in *E. coli* strain treated with 1.75 mg/mL (Figure 1B, lane 3 and 6) of ethanolic aerial parts extract for 2h and 6h. The band with an amplicon length of about 800-bp was less intense in *E. coli* strain treated with 3.5 mg/mL (Figure 1B, lane 7), and disappeared in *E. coli* strain treated with 1.75 mg/mL and 0.875 mg/mL (Figure 1B, lane 8 and 9) aqueous aerial parts extract for 24h. In addition, the band with an amplicon length of about 300-bp was less intense (Figure 1B, lanes 8 and 9) in comparison with the same band appeared in untreated control. ERIC-PCR profiles for *E. coli* strain untreated and treated with different concentrations of ethanolic aerial parts extract of *E. foeminea* at the different time intervals are shown in Figure 1A.

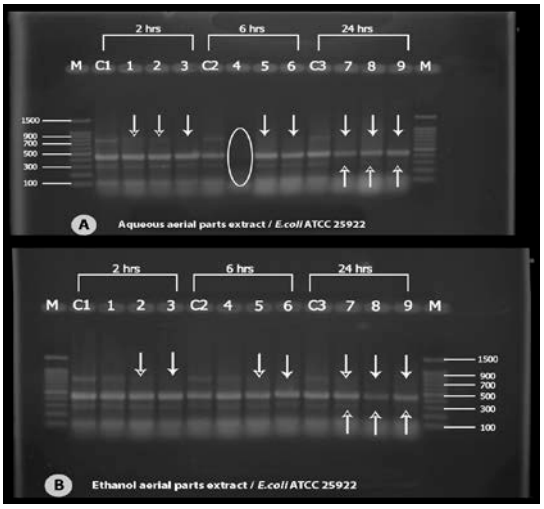


**Figure 1.** ERIC-PCR profile of *E. coli* strain untreated and treated with different aerial parts extract concentrations. A: aqueous aerial parts extract, B: ethanolic aerial parts extract of *E. foeminea* at different time intervals. Lanes C1, C2 and C3 are untreated (negative controls); lanes 1, 4 and 7 treated with 3.5 mg/ml; Lanes 2, 5 and 8 treated with 1.75 mg/ml; Lanes 3, 6 and 9 treated with 0.875 mg/ml of plant extract.

## 4. Discussion

In the present study broth microdilution method was used to examine the potential antimicrobial activity of both aqueous and ethanolic aerial parts extracts of *E. foeminea* against *E. coli*. The results confirmed that both aqueous and ethanolic aerial parts extracts of *E. foeminea* exhibited antibacterial activity against *E. coli* strain. Antimicrobial activity of some *Ephedra* species has been reported using different types of extracts (Al-Khalil *et al*., 1998; Feresin *et al*., 2001; Cottiglia *et al*., 2005; Parsaeimehr *et al*., 2010; Rustaiyan *et al*., 2011; Dehkordi *et al*., 2015; Dosari *et al*., 2016). According to previously conducted studies, phenolic compounds are the active ingredients of *Ephedra* plant (Dehkordi *et al*., 2015; Dosari *et al*., 2016).

In this study, the potential genotoxic effect of the aqueous and ethanolic aerial parts extracts of *E. foeminea* against *E. coli* was examined using ERIC-PCR technique. Reviewing the scientific literature showed that this study is the first of its kind that studied the genetoxicity of *E. foeminea* extracts on prokaryotes using ERICPCR technique. Besides, many plants were previously tested to detect their genotoxicity potential by different techniques (Basaran *et al*., 1996; Lalrotluanga *et al*., 2011; El-Tarras *et al*., 2013; Hajar and Gumgumjee, 2014; Ciğerci et al., 2016; Abu-Hijleh *et al*., 2018). ERIC-PCR profiles showed significant differences between the treated and untreated *E. coli* strain used in this study. The changes in the treated *E. coli* strain with both aqueous and ethanolic aerial parts extracts included the disappearance of certain bands as well as the change in the band intensity in comparison with untreated control. The changes in the profile of the treated *E. coli* strain in comparison with the untreated control samples could be explained due to the effect of the genotoxic molecules that were present in the plant extracts. These molecules can induce different

changes such as breakdown in DNA strands, point mutations and/or rearrangements in chromosomes. These changes in the DNA might have a potential effect on the primer binding sites and/or inter-priming distances (Abu-Hijleh *et al*., 2018). DNA sequencing or probing and other techniques can help in understanding the proposed mechanisms that lead to such differences in ERIC-PCR profiles (Lalrotluanga et al., 2011). Ma-huang is a traditional Chinese medicinal preparation derived from *Ephedra sinica* Stapf and other *Ephedra* species that are used to treat different diseases. Studies on cytotoxity of the ma-huang extracts showed that, cytotoxicity of all ma-huang extracts could not be totally accounted for by their ephedrine contents, suggesting the presence of other toxins in the extracts which may modify its pharmacological and toxicological activities (Lee *et al*., 2000).

## 5. Conclusion

The results of this study showed that aqueous and ethanolic aerial parts extracts of *E. foeminea* possess genotoxic and mutagenic potential against *E. coli*. In addition, the results also point out the capability of using *E. foeminea* to treat infections caused by *E. coli*. More studies are recommended to reveal the exact molecules that are responsible for *E. foeminea* genotoxicity as well as the mechanisms responsible for that genotoxicity.

## Competing Interests

Authors have declared that no competing interests exist.

## References


Abu-Hijleh A, Adwan G and Abdat W. 2018. Biochemical and molecular evaluation of the plant *Ecballium elaterium* extract effects on *Escherichia coli*. *J Adv Biol Biotechnol*., **9** (**2**): 1-11.

Adwan G, Adwan K, Jarrar N, Salama Y and Barakat A. 2013. Prevalence of *seg*, *seh* and *sei* genes among clinical and nasal *Staphylococcus aureus* isolates. *Br Microbiol Res J.*, **3**(**2**):139-149.

Al-Khalil S, Alkofahi A, El-Eisawi D and Al-Shibib A. 1998. Transtorine, a new quinoline alkaloid from Ephedra transitoria. *J Nat Prod*., **61**(**2**):262-263.

Al-Rimawi F, Abu-Lafi S, Abbadi J, Alamarneh AAA, Sawahreh RA and Odeh I. 2017. Analysis of phenolic and flavonoids of wild *Ephedra alata* plant extracts by LC/PDA and LC/MS and their antioxidant activity. *Afr J Tradit Complement Altern Med*., **14**(**2**): 130-141.

Amakura Y, Yoshimura M, Yamakami S, Yoshida T, Wakana D, Hyuga M, Hyuga S, Hanawa T and Goda Y.2013. Characterization of phenolic constituents from ephedra herb extract. *Molecules*, **18**(**5**):5326-5334.

Andrews, J. M. 2006. BSAC standardized disc susceptibility testing method (version 5). *J Antimicrob Chemother*., **58**(**3**): 511-529.

Atienzar FA, Venier P, Jha AN and Depledge MH. 2002. Evaluation of the random amplified polymorphic DNA (RAPD) assay for the detection of DNA damage and mutations. *Mutation Research/Genetic Toxicol and Environ Mutagen*., **521**(**1-2**): 151-163.

Basaran AA, Yu TW, Plewa MJ and Anderson D. 1996. An investigation of some Turkish herbal medicines in *Salmonella typhimurium* and in the COMET assay in human lymphocytes. *Teratogen, Carcinogen, and Mutagen*., **16**(**2**):125-138.

Caveney S, Charlet DA, Freitag H, Maier-Stolte M and Starratt AN. 2001. New observations on the secondary chemistry of world Ephedra (Ephedraceae). *Am J Bot*., **88**(**7**):1199-1208.

Ciğerci IH., Cenkci S, Kargıoğlu M and Konuk M. 2016. Genotoxicity of *Thermopsis turcica* on *Allium cepa L.* roots revealed by alkaline comet and random amplified polymorphic DNA assays. *Cytotechnol*., **68**(**4**):829-838.

Clinical and Laboratory Standards Institute (CLSI). 2017. **Performance Standards for Antimicrobial Susceptibility Testing**. 27th ed. CLSI supplement. M100S. Wayne, PA, USA.

Cottiglia F, Bonsignore L, Casu L, Deidda D, Pompei R, Casu M and Floris C. 2005. Phenolic constituents from *Ephedra nebrodensis*. *Nat Prod Res*., **19**(**2**):117-23.

Danin A. 2018. Flora of Israel on line. http://flora.huji.ac.il/browse asp. Accessed (Dec. 10, 2018).

Dehkordi NV, Kachouie MA, Pirbalouti AG, Malekpoor F and Rabei M. 2015.Total phenolic content, antioxidant and antibacterial activities of the extract of *Ephedra procera* fisch. et mey. *Acta Pol Pharm*., **72**(**2**):341-345.

Dosari AS, Amin Norouzi A, Moghadam MT and Satarzadeh N. 2016. Antimicrobial activity *of Ephedra pachyclada* methanol extract on some enteric gram negative bacteria which causes nosocomial infections by agar dilution method. *Zahedan J Res Med Sci.*, **18**(**11**):1-4.

El-Tarras AA, Hassan MM and El-Awady MA. 2013. Evaluation of the genetic effects of the *in vitro* antimicrobial activities of *Rhazya stricta* leaf extract using molecular techniques and scanning electron microscope. *Afr J Biotechnol*., **12**(**21**):3171-3180.

Eberhardt MV, Lee CY and Liu RH 2000. Antioxidant activity of fresh apples. *Nature* **405**:903–904.

Feresin GE, Tapia A, López SN and Zacchino SA. 2001. Antimicrobial activity of plants used in traditional medicine of San Juan province, Argentine. *J Ethnopharmacol.*, **78**(**1**):103-107.

Hajar AS and Gumgumjee NM. 2014. Antimicrobial activities and evaluation of genetic effects of *Moringa peregrina* (forsk) fiori using molecular techniques. *Inter J Plant and Animal Environ Sci.*, **4**(**1**):65-72.

Ibragic S and Sofić E. 2015. Chemical composition of various *Ephedra* species. *Bosn J Basic Med Sci.*, **15**(**3**): 21-27.

Lalrotluanga, Kumar NS and Gurusubramanian G. 2011. Evaluation of the random amplified polymorphic DNA (RAPD) assay for the detection of DNA damage in mosquito larvae treated with plant extracts. *Science Vision*, **11**(**3**): 155-158.

Lee MK, Cheng BW, Che CT and Hsieh DP. 2000. Cyto-toxicity assessment of Ma-huang (*Ephedra*) under different conditions of preparation. *Toxicol Sci*., **56**(**2**):424-430.

Mendelovich M, Shoshan M, Fridlender M, Mazuz M, Namder D, Nallathambi R, Selvaraj G, Kumari P, Ion A, Wininger S, Nasser A, Samara M, Sharvit Y, Kapulnik Y, Dudai N and Koltai H. 2017. Effect of *Ephedra foeminea* active compounds on cell viability and actin structures in cancer cell lines. *J Med Plants Res.*, **11**(**43**): 690-702.

O'Dowd NA, McCauley G, Wilson JAN, Parnell TAK and Kavanaugh D. 1998. *In vitro* culture, micropropagation and the production of ephedrine and other alkaloids. *In*: **Biotechnology in Agriculture and Forestry**; Bajaj YPS. (Ed.), p. 41, Springer, Berlin.

Parsaeimehr A, Sargsyan E and Javidnia K. 2010. A comparative study of the antibacterial, antifungal and antioxidant activity and total content of phenolic compounds of cell cultures and wild plants of three endemic species of *Ephedra*. *Molecules*, **15**(**3**): 1668-1678.

Pirbalouti AG, Azizi S, Amirmohammadi M and Craker L. 2013. Healing effect of hydro-alcoholic extract of *Ephedra pachyclada* Boiss. in experimentally gastric ulcer in rat. *Acta Pol Pharm*., **70** (**6**):1003-1009.

Rustaiyan A, Javidnia K, Farjam MH, Aboee-Mehrizi F and Ezzatzadeh E. 2011. Antimicrobial and antioxidant activity of the *Ephedra sarcocarpa* growing in Iran. *J Med Plants Res.,* **5** (**17**):4251-4255.

View publication stats

International Journal of
*Molecular Sciences*

MDPI

*Article*

# *Ephedra foeminea* as a Novel Source of Antimicrobial and Anti-Biofilm Compounds to Fight Multidrug Resistance Phenotype

**Shurooq Ismail [1,2], Rosa Gaglione [1,3], Marco Masi [1], Srichandan Padhi [4], Amit K. Rai [4], Ghadeer Omar [2], Alessio Cimmino [1,*] and Angela Arciello [1,3,*]**

1 Department of Chemical Sciences, University of Naples Federico II, Via Cintia 21, I-80126 Naples, Italy
2 Department of Biology and Biotechnology, An-Najah National University, Nablus 97300, Palestine
3 Istituto Nazionale di Biostrutture e Biosistemi (INBB), 00136 Rome, Italy
4 Institute of Bioresources and Sustainable Development, Imphal, Manipur 795004, India
* Correspondence: alessio.cimmino@unina.it (A.C.); anarciel@unina.it (A.A.)

**Abstract:** Plants are considered a wealthy resource of novel natural drugs effective in the treatment of multidrug-resistant infections. Here, a bioguided purification of *Ephedra foeminea* extracts was performed to identify bioactive compounds. The determination of antimicrobial properties was achieved by broth microdilution assays to evaluate minimal inhibitory concentration (MIC) values and by crystal violet staining and confocal laser scanning microscopy analyses (CLSM) to investigate the antibiofilm capacity of the isolated compounds. Assays were performed on a panel of three gram-positive and three gram-negative bacterial strains. Six compounds were isolated from *E. foeminea* extracts for the first time. They were identified by nuclear magnetic resonance (NMR) spectroscopy and mass spectrometry (MS) analyses as the well-known monoterpenoid phenols carvacrol and thymol and as four acylated kaempferol glycosides. Among them, the compound kaempferol-3-*O*-α-L-(2″,4″-di-*E*-*p*-coumaroyl)-rhamnopyranoside was found to be endowed with strong antibacterial properties and significant antibiofilm activity against *S. aureus* bacterial strains. Moreover, molecular docking studies on this compound suggested that the antibacterial activity of the tested ligand against *S. aureus* strains might be correlated to the inhibition of Sortase A and/or of tyrosyl tRNA synthase. Collectively, the results achieved open interesting perspectives to kaempferol-3-*O*-α-L-(2″,4″-di-*E*-*p*-coumaroyl)-rhamnopyranoside applicability in different fields, such as biomedical applications and biotechnological purposes such as food preservation and active packaging.

**Keywords:** multidrug resistant infections; plant-derived drugs; bioguided purification; antimicrobial monoterpenoid phenols; antimicrobial glycosylated flavonoids

check for updates

**Citation:** Ismail, S.; Gaglione, R.; Masi, M.; Padhi, S.; Rai, A.K.; Omar, G.; Cimmino, A.; Arciello, A. *Ephedra foeminea* as a Novel Source of Antimicrobial and Anti-Biofilm Compounds to Fight Multidrug Resistance Phenotype. *Int. J. Mol. Sci.* **2023**, *24*, 3284. https://doi.org/10.3390/ijms24043284

Academic Editors: Ángel Serrano-Aroca, Murtaza M. Tambuwala and Martin Birkett

Received: 22 December 2022
Revised: 28 January 2023
Accepted: 2 February 2023
Published: 7 February 2023

**Copyright:** © 2023 by the authors. Licensee MDPI, Basel, Switzerland. This article is an open access article distributed under the terms and conditions of the Creative Commons Attribution (CC BY) license (https://creativecommons.org/licenses/by/4.0/).

## 1. Introduction

Humans have always used plants as a natural source of food, animal feed and medical options to treat several diseases [1]. Indeed, conventional medicinal plants have been reported to contain compounds endowed with antimicrobial, antifungal, anti-inflammatory, antiviral and anticancer properties [2]. Among compounds responsible for these interesting and promising bioactivities, an important role is played by essential oils and other secondary metabolites, including alkaloids, terpenoids, tannins and flavonoids [2,3]. The secondary metabolites of several plants have been found to be endowed with antimicrobial properties exerted through different mechanisms of action, such as the ability to form complexes with extracellular and soluble proteins, thus sequestering them, or with membrane proteins of targeted microbes, thus determining a perturbation of membrane organization. Some secondary metabolites have also been reported to cause membrane disruption and bacterial enzyme inhibition [4–7]. The abundance and bioactivities of these compounds may greatly vary depending on plant species and environmental conditions. Traditional herbal medicine is gaining great attention in developing countries due to the strong demand for

natural compounds able to exert therapeutic effects in the absence of harmful side effects. However, it has to be highlighted that only a small percentage (1–10%) of available plant species is used by humans [8,9]. Furthermore, in many cases, the chemical composition of used plants has not been deeply characterized [3]. In recent years, the antimicrobial activity of several wild plants attracted the attention of scientists and researchers because of the fast spread of multidrug resistat (MDR) microorganisms, a worrying phenomenon requiring the urgent development of effective strategies alternative to conventional antibiotics [3].

Plants belonging to Ephedra genera falling in the Ephedraceae family represent a group of perennial gymnosperms distributed in arid and semiarid regions all over the world [10–13]. They have been largely employed in the practice of complementary and alternative medicine [14], even if it is not clear whether these practices are supported by the plants' effective pharmacological properties or if they are merely based on folklore [15]. In this scenario, researchers focused their efforts to search for and to identify novel effective drugs starting from still-unexplored folk medicinal wild plants [16]. In the case of Ephedra genera, the presence of five species, such as *E. foeminea*, *E. alata*, *E. aphyla*, *E. ciliata* and *E. fragilis* [17], has been observed. Alanda (*Ephedra foeminea* or *Ephedra campylopoda*) is the Arabic name for a low stalky Eurasian shrub from the Ephedraceae family, omnipresent in northern Palestine and across the southeastern Mediterranean. In Oriental Arab medicine, it is used to treat agitation and skin rash. Moreover, the aerial parts of various *Ephedra* species were proven to contain active alkaloids, such as phenylpropylamino, alkaloids, ephedrine and pseudoephedrine [18]. The phytochemical analysis of the aqueous, methanolic and ethanolic extracts of *E. foeminea* revealed the presence of different phytoconstituents, with the methanolic extract containing (i) high levels of phenols, carbohydrates, sterols/steroids, flavones and lignin; (ii) moderate levels of tannins, quinones, amino acids, cardiac glycosides and phlobatannins; (iii) low levels of resins, terpenoids, flavonoids, coumarins, reducing sugars and anthocyanins; and (iv) the absence of alkaloids, saponins, anthraquinones and fixed oils and lipids [19]. It has been also reported in other *Ephedra* species a high content of the alkaloids ephedrine and pseudoephedrine, which are known to be endowed with several pharmaceutical properties, being able to increase heartrate and blood pressure, to promote bronchodilatation and to affect the central nervous system [20]. Because of this, plants from *Ephedra* genera have been widely used throughout the history of humankind, having been employed as an ointment to improve wound healing or to treat bronchial asthma, chills, colds, coughs, edema, fever, allergies, syphilis and gonorrhea [21]. *Ephedra* extracts have even been used as a food supplement to enhance performance and weight loss until 2004 when they were banned by the Food and Drug Administration (FDA) because of several death events due to negative effects on the cardiac and cardiovascular systems [22]. In more recent studies, the ethanolic extracts of *E. foeminea* were found to be endowed with anticancer and antimicrobial properties [23,24]. However, while the alkaloid content of *Ephedra* species has been widely described, only a few papers focus on non-alkaloid content. Based on this, it appears promising to investigate the biological activities of these still-unexplored secondary metabolites that might represent a source of novel compounds with interesting bioactivities.

In this study, we performed a bioguided purification of *E. foeminea* extracts to isolate bioactive compounds that were identified by nuclear magnetic resonance (NMR) spectroscopy and mass spectrometry (MS) analyses. Following this experimental strategy, in addition to the well-known monoterpenoid phenols carvacrol and thymol, four acylated kaempferol glycosides namely kaempferol-3-*O*-α-L-(2″,4″-di-*E*-*p*-coumaroyl)-rhamnopyranoside, kaempferol-3-*O*-α-L(2″-*E*-*p*-coumaroyl,4″-*Z*-*p*-coumaroyl)- rhamnopyranoside, kaempferol-3-*O*-α-L(2″-*Z*-*p*-coumaroyl,4″-*E*-*p*-coumaroyl)- rhamnopyranoside and kaempferol-3-*O*-α-L(2″,4″-di-*Z*-*p*-coumaroyl)-rhamnopyranoside were also identified for the first time in *E. foeminea*. Furthermore, they were found to be endowed with strong antimicrobial properties and promising antibiofilm activity.

## 2. Results

### 2.1. Antimicrobial and Antibiofilm Activity of E. foeminea Extracts

*E. foeminea* ethanolic extract was firstly investigated for its antibacterial activity towards three gram-positive (*S. aureus* ATCC 29213, methicillin-resistant *S. aureus* MRSA WKZ-2, *E. faecalis* ATCC 29212) and three gram-negative (*A. baumannii* ATCC 17878, *E. coli* ATCC 25922 and *S. typhimurium* ATCC 14028) bacterial strains. The ethanolic extract was found to exert strong antimicrobial properties towards three out of six bacterial strains tested, with $MIC_{100}$ values ranging from 1.25 to 2.5 mg/mL (Table 1). Being effective on both gram-negative and gram-positive bacterial strains, the ethanolic extract was found to be endowed with a broad-spectrum antimicrobial activity (Table 1). Interestingly, significant antimicrobial effects were also detected on *S. aureus* MRSA WKZ-2, *E. faecalis* ATCC 29212 and *A. baumannii* ATCC 17878 bacterial strains, even if higher doses of the extract ($MIC_{100}$ values comprised between 5 and 10 mg/mL) were required to obtain the same effects recorded on the other tested strains (Table 1). To identify compounds responsible for the detected effects, further extraction procedures were sequentially performed as detailed in the Materials and Methods section. In particular, three solvents characterized by a different polarity, namely (i) hexane, (ii) dichloromethane and (iii) ethyl acetate were used. The antibacterial activity of each obtained fraction was investigated on the same bacterial strains described above and it was found that hexane, dichloromethane and ethyl acetate extracts were able to exert antimicrobial activity on three out of six bacterial strains tested with $MIC_{100}$ values comprised between 0.625 and 2.5 mg/mL (Table 1). This suggests that the extracts retain a significant broad-spectrum antimicrobial activity being effective on both gram-negative and gram-positive bacterial strains (Table 1). In the case of the water phase, no significant antimicrobial activity was detected on any of the tested strains. Based on this, it can be hypothesized that most of the compounds responsible for the antibacterial activity were extracted using organic solvents. The antibiofilm properties of the extracts were also evaluated by performing crystal violet assays. Interestingly, ethanolic, hexane, dichloromethane and ethyl acetate extracts were found to be endowed with antibiofilm properties, being able to affect the biofilm formation in the case of *S. typhimurium* ATCC 14028 (Figure 1a). No significant antibiofilm properties were, instead, detected for the water phase (Figure 1a). Ethanolic extract was also tested on *S. aureus* MRSA WKZ-2, *E. faecalis* ATCC 29212 and *A. baumannii* ATCC 17878 and found to be effective on these strains with significant inhibition of biofilm formation (about 50–70% inhibition) in the case of *A. baumannii* ATCC 17878 and *S. aureus* MRSA WKZ-2 (Figure 1b).

**Table 1.** $MIC_{100}$ values (mg/mL) determined for *E. foeminea* ethanolic, hexane, dichloromethane and ethyl-acetate extracts tested on a panel of gram-positive and gram-negative bacterial strains. (-) indicates not tested samples. Reported data refer to three biological replicates.

| | $MIC_{100}$ (mg/mL) | | | |
|---|---|---|---|---|
| **Gram-Positive Strains** | **Ethanol** | **Hexane** | **Dichloromethane** | **Ethyl Acetate** |
| *S. aureus* ATCC 29213 | 2.5 | 0.625 | 1.25 | 2.5 |
| *S. aureus* MRSA WKZ-2 | 10 | - | - | - |
| *E. faecalis* ATCC 29212 | 10 | - | - | - |
| **Gram-Negative Strains** | | | | |
| *E. coli* ATCC 25922 | 1.25 | 2.5 | 2.5 | 2.5 |
| *S. typhimurium* ATCC 14028 | 2.5 | 1.25 | 2.5 | 2.5 |
| *A. baumannii* ATCC 17878 | 5 | - | - | - |

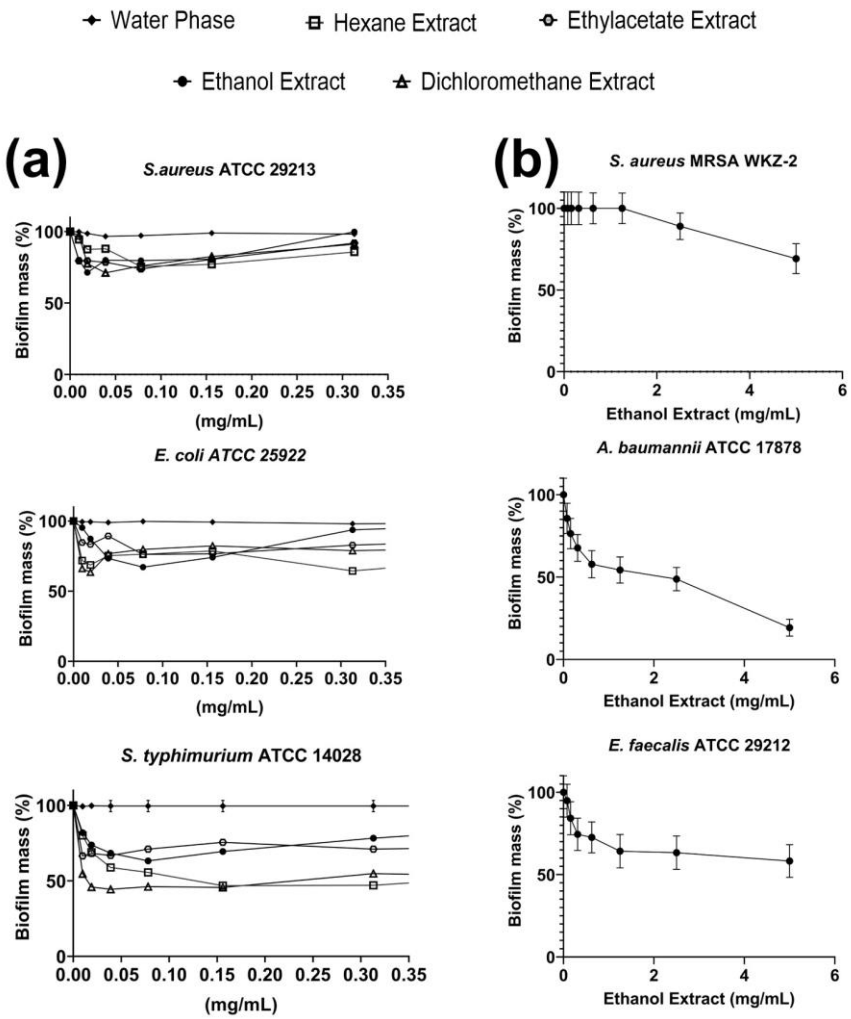


**Figure 1.** Antibiofilm activity of *E. foeminea* plant extracts on *S. aureus* ATCC 29213, *S. aureus* MRSA WKZ-2, *E. faecalis* ATCC 29212, *A. baumannii* ATCC 17878, *E. coli* ATCC 25922 and *S. typhimurium* ATCC 14028. (**a**) Extracts obtained in ethanol, hexane, dichloromethane, ethyl acetate or water phase were tested against *S. aureus* ATCC 29213, *E. coli* ATCC 25922 and *S. typhimurium* ATCC 14028. (**b**) Ethanolic extract was tested against *A. baumannii* ATCC 17878, *E. faecalis* ATCC 29212 and *S. aureus* MRSA WKZ-2. The effects of increasing concentrations of each extract were evaluated on biofilm formation. At the end of the incubations, biofilm samples were stained with crystal violet and measured at 630 nm. Data represent the mean (±standard deviation, SD) of at least three independent experiments, each one carried out with triplicate determinations.

### *2.2. Bioguided Fractionation of Plant Extracts Followed by Isolation and Identification of Active Compounds*

To isolate the compounds endowed with antibacterial and/or antibiofilm activities, the most promising extracts (hexane and dichloromethane extracts) obtained from *E. foeminea* were subjected to sequential purification steps by thin-layer chromatography (TLC) or column chromatography (CC) as reported in the Materials and Methods section and in Figure 2.

Fractions obtained upon extraction in hexane and two sequential steps of CC were found to be endowed with antimicrobial activity (Supplementary Table S1). Two main compounds were isolated from the hexane extract and identified as carvacrol (compound **1**, 4.72 mg) and as thymol (compound **2**, 1.72 mg) (Figure 3), comparing their spectroscopic data ($^1$H NMR and ESI MS) with those reported in the literature (Supplementary Figures S1 and S2). It is

noteworthy that no data in the literature exist about the presence of these two compounds in *E. foeminea* [21].

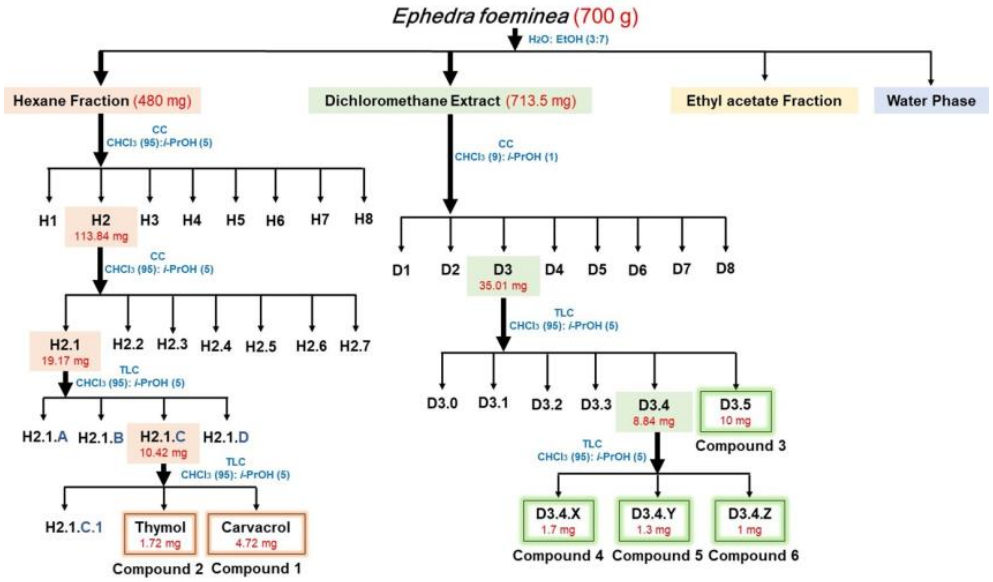


**Figure 2.** Schematic representation of the bioguided fractionation of extracts obtained from *E. foeminea* aerial parts.

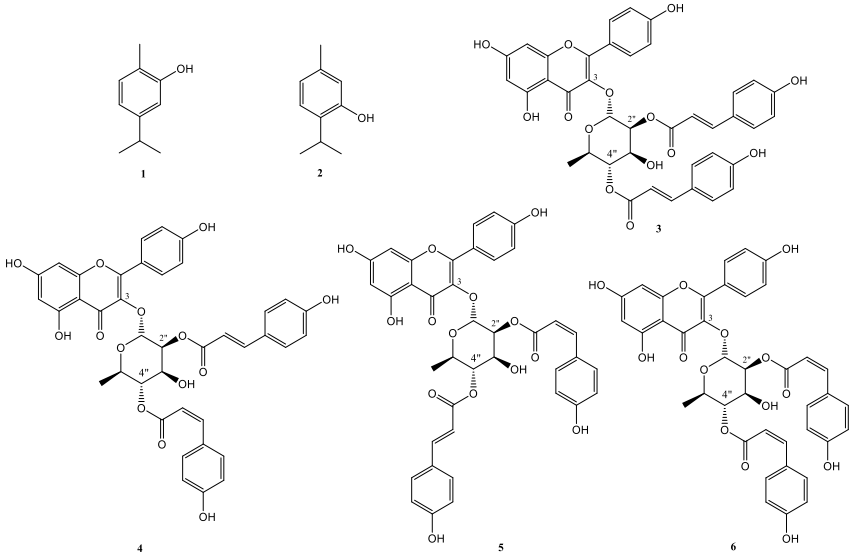


**Figure 3.** Chemical structures of isolated compounds **1**–**6**.

The active compounds from the $CH_2Cl_2$ extract were fractionated by combined CC and TLC on the direct and reverse phase to obtain four pure metabolites, as reported in detail in the Materials and Methods section. The first investigation of their $^1$H NMR spectra showed the signals of flavonol glycosides. In particular, the $^1$H NMR spectrum of compound **3** was recorded in acetone-$d_6$ [25] and in $CD_3OD$ [26] (Supplementary Figures S3–S13). In acetone-$d_6$, two broad signals at δ 6.28 (H-6) and 6.48 (H-8) were detected and the two doublet $A_2X_2$ aromatic system protons at δ 7.13 (H-3′,5′) and 7.91 (H-2′,6′), $J$ = 8.7 Hz, typical of a kaempferol residue. The presence of the anomeric proton at δ 5.83 (H-1″, brs), the methine protons at δ 5.62 (H-2, brs), 4.20 (H-3, dd, $J$ = 9.7 and 3.0 Hz), 4.98 (H-4, t, $J$ = 9.7 Hz), 3.39 (dd, $J$ = 9.7 and 6.1 Hz) and the secondary methyl group at δ 0.86 (H-6, d, $J$ = 6.1 Hz) suggested the presence of an α-rhamnopyranoside moiety substituted in position H-2″ and H-4″ by two *p*-coumaroyl residues, as observed from their typical signals. In particular, the signals

of the double bonds H-2‴ and H-3‴ at δ 6.44 and 7.68 ($J$ = 16.0 Hz) and H-2⁗ and H-3⁗ at δ 6.31 and 7.56 ($J$ = 16.1 Hz) revealed the presence of two *E*-configured double bounds. COSY spectrum (Supplementary Figures S7 and S8) confirmed the connections around the rhamnopyranoside and the positions of the *p*-coumaroyl residues at H-2″ and H-4″ of the sugar residue for the downfield shifts showed by these protons. Through an extensive study of 2D $^{13}$C NMR spectra (HSQC and HMBC), the chemical shifts were assigned to all the carbons and protons (Supplementary Figures S10–S13). In this way, compound **3** was identified as kaempferol-3-*O*-α-L-(2″,4″-di-*E*-*p*-coumaroyl)-rhamnopyranoside as previously reported [25–28]. The identification was also supported by the data collected by the electrospray ionization (ESI) MS spectrum, which showed the protonated $[M + H]^+$ ion at $m/z$ 725.

Compounds **4**–**6** showed similar 1D and 2D $^1$H and $^{13}$C NMR spectra indicating that they differ from compound **3** for the configuration of the double bonds on the two *p*-coumaroyl residues (Supplementary Figures S14–S24). In particular, the $^1$H NMR spectrum of compound **4** differed from that of compound **3** for the signals of the double bonds H-2‴ and H-3‴ at δ 6.45 and 7.70 ($J$ = 15.9 Hz) and H-2⁗ and H-3⁗ at δ 5.78 and 6.92 ($J$ = 10.0 Hz), thus suggesting the presence of *trans*- and *cis*-*p*-coumaroyl moieties. Compound **4** was identified kaempferol-3-*O*-α-L-(2″-*E*-*p*-coumaroyl,4″-*Z*-*p*-coumaroyl)-rhamnopyranoside, as previously reported [28]. The $^1$H NMR spectrum of compound **5** differed from that of compound **3** for the signals of the double bonds H-2‴ and H-3‴ at δ 5.88 and 6.93 ($J$ = 11.8 Hz) and H-2⁗ and H-3⁗ at δ 6.33 and 7.59 ($J$ = 16.0 Hz), thus suggesting the presence of *trans*- and *cis*-*p*-coumaroyl moieties. Thus, compound **5** was identified as kaempferol-3-*O*-α-L-(2″-*Z*-*p*-coumaroyl,4″-*E*-*p*-coumaroyl)-rhamnopyranoside, as previously reported [29]. Compound **6** was, instead, identified as kaempferol-3-*O*-α-L-(2″,4″-di-*Z*-*p*-coumaroyl)-rhamnoside. In fact, its $^1$H NMR spectrum differed from that of compound **3** for the signals of the double bonds H-2‴ and H-3‴ at δ 5.77 and 6.87 ($J$ = 12.0 Hz) and H-2⁗ and H-3⁗ at δ 5.89 and 6.92 ($J$ = 12.0 Hz) [26]. Through extensive use of 1D and 2D $^1$H and $^{13}$C NMR spectra, the chemical shifts were assigned to all the carbons and protons of compounds **4**–**6** (Supplementary Figures S14–S24).

### 2.3. Evaluation of the Antimicrobial Activity of Isolated Compounds **1**–**6**

To verify whether the isolated compounds might account for the antimicrobial activity of the whole extract, antimicrobial activity assays were performed by testing increasing concentrations of each isolated compound on *S. aureus* ATCC 29213, *S. aureus* MRSA WKZ-2, *E. faecalis* ATCC 29212, *A. baumannii* ATCC 17878, *E. coli* ATCC 25922 and *S. typhimurium* ATCC 14028. As shown in Supplementary Table S2, carvacrol was found to be active on all the strains tested, with the strongest effects observed on *S. aureus* ATCC 29213 and *S. aureus* MRSA WKZ-2, with $MIC_{100}$ values of 100 and 50 μg/mL, respectively (Supplementary Table S2). The *E. coli* bacterial strain was found to be the least sensitive to carvacrol antimicrobial activity, with an $MIC_{100}$ value of 200 μg/mL (Supplementary Table S2). In the case of thymol, higher $MIC_{100}$ values were detected with respect to carvacrol on the same bacterial strains, with *S. typhimurium* found to be the most susceptible bacterial strain ($MIC_{100}$ = 300 μg/mL) and *S. aureus* MRSA WKZ-2 found to be the least sensitive to thymol antimicrobial effects ($MIC_{100}$ = 2400 μg/mL) (Supplementary Table S2). The antimicrobial activity was also tested for the isolated isomer kaempferol-3-*O*-α-L-(2″,4″-di-*E*-*p*-coumaroyl)-rhamnopyranoside compound **3** on *S. aureus* ATCC 29213, *S. aureus* MRSA WKZ-2, *E. coli* ATCC 25922, *E. faecalis* ATCC 29212, *E. coli* ATCC 25922, *S. typhimurium* ATCC 14028 and *A. baumannii* ATCC 17878. A very strong antimicrobial activity towards gram-positive *S. aureus* ATCC 20213 and *S. aureus* MRSA WKZ-2 was found, with $MIC_{100}$ values as low as 0.49 μg/mL in the case of both bacterial strains (Table 2). Significantly higher $MIC_{100}$ values were detected in the case of the other bacterial strains tested, with values comprised between 250 and 1000 μg/mL (Table 2 and Supplementary Table S3). Kinetic killing curves were also obtained by treating *S. aureus* ATCC 29213 and *S. aureus* MRSA WKZ-2 with 0.49 μg/mL compound **3** for different times

(0–19 h). We observed that, in the case of both bacterial strains, about 90% cell death was observed upon 19 h incubation (Figure 4), thus indicating the ability of kaempferol-3-*O*-α-L-(2″,4″-di-*E*-*p*-coumaroyl)-rhamnopyranoside compound **3** to exert bactericidal effects. Very interesting is also the evidence that the analyzed compound **3** was the only one to be endowed with this strong antimicrobial activity on *S. aureus* strains. Indeed, the other tested isomers (compound **4**–**6**) were found to be endowed with $MIC_{100}$ values higher than 1000 μg/mL when tested on *S. aureus* MRSA WKZ-2 (Supplementary Table S3). This might open interesting perspectives to the applicability of the isolated compound **3** in the biomedical field.

**Table 2.** $MIC_{100}$ values (μg/mL) determined for the compound kaempferol-3-*O*-α-L-(2″,4″-di-*E*-*p*-coumaroyl)-rhamnopyranoside (compound **3**) purified from *E. foeminea* dichloromethane extract.

| | $MIC_{100}$ (μg/mL) | |
|---|---|---|
| **Gram-Positive Strains** | **Compound 3** | **Gentamycin** |
| *S. aureus* ATCC 29213 | 0.49 | ≤1 |
| *S. aureus* MRSA WKZ-2 | 0.49 | ≤1 |
| *E. faecalis* ATCC 29212 | 500 | ≤8 |
| **Gram-Negative Strains** | | |
| *E. coli* ATCC 25922 | 250 | ≤4 |
| *S. typhimurium* ATCC 14028 | 1000 | ≤15 |
| *A. baumannii* ATCC 17878 | 1000 | ≤2 |

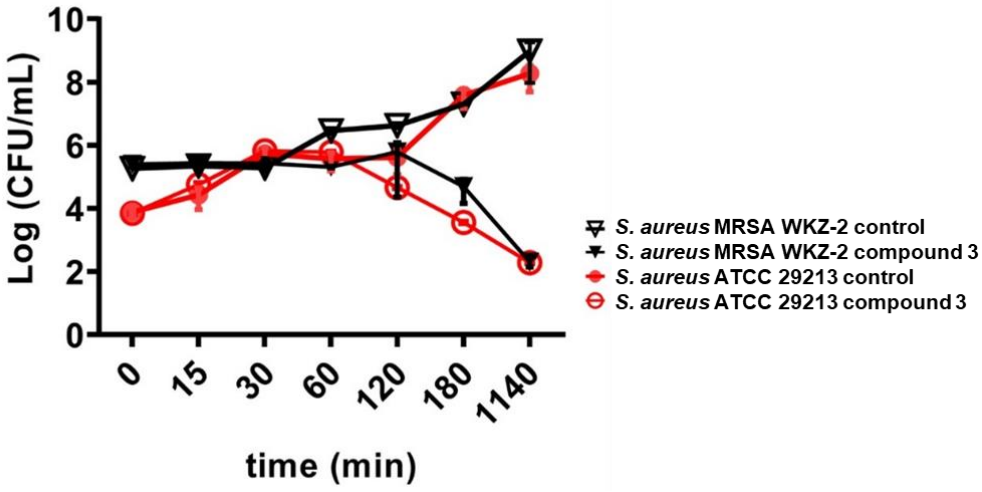


**Figure 4.** Time-killing curves obtained by incubating *S. aureus* ATCC 29213 (red lines) and *S. aureus* MRSA WKZ-2 (black lines) with kaempferol-3-*O*-α-L-(2″-*E*-*p*-coumaroyl,4″-*E*-*p*-coumaroyl)-rhamnoside (compound **3**) for different time intervals. Data represent the mean (±standard deviation, SD) of at least three independent experiments, each one carried out with triplicate determinations.

### *2.4. Evaluation of the Antibiofilm Activity of Kaempferol-3-O-α-L-(2″,4″-di-E-p-coumaroyl)-rhamnopyranoside (Compound 3)*

The antibiofilm properties of the purified compound **3** were also evaluated by performing crystal violet assays on the *S. aureus* ATCC 29213, *S. aureus* MRSA WKZ-2, *E. faecalis* ATCC 29212, *A. baumannii* ATCC 17878, *E. coli* ATCC 25922 and *S. typhimurium* ATCC 14028 bacterial strains incubated with increasing concentrations of the isolated compound. In all the cases, a significant inhibition (about 30–80%) of biofilm formation was observed, with the strongest effects obtained in the case of the *A. baumannii* ATCC 17878 and *S. aureus* MRSA WKZ-2 bacterial strains (Figure 5). It is noteworthy that significant effects on biofilm formation were obtained at concentrations significantly lower than the $MIC_{100}$ values

detected on the same bacterial strains. To deepen on compound **3** antibiofilm activity, confocal laser scanning microscopy (CLSM) analyses were also performed. As first, the *E. foeminea* crude ethanolic extract was analyzed for its effects on the formation of *S. aureus* MRSA WKZ-2 and *A. baumannii* ATCC 17878 biofilm. As observed in Figure 6, significant effects on biofilm architecture and thickness were evaluated upon treatment of both bacterial strains with the extract for 24 h. When the pure compound **3** was analyzed on the same bacterial strains, significant effects on biofilm architecture and thickness were also evaluated (Figure 7). Furthermore, when the pure compound **3** was tested on *A. baumannii* ATCC 17878 biofilm, changes in the biofilm morphology were found to be associated with a strong aggregation of bacterial cells that appear to form groove-like structures (Figure 7a) and filamentous structures (Figure 7b), which is indicative of an interference with cell division, probably due to a septation block, as previously reported for different antibiofilm compounds [30]. A significant decrease in cell density also appears clear upon treatment with the pure compound (Figure 7), indicative of a high percentage of cell death. When the total protein content was analyzed, a significant effect of compound **3** was detected only in the case of the *S. aureus* MRSA WKZ-2 bacterial strain (Figure 7a). Indeed, in this case, the total protein content was found to be lower in the presence of compound **3** with respect to control untreated cells, both in the case of attached biofilm (sediment) and in the case of floating cells (supernatant). A different result was, instead, obtained in the case of the *A. baumannii* ATCC 17878 bacterial strain. In this case, a slight effect on the total protein content was detected only in the case of the supernatant (Figure 7b), probably because compound **3** exerts antibiofilm properties with different mechanisms depending on the specific features of the target bacterial cells. It is noteworthy that, when the antibiofilm activity of the isomers, i.e., compounds **4**–**6**, has been analyzed, different results were obtained. Also in this case, CLSM analyses were performed to test effects of isomers on *S. aureus* MRSA WKZ-2 and *A. baumannii* ATCC 17878 biofilm formation. In the case of compound **5**, a small effect on biofilm thickness was evaluated on *A. baumannii* ATCC 17878 upon 24 h incubation (Supplementary Figure S25), whereas no significant effects were detected on *S. aureus* MRSA WKZ-2 (Supplementary Figure S26). A similar result was obtained also in the case of the isomer compound **4** (Supplementary Figure S25), whereas no significant effects on either bacterial strain were detected in the case of compound **6** (Supplementary Figure S27).

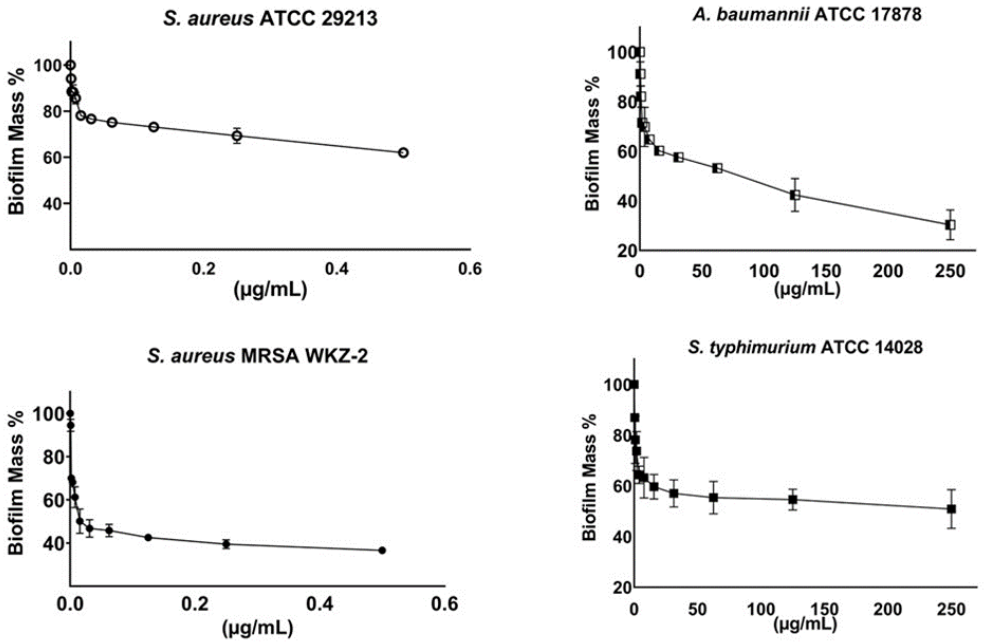


**Figure 5.** *Cont.*

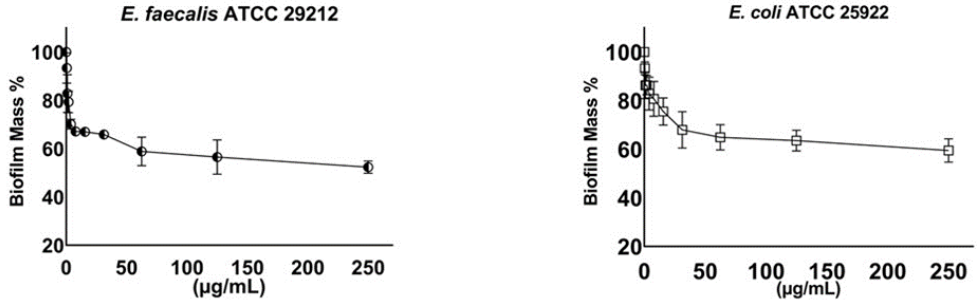


**Figure 5.** Antibiofilm activity of kaempferol-3-*O*-α-L-(2″,4″-di-*E*-*p*-coumaroyl)-rhamnoside (compound **3**) evaluated by crystal violet assays on *S. aureus* ATCC 29213, *S. aureus* MRSA WKZ-2, *E. faecalis* ATCC 29212, *A. baumannii* ATCC 17878, *S. typhimurium* ATCC 14028 and *E. coli* ATCC 25922. The effects of increasing concentrations of the compound were evaluated on biofilm formation. Biofilm was stained with crystal violet and samples were analyzed by using a plate reader to measure absorbance at 630 nm. Data represent the mean (±standard deviation, SD) of at least three independent experiments, each one carried out with triplicate determinations.

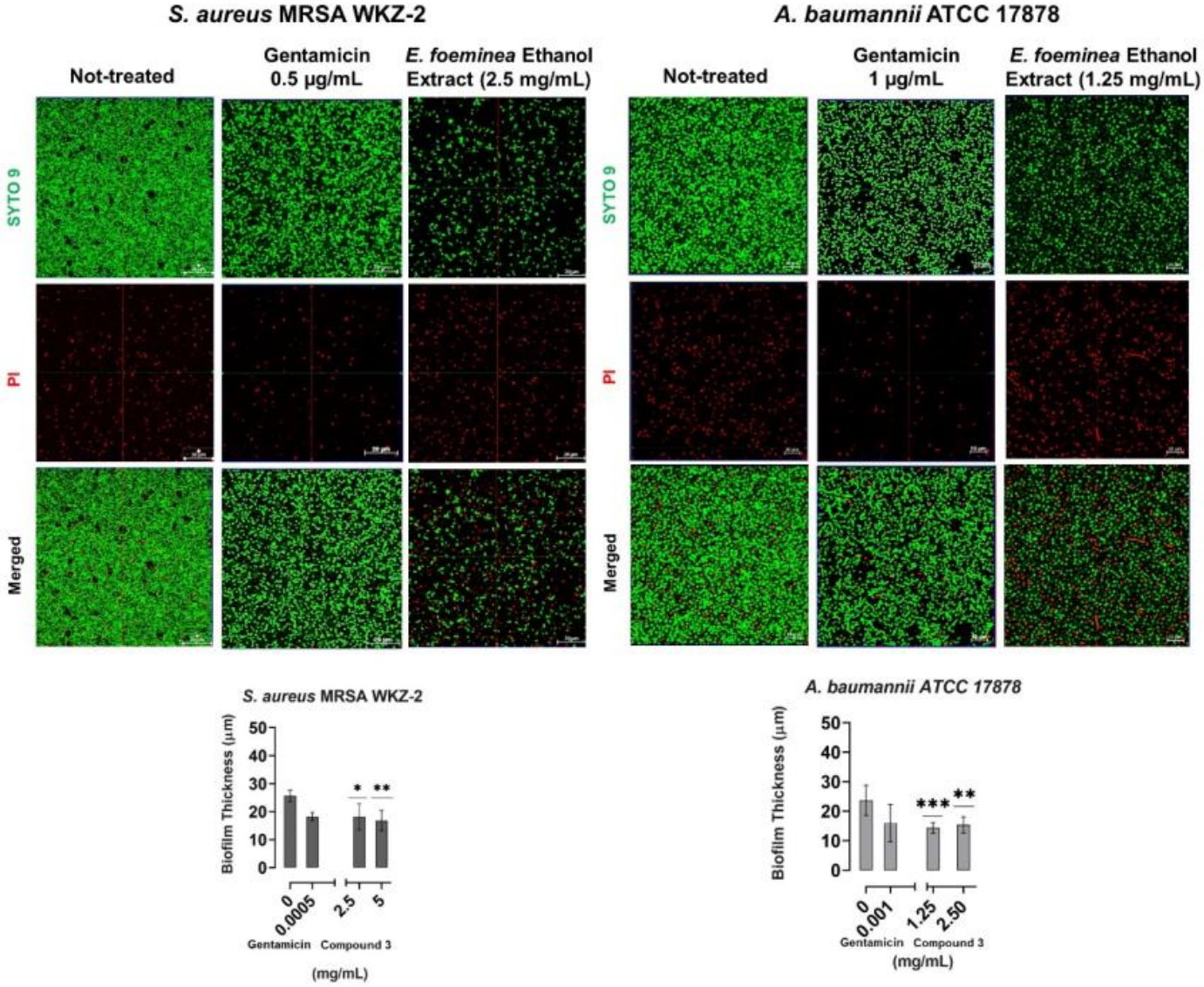


**Figure 6.** Antibiofilm activity of *E. foeminea* ethanolic extract. Effects of *E. foeminea* ethanolic extract were evaluated on biofilm formation in the case of *S. aureus* MRSA WKZ-2 and *A. baumannii* ATCC

17878 by CLSM. Gentamicin antibiotic was tested as a positive control. Not-treated sample contains the same amount of solvent present in the sample incubated with the highest concentration of ethanolic extract. Biofilm cells were stained with LIVE/DEAD BacLight bacterial viability kit (molecular probes, Eugene, OR) containing a 1:1 mol/mol ratio of SYTO-9 (green fluorescence, all cells) and propidium iodide (PI; red fluorescence, dead cells). The biofilm images were obtained by confocal z-stack using Zen Lite 2.3 software. All the images were taken under identical conditions. Significant differences were indicated as (* $p < 0.05$), (** $p < 0.001$) or (*** $p < 0.0001$) for treated versus control samples. Each experiment was carried out in triplicate.

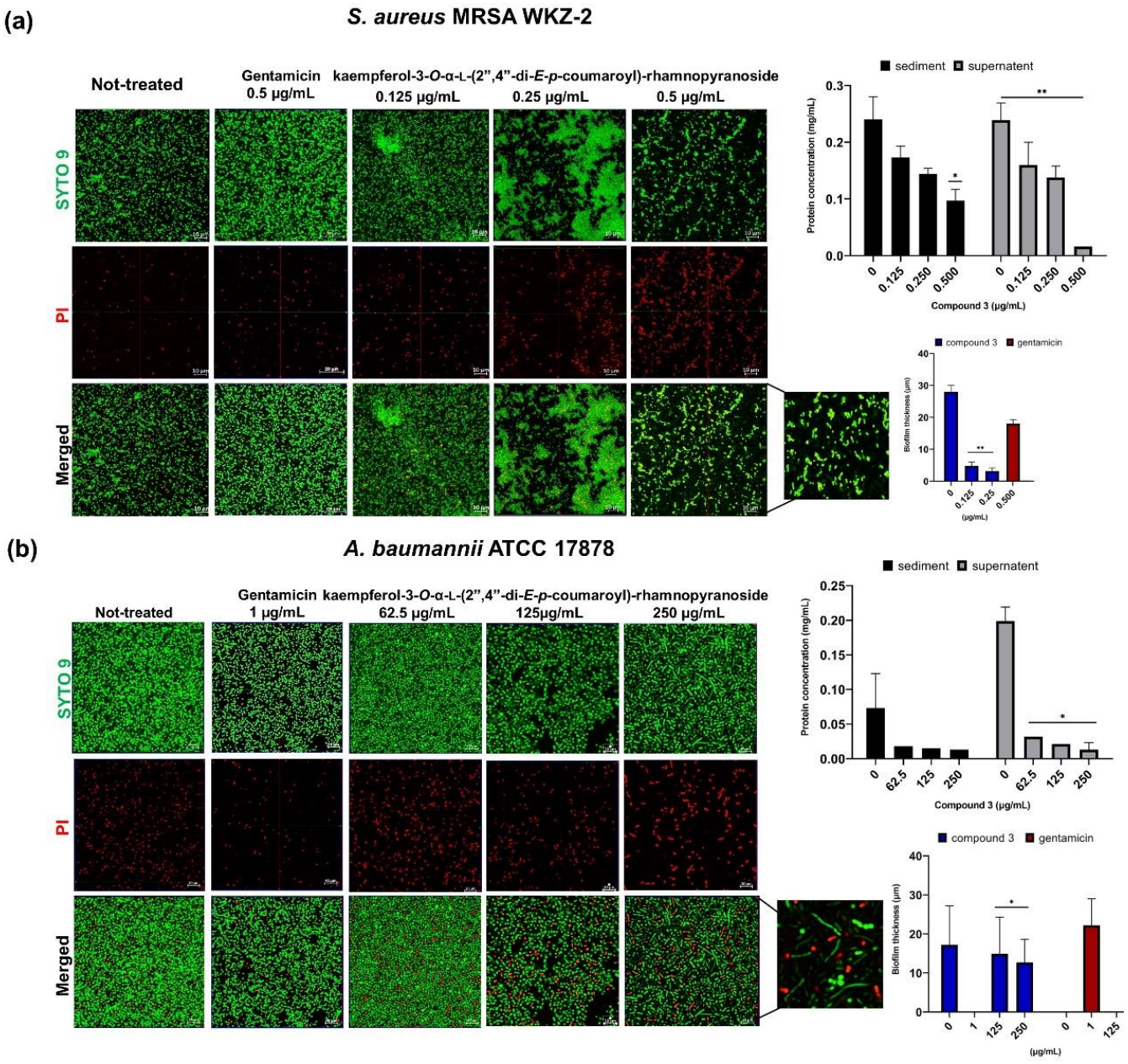


**Figure 7.** Antibiofilm activity of purified kaempferol-3-*O*-α-L-(2″,4″-di-*E*-*p*-coumaroyl)-rhamnopyranoside (compound **3**). Effects of compound **3** were evaluated on biofilm formation in the case of *S. aureus* MRSA WKZ-2 (**a**) and *A. baumannii* ATCC 17878 (**b**) by CLSM. Gentamicin antibiotic was tested as a positive control. Not-treated sample contains the same amount of solvent present in the sample incubated with the highest concentration of tested compound **3**. Biofilm cells were stained with LIVE/DEAD BacLight bacterial viability kit (molecular probes,

Eugene, OR) containing a 1:1 mol/mol ratio of SYTO-9 (green fluorescence, all cells) and propidium iodide (PI; red fluorescence, dead cells). Biofilm images were obtained by confocal z-stack using Zen Lite 2.3 software. All the images were taken under identical conditions. Significant differences were indicated as (* $p < 0.05$) or (** $p < 0.001$) for treated versus control samples. Each experiment was carried out in triplicate.

### *2.5. Prediction of the Target of Kaempferol-3-O-α-L-(2″, 4″-di-E-p-coumaroyl)-rhamnopyranoside Antimicrobial and Antibiofilm Activity by Molecular Docking*

Among the well-known proteins responsible for bacterial biofilm adhesion, formation and aggregation, Sortase A (Srt A) [31] attracted our attention. This enzyme catalyzes the covalent linkage of the cell wall proteins (CWA) to the peptidoglycan [31]. Indeed, the inactivation of their enzymatic activity has been reported to interfere with the ability of bacterial cells to cause infections because of the failure of fibronectin protein attachment to the cell wall [32]. For this reason, the Srt A protein attracted the attention of the researchers as an interesting target for the development of antimicrobial and antibiofilm drugs [33]. Another interesting target is represented by aminoacyl–tRNA synthases (aaRSs) [34] playing a key role in the translation of nucleic acid sequences into a polypeptide sequence [35]. Indeed, their inhibition is associated with a blockage of bacterial cell growth due to the interference with protein synthesis [34]. Furthermore, it has to be highlighted that significant differences in the topology of ATP binding domain have been reported between human and bacterial aaRS, probably due to the different functions that these enzymes play in human cells [36], thus opening the way to the possibility of selectively targeting bacterial aaRSs enzymes [34]. Based on this, a preliminary evaluation of the putative molecular bases of compound **3** antimicrobial and antibiofilm properties was performed by selecting Sortase A (Srt A) protein and aminoacyl–tRNA synthases (aaRSs) as targets in molecular docking analyses. The tested compound **3** demonstrated substantial binding to both selected targets. The binding free energy, in the case of the complex with tyrosyl tRNA synthetase, was computed to be higher (−9.5 kcal/mol) than that determined in the case of Sortase A (−8.3 kcal/mol). In the case of all the analyzed complexes, the binding of the ligand to the active site of the proteins was found to be mediated by representative hydrogen bonding, hydrophobic and various van der Waal's force interactions (Supplementary Table S4, Figure 8a–d). Furthermore, in the case of the complex with tyrosyl tRNA synthetase, the binding was found to be supported by a carbon-hydrogen bond and several hydrophobic interactions. Indeed, the tested ligand was found to be bonded to several amino acid residues, such as Gly 38, Ala 43, His 47, His 50 and Leu 223 (Supplementary Table S4). The maximum number of interactions was observed in the case of His 47 residue. It is noteworthy that the residues His 47 and His 50 were reported as suitable targets of specific inhibitors of the enzyme tyrosyl tRNA synthetase [35]. In the case of the complex with Sortase A, various non-covalent forces were described including conventional hydrogen bonding, carbon–hydrogen bonding and hydrophobic interactions. Amino acids Ala 92, Ala 104, Val 168, Thr 180, Val 193, Arg 197 and Ile 199 were predicted to mediate the interaction between the test ligand and the Sortase A enzyme (Supplementary Table S4). It is noteworthy that residue Arg 197 represents a suitable target f an inactivating drug, since it has been reported to play a crucial role in the active site of the Sortase A enzyme [33]. It has to be highlighted that non-covalent forces generally mediate the biological activity of effective drugs and are of great importance in the design and development of novel drugs. Hydrogen bonds generally deliver structural strength and stability to protein–ligand complexes, whereas hydrophobic forces play a crucial role in amplifying the ligand's binding affinity toward the surface of the target in a physiological environment [37,38]. Van der Waal's interactions, being weak electrostatic forces, play an important role in stabilizing the three-dimensional structure of protein–ligand complexes [39]. Based on our findings, it can be hypothesized that the strong antibacterial activity of kaempferol-3-*O*-α-L-(2″,4″-di-*E*-*p*-coumaroyl)-rhamnoside against *S. aureus* bacterial cells might be mediated by its binding to these two selected enzymes (tyrosyl tRNA synthetase and Sortase-A) and to the consequent blockage of key residues present in the active site determining the inhibition of the enzymatic activity.

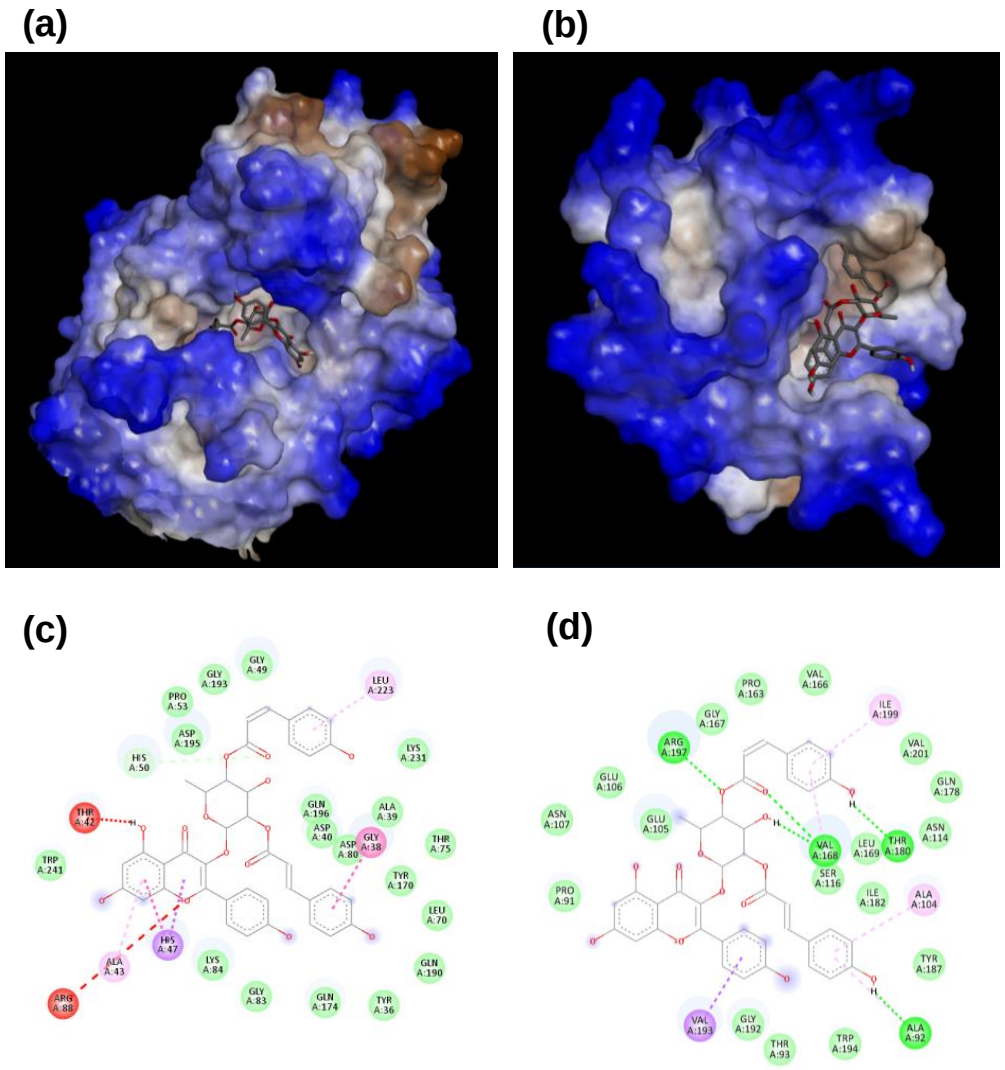


**Figure 8.** 3D orientation of kaempferol-3-*O*-α-L-(2″,4″-di-*E*-*p*-coumaroyl)-rhamnopyranoside (compound **3**) (shown in stick) at the active pocket of tyrosyl tRNA synthetase (**a**) and Sortase A (**b**); 2D representation of intermolecular interactions between the antimicrobial compound and enzyme targets tyrosyl tRNA synthetase (**c**) and Sortase A (**d**).

### *2.6. Analysis of Kaempferol-3-O- α-L-(2″,4″-di-E-p-coumaroyl)-rhamnopyranoside Biocompatibility*

To verify whether compound **3** satisfies the requirements to be employed in the future as a bioactive molecule in the biomedical field, biocompatibility analyses on eukaryotic cells were performed. For this purpose, immortalized human keratinocytes (HaCaT) and human dermal fibroblasts (HDF) were incubated with increasing concentrations (from 0.5 μg/mL to 5 μg/mL) of the compound under test for 72 h. As shown in Figure 9a,b, no significant toxic effects were detected under the experimental conditions tested, thus indicating that the identified compound is selectively toxic toward prokaryotic cells. Slight toxicity was detected only in the case of HDF cells at the highest concentrations tested (Figure 9b).

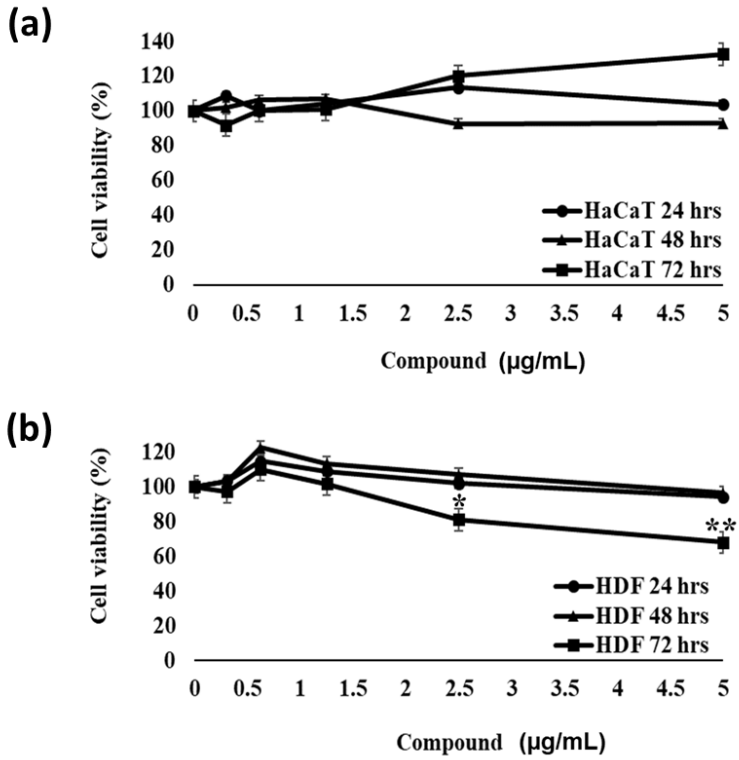


**Figure 9.** Effect of kaempferol-3-*O*-α-L-(2″,4″-di-*E*-*p*-coumaroyl)-rhamnopyranoside (compound **3**) on the viability of HaCat (**a**) and HDF cells (**b**). Cell viability was expressed as the percentage of MTT reduction with respect to control cells tested under the same conditions but in the absence of the compound under test. The experimental data represent the average of three independent experiments, each one carried out with triplicate determinations. Significant differences were indicated as (* $p < 0.05$) or (** $p < 0.001$) for treated versus control samples. Each experiment was carried out in triplicate.

## 3. Discussion

In the present manuscript, a bioguided purification of *E. foeminea* extracts was carried out to isolate compounds with antimicrobial and antibiofilm properties. A total of six compounds were isolated and identified as carvacrol, thymol and four acylated kaempferol glycosides, i.e., kaempferol-3-*O*-α-L-(2″,4″-di-*E*-*p*-coumaroyl)-rhamnopyranoside, kaempferol-3-*O*-α-L-(2″-*E*-*p*-coumaroyl,4″-*Z*-*p*-coumaroyl)-rhamnopyranoside, kaempferol-3-*O*-α-L-(2″-*Z*-*p*-coumaroyl,4″-*E*-*p*-coumaroyl)-rhamnopyranoside and kaempferol-3-*O*-α-L-(2″,4″-di-*Z*-*p*-coumaroyl)-rhamnopyranoside (compounds **1**–**6** in Figure 3). These metabolites were identified for the first time in *E. foeminea* organic extracts and compounds **1**–**3** were found to be endowed with strong antimicrobial properties and promising antibiofilm activity.

Carvacrol and thymol have been largely investigated and are known for their medical properties. They have also been employed as food preservatives and food additives because of their well-known antimicrobial activity [40], probably due to their physicochemical properties, such as hydrophobicity, partition coefficient and ability to form H-bonds with interacting target molecules [41]. Carvacrol is an aromatic monoterpene generally present in aromatic plants such as thyme and oregano, and thymol is an isomer of carvacrol. Carvacrol has been reported to be endowed with significant antimicrobial properties when tested on a wide range of bacterial strains such as *E. coli*, *S. aureus*, *L. monocytogenes* and *S. typhimurium* [42–45]. Molecular mechanisms underlying carvacrol antimicrobial activity imply bacterial membrane disruption due to an alteration of its fluidity, integrity and functionality [40,41]. Carvacrol has been also reported to cause a depletion of intracellular ATP due to an alteration of intracellular pH value consequent to an interference with protons influx [40,41]. In the literature, further mechanisms have been also described to explain carvacrol effects on the viability of bacterial cells, such as the induction of reactive

oxygen species (ROS) and the inhibition of efflux pumps [40,41]. Due to its hydrophobicity, carvacrol has also been reported to penetrate the hydrophobic environment of bacterial biofilm matrix, to interact with bacterial membranes and to interfere with their ability to form biofilms by altering the motility of bacterial cells and by reducing the cells' ability to adhere to substrates [40,41]. Carvacrol antibiofilm activity has been also reported to be mediated by its ability to interfere with signaling pathways of quorum sensing (QS) by blocking the expression of specific involved genes [40,41]. Based on these observations, it is plausible that carvacrol might be, at least in part, responsible for the antimicrobial and antibiofilm activity observed by testing *E. foeminea* hexane extract (Table 1 and Figure 5).

We also identified for the first time in the *E. foeminea* dichloromethane extract four glycosilated isomers of kaempferol (compounds **3**–**6** in Figure 3). It has to be highlighted that compound **3** was isolated for the first time from *Pentachondra pumila* collected in New Zealand [25] and from unripe fruits of *Ocotea vellosiana* [46]. Subsequently, it was isolated from several sources, such as the leaves of *Laurus nobilis* [26], the buds of *Mammea longifolia* [27], the leaves of *Eriobotrya japonica* [47], the leaves of *Cinnamomun kotoense* [29], the aerial parts of *Epimedium sagittatum* and the leaves of *Machilus philippinens* [48]. Compound **4** was isolated for the first time from the aerial parts of *Epimedium sagittatum* together with compounds **3** and **5** and other related compounds [28]. Regarding compound **5**, it was isolated for the first time together with compound **3** from the leaves of *Cinnamomun kotoense*, and a mixture of both compounds was found to be able to suppress peripheral blood mononuclear cell (PBMC) production induced by phytohemagglutinin (PHA) [29]. Finally, compound **6** was isolated for the first time from several sources together with other isomers, such as from the leaves of *Laurus nobilis* [26] together with compound **3**, from the leaves of *Machilus philippinens* together with compound **4** [48] and from the leaves of *Eriobotrya japonica* together with compound **3** [47]. Very interestingly, here, we found that, despite other isomers, compound **3** is the only one to be endowed with a very strong antimicrobial activity towards *S. aureus* strains sensitive or resistant to conventional antibiotics (Table 2). In the past, strong antimicrobial properties have been reported for compounds **3** and **4** isolated from *Laurus nobilis* against methicillin-resistant *S. aureus* strains and against vancomycin-resistant Enterococci [49]. Considering the strong antibacterial activity of compound **3** (Table 2) with respect to that shown by its isomers (compounds **4–6** in Table S3), it is plausible that stereochemistry of the double bonds of the *p*-coumaroyl residues is a key structural feature associated to the antibiotic activity. In particular, the *E*,*E* stereochemistry of the double bonds of the *p*-coumaroyl residues seems to be fundamental (Table 2).

As compound **3** was the most promising antimicrobial agent among the identified compounds, we also performed docking studies, with the main aim being to predict suitable molecular targets of compound **3** antibiofilm activity. Obtained results suggest that the antibiofilm activity of the test ligand against *S. aureus* strains might be correlated to the inhibition of Sortase A and/or tyrosyl tRNA synthetase. Sortase A (Srt A) is one of the well-known proteins responsible for biofilm adhesion, formation and aggregation [31]. This enzyme catalyzes the formation of covalent bonds between cell wall proteins (CWA) and peptidoglycan molecules of the bacterial cell wall [31]. It has been reported that, in the presence of inactivating mutations of Srt A, bacterial cells are no longer able to cause infections because of the failure of the attachment of fibronectin proteins to the cell wall [32]. This makes Srt A a suitable target for the development of novel and effective antibiofilm drugs [33]. Aminoacyl–tRNA synthases (aaRSs) also represent good candidates as targets of antimicrobial strategies [34]. Indeed, their inhibition is associated with a blockage of cell growth due to interference with protein synthesis processes [34]. Furthermore, differences in the topology of the ATP binding domain between human and bacterial enzymes are the basis of the possibility to selectively target bacterial enzymes [36]. Indeed, this is in line with the data obtained here by treating human eukaryotic cells with kaempferol-3-*O*-α-L-(2″,4″-di-*E*-*p*-coumaroyl)-rhamnopyranoside. Indeed, compound **3**, while exerting toxic effects on *S. aureus* bacterial cells, was found to be harmless towards immortalized human

keratinocytes (HaCaT) and human dermal fibroblasts (HDF) at concentrations effective on bacterial cells under the experimental conditions tested (Figure 8).

Altogether, obtained data open interesting perspectives to the future applicability of the identified compound **3** in several fields to counteract bacterial infections. In the future, it the possibility of using this compound in combination with conventional antibiotics will be also explored, in order to develop effective combinatorial therapeutic approaches with the main aim of counteracting the worrying phenomenon of multidrug resistance.

## 4. Materials and Methods

### *4.1. Materials*

All the reagents were purchased from Sigma-Merck (Milan, Italy), unless specified otherwise. Optical rotations were measured on a Jasco P-1010 digital polarimeter (Tokyo, Japan); $^{1}H$ and $^{13}C$ nuclear magnetic resonance (NMR) spectra were recorded at 400 and 100 MHz, respectively, in $CDCl_3$, acetone-$d_6$ and $CD_3OD$ on a Bruker spectrometer (Billerica, MA, USA). The same solvents were used as internal standards. DEPT, COSY-45, HSQC, HMBC and NOESY experiments [50] were performed using Bruker microprograms. Electrospray ionization mass spectra (ESIMS) were performed using the LC/MS TOF system AGILENT 6230B (Agilent Technologies, Milan, Italy). Analytical and preparative thin layer chromatography (TLC) were performed on silica gel plates (Kieselgel 60, $F_{254}$, 0.25 and 0.5 mm respectively) or on reverse phase (Kieselgel 60 RP-18 $F_{254}$, 0.20 mm) plates and the compounds were visualized by exposure to UV light and/or iodine vapors and/or by spraying firstly with 10% $H_2SO_4$ in MeOH and then with 5% phosphomolybdic acid in EtOH, followed by heating at 110 °C for 10 min. Column chromatography (CC) was performed using silica gel (Merck, Kieselgel 60, 0.063–0.200 mm).

### *4.2. Ephedra Foeminea Plant Collection and Identification*

The aerial parts of *E. foeminea* were collected from their natural habitat in West Bank-Palestine during September 2020. Identification of the plant was carried out at the Department of Biology and Biotechnology, An-Najah National University, Palestine. Representative plant specimens were collected, pressed until dried, then chemically poisoned to prevent bacterial and fungal infections and finally mounted on herbarium sheets and provided with a voucher number (ANUH1895). Subsequently, they were deposited at An-Najah National University herbarium. The aerial parts of *E. foeminea* collected were washed with water to remove soil and dust particles and then dried. Exposure to light was avoided to prevent possible loss of effective ingredients. The dried aerial parts were made into a fine powder using a blender in order to make them ready for subsequent extraction processes.

### *4.3. Plant Extract Preparation and Purification*

Starting with the plants collected from their natural habitat in West Bank-Palestine during September 2020 (voucher number ANUH1895), plant material (700 g) was extracted (1 × 2000 mL) using ethanol/$H_2O$ (7/3, *v*/*v*) under stirring conditions at room temperature for 48 h. Afterward, the sample was centrifuged at 7000 rpm for 40 min. An amount of 10 mL of the supernatant was concentrated under reduced pressure in order to evaporate the ethanol and lyophilized to obtain 120 mg of ethanol extract. The rest of the supernatant was firstly extracted by hexane (3 × 800 mL), then with $CH_2Cl_2$ (3 × 800 mL) and, after removing the ethanol under reduced pressure, with EtOAc (3 × 700 mL). Each kind of extract and the residual water phase were then tested for antimicrobial properties on six bacterial strains. Since hexane organic extract (280 g) displayed interesting antibacterial activity, it was purified using column chromatography (CC) and eluted with $CHCl_3$/i-PrOH (95/5, *v*/*v*), thus obtaining eight homogeneous fractions (H1–H8). Among them, fraction H2 was found to retain antibiotic activity and was further purified by using different steps of CC and TLC (Figure 2). Briefly, fraction H2 (113.8 mg) was purified by CC and eluted with ethyl acetate/hexane (40/60, *v*/*v*). The first obtained fraction (H2.1 in Figure 2) was further purified using two steps of TLC and eluted with $CHCl_3$/i-PrOH (98/2, *v*/*v*), to

obtain four homogeneous fractions. Among these, fraction H2.1.C (10.42 mg) was further purified to obtain a pure oil identified as carvacrol (compound **1**, 4.7 mg) and a pure amorphous solid identified as thymol (compound **2**, 1.7 mg).

The organic extract obtained in $CH_2Cl_2$ (713.5 mg) was found to retain interesting antimicrobial properties and was purified using CC and eluted with $CH_2Cl_2$/i-PrOH (9/1, *v*/*v*), thus obtaining eight homogeneous fractions (D1–D8) (Figure 2). Among them, fraction D3 (35.01 mg) was found to retain antibiotic activity and was further purified using two steps of TLC (Figure 2). Briefly, fraction D3 was purified using TLC and eluted in $CHCl_3$/i-PrOH (9/1, *v*/*v*), thus obtaining six homogeneous fractions (Figure 2). Fraction D3.5 (10.06 mg) in Figure 2 was found to be a pure yellow powder identified as kaempferol-3-O-α-L-(2″,4″-di-*E*-*p*-coumaroyl)-rhamnopyranoside (compound **3**, 10.06 mg). Fraction D3.4 (8.84 mg) in Figure 2 was further purified using TLC to obtain three pure amorphous solids, fractions D3.4.X, D3.4.Y and D3.4.Z in Figure 2. The fractions were analyzed using NMR and mass spectrometry and identified as kaempferol-3-O-α-L-(2″-E-p-coumaroyl,4″-Z-p-coumaroyl)-rhamnopyranoside (compound **4**, 1.65 mg), kaempferol-3-O-α-L-(2″-*Z*-*p*-coumaroyl,4″-*E*-*p*-coumaroyl)-rhamnopyranoside (compound **5**, 1.56 mg) and kaempferol-3-O-α-L-(2″,4″-di-*Z*-*p*-coumaroyl)-rhamnopyranoside (compound **6**, 0.88 mg), respectively.

### 4.4. Bacterial Strains and Growth Conditions

A total of six bacterial strains were used in the present study, i.e., *S. aureus* ATCC 29213, methicillin-resistant *S. aureus* (MRSA WKZ-2), *E. faecalis* ATCC 29212, *A. baumannii* ATCC 17878, *E. coli* ATCC 25922 and *S. typhimurium* ATCC 14028. All the bacterial strains were grown in Muller Hinton Broth (MHB; Becton Dickinson Difco, Franklin Lakes, NJ, USA) and on Tryptic Soy Agar (TSA; Oxoid Ltd., Hampshire, UK). In all the experiments, the bacteria were inoculated and grown overnight in MHB at 37 °C. The next day, the bacteria were transferred to a fresh MHB tube and grown to the mid-logarithmic phase.

### 4.5. Antimicrobial Activity

The antimicrobial activity of *E. foeminea* extracts and its derived compounds were tested against six bacterial strains, i.e., *S. aureus* ATCC 29213, methicillin-resistant *S. aureus* (MRSA WKZ-2), *E. faecalis* ATCC 29212, *A. baumannii* ATCC 17878, *E. coli* ATCC 25922 and *S. typhimurium* ATCC 14028 by using the broth microdilution method [51,52]. All the bacterial strains were obtained from ATCC (American Type Culture Collection), with the only exception of *S. aureus* (MRSA WKZ-2), which was kindly provided by Dr. E.J.A. Veldhuizen from Utrecht University, Netherlands. The bacteria were grown to the mid-logarithmic phase in MHB at 37 °C and then diluted to $2 \times 10^6$ CFU/mL in nutrient broth (NB, Difco, Becton Dickinson, Franklin 12 Lakes, NJ). To perform the assay, the bacterial samples were mixed 1:1 *v*/*v* with two-fold serial dilutions of the compound under test and incubated for 20 h at 37 °C. Following the incubation, each sample was diluted and plated on TSA in order to count the number of colonies. All the experiments were carried out in three independent replicates. The $MIC_{100}$ values were determined as the lowest compound concentration responsible for no visible bacterial growth after overnight incubation. To kinetically analyze the antimicrobial activity of kaempferol-3-O-α-L-(2″,4″-di-E-p-coumaroyl)-rhamnoside (compound **3**), *S. aureus* ATCC 29213 and *S. aureus* MRSA WKZ-2, bacterial cells were grown overnight in the MHB medium at 37 °C. The bacteria were then diluted to $4 \times 10^6$ CFU/mL in NB 0.5× and mixed with 0.5 µg/mL compound **3** (1:1 *v*/*v*) for defined time intervals. The samples (20 µL) were serially diluted (from 10- to 100,000-fold) and 100 µL of each dilution was plated on TSA. Following an incubation of 16 h at 37 °C, the bacterial colonies were counted [51].

### 4.6. Antibiofilm Activity Assays

To evaluate antibiofilm effects, bacteria inocula were grown overnight at 37 °C, then diluted to $1 \times 10^8$ CFU/mL in 0.5× MHB containing increasing concentrations of the compound under test. The gentamicin antibiotic was tested as a positive control at a con-

centration of 0.5 or 1 µg/mL on the *S. aureus* (MRSA WKZ-2) and *A. baumannii* ATCC 17878 bacterial strains, respectively. Not-treated samples contained the same amount of solvent present in the sample incubated with the highest concentration of the tested compound. The samples were then incubated at 37 °C for 24 h in order to test the effects on biofilm formation. In the case of crystal violet assay, the bacterial biofilm was washed three times with phosphate buffer (PBS 1X) and then incubated with the dye (0.04%) for 20 min at room temperature. Following the incubation, the samples were washed with PBS and then the dye bound to cells was dissolved in 33% acetic acid. Spectrophotometric measurements were then carried out at a wavelength of 630 nm by using a microtiter plate reader (FLUOstar Omega, BMG LABTECH and Germany) [51–53]. Confocal laser scanning microscopy (CLSM) analyses in static conditions were carried out by using Thermo Scientific™ Nunc™ Lab-Tek™ Chambered Coverglass systems (Thermo Fisher Scientific, Waltham, MA, USA). The viability of the cells within the biofilm structure was evaluated using sample staining with a LIVE/DEAD® Bacterial Viability kit (Molecular Probes Thermo Fisher Scientific, Waltham, MA, USA). The staining was performed according to the manufacturer's instructions. Biofilm images were collected by using a confocal laser scanning microscope (Zeiss LSM 710, Zeiss, Germany) and a 63× objective oil-immersion system. The biofilm architecture was analyzed by using the Zen Lite 2.3 software package. Each experiment was performed in triplicate and all images were taken under identical conditions [54]. The total protein content was determined by Bradford assay. Briefly, bacterial cells were grown overnight in MHB at 37 °C. The bacteria were then diluted to $4 \times 10^8$ CFU/mL in 100 µL of 0.5× MHB 0.5× along with increasing concentrations of kaempferol-3-O-α-L-(2″,4″-di-E-p-coumaroyl)-rhamnoside compound 3 (1:1 *v*/*v*). The samples were then incubated at 37 °C for 24 h. Afterward, the biofilm supernatant was separated from the pellet by centrifugation and the protein content of obtained samples was determined by Bradford assay [55].

### 4.7. Eukaryotic Cell Cultures and Biocompatibility Evaluation

The immortalized human keratinocytes (HaCaT) and human dermal fibroblasts (HDF) were from Thermo Fisher Scientific, Waltham, MA, USA. Both cell lines were cultured in high-glucose Dulbecco's modified Eagle's medium (DMEM) supplemented with 10% fetal bovine serum (FBS), 1% antibiotics (Pen/strep) and 1% L-glutamine and grown at 37 °C in a humidified atmosphere containing 5% $CO_2$. To evaluate the biocompatibility of kaempferol-3-O-(2″,4″-di-E-p-coumaroyl)-α-L-rhamno-pyiranoside, the cells were seeded into 96-well plates at a density of $3 \times 10^3$ cells/well in 100 µL of complete DMEM 24 h before the treatment. They were then incubated in the presence of increasing compound concentrations (0.5–5 µg $mL^{-1}$) for 72 h. Following the treatment, the cell culture supernatants were replaced with 0.5 mg/mL MTT (3-(4,5-dimethylthiazol-2-yl)-2,5-diphenyltetrazolium bromide) reagent dissolved in a DMEM medium without red phenol (100 µL/well). After 4 h of incubation at 37 °C, the resulting insoluble formazan salts were solubilized in 0.01 N HCl in anhydrous isopropanol and quantified by measuring the absorbance at λ = 570 nm using an automatic plate reader spectrophotometer (Synergy™ H4 Hybrid Microplate Reader, BioTek Instruments, Inc., Winooski, VT, USA), as previously described. Cell survival was expressed as the mean of the percentage values compared to the control untreated cells.

### 4.8. Molecular Docking Analyses

The chemical structure of kaempferol-3-O-α-L-(2″,4″-di-*E*-*p*-coumaroyl)-rhamnopyranoside was prepared and used as a ligand in molecular docking analyses with the main aim to predict the ligand's binding affinity and possible chemical interactions with two putative interactors present in *S. aureus* cells, i.e., Sortase A (PDB ID-1T2P) and tyrosyl tRNA synthetase (TyRS) (PDB ID- 1JIL). To do this, the crystallographic 3D structures of the target enzymes were retrieved from the protein data bank. The Autodock tool 1.5.6 was used to optimize the structures of the putative receptor and of the ligand. This was performed upon removal of the water molecules and heteroatoms and addition of polar hydrogens and Kollman charges. Molecular docking was performed by using the CB Dock web server, which represents an implementation of the popular

docking program Autodock Vina [56]. The docked complexes were visualized to identify putative receptor– ligand interactions by using Discovery Studio (DS) Visualizer 2020 (Biovia, San Diego, USA). The binding affinity of the compound under test towards the targets was estimated on the basis of intermolecular interactions and the bonds' lengths (Supplementary Table S4).

### *4.9. Statistical Analyses*

Statistical analyses were performed by using Student's *t*-test. Significant differences were indicated as * ($p < 0.05$), ** ($p < 0.01$), *** ($p < 0.001$) or **** ($p < 0.0001$). Graphs were obtained by using GraphPad Prism 8 software.

**Supplementary Materials:** The following supporting information can be downloaded at: https://www.mdpi.com/article/10.3390/ijms24043284/s1.

**Author Contributions:** Conceptualization, S.I., A.C. and A.A.; methodology, S.I., R.G., M.M., S.P., A.K.R. and A.C.; validation, S.I., A.C. and A.A.; formal analysis, S.I., A.C. and A.A.; investigation, S.I., R.G., M.M., S.P. and G.O.; data curation, S.I., A.C. and A.A.; writing—original draft preparation, S.I., A.C. and A.A.; writing—review and editing, S.I., M.M., S.P., A.C. and A.A.; supervision, A.C. and A.A.; project administration, A.C. and A.A.; funding acquisition, A.C. and A.A. All authors have read and agreed to the published version of the manuscript.

**Funding:** This research received no external funding.

**Institutional Review Board Statement:** Not applicable.

**Informed Consent Statement:** Not applicable.

**Data Availability Statement:** The data presented in this study are available within the article or supplementary material.

**Conflicts of Interest:** The authors declare no conflict of interest.

## References

1. Svoboda, K.; Brooker, J.D.; Zrustova, J. Antibacterial and Antioxident Properties of Essential Oils: Their Potential Applications in the Food Industries. *Acta Hortic.* **2006**, *709*, 35–44. [CrossRef]
2. Valle, D.L., Jr.; Andrade, J.I.; Puzon, J.J.M.; Cabrera, E.C.; Rivera, W.L. Antibacterial activities of ethanol extracts of Philippine medicinal plants against multidrug-resistant bacteria. *Asian Pac. J. Trop. Biomed.* **2015**, *5*, 532–540. [CrossRef]
3. Savoia, D. Plant-derived antimicrobial compounds: Alternatives to antibiotics. *Future Microbiol.* **2012**, *7*, 979. [CrossRef] [PubMed]
4. Cowan, M.M. Plant product as antimicrobial agents. *Clin. Microbiol. Rev.* **1999**, *12*, 564–582. [CrossRef] [PubMed]
5. Garcia, A.; Bocanegra-Garcia, V.; Palma-Nicolas, J.P.; Rivera, G. Recent advances in antitubercular natural products. *Eur. J. Med. Chem.* **2012**, *49*, 1–23. [CrossRef]
6. Kurek, A.; Grudniak, A.M.; Kraczkiewicz, D.A.; Wolska, K.I. New antibacterial therapeutics and strategies. *Pol. J. Microbiol.* **2011**, *60*, 3–12. [CrossRef]
7. Fowler, Z.L.; Baron, C.M.; Panepinto, J.C.; Koffas, M.A. Melanization of flavonoids by fungal and bacterial laccases. *Yeast* **2011**, *28*, 181–188. [CrossRef]
8. WHO. *WHO Traditional Medicine Strategy*; WHO: Geneva, Switzerland, 2002.
9. Sahib, N.G.; Anwar, F.; Gilani, A.H.; Hamid, A.A.; Saari, N.; Alkharfy, K.M. Coriander *Coriandrum sativum* L.: A potential source of high-value components for functional foods and nutraceuticals—A review. *Phytother. Res.* **2013**, *27*, 1439–1456. [CrossRef]
10. O'Dowd, N.A.; McCauley, G.; Wilson, J.A.N.; Parnell, T.A.K.; Kavanaugh, D. In vitro culture, micropropagation and the production of ephedrine and other alkaloids. In *Biotechnology in Agriculture and Forestry*; Bajaj, Y.P.S., Ed.; Springer: Berlin/Heidelberg, Germany, 1998; p. 41. [CrossRef]
11. Pirbalouti, A.G.; Azizi, S.; Amirmohammadi, M.; Craker, L. Healing effect of hydro-alcoholic extract of *Ephedra pachyclada* Boiss. in experimentally gastric ulcer in rat. *Acta Pol. Pharm.* **2013**, *70*, 1003–1009.
12. Hollander, J.L.; Vander Wall, S.B.; Baguley, J.G. Evolution of seed dispersal in North American Ephedra. *Evol. Ecol.* **2010**, *24*, 333–345. [CrossRef]
13. Ickert-Bond, S.M.; Rydin, C.; Renner, S.S. A fossil-calibrated relaxed clock for Ephedra indicates an Oligocene age for the divergence of Asian and New World clades and Miocene dispersal into South America. *J. Syst. Evol.* **2009**, *47*, 444–456. [CrossRef]
14. Sawalha, A.F. Complementary and alternative medicine (CAM) in Palestine: Use and safety implications. *J. Altern. Complement. Med.* **2007**, *13*, 263–270. [CrossRef] [PubMed]
15. Abou-Elkhair, E.; Fadda, H.; Abu-Mohsen, U. Antibacterial activity and Phytochemical analysis of some medicinal plants from Gaza Strip-Palestine. *J. Al-Azhar Univ.-Gaza* **2010**, *12*, 45–54.

16. Ickert-Bond, S.M.; Renner, S.S. The Gnetales: Recent insights on their morphology, reproductive biology, chromosome numbers, biogeography and divergence times. *J. Syst. Evol.* **2016**, *54*, 1–16. [CrossRef]
17. Danin, A. Flora of Israel. Available online: http://flora.huji.ac.il/browseasp (accessed on 10 December 2018).
18. Yeung, E.C. Embryogeny of Pbaseolus: The role of the suspensor. *Z. Pflanzenphysiol.* **1980**, *96*, 17–28. [CrossRef]
19. Kallassy, H.; Fayyad-Kazan, M.; Makki, R.; Yolla, E.M.; Rammal, H.; Leger, D.Y.; Badran, B. Chemical composition and antioxidant, anti-inflammatory and antiproliferative activities of Lebanese *Ephedra campylopoda* plant. *Med. Sci. Monit. Basic Res.* **2017**, *23*, 313. [CrossRef]
20. Ibragic, S.; Sofic, E. Chemical composition of various Ephedra species. *Bosn. J. Basic Med. Sci.* **2015**, *15*, 21–27. [CrossRef] [PubMed]
21. González-Juárez, D.E.; Escobedo-Moratilla, A.; Flores, J.; Hidalgo-Figueroa, S.; Martínez-Tagüeña, N.; Morales-Jiménez, J.; Muñiz-Ramírez, A.; Pastor-Palacios, G.; Pérez-Miranda, S.; Ramírez-Hernández, A.; et al. A Review of the Ephedra genus: Distribution, Ecology, Ethnobotany, Phytochemistry and Pharmacological Properties. *Molecules* **2020**, *25*, 3283. [CrossRef]
22. Mills, S.; Bone, K. *The Essential Guide to Herbal Safety*; Elsevier Inc.: St. Louis, MO, USA, 2004.
23. Mendelovich, M.; Shoshan, M.; Fridlender, M.; Mazuz, M.; Namder, D.; Nallathambi, R.; Selvaraj, G.; Kumari, P.; Ion, A.; Wininger, S.; et al. Effect of *Ephedra foeminea* active compounds on cell viability and actin structures in cancer cell lines. *J. Med. Plants Res.* **2017**, *11*, 690–702. [CrossRef]
24. Ismail, S.M.; Adwan, G.B.; Jarrar, N.R. Evaluation of Antimicrobial and Genotoxic Activity of *Ephedra foeminea* Ethanolic and Aqueous Extracts on *Escherichia coli*. *Jordan J. Biol. Sci.* **2020**, *13*, 123–126.
25. Bloor, S.J. An antimicrobial kaempferol-diacyl-rhamnoside from Pentachondra pumila. *Phytochemistry* **1995**, *38*, 1033–1035. [CrossRef] [PubMed]
26. Fiorini, C.; David, B.; Fourasté, I.; Vercauteren, J. Acylated kaempferol glycosides from Laurus nobilis leaves. *Phytochemistry* **1998**, *47*, 821–824. [CrossRef]
27. Rao, J.M.L.; Yada, H.; Ono, H.; Yoshida, M. Acylated and non-acylated flavonol monoglycosides from the Indian minor spice nagkesar (*Mammea longifolia*). *J. Agric. Food Chem.* **2002**, *50*, 3143–3146. [CrossRef]
28. Wang, G.J.; Tsai, T.H.; Lin, L.C. Prenylflavonol, acylated flavonol glycosides and related compounds from *Epimedium sagittatum*. *Phytochemistry* **2007**, *68*, 2455–2464. [CrossRef]
29. Kuo, Y.C.; Lu, C.K.; Huang, L.W.; Kuo, Y.H.; Chang, C.; Hsu, F.L.; Lee, T.H. Inhibitory effects of acylated kaempferol glycosides from the leaves of *Cinnamomum kotoense* on the proliferation of human peripheral blood mononuclear cells. *Planta Med.* **2005**, *71*, 412–415. [CrossRef] [PubMed]
30. Gaglione, R.; Cesaro, A.; Dell'Olmo, E.; Della Ventura, B.; Casillo, A.; Di Girolamo, R.; Velotta, R.; Notomista, E.; Veldhuizen, E.J.A.; Corsaro, M.M.; et al. Effects of human antimicrobial cryptides identified in apolipoprotein B depend on specific features of bacterial strains. *Sci. Rep.* **2019**, *9*, 6728. [CrossRef]
31. Mazmanian, S.K.; Liu, G.; Ton-That, H.; Schneewind, O. *Staphylococcus aureus* sortase, an enzyme that anchors surface proteins to the cell wall. *Science* **1999**, *285*, 760–763. [CrossRef]
32. Weiss, W.J.; Lenoy, E.; Murphy, T.; Tardio, L.; Burgio, P.; Projan, S.J.; Schneewind, O.; Alksne, L. Effect of srtA and srtB gene expression on the virulence of *Staphylococcus aureus* in animal models of infection. *J. Antimicrob. Chemother.* **2004**, *53*, 480–486. [CrossRef]
33. Lei, S.; Hu, Y.; Yuan, C.; Sun, R.; Wang, J.; Zhang, Y.; Zhang, Y.; Lu, D.; Fu, L.; Jiang, F. Discovery of Sortase A covalent inhibitors with benzofuranene cyanide structures as potential antibacterial agents against *Staphylococcus aureus*. *Eur. J. Med. Chem.* **2022**, *229*, 114032. [CrossRef]
34. Xiao, Z.P.; Wei, W.; Wang, P.F.; Shi, W.K.; Zhu, N.; Xie, M.Q.; Sun, Y.W.; Li, L.X.; Xie, Y.X.; Zhu, L.S.; et al. Synthesis and evaluation of new tyrosyl-tRNA synthetase inhibitors as antibacterial agents based on a N2-(arylacetyl) glycinanilide scaffold. *Eur. J. Med. Chem.* **2015**, *102*, 631–638. [CrossRef]
35. Lapointe, J. Mechanism and evolution of multidomain aminoacyl-tRNA synthetases revealed by their inhibition by analogues of a reaction intermediate and by properties of truncated forms. *J. Biomed. Sci. Eng.* **2013**, *6*, 943–946. [CrossRef]
36. Giegé, R.; Springer, M. Aminoacyl-tRNA Synthetases in the Bacterial World. *EcoSal Plus* **2012**, *5*. [CrossRef]
37. Padhi, S.; Masi, M.; Chourasia, R.; Rajashekar, Y.; Rai, A.K.; Evidente, A. ADMET profile and virtual screening of plant and microbial natural metabolites as SARS-CoV-2 S1 glycoprotein receptor binding domain and main protease inhibitors. *Eur. J. Pharmacol.* **2020**, *890*, 2021. [CrossRef] [PubMed]
38. Talukdar, R.; Padhi, S.; Rai, A.K.; Masi, M.; Evidente, A.; Jha, D.K.; Cimmino, A.; Tayung, K. Isolation and Characterization of an Endophytic Fungus *Colletotrichum coccodes* Producing Tyrosol from *Houttuynia cordata* Thunb. Using ITS2 RNA Secondary Structure and Molecular Docking Study. *Front. Bioeng. Biotechnol.* **2021**, *9*, 650247. [CrossRef] [PubMed]
39. Righetti, P.G.; Boschetti, E. Low-Abundance Protein Access by Combinatorial Peptide Libraries. In *Low-Abundance Proteome Discovery*; Elsevier: Amsterdam, The Netherlands, 2013; pp. 79–157. [CrossRef]
40. Zhang, D.; Gan, R.; Ge, Y.; Yang, Q.; Ge, J.; Li, H.; Corke, H. Research Progress on the Antibacterial Mechanisms of Carvacrol: A Mini Review. *Bioact. Compd. Health Dis.* **2018**, *1*, 71–81. [CrossRef]
41. Marinelli, L.; Di Stefano, A.; Cacciatore, I. Carvacrol and its derivatives as antibacterial agents. *Phytochem. Rev.* **2018**, *17*, 903–921. [CrossRef]

42. Stratakos, A.C.; Sima, F.; Ward, P.; Linton, M.; Kelly, C.; Pinkerton, L.; Stef, L.; Pet, I.; Corcionivoschi, N. The in vitro effect of carvacrol, a food additive, on the NBpathogenicity of O157 and non-O157 Shiga-toxin producing *Escherichia coli*. *Food Control* **2017**, *84*, 290–296. [CrossRef]
43. Engel, J.B.; Heckler, C.; Tondo, E.C.; Daroit, D.J.; da Silva Malheirosm, P. Antimicrobial activity of free and liposome-encapsulated thymol and carvacrol against Salmonella and *Staphylococcus aureus* adhered to stainless steel. *Int. J. Food Microbiol.* **2017**, *252*, 18–23. [CrossRef] [PubMed]
44. Carvalho, R.I.; Medeiros, A.S.D.J.; Chaves, M.; Souza, E.L.D.; Magnani, M. Lipids, pH and their interaction affect the inhibitory effects of carvacrol against Salmonella typhimurium PT4 and *Escherichia coli* O157:H7. *Front. Microbiol.* **2017**, *8*, 2701. [CrossRef]
45. Chung, D.; Cho, T.J.; Rhee, M.S. Citrus fruit extracts with carvacrol and thymol eliminated 7-log acid-adapted *Escherichia coli* O157:H7, Salmonella typhimurium and Listeria monocytogenes: A potential of effective natural antibacterial agents. *Food Res. Int.* **2018**, *107*, 578. [CrossRef]
46. Garcez, W.S.; Yoshida, M.; Gottlieb, O.R. Benzylisoquinoline alkaloids and flavonols from Ocotea vellosiana. *Phytochemistry* **1995**, *39*, 815–816. [CrossRef]
47. Kawahara, N.; Satake, M.; Goda, Y. A new acylated flavonol glycoside from the leaves of Eriobotrya japonica. *Chem. Pharm. Bull.* **2002**, *50*, 1619–1620. [CrossRef]
48. Lee, S.S.; Lin, H.C.; Chen, C.K. Acylated flavonol monorhamnosides, α-glucosidase inhibitors, from Machilus philippinensis. *Phytochemistry* **2008**, *69*, 2347–2353. [CrossRef] [PubMed]
49. Otsuka, N.; Liu, M.H.; Shiota, S.; Ogawa, W.; Kuroda, T.; Hatano, T.; Tsuchiya, T. Anti-methicillin resistant *Staphylococcus aureus* (MRSA) compounds isolated from Laurus nobilis. *Biol. Pharm. Bull.* **2008**, *31*, 1794–1797. [CrossRef] [PubMed]
50. Berger, S.; Braun, S. *200 and More NMR Experiments*; Wiley-Vch: Weinheim, Germany, 2004; pp. 305–307.
51. Gaglione, R.; Dell'Olmo, E.; Bosso, A.; Chino, M.; Pane, K.; Ascione, F.; Itri, F.; Caserta, S.; Amoresano, A.; Lombardi, A.; et al. Novel human bioactive peptides identified in apolipoprotein B: Evaluation of their therapeutic potential. *Biochem. Pharmacol.* **2017**, *130*, 34–50. [CrossRef] [PubMed]
52. Pizzo, E.; Pane, K.; Bosso, A.; Landi, N.; Ragucci, S.; Russo, R.; Gaglione, R.; Torres, M.D.T.; de la Fuente-Nunez, C.; Arciello, A.; et al. Novel bioactive peptides from PD-L1/2, a type 1 ribosome inactivating protein from *Phytolacca dioica* L. Evaluation of their antimicrobial properties and antibiofilm activities. *Biochim. Biophys. Acta Biomembr.* **2018**, *1860*, 1425–1435. [CrossRef]
53. Monti, D.M.; Guglielmi, F.; Monti, M.; Cozzolino, F.; Torrassa, S.; Relini, A.; Pucci, P.; Arciello, A.; Piccoli, R. Effects of a lipid environment on the fibrillogenic pathway of the N-terminal polypeptide of human apolipoprotein A-I, responsible for in vivo amyloid fibril formation. *Eur. Biophys. J.* **2010**, *39*, 1289–1299. [CrossRef]
54. Gaglione, R.; Cesaro, A.; Dell'Olmo, E.; Di Girolamo, R.; Tartaglione, L.; Pizzo, E.; Arciello, A. Cryptides Identified in Human Apolipoprotein B as New Weapons to Fight Antibiotic Resistance in Cystic Fibrosis Disease. *Int. J. Mol. Sci.* **2020**, *21*, 2049. [CrossRef]
55. Guo, J.; Qin, S.; Wei, Y.; Liu, S.; Peng, H.; Li, Q.; Luo, L.; Lv, M. Silver nanoparticles exert concentration-dependent influences on biofilm development and architecture. *Cell Prolif.* **2019**, *52*, e12616. [CrossRef]
56. Liu, Y.; Grimm, M.; Dai, W.-T.; Hou, M.C.; Xiao, Z.X.; Cao, Y. CB-Dock: A web server for cavity detection-guided protein–ligand blind docking. *Acta Pharm. Sin.* **2020**, *41*, 138–144. [CrossRef]


**Disclaimer/Publisher's Note:** The statements, opinions and data contained in all publications are solely those of the individual author(s) and contributor(s) and not of MDPI and/or the editor(s). MDPI and/or the editor(s) disclaim responsibility for any injury to people or property resulting from any ideas, methods, instructions or products referred to in the content.

# SUPPORTING INFORMATION

# *Ephedra foeminea* plant as a novel source of antimicrobial and anti-biofilm compounds to fight multidrug resistance phenotype

**Shurooq Ismail [1,2], Rosa Gaglione [1,3], Marco Masi [1], Srichandan Padhi [4], Amit K. Rai[4] ,Ghadeer Omar [2], Alessio Cimmino [1,*], Angela Arciello [1,3,*]**

[1] Department of Chemical Sciences, University of Naples Federico II, Via Cintia 21, I-80126, Naples, Italy; shurooq.ismail@unina.it (S.I.); rosa.gaglione@unina.it (R.G.); marco.masi@unina.it (M.M.); alessio.cimmino@unina.it (A.C.); anarciel@unina.it (A.A.)

[2] Department of Biology and Biotechnology, An-Najah National University, Nablus, Palestine; ghaderomar@najah.edu (G.O.)

[3] Istituto Nazionale di Biostrutture e Biosistemi (INBB), Rome, Italy

[4] Institute of Bioresources and Sustainable Development, Imphal, Manipur, India; srichandan1989@gmail.com (S.P.) * Correspondence: alessio.cimmino@unina.it (A.C.); anarciel@unina.it (A.A.)

**Supporting information list**

**Supplementary Table S1.** Minimal Inhibitory Concentration ($MIC_{100}$) values (mg/mL) determined for fractions obtained upon extraction in hexane and two sequential steps of CC.

**Supplementary Figure S1**. $^{1}H$ NMR spectrum of carvacrol, **compound 1** ($CDCl_3$, 400 MHz).

**Supplementary Figure S2**. $^{1}H$ NMR spectrum of thymol, **compound 2** ($CDCl_3$, 400 MHz).

**Supplementary Figure S3**. $^{1}H$ NMR spectrum of kaempferol-3-*O*-α-L-(2",4"-di-*E*-*p*-coumaroyl)-rhamnopyranoside **compound 3** (MeOD, 400 MHz).

**Supplementary Figure S4**. $^{1}H$ NMR spectrum of kaempferol-3-*O*-α-L-(2",4"-di-*E*-*p*-coumaroyl)-rhamnopyranoside **compound 3** (MeOD, 400 MHz) in the range 8.1 to 5.4 ppm.

**Supplementary Figure S5**. $^{1}H$ NMR spectrum of kaempferol-3-*O*-α-L-(2",4"-di-*E*-*p*-coumaroyl)-rhamnopyranoside **compound 3** (acetone-$d_6$, 400 MHz).

**Supplementary Figure S6**. $^{1}H$ NMR spectrum of kaempferol-3-*O*-α-L-(2",4"-di-*E*-*p*-coumaroyl)-rhamnopyranoside **compound 3** (acetone-$d_6$, 400 MHz) in the range 8.0 to 5.5 ppm.

**Supplementary Figure S7**. COSY spectrum of kaempferol-3-*O*-α-L-(2",4"-di-*E*-*p*-coumaroyl)-rhamnopyranoside, **compound 3** (acetone-$d_6$, 400 MHz).

**Supplementary Figure S8**. COSY spectrum of kaempferol-3-*O*-α-L-(2",4"-di-*E*-*p*-coumaroyl)-rhamnopyranoside **compound 3** (acetone-$d_6$, 400 MHz) in the range 8.0 to 5.6 ppm.

**Supplementary Figure S9**. NOESY spectrum of kaempferol-3-*O*-α-L-(2",4"-di-*E*-*p*-coumaroyl)-rhamnopyranoside **compound 3** (acetone-$d_6$, 400 MHz).

**Supplementary Figure S10**. $^{13}C$ NMR spectrum of kaempferol-3-*O*-α-L-(2",4"-di-*E*-*p*-coumaroyl)-rhamnopyranoside **compound 3** (acetone-$d_6$, 400 MHz).

**Supplementary Figure S11**. HSQC spectrum of kaempferol-3-*O*-α-L-(2",4"-di-*E*-*p*-coumaroyl)-rhamnopyranoside **compound 3** (acetone-$d_6$, 400 MHz).

**Supplementary Figure S12**. HMBC spectrum of kaempferol-3-*O*-α-L-(2",4"-di-*E*-*p*-coumaroyl)-rhamnopyranoside, **compound 3** (acetone-$d_6$, 400 MHz).

**Supplementary Figure S13**. ESI MS spectrum of kaempferol-3-*O*-α-L-(2",4"-di-*E*-*p*-coumaroyl)-rhamnopyranoside **compound 3** recorded in positive modality.

**Supplementary Figure S14**. $^{1}H$ NMR spectrum of kaempferol-3-*O*-α-L-(2"-*E*-*p*-coumaroyl,4"-*Z*-*p*-coumaroyl)-rhamnopyranoside **compound 4** (MeOD, 400 MHz).

**Supplementary Figure S15**. $^{1}H$ NMR spectrum of kaempferol-3-*O*-α-L-(2"-*E*-*p*-coumaroyl,4"-*Z*-*p*-coumaroyl)-rhamnopyranoside **compound 4** (MeOD, 400 MHz) in the range 8.0 to 5.3 ppm.

**Supplementary Figure S16**. COSY spectrum of kaempferol-3-*O*-α-L-(2"-*E*-*p*-coumaroyl,4"-*Z*-*p*-coumaroyl)-rhamnopyranoside **compound 4** (acetone-$d_6$, 400 MHz).

**Supplementary Figure S17**. $^{1}H$ NMR spectrum of kaempferol-3-*O*-α-L-(2"-*E*-*p*-coumaroyl,4"-*Z*-*p*-coumaroyl)-rhamnopyranoside **compound 4** (acetone-$d_6$, 400 MHz).

**Supplementary Figure S18**. $^{1}H$ NMR spectrum of kaempferol-3-*O*-α-L-(2"-*E*-*p*-coumaroyl,4"-*Z*-*p*-coumaroyl)-rhamnopyranoside **compound 4** (acetone-$d_6$, 400 MHz) in the range 8.0 to 5.4 ppm.

**Supplementary Figure S19**. $^{1}H$ NMR spectrum of kaempferol-3-*O*-α-L-(2"-*Z*-*p*-coumaroyl,4"-*E*-*p*-coumaroyl)-rhamnopyranoside **compound 5** (MeOD, 400 MHz).

**Supplementary Figure S20**. $^{1}H$ NMR spectrum of kaempferol-3-*O*-α-L-(2"-*Z*-*p*-coumaroyl,4"-*E*-*p*-coumaroyl)-rhamnopyranoside **compound 5** (MeOD, 400 MHz) in the range 8.0 to 5.4 ppm.

**Supplementary Figure S21**. $^{1}$H NMR spectrum of kaempferol-3-*O*-α-L-(2”,4”-di-*Z*-*p*-coumaroyl)-rhamnopyranoside **compound 6** (MeOD, 400 MHz).

**Supplementary Figure S22**. $^{1}$H NMR spectrum of kaempferol-3-*O*-α-L-(2”,4”-di-*Z*-*p*-coumaroyl)-rhamnopyranoside **compound 6** (MeOD, 400 MHz) in the range 7.9 to 5.5 ppm.

**Supplementary Figure S23**. $^{1}$H NMR spectrum of kaempferol-3-*O*-α-L-(2”,4”-di-*Z*-*p*-coumaroyl)-rhamnopyranoside **compound 6** (acetone-$d_6$, 400 MHz).

**Supplementary Figure S24**. $^{1}$H NMR spectrum of kaempferol-3-*O*-α-L-(2”,4”-di-*Z*-*p*-coumaroyl)-rhamnopyranoside **compound 6** (acetone-$d_6$, 400 MHz) in the range 8.0 to 5.4 ppm.

**Supplementary Table S2**. $MIC_{100}$ values (µg/mL) determined for the compounds carvacrol and thymol purified from *E. foeminea* hexane extract.

**Supplementary Table S3.** $MIC_{100}$ values (µg/mL) determined for the compounds: kaempferol-3-*O*-α-L-(2”,4”-di-*E*-*p*-coumaroyl)-rhamnopyranoside (compound **3**),kaempferol-3-*O*-α-L-(2”-*E*-*p*-coumaroyl,4”-*Z*-*p*-coumaroyl)-rhamnopyranoside (compound **4**), kaempferol-3-*O*-α-L-(2”-*Z*-*p*-coumaroyl,4”-*E*-*p*-coumaroyl)-rhamnopyranoside (compound **5**) and kaempferol-3-*O*-α-L-(2”,4”-di-*Z*-*p*-coumaroyl)-rhamnopyranoside (compound **6**) purified from *E. foeminea* dichloromethane extract.

**Supplementary Figure S25.** Anti-biofilm activity of purified kaempferol-3-*O*-α-L-(2”-*E*-*p*-coumaroyl,4”-*Z*-*p*-coumaroyl)-rhamnopyranoside (compound **4**).

**Supplementary Figure S26.** Anti-biofilm activity of purified kaempferol-3-*O*-α-L-(2”-*Z*-*p*-coumaroyl,4”-*E*-*p*-coumaroyl)-rhamnopyranoside (compound **5**).

**Supplementary Figure S27.** Anti-biofilm activity of purified kaempferol-3-*O*-α-L-(2”,4”-di-*Z*-*p*-coumaroyl)-rhamnopyranoside (compound **6**).

**Supplementary Table S4.** Details of the intermolecular interactions between the test ligand and *S. aureus* target enzymes tyrosyl tRNA synthetase and sortase A.

**Supplementary Table S1**. $MIC_{100}$ values (mg/mL) determined for fractions obtained upon extraction in hexane and two sequential steps of column chromatography.

| | **$MIC_{100}$ (mg/mL) of fractions extracted in hexane** | | | | | | |
|---|---|---|---|---|---|---|---|
| **Bacterial strains** | **1** | **2** | **3** | **4** | **5** | **6** | **7** |
| *S. aureus* ATCC 29213 | 2.5 | 2.5 | 2.5 | 0.313 | 0.313 | 2.5 | 1.25 |
| *E. coli* ATCC 25922 | 2.5 | 2.5 | 2.5 | 2.5 | 2.5 | 2.5 | 2.5 |
| *S. typhimurium* ATCC 14028 | 2.5 | 2.5 | 2.5 | 2.5 | 2.5 | 2.5 | 2.5 |

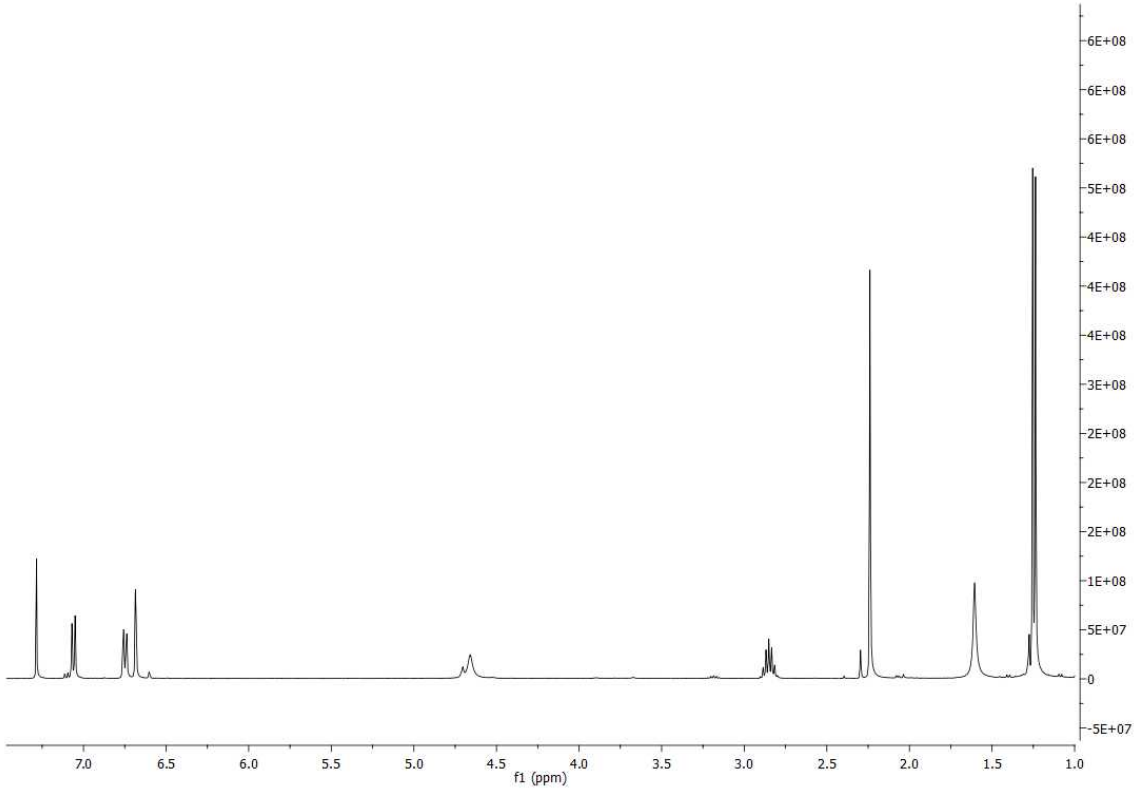


**Supplementary Figure S1**. $^{1}H$ NMR spectrum of carvacrol **compound 1** ($CDCl_3$, 400 MHz).

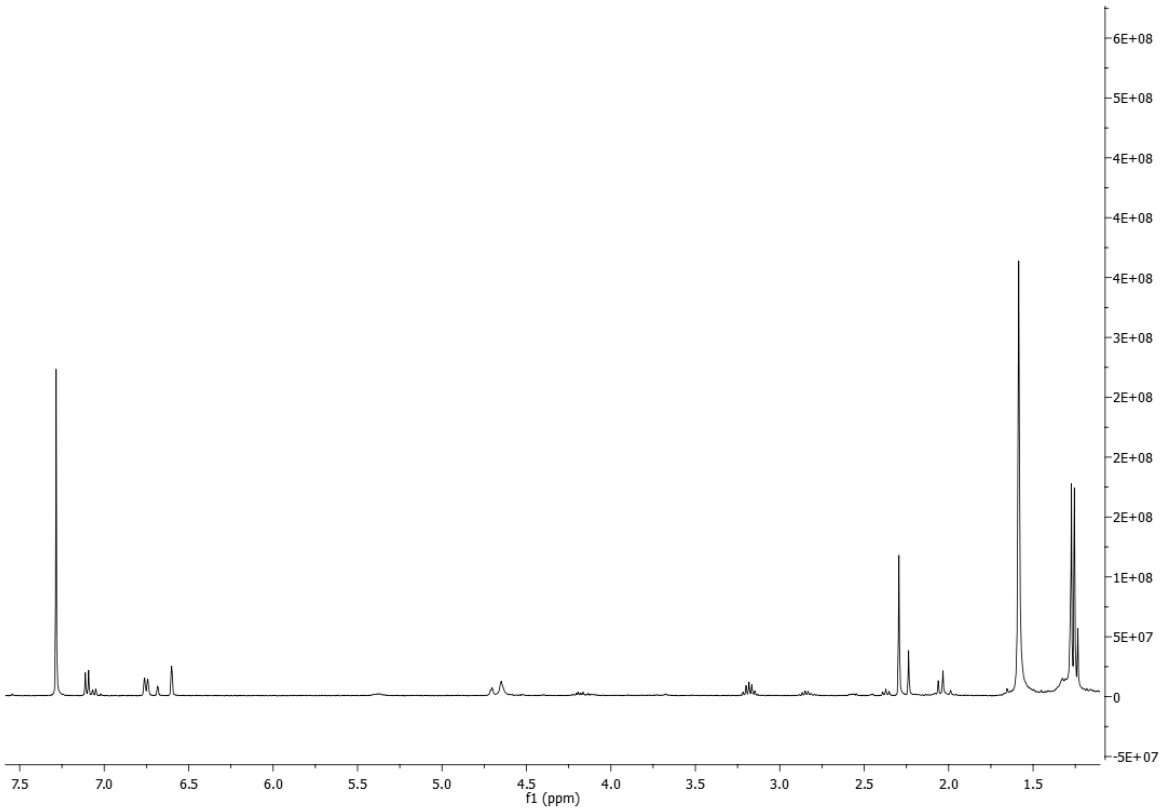


**Supplementary Figure S2**. $^{1}H$ NMR spectrum of thymol **compound 2** ($CDCl_3$, 400 MHz).

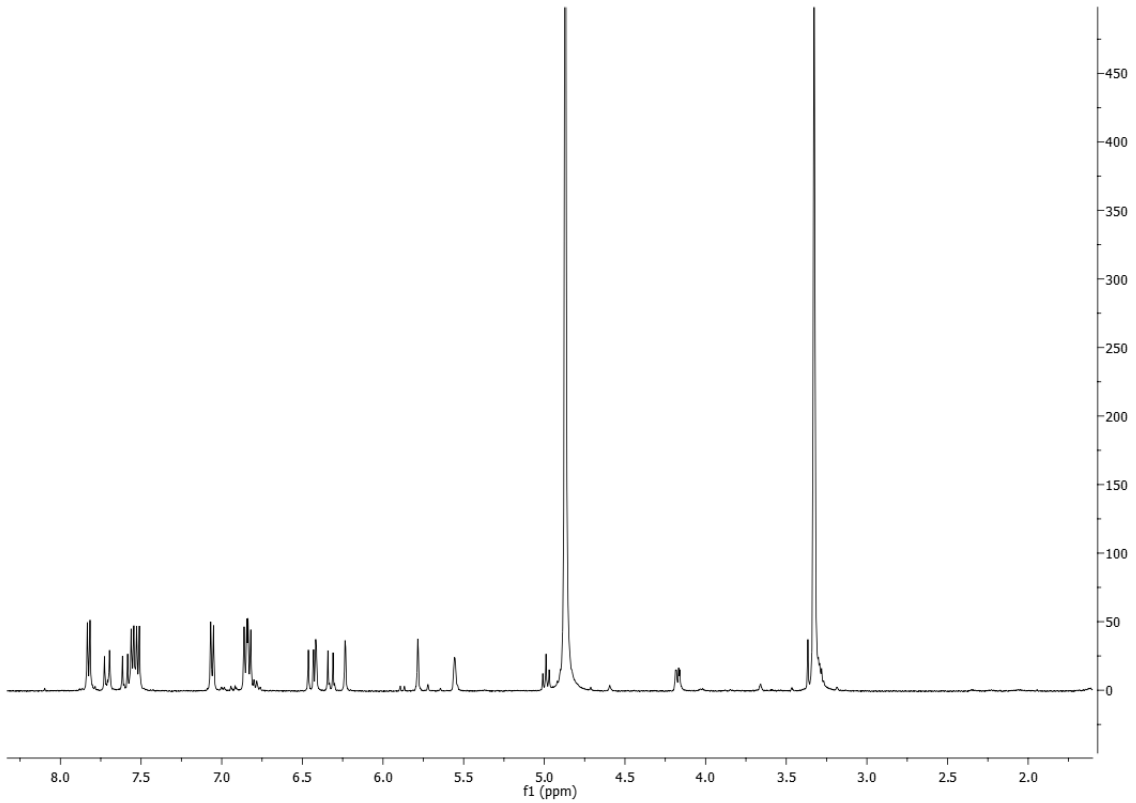


**Figure S3**. $^{1}$H NMR spectrum of kaempferol-3-*O*-α-L-(2”,4”-di-*E*-*p*-coumaroyl)-rhamnopyranoside **compound 3** (MeOD, 400 MHz).

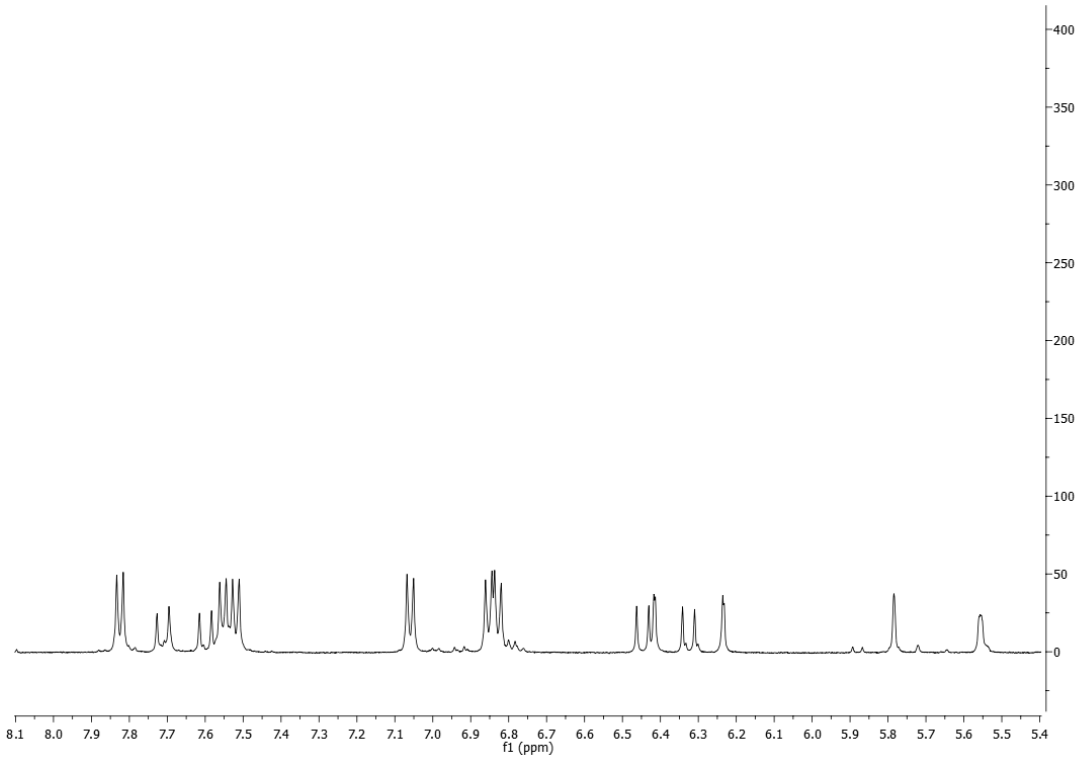


**Figure S4**. $^{1}$H NMR spectrum of kaempferol-3-*O*-α-L-(2”,4”-di-*E*-*p*-coumaroyl)-rhamnopyranoside **compound 3** (MeOD, 400 MHz) in the range 8.1 to 5.4 ppm.

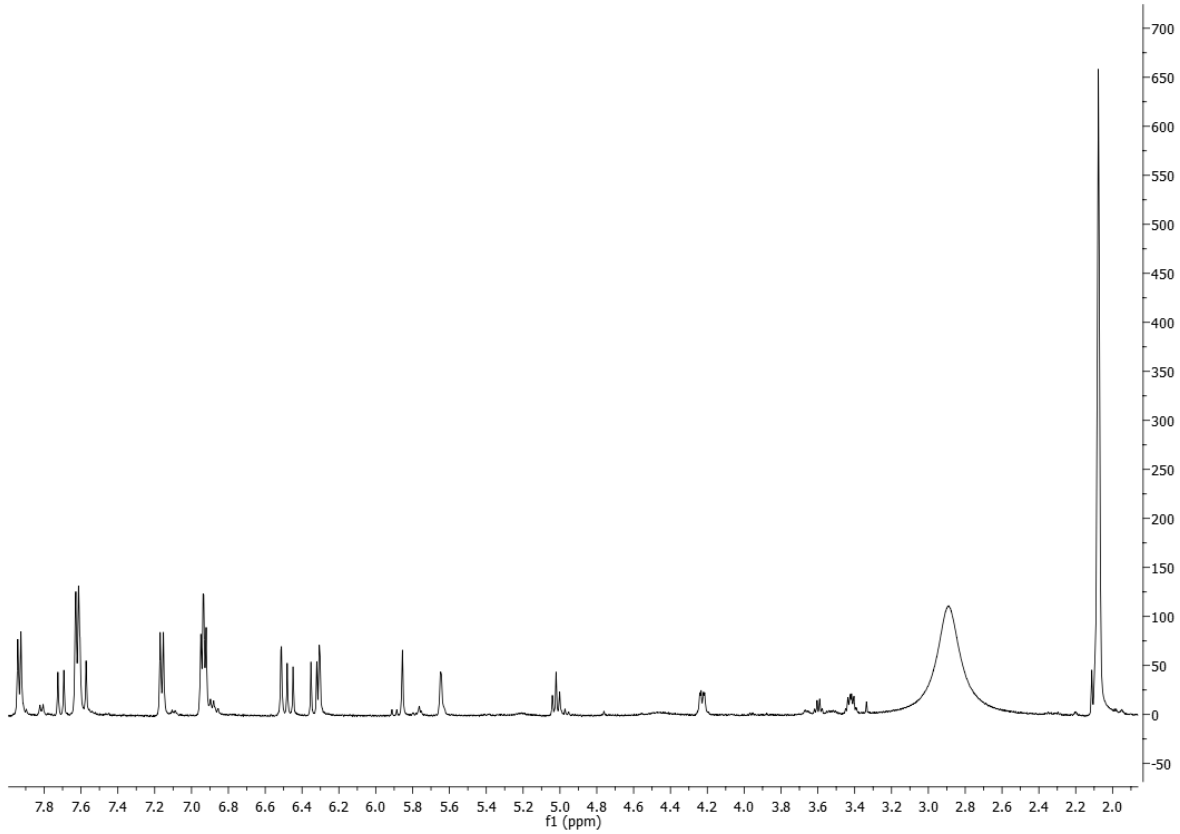


**Figure S5**. $^{1}$H NMR spectrum of kaempferol-3-*O*-α-L-(2”,4”-di-*E*-*p*-coumaroyl)-rhamnopyranoside **compound 3** (acetone-$d_6$, 400 MHz).

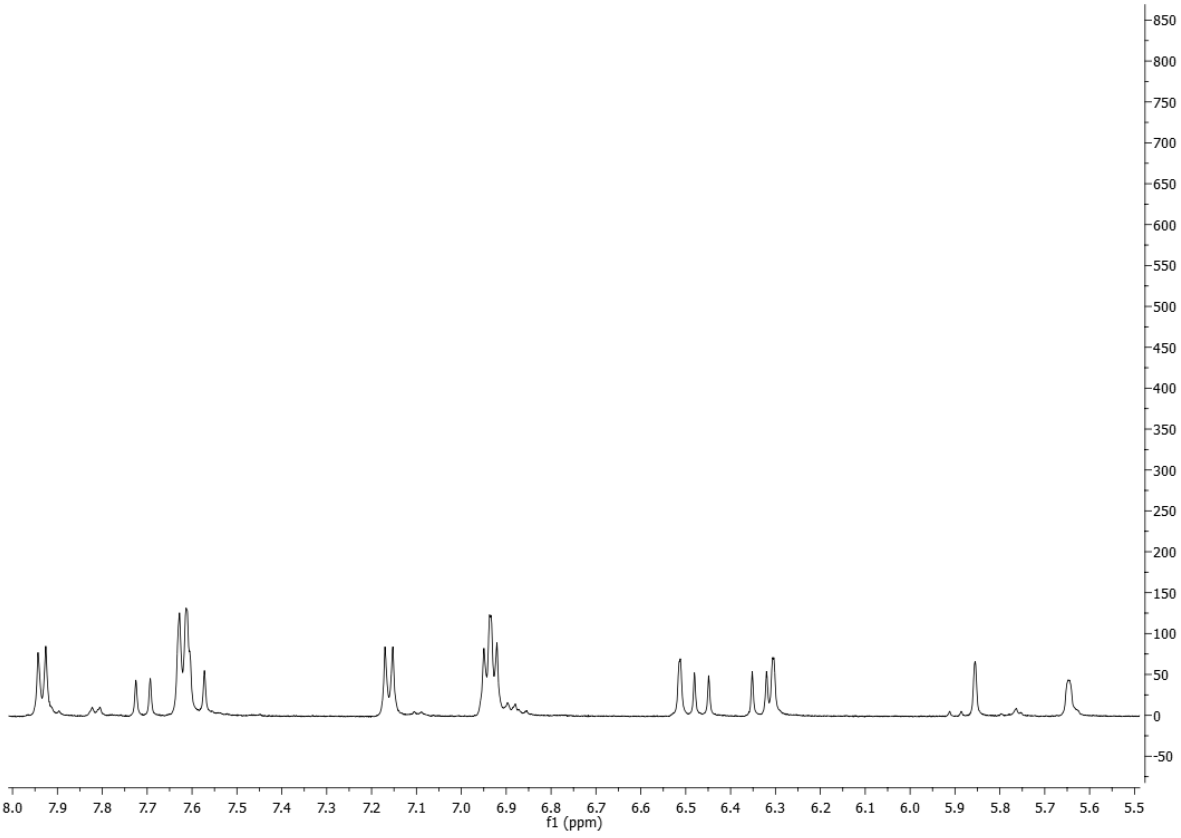


**Figure S6**. $^{1}$H NMR spectrum of kaempferol-3-*O*-α-L-(2”,4”-di-*E*-*p*-coumaroyl)-rhamnopyranoside **compound 3** (acetone-$d_6$, 400 MHz) in the range 8.0 to 5.5 ppm.

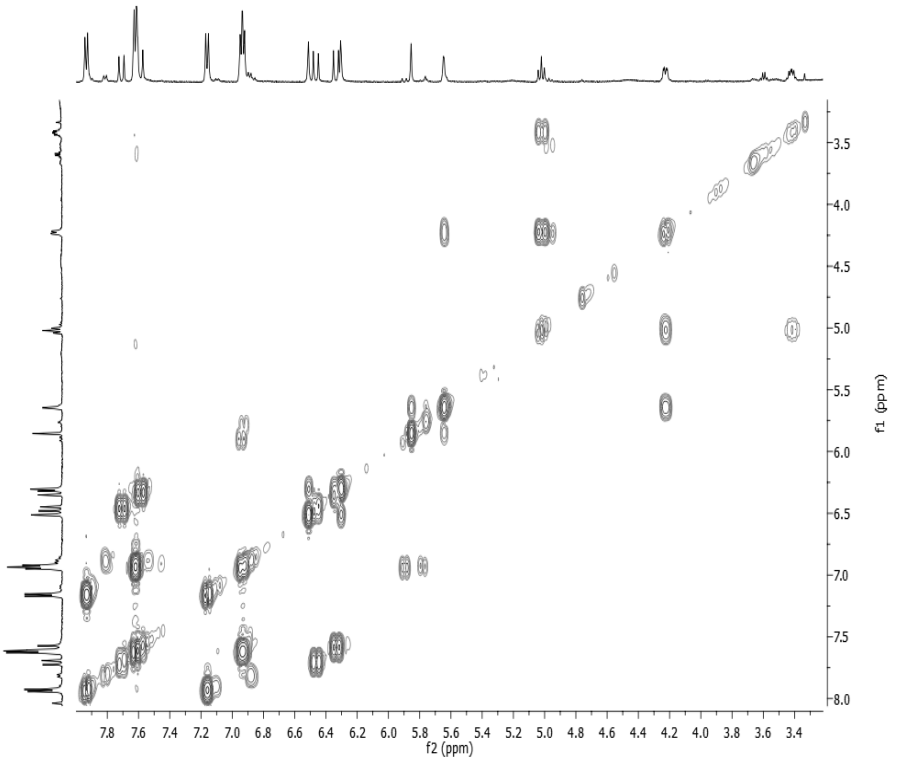


**Figure S7**. COSY spectrum of kaempferol-3-*O*-α-L-(2”,4”-di-*E*-*p*-coumaroyl)-rhamnopyranoside **compound 3** (acetone-$d_6$, 400 MHz).

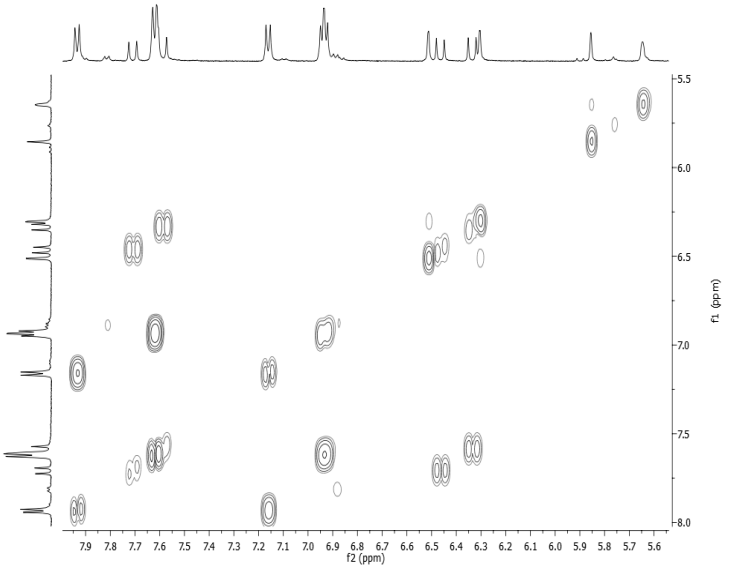


**Figure S8**. COSY spectrum of kaempferol-3-*O*-α-L-(2”,4”-di-*E*-*p*-coumaroyl)-rhamnopyranoside **compound 3** (acetone-$d_6$, 400 MHz) in the range 8.0 to 5.6 ppm.

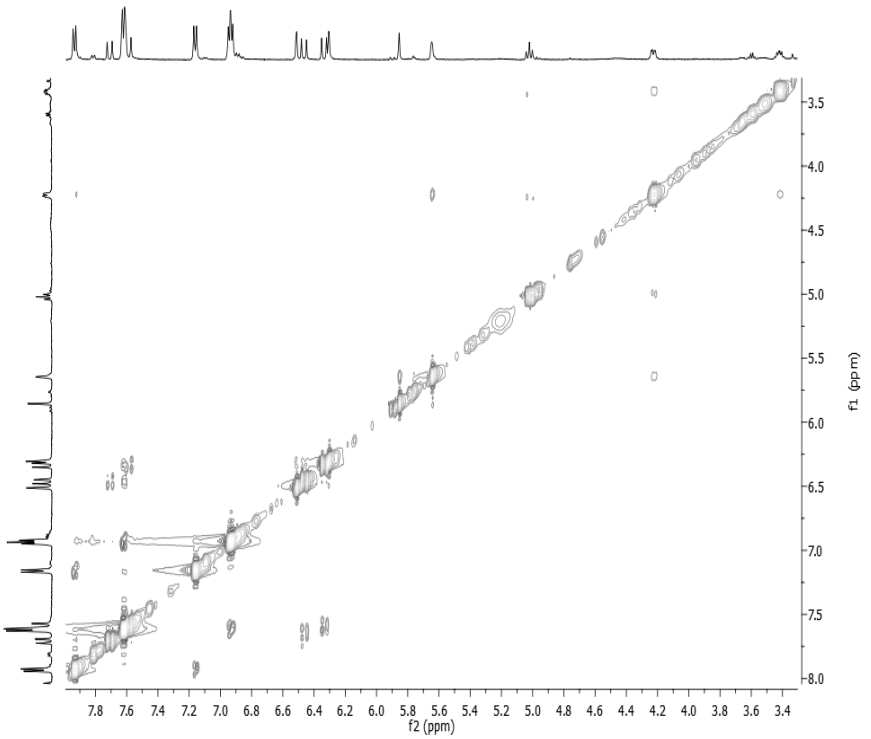


**Figure S9**. NOESY spectrum of kaempferol-3-*O*-α-L-(2”,4”-di-*E*-*p*-coumaroyl)-rhamnopyranoside **compound 3** (acetone-$d_6$, 400 MHz).

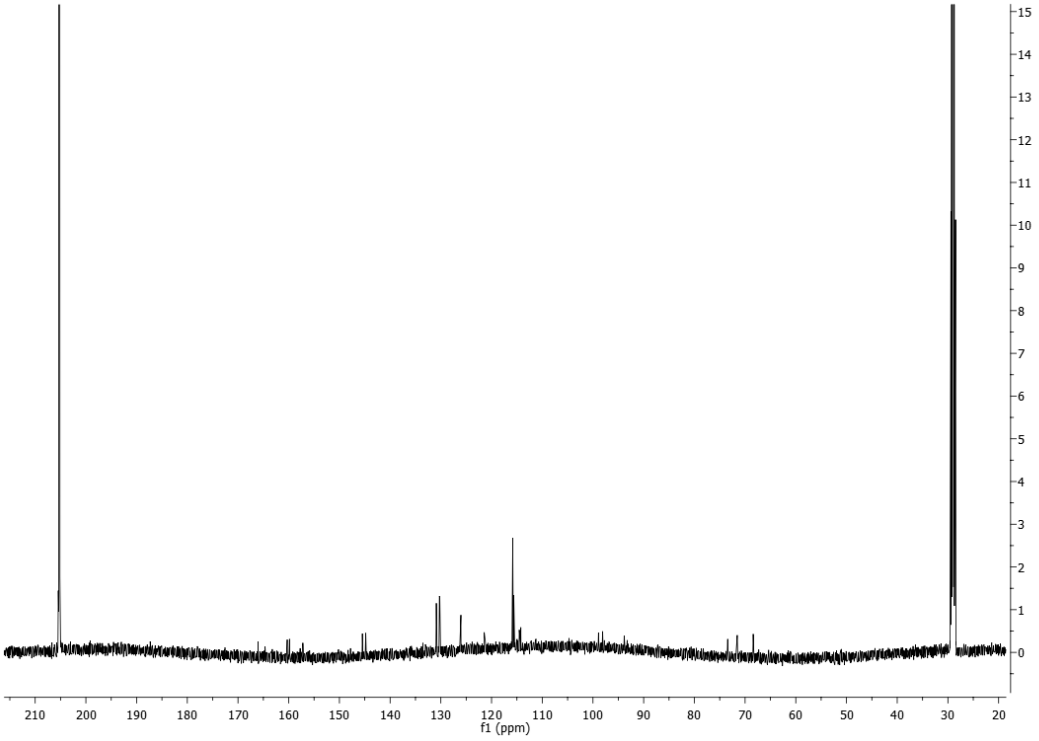


**Figure S10**. $^{13}C$ NMR spectrum of kaempferol-3-*O*-α-L-(2”,4”-di-*E*-*p*-coumaroyl)-rhamnopyranoside **compound 3** (acetone-$d_6$, 400 MHz).

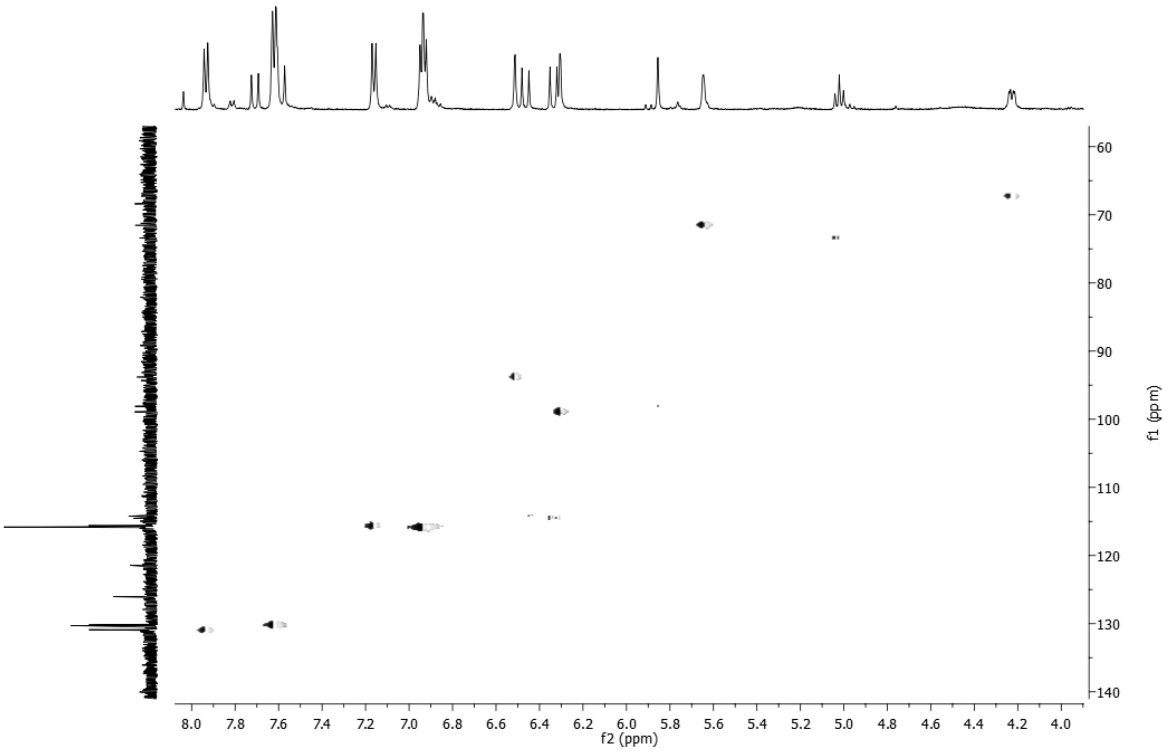


**Figure S11**. HSQC spectrum of kaempferol-3-*O*-α-L-(2”,4”-di-*E*-*p*-coumaroyl)-rhamnopyranoside **compound 3** (acetone-$d_6$, 400 MHz).

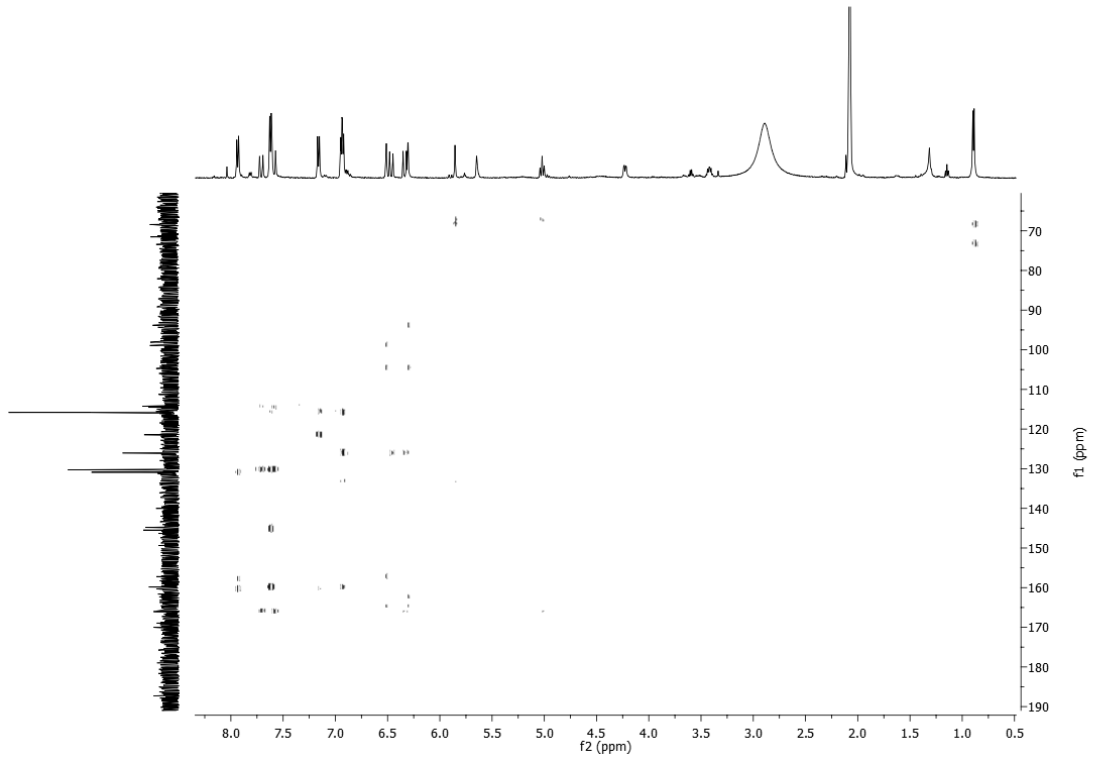


**Figure S12**. HMBC spectrum of kaempferol-3-*O*-α-L-(2”,4”-di-*E*-*p*-coumaroyl)-rhamnopyranoside **compound 3** (acetone-$d_6$, 400 MHz).

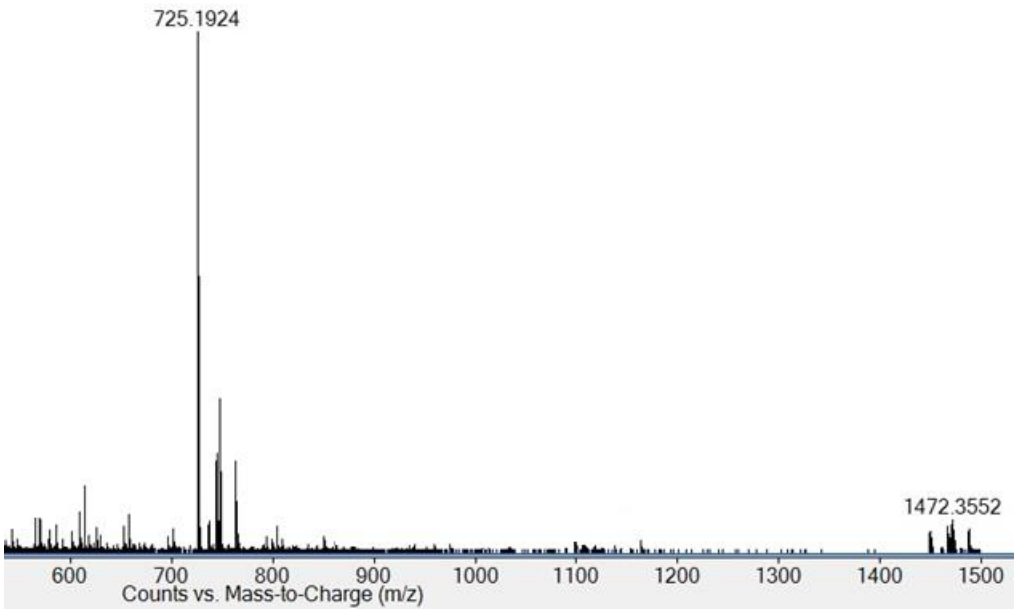


**Figure S13**. ESI MS spectrum of kaempferol-3-*O*-α-L-(2”,4”-di-*E*-*p*-coumaroyl)-rhamnopyranoside **compound 3** recorded in positive modality.

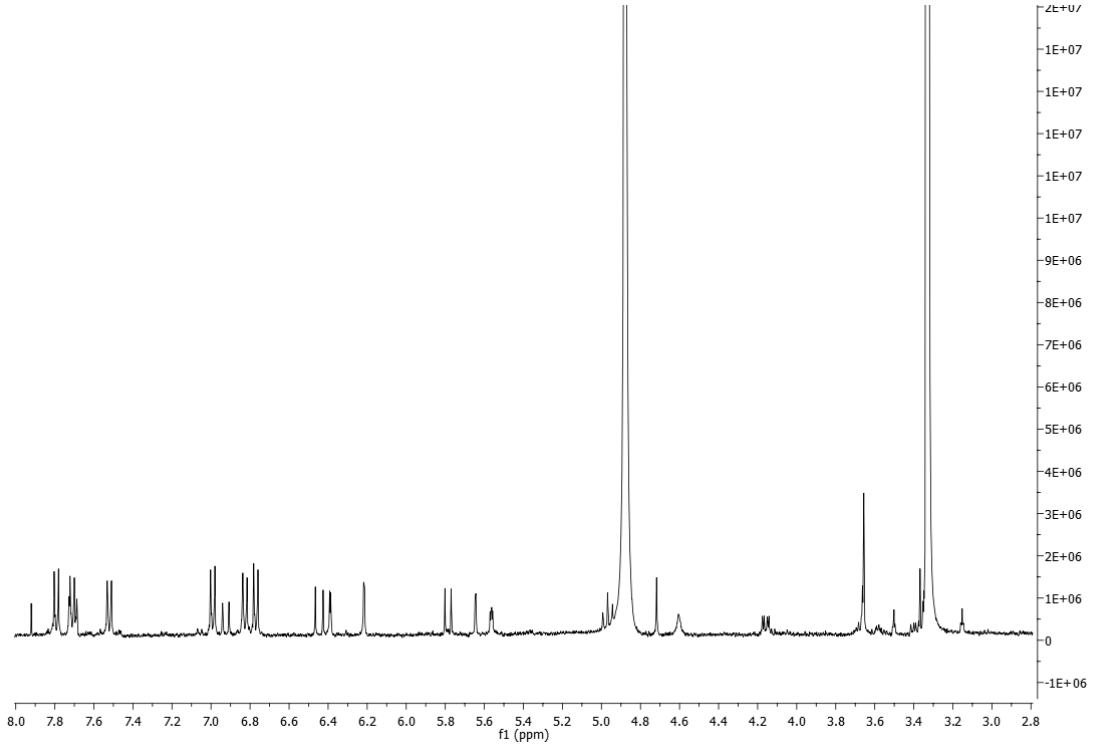


**Figure S14**. $^{1}$H NMR spectrum of kaempferol-3-*O*-α-L-(2”-*E*-*p*-coumaroyl,4”-*Z*-*p*-coumaroyl)-rhamnopyranoside **compound 4** (MeOD, 400 MHz).

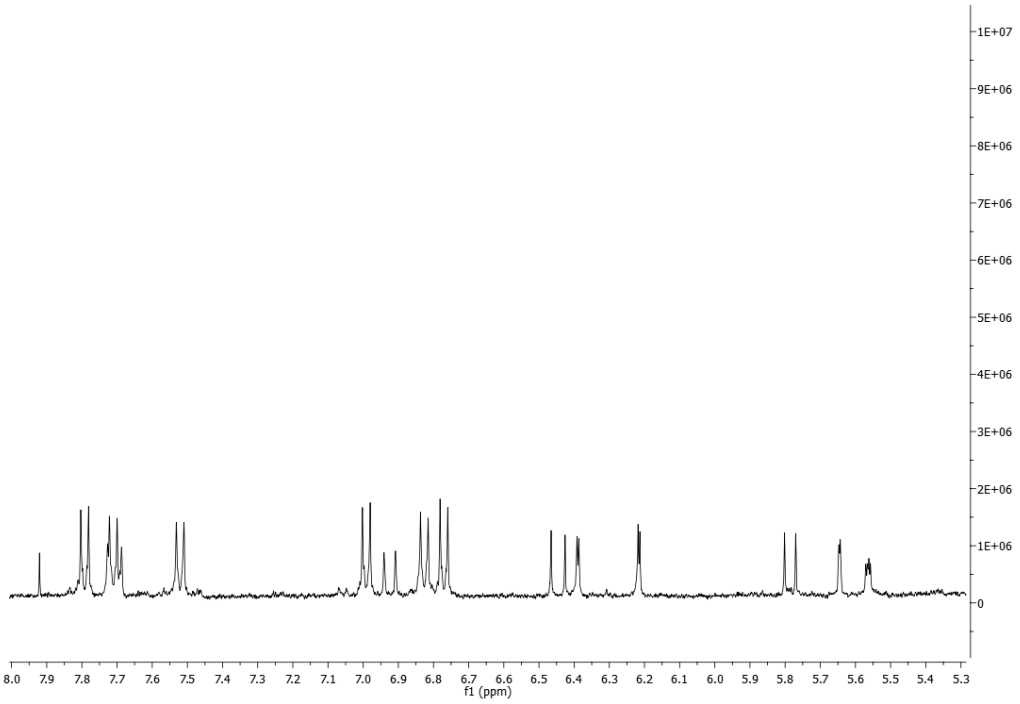


**Figure S15**. $^{1}$H NMR spectrum of kaempferol-3-*O*-α-L-(2”-*E*-*p*-coumaroyl,4”-*Z*-*p*-coumaroyl)-rhamnopyranoside **compound 4** (MeOD, 400 MHz) in the range 8.0 to 5.3 ppm.

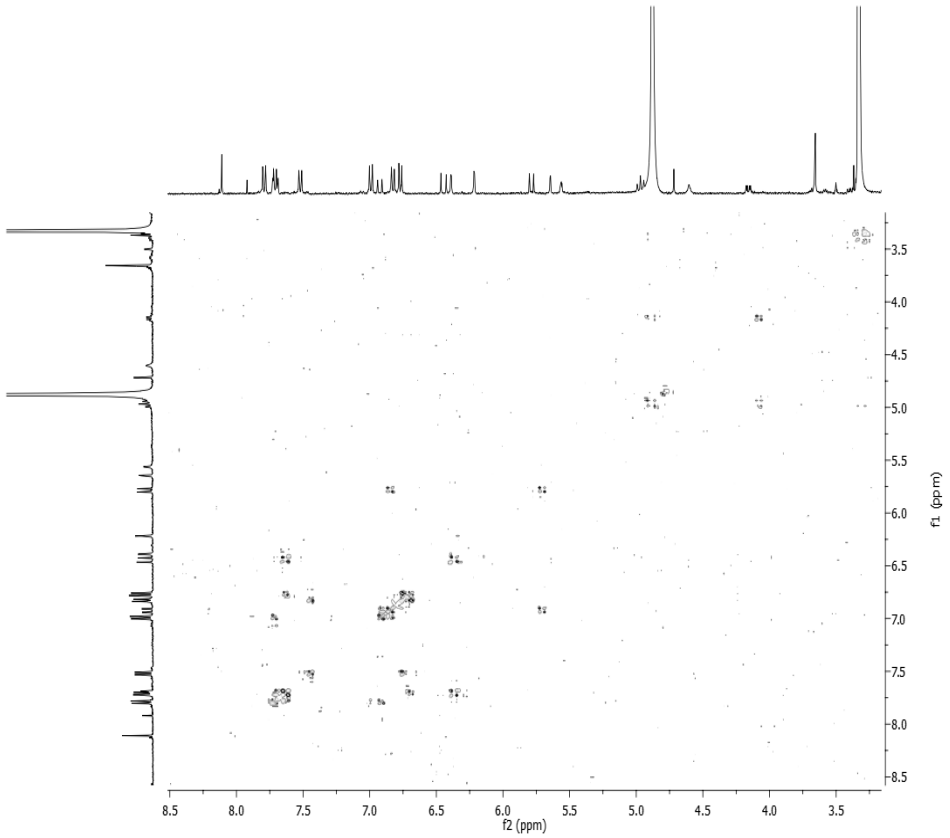


**Figure S16**. COSY spectrum of kaempferol-3-*O*-α-L-(2”-*E*-*p*-coumaroyl,4”-*Z*-*p*-coumaroyl)-rhamnopyranoside **compound 4** (acetone-$d_6$, 400 MHz).

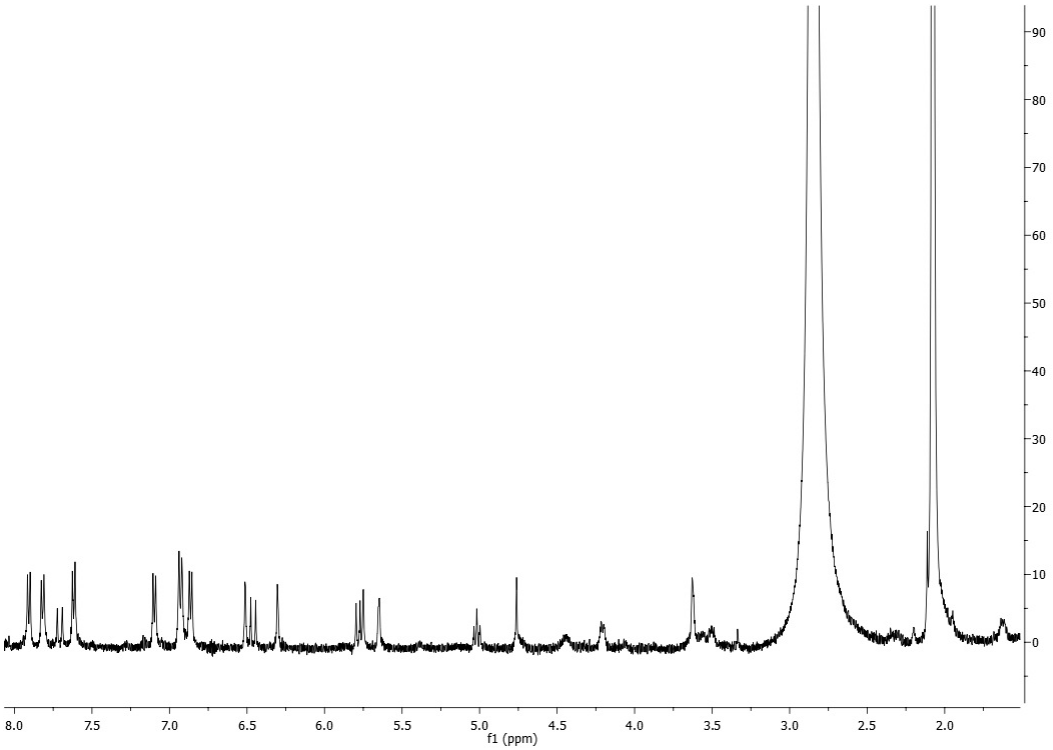


**Figure S17**. $^{1}$H NMR spectrum of kaempferol-3-*O*-α-L-(2”-*E*-*p*-coumaroyl,4”-*Z*-*p*-coumaroyl)-rhamnopyranoside **compound 4** (acetone-$d_6$, 400 MHz).

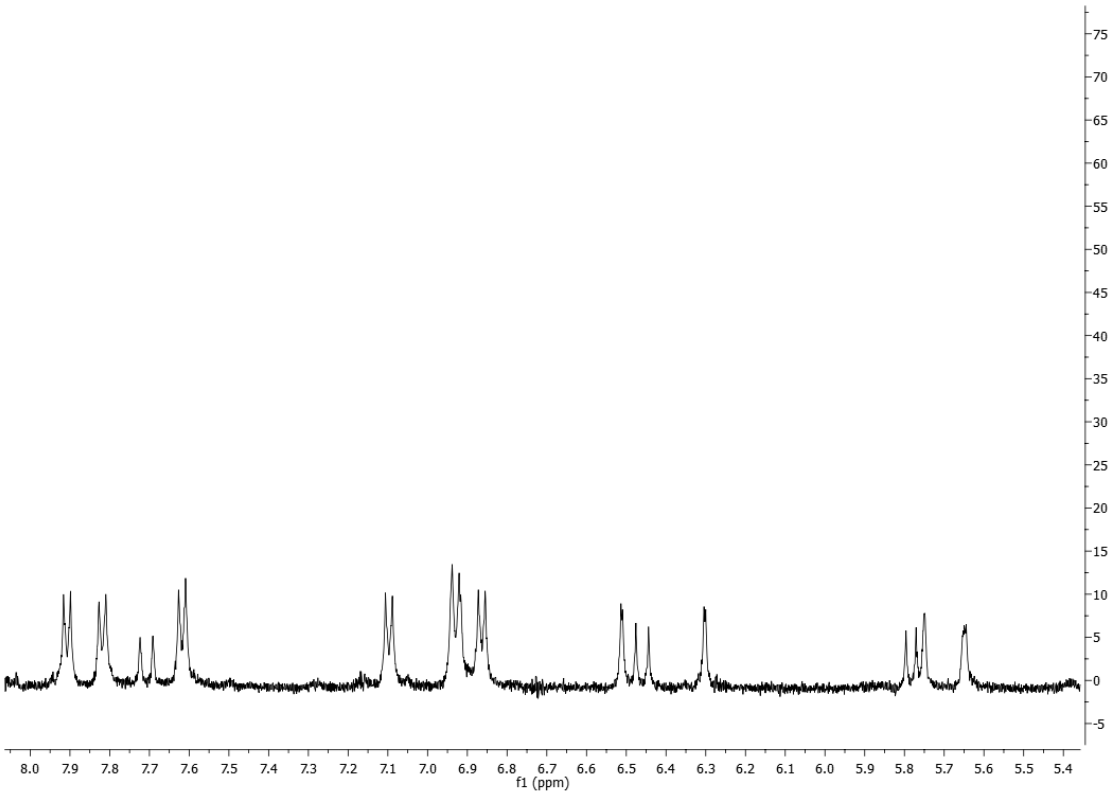


**Figure S18**. $^{1}$H NMR spectrum of kaempferol-3-*O*-α-L-(2”-*E*-*p*-coumaroyl,4”-*Z*-*p*-coumaroyl)-rhamnopyranoside **compound 4** (acetone-$d_6$, 400 MHz) in the range 8.0 to 5.4 ppm.

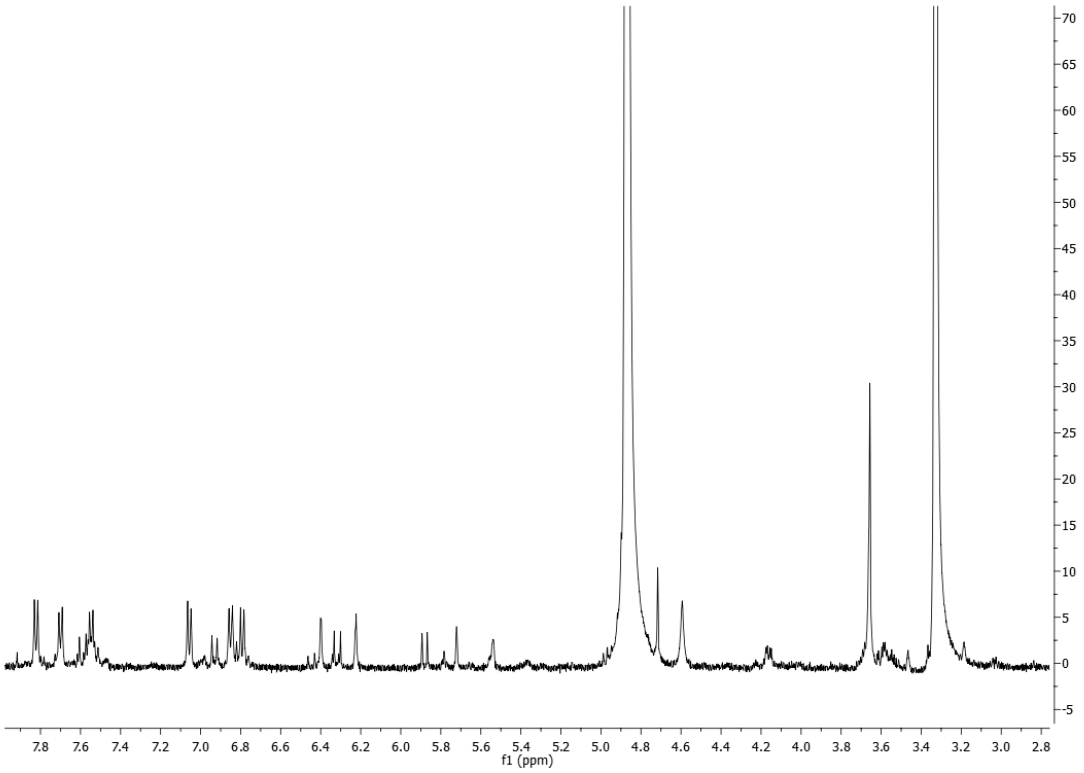


**Figure S19**. $^{1}$H NMR spectrum of kaempferol-3-*O*-α-L-(2”-*Z*-*p*-coumaroyl,4”-*E*-*p*-coumaroyl)-rhamnopyranoside **compound 5** (MeOD, 400 MHz).

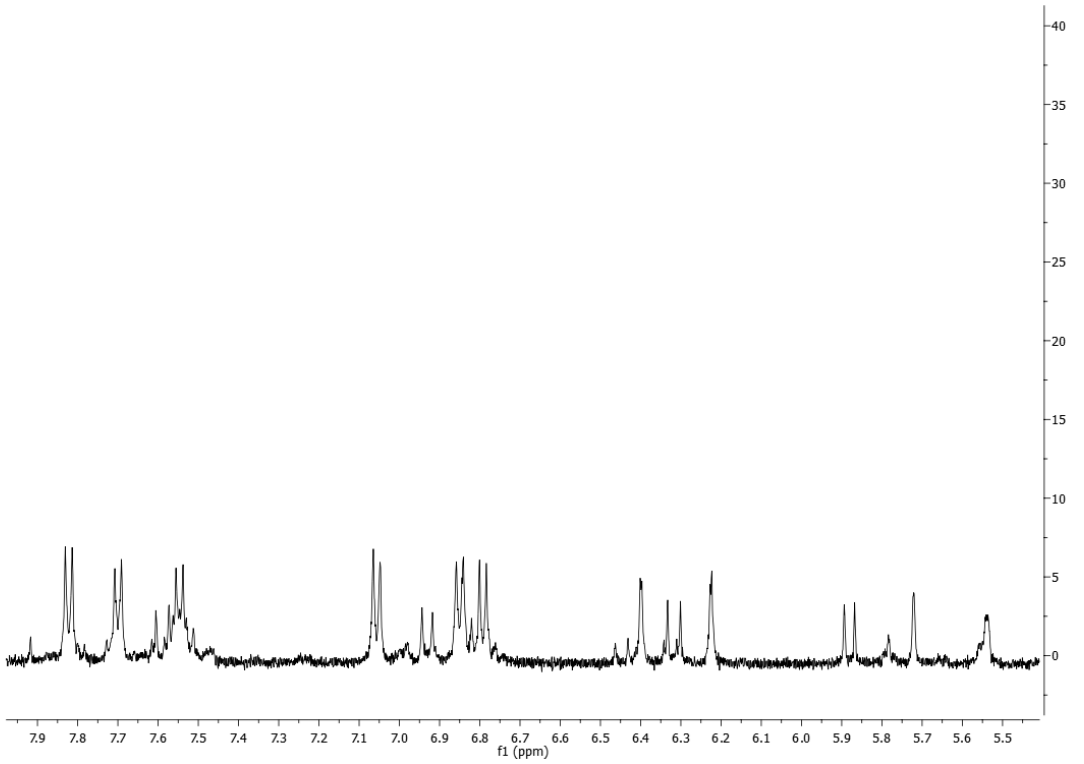


**Figure S20**. $^{1}$H NMR spectrum of kaempferol-3-*O*-α-L-(2”-*Z*-*p*-coumaroyl,4”-*E*-*p*-coumaroyl)-rhamnopyranoside **compound 5** (MeOD, 400 MHz) in the range 8.0 to 5.4 ppm.

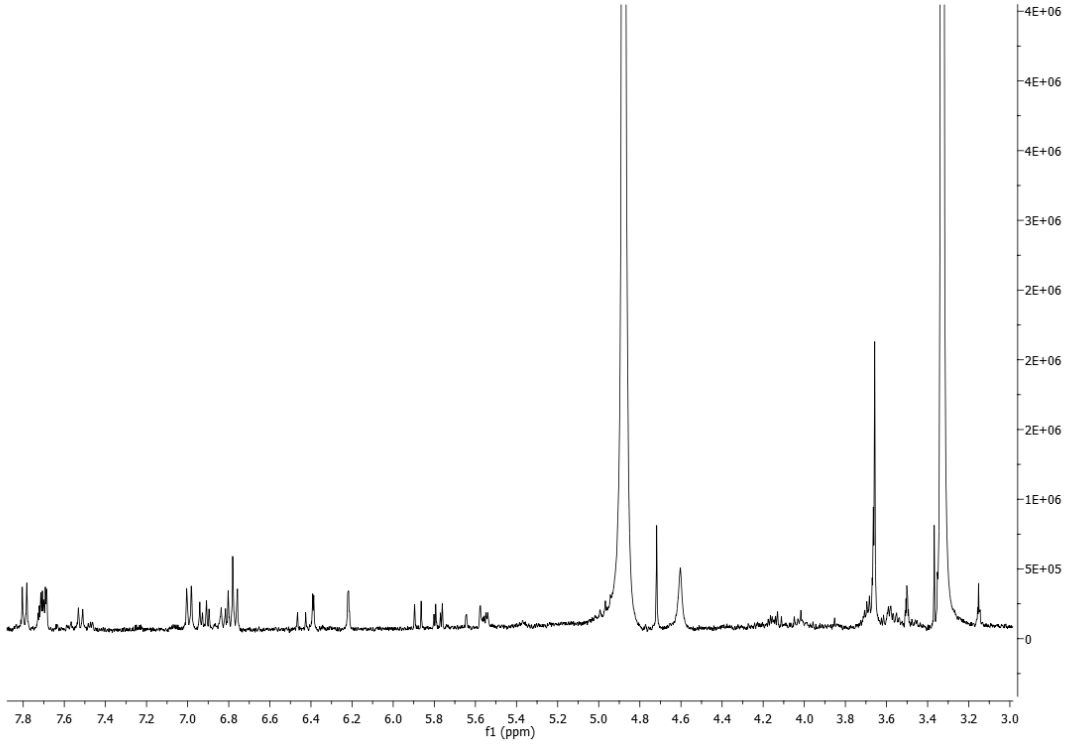


**Figure S21**. $^{1}$H NMR spectrum of kaempferol-3-*O*-α-L-(2”,4”-di-*Z*-*p*-coumaroyl)-rhamnopyranoside, **compound 6** (MeOD, 400 MHz).

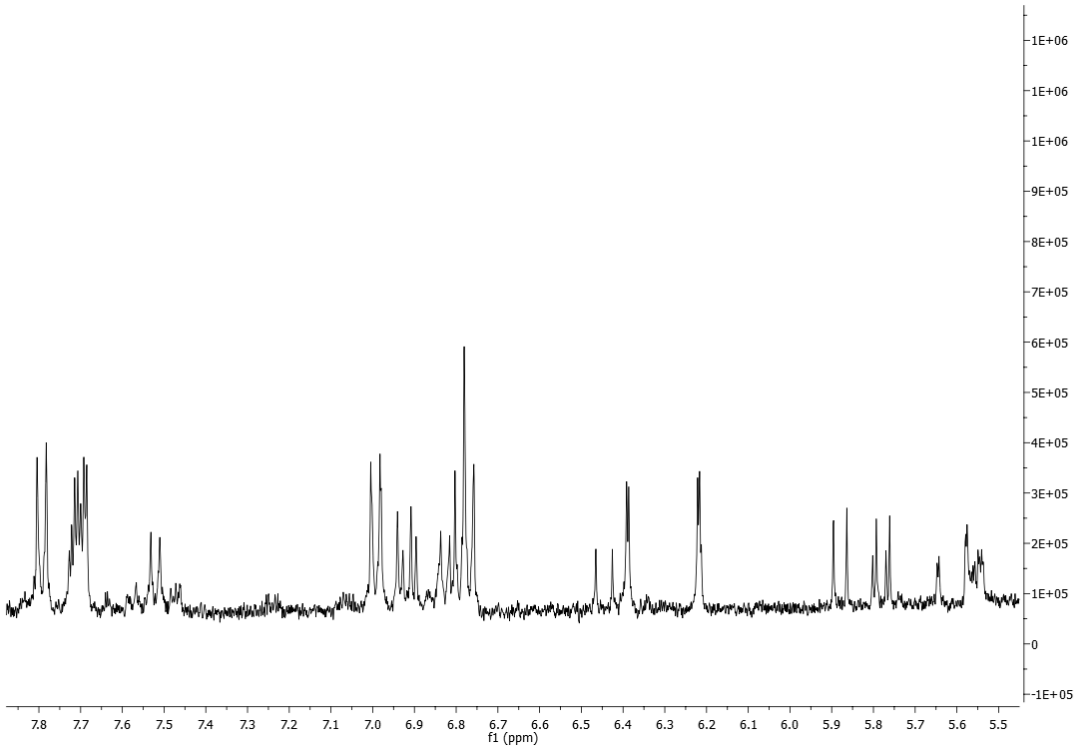


**Figure S22**. $^{1}$H NMR spectrum of kaempferol-3-*O*-α-L-(2”,4”-di-*Z*-*p*-coumaroyl)-rhamnopyranoside **compound 6** (MeOD, 400 MHz) in the range 7.9 to 5.5 ppm.

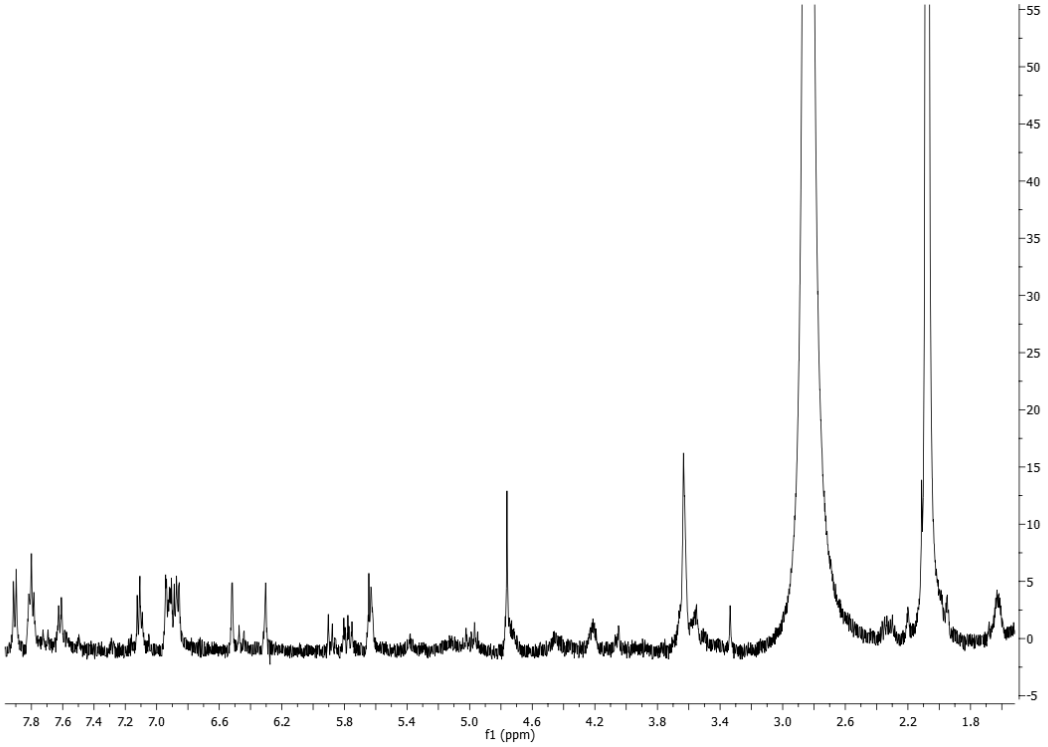


**Figure S23**. $^{1}$H NMR spectrum of kaempferol-3-*O*-α-L-(2”,4”-di-*Z*-*p*-coumaroyl)-rhamnopyranoside **compound 6** (acetone-$d_6$, 400 MHz).

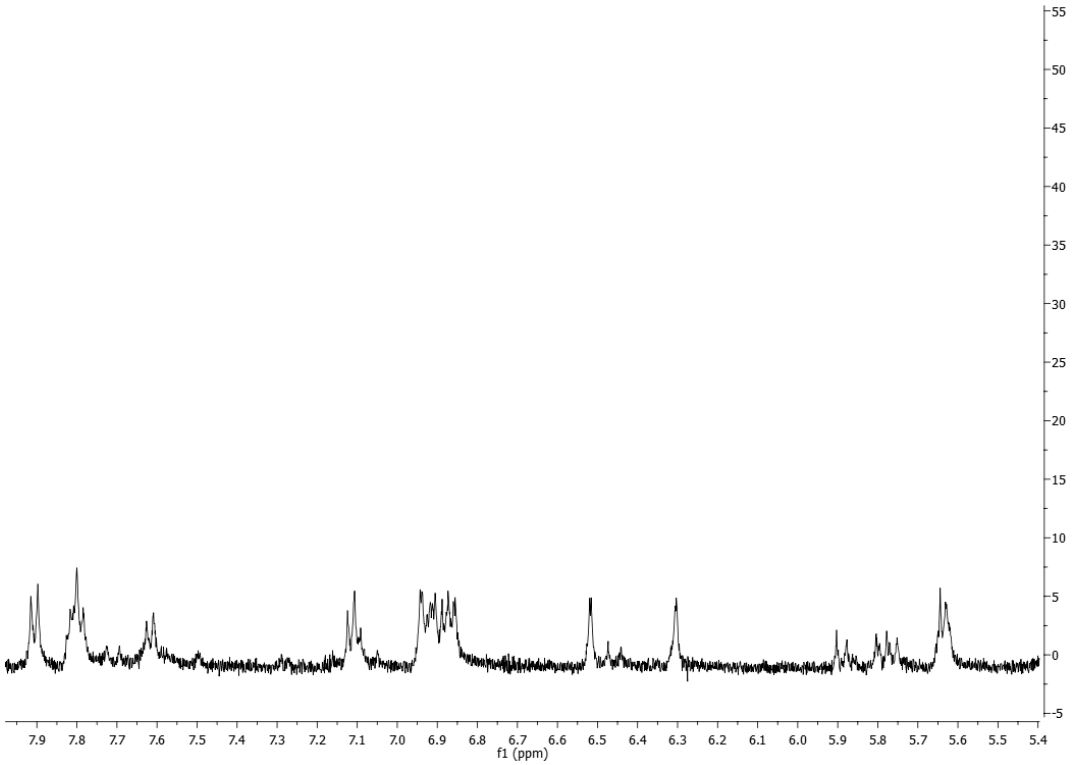


**Figure S24**. $^{1}$H NMR spectrum of kaempferol-3-*O*-α-L-(2”,4”-di-*Z*-*p*-coumaroyl)-rhamnopyranoside **compound 6** (acetone-$d_6$, 400 MHz) in the range 8.0 to 5.4 ppm.

**Supplementary Table S2**. $MIC_{100}$ values (µg/mL) determined for ~~the essential oils~~ carvacrol and thymol purified from *E. foeminea* hexane extract.

| | $MIC_{100}$ (µg/mL) | |
|---|---|---|
| **Gram-positive strains** | **Carvacrol** | **Thymol** |
| *S. aureus* ATCC 29213 | 100 | 600 |
| *S. aureus* MRSA WKZ-2 | 50 | 2,400 |
| *E. faecalis* ATCC 29212 | 100 | 1,200 |
| **Gram-negative Strains** | | |
| *E. coli* ATCC 25922 | 200 | 600 |
| *S. typhimurium* ATCC 14028 | 100 | 300 |
| *A. baumannii* ATCC 17878 | 100 | 1,200 |

**Supplementary Table S3.** $MIC_{100}$ values (µg/mL) determined for the compounds (**3-6**) purified from *E. foeminea* dichloromethane extract.

| | **$MIC_{100}$ (µg/mL)** | |
|---|---|---|
| | ***S. aureus* MRSA WKZ-2** | ***A. baumannii* ATCC 17878** |
| **kaempferol-3-*O*-α-L-(2",4"-di-*E*-*p*-coumaroyl)-rhamnopyranoside** | 0.49 | 1,000 |
| **kaempferol-3-*O*-α-L-(2"-*Z*-*p*-coumaryl,4"-di-*E*-*p*-coumaryl rhamnopyranoside** | >1,000 $MIC_{95}$ = 1,000 | 1,000 |
| **kaempferol-3-*O*-α-L-(2"-*E*- *p*-coumaryl,4"-di-*Z*-*p*-coumaryl)-rhamnopyranoside** | >1,000 $MIC_{98}$ = 1,000 | 1,000 |
| **kaempferol-3-*O*-α-L-(2",4"-di-*Z*-*p*-coumaryl)-rhamnopyranoside** | >1,000 $MIC_{98}$ = 1,000 | 1,000 |

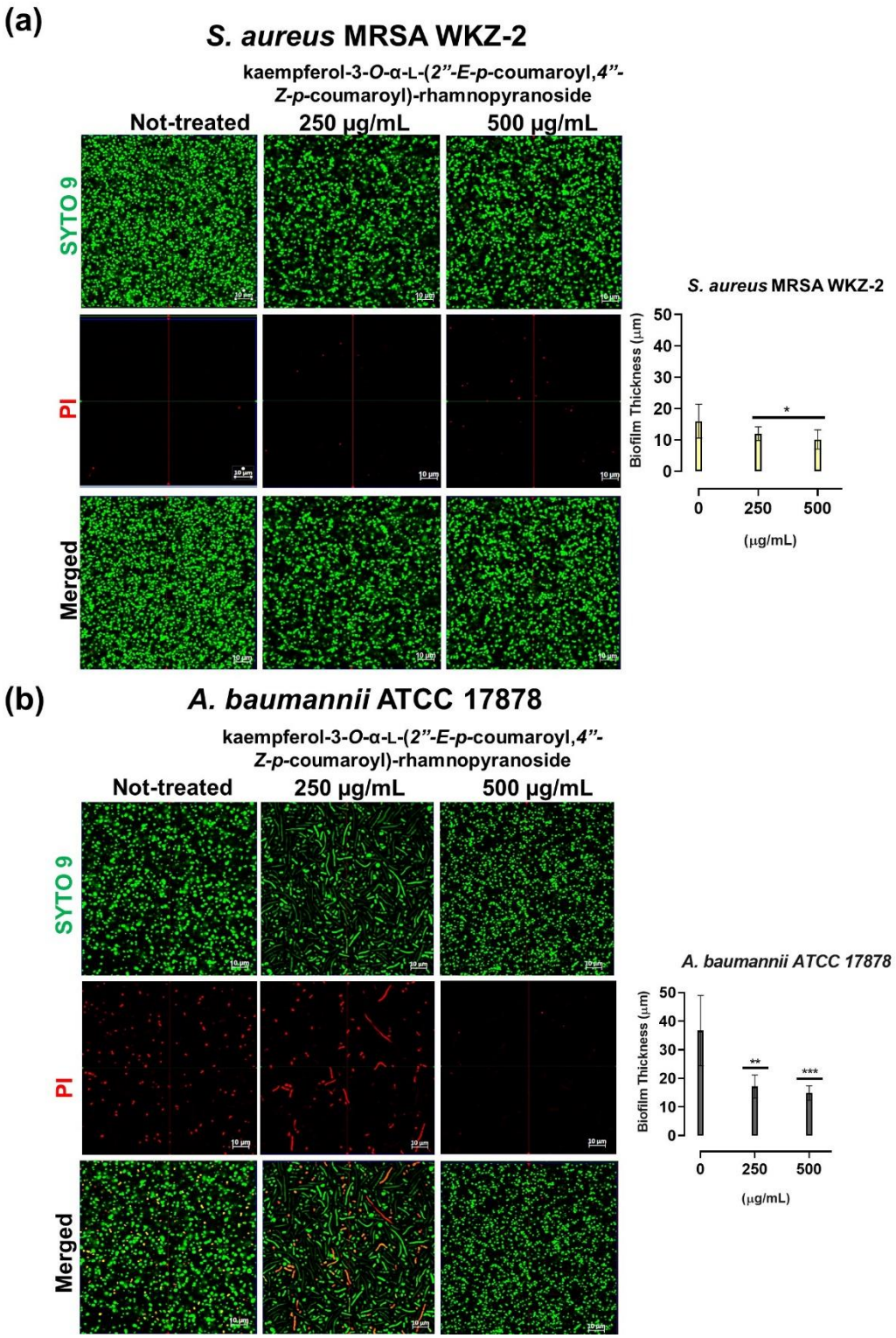


**Figure S25.** Anti-biofilm activity of purified kaempferol-3-*O*-α-L-(*2''-E-p*-coumaroyl,*4''-Z-p*-coumaroyl)-rhamnopyranoside (compound **4**). Effects of compound **4** have been evaluated on biofilm formation in the case of *S. aureus* MRSA WKZ-2 **(a)**, and *A. baumannii* ATCC 17878 **(b)** by CLSM. Biofilm cells were stained with LIVE/DEAD BacLight bacterial viability kit (Molecular Probes, Eugene, OR) containing a 1:1 mol/mol ratio of SYTO-9 (green fluorescence, all cells) and propidium iodide (PI; red fluorescence, dead cells). The biofilm images were obtained by confocal z-stack using Zen Lite 2.3 software. All the images were taken under identical conditions. Significant differences were indicated as (*P< 0.05), (**P< 0.001) or (***P< 0.0001) for treated *versus* control samples. Each experiment was carried out in triplicate.

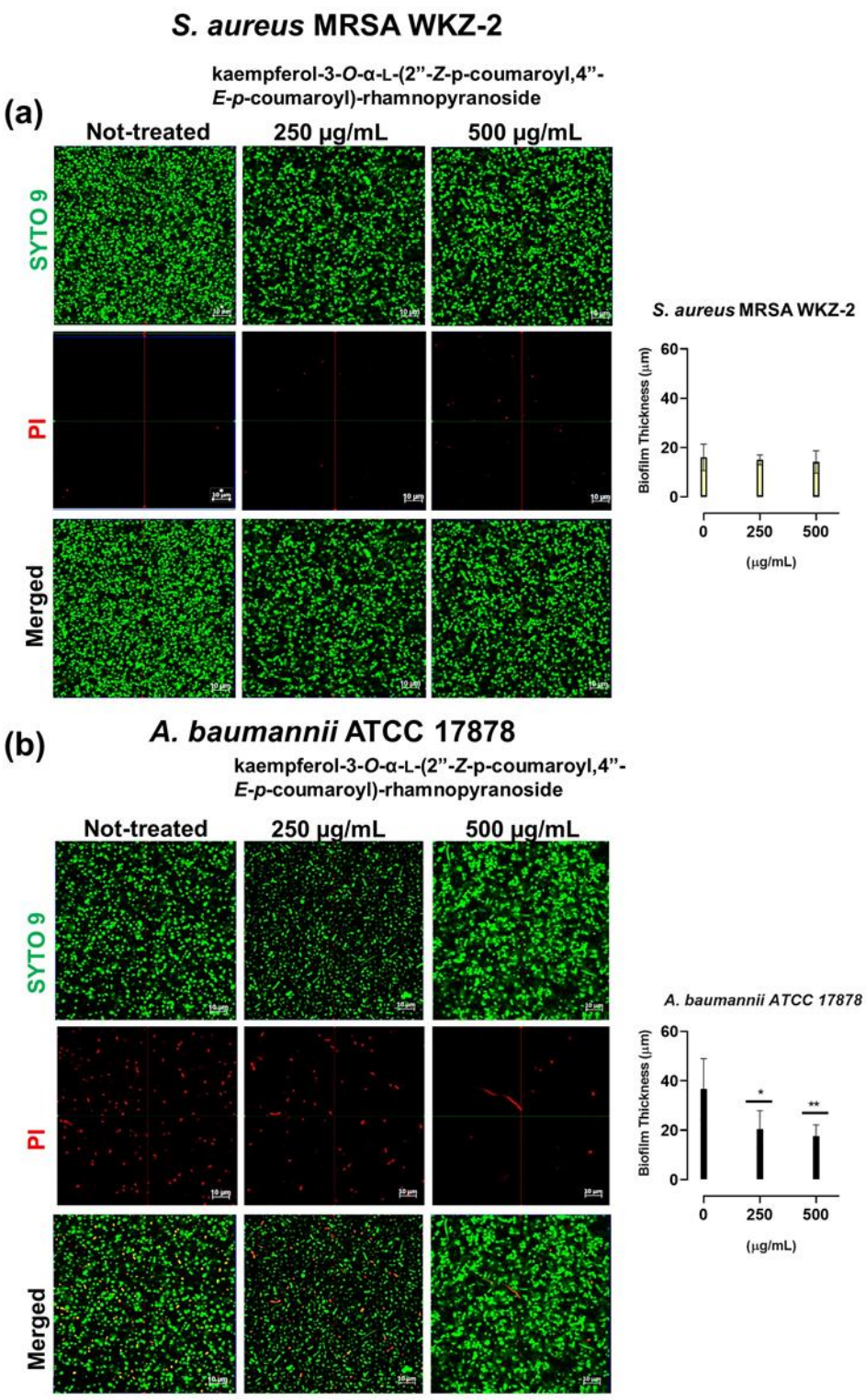


**Figure S26.** Anti-biofilm activity of purified kaempferol-3-*O*-α-L-(*2''-Z-p*-coumaroyl,*4''-E-p*-coumaroyl)-rhamnopyranoside (compound **5)**. Effects of compound **5** have been evaluated on biofilm formation in the case of *S. aureus* MRSA WKZ-2 **(a)**, and *A. baumannii* ATCC 17878 **(b)**. Biofilm cells were stained with LIVE/DEAD BacLight bacterial viability kit (Molecular Probes, Eugene, OR) containing a 1:1 mol/mol ratio of SYTO-9 (green fluorescence, all cells) and propidium iodide (PI; red fluorescence, dead cells). The biofilm images were obtained by confocal z-stack using Zen Lite 2.3 software. All the images were taken under identical conditions. Significant differences were indicated as (*P< 0.05) or (**P< 0.001) for treated *versus* control samples. Each experiment was carried out in triplicate.

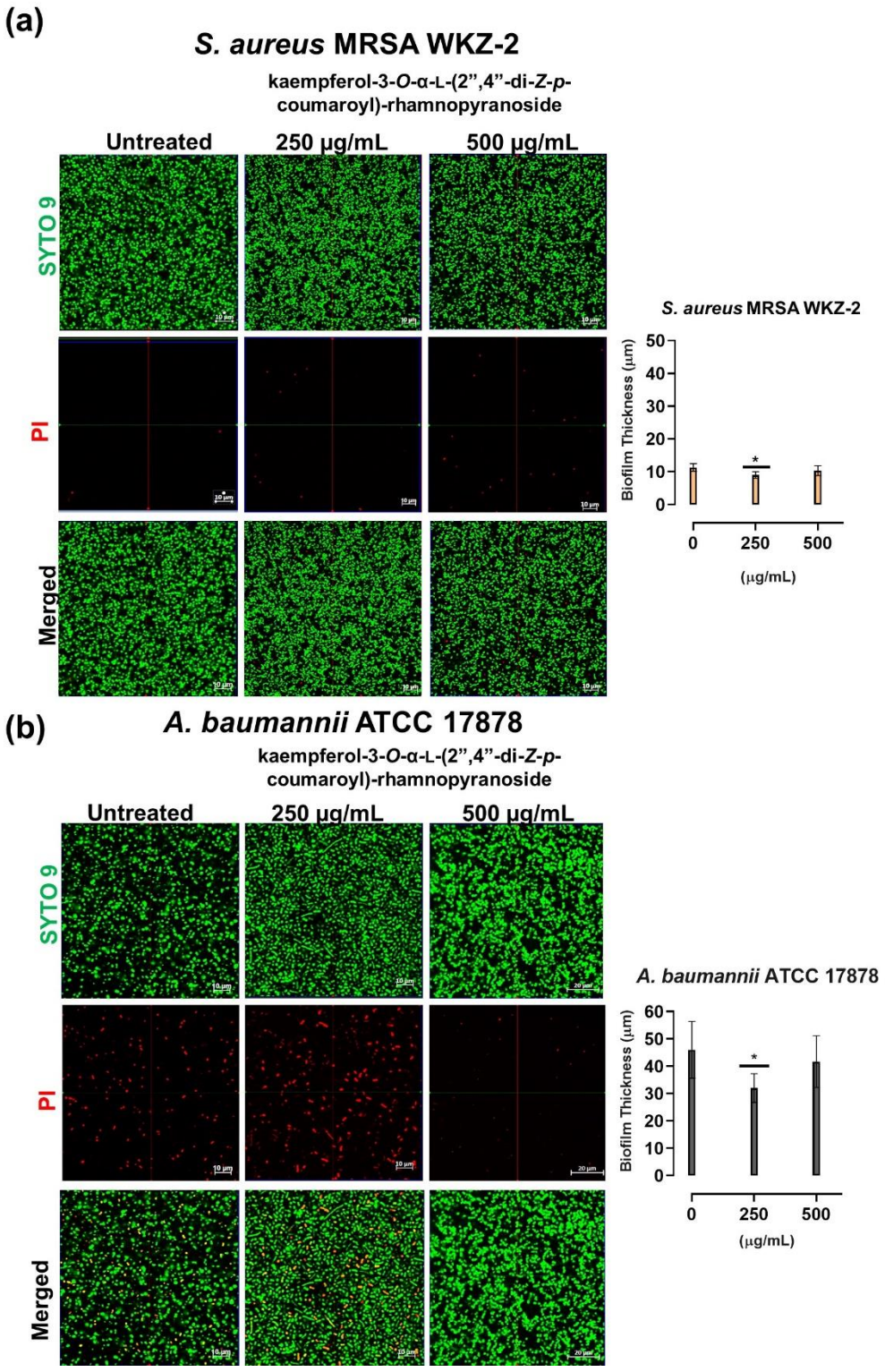


**Figure S27.** Anti-biofilm activity of purified kaempferol-3-*O*-α-L-(2",4"-di-*Z*-*p*-coumaroyl)-rhamnopyranoside (compound **6**). Effects of compound **6** have been evaluated on biofilm formation in the case of *S. aureus* MRSA WKZ-2 **(a)**, and *A. baumannii* ATCC 17878 **(b)** by CLSM. Biofilm cells were stained with LIVE/DEAD BacLight bacterial viability kit (Molecular Probes, Eugene, OR) containing a 1:1 mol/mol ratio of SYTO-9 (green fluorescence, all cells) and propidium iodide (PI; red fluorescence, dead cells). The biofilm images were obtained by confocal z-stack using Zen Lite 2.3 software. All the images were taken under identical conditions. Significant differences were indicated as (*P< 0.05) for treated *versus* control samples. Each experiment was carried out in triplicate.

| **Supplementary Table S4.** Details of the intermolecular interactions between the tested ligand and *S. aureus* target enzymes tyrosyl tRNA synthetase and sortase A. | | | | | |
|---|---|---|---|---|---|
| **Interaction between antimicrobial compound and tyrosyl tRNA synthetase** | | | **Interaction between antimicrobial compound and sortase A** | | |
| **Interacting amino acid** | **Type of interaction** | **Bond length (Å)** | **Interacting amino acid** | **Type of interaction** | **Bond length (Å)** |
| His 50 | Carbon-hydrogen bond | 3.57 | Val 168 | Hydrogen bond | 2.21 |
| His 47 | Pi-Sigma | 3.92 | Arg 197 | Hydrogen bond | 2.35 |
| His 47 | Pi-Pi T shaped | 5.02 | Ala 92 | Hydrogen bond | 2.66 |
| His 47 | Pi-Pi T shaped | 4.96 | Val 168 | Hydrogen bond | 2.70 |
| Gly 38 | Amide Pi Stacked | 3.52 | Thr 180 | Hydrogen bond | 2.49 |
| Ala 43 | Pi -Alkyl | 5.00 | Val 193 | Pi-Sigma | 3.79 |
| Leu 223 | Pi -Alkyl | 5.37 | Ala 92 | Pi-alkyl | 5.11 |
| | | | Ala 104 | Pi-Alkyl | 5.07 |
| | | | Val 168 | Pi-Alkyl | 4.65 |
| | | | Ile 199 | Pi-Alkyl | 4.54 |

# Host defence peptides identified in human apolipoprotein Bas natural food bio-preservatives: evaluation of their biosafety and digestibility

| | |
|---|---|
| Journal: | *Peptide Science* |
| Manuscript ID | PEP-2022-07-00052.R2 |
| Wiley - Manuscript type: | Article |
| Date Submitted by the Author: | 11-Jan-2023 |
| Complete List of Authors: | Dell'Olmo, Eliana; University of Naples Federico II, Chemical Sciences<br>Pane, Katia; IRCCS SDN SpA, IRCSS SDB SpA<br>Schibeci, Martina; University of Naples Federico II, Chemical Sciences<br>Cesaro, Angela; University of Naples Federico II, Chemical Sciences<br>De Luca, Maria; University of Naples Federico II, Chemical Sciences<br>Ismail, Shurooq; University of Naples Federico II, Chemical Sciences<br>Gaglione, Rosa; University of Naples Federico II, Chemical Sciences<br>Arciello, Angela; University of Naples Federico II, Chemical Sciences |
| Keywords: | host defence peptides, antimicrobial peptides, food bio-preservatives, peptide biocompatibility, antimicrobial resistance |
| | |

SCHOLARONE™
Manuscripts

## Answers to reviewer 1

**QUESTION 1**. A general comment is that the MS lacks adequate focus on the actual anti-microbial activity of the tested peptides and ranges of MIC.
**ANSWER 1**. Based on reviewer's comment, we added information on peptides' MIC values in the Introduction Section of the revised version of the manuscript and cited proper references reporting data previously obtained by our research group.

**QUESTION 2**. The data on development of resistance should be presented in Table format showing the initial anti-microbial activity, and changes that indicate development of resistance or not.
**ANSWER 2**. Following reviewer's suggestion, data on MIC values obtained at time 0 and after prolonged exposure of bacterial cells to ciprofloxacin or to r(P)ApoB$_{L}^{Pro}$ peptide have been presented in table format in panel C of the revised version of Figure 2.

**QUESTION 3**. Likewise in the Discussion, more attention should be given to the anti-microbial activity and comparison with other AMPs, that justifies the rest of the research.
**ANSWER 3**. Following reviewer's suggestion, these aspects have been included in the Discussion Section of the revised version of the manuscript.

**QUESTION 4**. The focus of the Discussion mostly on digestive and proteolytic break-down of peptides is disproportionate to the other data presented.
ANSWER 4. Following reviewer's suggestion, we modified the Discussion in the revised version of the manuscript.

**QUESTION 5**. Considering the high expectation of break down of the peptides, what is the relevance of the cytotoxicity data for intact peptides?
**ANSWER 5**. We thank the reviewer for his/her observation that allowed us to explain the meaning of our cytocompatibility experiments. Even if the peptide is expected to be degraded with high probability, we propose to use the full-length peptide as novel food bio-preservative. For this reason, we believe that it is important to determine, as first, the cytocompatibility of the intact peptide. On the other hand, we cannot exclude that proteases secreted from the cells during the 72 hrs incubation time might degrade the peptide. The important point is that no toxic effects of the peptide towards eukaryotic cells are detected under the experimental conditions tested.

**QUESTION 6**. Abstract L50: specify which cell types; P9-L14: complicated P9-L58: what about possible flavor effects as peptides can be bitter
**ANSWER 6**. We modified the manuscript accordingly. About the last point, we only affirm that the use of the peptides might non affect food quality, a concept that is generally accepted. About the bitter flavor of the peptides, it is a hypothesis since this feature will surely depend on peptide concentration.

**QUESTION 7**. Methods Section 2.1 define peptides and their sequences that were studied in the MS L14-16: move to relevant section
**ANSWER 7**. We modified the manuscript accordingly.

## Answers to Editor

**QUESTION 1**. The table containing the MIC data (currently figure 2 C) needs to be an individual table, complete with proper caption explaining the data. The table should contain the initial values as well as those after treatment. The text should describe and discuss the data; the change in anti-microbial activity needs to be better explained.
**ANSWER 1**. Following Editor's suggestion, we separated the Table 1 from Figure 2 in the revised version of the manuscript, provided a proper caption for the Table the initial MIC values and those after treatment. We also revised Results Section in the revised version of the manuscript to better explain and discuss the observed changes in the antimicrobial activity.

**QUESTION 2**. More comparisons to earlier work - both to yours and to that of others - needs to be added. At present the advantages of these specific peptides over alternatives documented in the current literature is not well evidenced.
**ANSWER 2**. Following Editor's suggestion, we improved Discussion Section in the revised version of the manuscript to highlight the specific features of these specific peptides and their potentialities as novel food biopreservatives.

**Title: Host defence peptides identified in human apolipoprotein B as natural food bio-preservatives: evaluation of their biosafety and digestibility**

Eliana Dell'Olmo[a], Katia Pane[b], Martina Schibeci[a], Angela Cesaro[a], Maria De Luca[a], Shurooq Ismail[a], Rosa Gaglione[a,c,*], Angela Arciello[a,c,*]

[a] *Department of Chemical Sciences, University of Naples 'Federico II', 80126 Naples, Italy;*

[b] *IRCCS Synlab SDN, Naples, Italy;*

[c] *Istituto Nazionale di Biostrutture e Biosistemi (INBB), Rome, Italy.*

*** Correspondence:** Dr. Rosa Gaglione, rosa.gaglione@unina.it; Prof. Angela Arciello, anarciel@unina.it.

**Abstract**

The employment of chemical agents in food industry is raising several concerns by consumers and is leading to an increasing interest in natural food preservatives. Among alternatives, Host Defence Peptides (HDPs) attracted great interest for their ability to preserve food samples from contaminations without altering their quality, taste and organoleptic properties. Recently, we evaluated the applicability of ApoB-derived peptides as novel food bio-preservatives and demonstrated their ability to prevent chicken meat sample contamination when immobilized on chitosan films. To perform a further step towards the applicability of these peptides in food field, here we evaluated peptides biosafety and digestibility. To do this, we used a multidisciplinary approach including the evaluation of peptides toxicity and antimicrobial activity, the analysis of resistance phenotype development, an *in silico* prediction of peptides susceptibility to proteases and the evaluation of peptides stability in simulated gastric and intestinal fluids. ApoB-derived peptides were found to be not toxic when tested on human gastric carcinoma cells SNU-1 and on human colon-rectal adenocarcinoma cells HT-29 and not to induce resistance phenotype in *Salmonella* strains. Bioinformatic analyses showed that peptides are susceptible to several proteases, as also confirmed by experiments in simulated gastric and intestinal fluids. Altogether, these findings open interesting perspectives to the future applicability of ApoB-derived peptides as novel food bio-preservatives.

**Keywords:** host defence peptides; antimicrobial peptides; food bio-preservatives; peptide biocompatibility; peptide digestibility; antimicrobial resistance.

**Abbreviations**. HDPs, Host Defence Peptides; AMPs, Antimicrobial Peptides; ApoB, apolipoprotein B; MTT, 3-(4,5-dimethylthiazol-2-yl)-2,5-diphenyltetrazolium bromide; MIC, minimum inhibitory concentration; SGF, Simulated Gastric Fluid; SIF, Simulated Intestine Fluid.

## 1. Introduction

### Cryptic bioactive peptides

In the last decades, it was evidenced that the limited number of genes is not enough to explain the complexity of the organism and it was highlighted the key role played by the proteins [1] present in a cell, tissue or organ in a given time and under specific conditions [2]. The situation is even more complicated if we consider that most of the proteins are processed to produce a pool of bioactive encrypted peptides endowed with functions often not directly related to those of the precursor proteins. Indeed, the term "cryptome" has been used to define a subset of the proteome comprising cryptic peptides with distinct bioactivities, that have been named cryptides [3,4]. They have been found to be endowed with a wide range of bioactivities, such as host defence, antithrombotic, protease inhibition, blood pressure regulation, opioid, analgesic, signalling, angiogenesis, and wound healing [5–10].

### Host defence peptides

Among cryptides, a special class is represented by Antimicrobial Peptides (AMPs), then named Host Defence Peptides (HDPs) because of their involvement in the innate immune system of living organisms. HDPs generally share crucial features, such as the length ranging between 12 and 50 amino acids, the high content of hydrophobic aminoacidic residues (+50%) and the positive net charge at physiological pH values [11]. These features are the basis of HDPs ability to selectively interact with and target negatively charged bacterial membranes [10]. In the case of vertebrates, HDPs are not only able to directly affect and kill bacteria but they also play a role in augmenting the adaptive response [6–8,10].

### Applicability of HDPs in food industry

Because of their wide range of activities and their peculiar mechanism of action, HDPs have attracted great interest as good candidates to be employed in biomedical, cosmeceutical and food fields. In the case of food industry, traditional procedures, such as the addition of chemical additives or food thermal processing, have been found to negatively affect food quality and nutritional properties [12], with a consequent increase of the interest of consumers towards untreated foods and natural biopreservatives. In this scenario, HDPs have attracted the interest of researchers as novel biopreservatives able to protect food samples from microbial contaminations while not affecting food quality. The introduction in the market of a novel food ingredient requires detailed analyses on its biocompatibility, allergenicity and safety for human health [13].

## ApoB-derived HDPs

In the present work, we analysed HDPs previously identified in human apolipoprotein B (ApoB) and found to be endowed with antimicrobial, anti-biofilm, antifungal, wound healing, and immunomodulatory properties [14–17]. MIC values determined for ApoB-derived peptides were found to be comprised between 1.25 and 20 μM depending on the bacterial strains tested [15]. Moreover, peptides were also found to be able to synergistically act in combination with conventional antibiotics [18–22] and to exert antimicrobial and antibiofilm properties when tested on *Salmonella* cells [23]. Indeed, ApoB-derived peptides were found to be effective on both *Salmonella enteriditis* 706 RIVM and *Salmonella typhimurium* ATCC® 14028 bacterial strains with MIC values ranging from 2.5 to 5 μM [23]. Furthermore, a cost-effective production procedure of peptides in bacterial cells has been set up and it has been estimated that, when peptides production scale is 1,000 mg/batch, the production cost is about 42 €/mg, a competitive value for a new compound that has to be introduced in the market [16]. The production procedure has been also scaled-up and found to be suitable to produce the amounts of peptides required for their applicability [16]. Even more importantly, ApoB-derived peptides were found to be able to preserve chicken meat samples from microbial contamination when employed to functionalize chitosan edible films [24-26]. Starting from these very promising results, here we investigated ApoB-derived peptides biosafety as novel food biopreservatives. We demonstrated that peptides are biocompatible, do not induce the development of resistance phenotype upon a prolonged incubation with *Salmonella* cells, and are characterized by a high propensity to be fragmented during simulated digestion. Altogether, obtained results open interesting perspectives to the applicability of ApoB-derived peptides as novel biopreservatives to be employed in food industry.

## 2. Materials and methods

According to material data sheets, all the necessary precautions for potential safety or environmental hazards were followed.

### 2.1 Chemical reagents

All the reagents were purchase from Sigma-Merck (Milan, Italy), unless differently specified. ApoB-derived peptides r(P)ApoB$^{Pro}_{S}$ PHVALKPGKLKFIIPSPKRPVKLLSG, r(P)ApoB$^{Pro}_{L}$ PHVALKPGKLKFIIPSPKRPVKLLSGGNTLHLVSTTKT, and r(P)ApoB$_L^{Ala}$ PHVALKAGKLKFIIPSPKRPVKLLSGGNTLHLVSTTKT were recombinantly produced in bacterial cells as previously described [17].

### 2.2 Cell cultures and their authentication

Human gastric carcinoma cells SNU-1 (ATCC® CRL-5971™) and human colon-rectal adenocarcinoma cells HT-29 (ATCC® HTB-38™) were purchased from American Type Culture Collection (ATCC) that validated them *via* short tandem repeat (STR) profiling. Cells were cultured in the laboratory for less than 6 months and were routinely tested for mycoplasma by MycoSEQ™ Mycoplasma Detection Kit (Applied Biosystems™, Thermo Fisher Scientific, Milan, Italy). Adherent human HT-29 cells were cultured in Dulbecco's modified Eagle's medium, whereas human SN-1 cells were grown in suspension in RPMI-1640 medium. In both cases, media were supplemented with 10% fetal bovine serum (HyClone, GE Healthcare Lifescience, Chicago, IL) and antibiotics, and cells were grown in a 5% $CO_2$ humidified atmosphere at 37 °C.

### 2.2 Cytocompatibility assays

Cytocompatibility of r(P)ApoB$_L^{Pro}$, r(P)ApoB$^{Pro}_{S}$ and r(P)ApoB$^{Ala}_{L}$ has been evaluated by performing experiments on human HT-29 and SNU-1 cells by 3-(4,5-dimethylthiazol-2-yl)-2,5-diphenyltetrazolium bromide (MTT) assay as previously described [27]. To this purpose, HT-29 and SNU-1 cells were plated into 96-well plates at a density of $5x10^3$ cells/well in 100 µL of medium, and incubated overnight at 37 °C. Afterwards, cells were treated with increasing concentrations (0 – 20 µM) of ApoB-derived peptides for 24 h and 48 h at 37 °C.

Following incubation, in the case of HT-29 cells, peptide-containing medium was removed, and 100 µL of MTT reagent, dissolved in DMEM without phenol red, were added to the cells (100 µL/well) at a final concentration of 0.5 mg/mL. After 4 h at 37 °C, culture medium was removed, and the resulting formazan salts were dissolved by the addition of isopropanol containing 0.1 N HCl (100

μL/well). Absorbance values of blue formazan were determined at 570 nm by using an automatic plate reader (Microbeta Wallac 1420, Perkin Elmer). In the case of SNU-1 cell line, instead, upon treatment with peptides, plates were centrifuged at 1,000 rpm for 10 min. Following incubation, 50 μL of MTT solubilized in DMEM without phenol red were added to the cells. Upon 4 h at 37 °C, DMSO was added to each sample in a ratio of 1:5 (vol/vol) and samples were incubated for 24 h at room temperature. Absorbance values of blue formazan were determined at 570 nm by using an automatic plate reader (Microbeta Wallac 1420, Perkin Elmer). In all the cases, cell survival was expressed as the percentage of viable cells in the presence of the peptides with respect to control cells grown in the absence of peptides. The experiments have been carried out in triplicate with triplicate determinations.

### 2.3 Bacterial strains and growth conditions

Bacterial strains *Salmonella typhimurium* ATCC® 14028 and *Salmonella enteritidis* RIVM 706 were grown in Muller Hinton Broth (MHB, Becton Dickinson Difco, Franklin Lakes, NJ) and on Tryptic Soy Agar (TSA; Oxoid Ltd., Hampshire, UK). In all the experiments, bacteria were inoculated and grown overnight in MHB at 37 °C. After about 24 h, bacteria were transferred into a fresh MHB tube and grown to mid-logarithmic phase.

### 2.4 Evaluation of resistance development in *Salmonella* strains

To verify whether *Salmonella typhimurium* (ATCC® 14028) and *Salmonella enteritidis* RIVM 706 bacterial cells develop resistance to r(P)ApoB$_L^{Pro}$ or to conventional antibiotic ciprofloxacin, first of all $MIC_{100}$ values of the antimicrobial agents were determined. To this purpose, bacterial cells were grown to mid-logarithmic phase in Nutrient Broth (NB, Difco, Becton Dickinson, Franklin Lakes, NJ) at 37 °C. Cells were then diluted to a final concentration of $2x10^6$ CFU/mL in 0.5X NB and were plated into 96-well plates in the presence of increasing amounts of the antimicrobials. For each agent under test, starting from a stock solution, two-fold serial dilutions were carried out, accordingly to broth microdilution method [28]. Following an over-night incubation, $MIC_{100}$ values were determined as the lowest drug concentration responsible for no visible bacterial growth. Moreover, for each treatment, the $MIC_{100}$ value was verified by plating the cells on LB agar. Once detected the $MIC_{100}$ values for each antimicrobial compound against the bacterial strains tested, bacterial cells that survived to exposure at a subinhibitory (MIC/2) concentration were regrown and re-exposed to the peptide or the antibiotic. Strains that developed resistance to the compound under test were characterized by higher $MIC_{100}$ values at subsequent passages.

### 2.5 *In silico* analyses to verify ApoB-derived peptides susceptibility to proteases

Prediction of cutting sites for pepsin and trypsin enzymes has been performed by using "Peptide cutter tool" available on ExPASy server as previously described [29]. In addition, PROSPER software was used to perform an *in silico* prediction of ApoB-derived peptides susceptibility to 24 proteases [30]. Peptide cutter tool was used to generate the scoring function based on the occurrence of aminoacidic consensus sequences. PROSPER, instead, integrates substrate specificity profiles derived from the MEROPS, CutDB and PMAP database to construct trained models for 24 proteases that have at least 40 experimentally verified substrates and include the four major catalytic types (aspartic, cysteine, metallo and serine proteases) [30]. The 24 proteases contained in PROSPER dataset are cathepsin K, calpain-1, caspases (-1, -3, -7, -6, -8), matrix metallopeptidase (-2, -9, -3, -7), chymotrypsin A, granzyme B (human), elastase-2, cathepsin-G, granzyme B (mouse), thrombin, plasmin, glutamyl peptidase I, furin, signal peptidase I, thylakoidalpeptidase I, signalase and the HIV-1 retropepsin.

### 2.6 Evaluation of ApoB-derived peptides stability in *in vitro* Simulated Gastric Fluid (SGF) and Simulated Intestine Fluid (SIF)

Evaluation of *in vitro* stability of ApoB-derived peptides has been performed as previously described [31] with some modifications. Briefly, total amount of 20 µg of r(P)ApoB$_L^{Pro}$, r(P)ApoB$_S^{Pro}$ or r(P)ApoB$_L^{Ala}$ have been analysed in 100 µL of simulated gastric fluid (SGF) containing 0.32% (w/v) pepsin and 34 mM NaCl at pH 1.2 [32], and in simulated intestinal fluid (SIF) containing 10 mg/mL trypsin in 50 mM $KH_2PO_4$ at pH 7.5 [31]. Preliminarily to the assay, both SGF and SIF mixtures have been pre-incubated at 37 °C for 3 min in the absence of ApoB-derived peptides. Then, 20 µg of each peptide have been added to SGF or SIF at 1:1 and 1:20 ratio (v/v), respectively. The reaction mixtures have been subsequently incubated at 37 °C for 0, 10, 30-, 60, 120, and 180 min. Assays have been performed in duplicate for each experimental condition. Reactions have been stopped by adding 200 mM $Na_2CO_3$ (1:1 v/v ratio) and by heating at 100 °C for 3 min. Degradation of full-length peptides r(P)ApoB$_L^{Pro}$, r(P)ApoB$_S^{Pro}$ and r(P)ApoB$_L^{Ala}$ upon incubation in SGF and SIF have been monitored by SDS-PAGE 18% [33] followed by densitometric analyses. Experiments have been carried out in duplicate.

### 2.7 Statistical analyses

Statistical analyses were performed by using a Student's t-Test. Significant differences were indicated as *($P < 0.05$), **($P < 0.01$) or ***($P < 0.001$).

## 3. Results

### 3.1 Analysis of ApoB-derived peptides cytocompatibility

The employment of ApoB-derived peptides as novel food additives and bio-preservatives is strictly dependent from their cytocompatibility. For this reason, we performed experiments to evaluate peptides' effects on the viability of human colon-rectal adenocarcinoma cells HT-29 and human gastric carcinoma cells SNU-1, selected as prototypes of stomach and intestine targets of peptide deposition during digestion. To this purpose, cells were plated and incubated with increasing concentrations of r(P)ApoB$_L^{Pro}$, r(P)ApoB$_L^{Ala}$ or r(P)ApoB$_S^{Pro}$ for 24 and 48 h. Interestingly, all the three peptides were found not to affect cell viability. Slight toxic effects were detected only upon incubation of SNU-1 cells with r(P)ApoB$_L^{Ala}$ peptide at concentrations starting from 20 µM. Altogether, obtained results suggest that peptides are cytocompatible when tested at concentrations known to affect the viability of bacterial *Salmonella* cells (2.5 – 5 µM) [16].

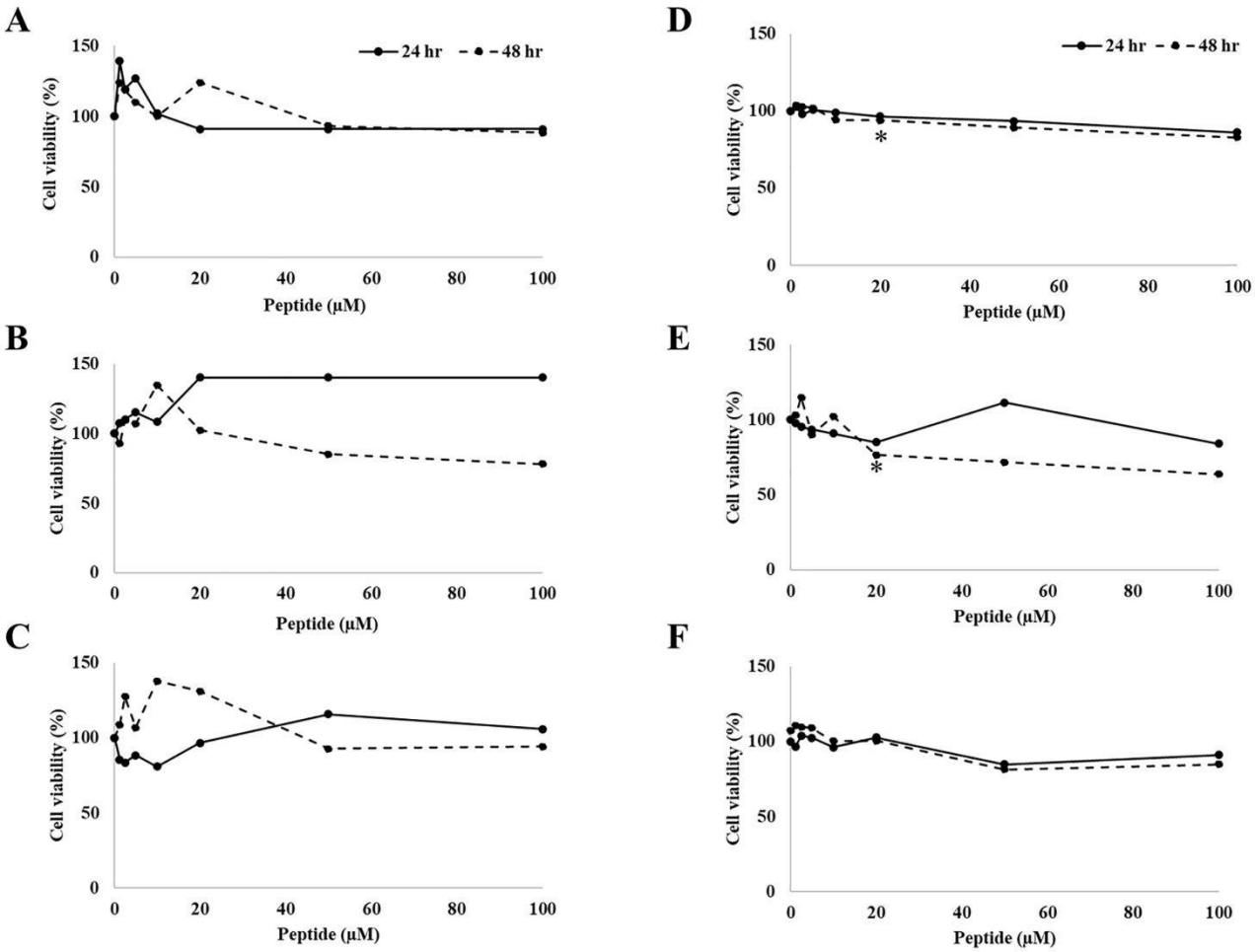


**Figure 1.** Effects of r(P)ApoB$_L^{Pro}$ (**A**, **D**), r(P)ApoB$_L^{Ala}$ (**B**, **E**) or r(P)ApoB$_S^{Pro}$ (**C**, **F**) on the viability of HT-29 (**A**, **B**, **C**) and SNU-1 (**D**, **E**, **F**) cell lines. MTT reduction assays were performed by treating

cells with increasing concentrations (0-100 µM) of each peptide for 24 and 48 h. Experiments were performed in triplicate with triplicate determinations. Significant differences were indicated as *($P < 0.05$) for treated *versus* untreated samples.

### 3.2 Analysis of resistance evolution upon treatment of bacterial cells with ApoB-derived peptides

Since most of conventional antibiotics employed in food field are responsible for the development of resistance phenotype in foodborne pathogens, we decided to evaluate whether a prolonged exposure of *Salmonella* cells to ApoB-derived peptides is responsible for the insurance of resistance. To this purpose, we treated *S. typhimurium* ATCC® 14028 and the clinically isolated *S. enteritidis* RIVM 706 strains with either r(P)ApoB$_L^{Pro}$ peptide or with conventional antibiotic ciprofloxacin for a prolonged time. As shown in **Figures 2A and B**, upon reiterated treatments with concentration gradients of the above-mentioned antimicrobials, both *Salmonella* strains were found to remain sensitive to r(P)ApoB$_L^{Pro}$ peptide antimicrobial activity. Indeed, peptide MIC values were found to remain stable upon treatment of *S. enteritidis* RIVM 706 cells for a prolonged time interval (**Figure 2B** and **Table 1**). As shown in **Table 1**, MIC value detected for r(P)ApoB$_L^{Pro}$ peptide in the case of *S. enteritidis* RIVM 706 strain was found to be 5 µM both at time 0 and after 7 rounds of treatment. In the case of *S. typhimurium* ATCC® 14028 strain, only a slight increase of peptide MIC value, which was found to be about 4-fold higher with respect to treatment 1, was observed from treatment 3 to treatment 7 (**Figure 2A** and **Table 1**). Indeed, as shown in **Table 1**, MIC values were found to be 2.5 µM and 10 µM at time 0 and after 3 rounds of treatment, respectively. However, it has to be highlighted that no further increase of MIC values was detected from treatment 3 to treatment 7 (**Figure 2A** and **Table 1**), thus indicating that bacterial cells remain sensitive to peptide toxic effects even if a slightly higher dose of peptide is required to completely inhibit bacterial growth. Resistance development was, instead, detected upon treatment of both *Salmonella* strains with the conventional antibiotic ciprofloxacin. Indeed, as shown in **Figure 2**, at treatment 3, which corresponds to the third day of treatment with ciprofloxacin, a MIC value 67-fold higher with respect to treatment 1 was detected for both *Salmonella* strains, what is indicative of resistance acquisition. Indeed, as shown in **Table 1**, in the case of both *Salmonella* strains, ciprofloxacin MIC value was found to increase from 0.3 µg/mL at time 0 to 20 µg/mL after 3 rounds of treatment. In the case of both strains, at treatment 4, it is observed a reversion of resistance development with a MIC value found to be only 4-fold higher with respect to treatment 1. Indeed, at treatment 4, ciprofloxacin MIC value was found to decrease from 20 to 1.25 µg/mL in the case of both *Salmonella* strains. However, it has to be highlighted that, in the case of *S. typhimurium* ATCC® 14028, MIC value was found to further increase at treatment 7 becoming again 20 µg/mL, *i.e.*, 67-fold higher with respect to treatment 1

(**Figure 2A** and **Table 1**), a trend that is indicative of a two-step selection of resistant cells and that indicates the occurrence of different mechanisms of resistance [34,35]. This generally happens when the fitness costs of antibiotic resistance development are not fully tolerated by bacterial cells that try to find alternative ways to overcome antibiotic effects. In the case of *S. enteriditis* RIVM 706, instead, upon reversion of resistance, MIC value was found to remain substantially stable at 1.25 µg/mL from treatment 4 to treatment 7, *i.e.*, 4-fold higher with respect time 0, thus indicating a more robust reversion of resistance. However, it has to be highlighted that the development of resistance, even if temporary, provides an obstacle to the successful eradication of bacterial infections also considering that a greatly higher dose of effective antibiotic drug is consequently required.

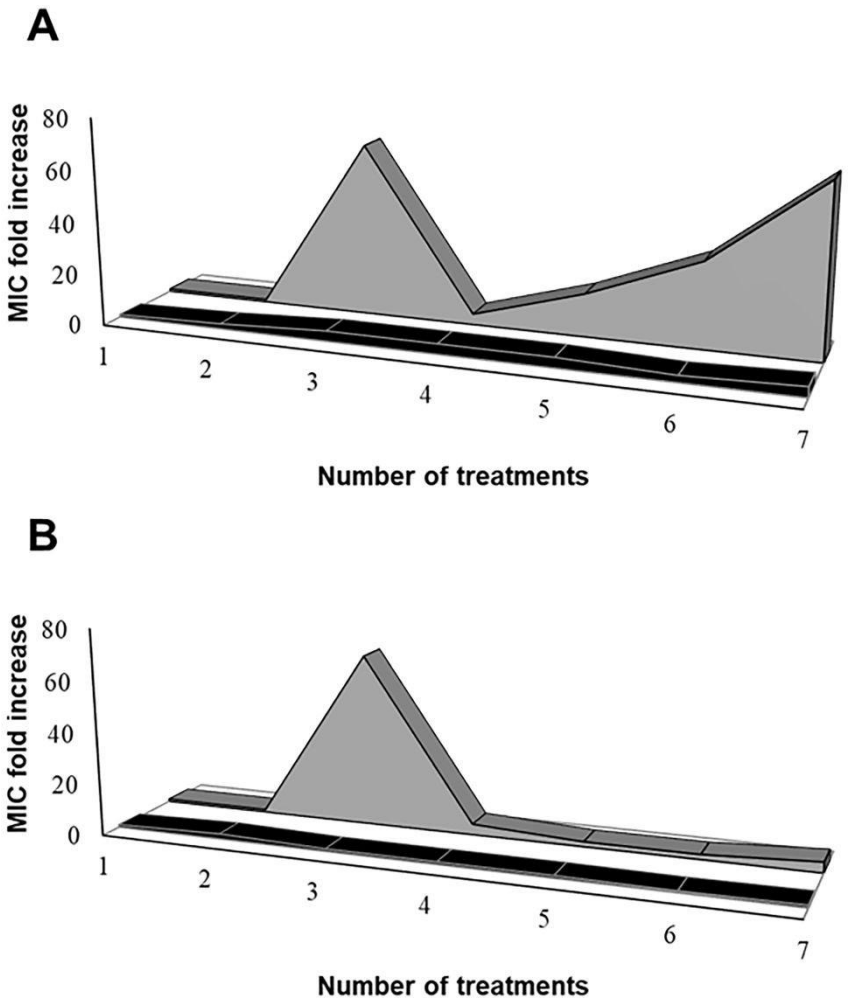


**Figure 2.** Analysis of MIC fold increase upon treatment of *S. typhimurium* ATCC® 14028 (**A**) or *S. enteriditis* RIVM 706 (**B**) with r(P)ApoB$_L^{Pro}$ (black) or ciprofloxacin (gray) for a prolonged time interval.

**Table 1. MIC values obtained at time 0 and after several rounds of treatment of bacterial cells with ciprofloxacin or r(P)ApoB$_L^{Pro}$ peptide**

| | CIPROFLOXACIN | | | | r(P)ApoB$_L^{Pro}$ | | | |
|---|---|---|---|---|---|---|---|---|
| | *S. typhimurium* ATCC 14028 | | *S. enteriditis* 706 RIVM | | *S. typhimurium* ATCC 14028 | | *S. enteriditis* 706 RIVM | |
| **Number of treatments** | **MIC (μg/mL)** | **Fold increase** | **MIC (μg/mL)** | **Fold increase** | **MIC (μM)** | **Fold increase** | **MIC (μM)** | **Fold increase** |
| 1 | 0.3 | 1 | 0.3 | 1 | 2.5 | 1 | 5 | 1 |
| 2 | 0.3 | 1 | 0.3 | 1 | 5 | 2 | 5 | 1 |
| 3 | 20 | 67 | 20 | 67 | 10 | 4 | 5 | 1 |
| 4 | 1.25 | 4 | 1.25 | 4 | 10 | 4 | 5 | 1 |
| 5 | 5 | 17 | 0.6 | 2 | 10 | 4 | 5 | 1 |
| 6 | 10 | 33 | 0.6 | 2 | 10 | 4 | 5 | 1 |
| 7 | 20 | 67 | 1.25 | 4 | 10 | 4 | 5 | 1 |

### 3.3 *In silico* analyses to identify cleavage sites in ApoB-derived peptides sequence

In order to evaluate ApoB-derived peptides digestibility in the gastro-intestinal tract, an *in silico* prediction of peptides proteolysis has been performed as first by using Peptide Cutter software [29]. As shown in **Figures 3A** and **B**, pepsin and trypsin cleavage sites have been identified in all the peptides even if a different number of cutting sites has been detected for the three peptides. In particular, r(P)ApoB$_L^{Pro}$ peptide was found to contain 9 proteolytic cleavage sites recognized by pepsin enzyme (**Figure 3A**), whereas an additional site was found to be present in r(P)ApoB$_L^{Ala}$ peptide in correspondence of leucine residue preceding the substituted alanine (**Figure 3A**). Peptide r(P)ApoB$_S^{Pro}$, lacking the last 12 amino acids, was found to contain only 5 cleavage sites recognized by pepsin enzyme. Similar findings have been obtained when trypsin cleavage sites have been analysed. Indeed, r(P)ApoB$_L^{Ala}$ has been found to contain the highest number (6) of trypsin cutting sites, with an additional cleavage site with respect to r(P)ApoB$_L^{Pro}$ in correspondence of a lysine residue adjacent to the substituted alanine (**Figure 3B**). Due to its shorter sequence, also in this case, r(P)ApoB$_S^{Pro}$ was found to contain the lowest number (4) of trypsin cleavage sites (**Figure 3B**). The differences in proteolytic susceptibility between r(P)ApoB$_L^{Ala}$ and r(P)ApoB$_L^{Pro}$ peptides appear related to the high influence exerted by amino acid residues flanking the cleavage site recognized by pepsin and trypsin enzymes [36,37].

Starting from these findings, we decided to perform an *in silico* analysis of ApoB-derived peptides susceptibility to 24 proteases by using PROSPER integrated feature-based server [30]. As shown in **Table 1**, we found that all the three peptides are susceptible to some of the analysed proteases comprising cysteine, metallo- and serine proteases. Peptides r(P)ApoB$_L^{Pro}$ and r(P)ApoB$_L^{Ala}$ have been found to contain overall 7 proteolytic sites recognized by the analysed proteases. It is interesting

to notice that the presence in position 7 of Pro or Ala residue is responsible for a different susceptibility of the peptide molecules to analysed proteases. Indeed, r(P)ApoB$_L^{Ala}$ was found to be susceptible to chymotrypsin A (cattle-type) cleavage (AGKL | KFII) in position 10, whereas r(P)ApoB$_L^{Pro}$ was found to be susceptible to matrix metallopeptidase-9 cleavage in position 9 (**Table 1**). In agreement with its shorter length, r(P)ApoB$_S^{Pro}$ peptide was found to contain only 5 sites recognized by the analysed proteases (**Table 1**).

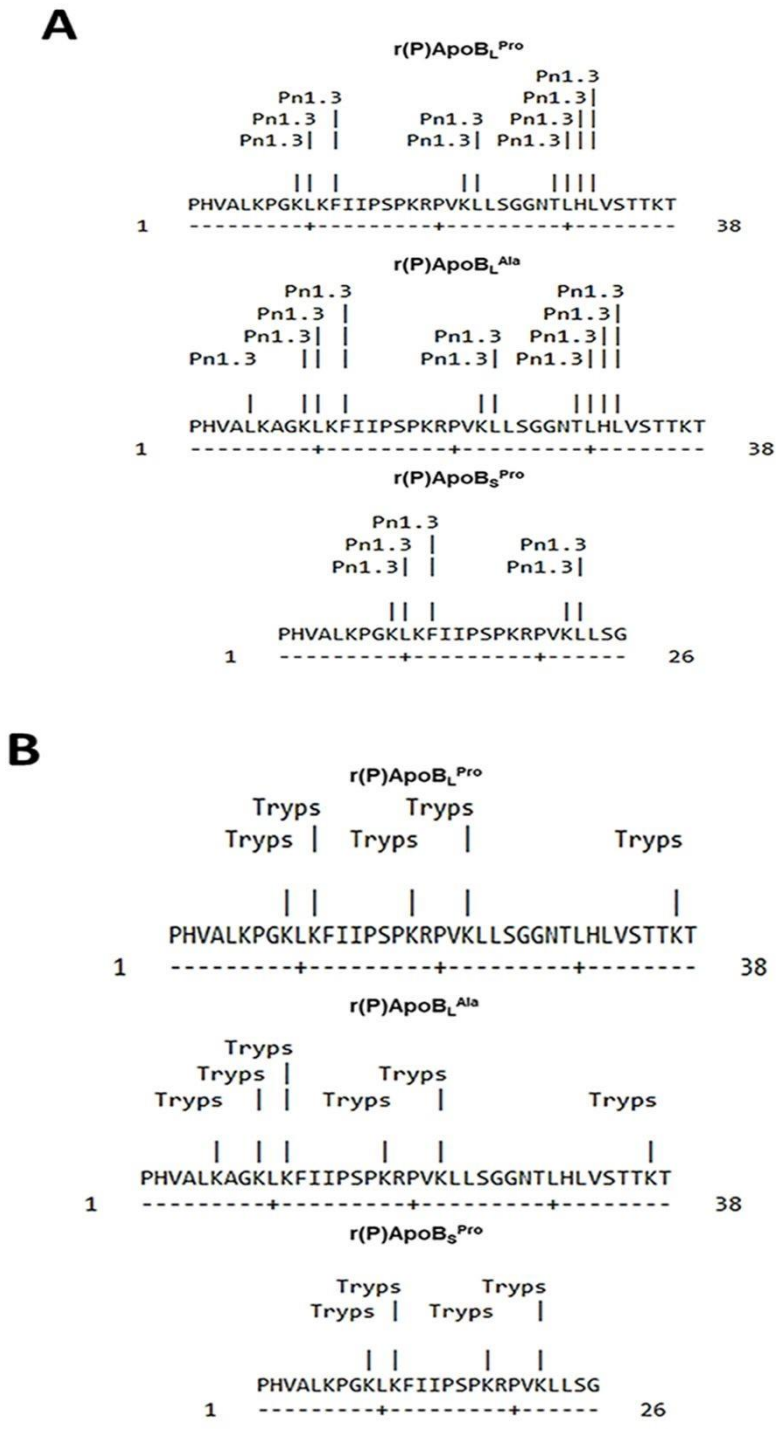

**Figure 3.** *In silico* identification of pepsin cleavage sites (**A**) and trypsin cleavage sites (**B**) in ApoB-derived peptides sequences. Analyses have been performed by using Peptide Cutter tool on ExSPAsy database. The total number and the position of pepsin and trypsin cleavage sites are shown in r(P)ApoB$_L^{Pro}$, r(P)ApoB$_L^{Ala}$, and r(P)ApoB$_S^{Pro}$.

**Table 2.** PROSPER prediction of protease cleavage sites in ApoB-derived peptides.

| Protease Family | Protease Name | Position | P4-P4' site | N-fragment (kDa) | C-fragment (kDa) | Cleavage score[a] |
|---|---|---|---|---|---|---|
| **r(P)ApoB$_L^{Pro}$ PHVALKPGKLKFIIPSPKRPVKLLSGGNTLHLVSTTKT** | | | | | | |
| CYSTEINE | cathepsin K | 24 | VKLL\|SGGN | 2.77 | 1.62 | 1.24 |
| METALLO | matrix metallopeptidase-9 | 9 | KPGK\|LKFI | 1.04 | 3.35 | 1.1 |
| | matrix metallopeptidase-9 | 31 | NTLH\|LVST | 3.67 | 0.73 | 1.06 |
| | matrix metallopeptidase-3 | 17 | IPSP\|KRPV | 1.93 | 2.46 | 1.02 |
| SERINE PROTEASE | elastase-2 | 33 | LHLV\|STTK | 3.88 | 0.51 | 1.04 |
| | elastase-2 | 21 | KRPV\|KLLS | 2.41 | 1.98 | 1.01 |
| | cathepsin G | 24 | VKLL\|SGGN | 2.77 | 1.62 | 1.25 |
| **r(P)ApoB$_L^{Ala}$ PHVALKAGKLKFIIPSPKRPVKLLSGGNTLHLVSTTKT** | | | | | | |
| CYSTEINE | cathepsin K | 24 | VKLL\|SGGN | 2.74 | 1.62 | 1.24 |
| METALLO | matrix metallopeptidase-9 | 31 | NTLH\|LVST | 3.64 | 0.73 | 1.06 |
| | matrix metallopeptidase-3 | 17 | IPSP\|KRPV | 1.91 | 2.46 | 1.02 |
| SERINE PROTEASE | chymotrypsin A (cattle-type) | 10 | AGKL\|KFII | 1.13 | 3.24 | 1.08 |
| | elastase-2 | 33 | LHLV\|STTK | 3.85 | 0.51 | 1.04 |
| | elastase-2 | 21 | KRPV\|KLLS | 2.39 | 1.98 | 1.01 |
| | cathepsin G | 24 | VKLL\|SGGN | 2.74 | 1.62 | 1.25 |
| **r(P)ApoB$_S^{Pro}$ PHVALKPGKLKFIIPSPKRPVKLLSG** | | | | | | |
| CYSTEINE | cathepsin K | 24 | VKLL\|SG | 2.77 | 0.26 | 1.24 |
| METALLO | matrix metallopeptidase-9 | 9 | KPGK\|LKFI | 1.04 | 1.99 | 1.1 |
| | matrix metallopeptidase-3 | 17 | IPSP\|KRPV | 1.93 | 1.09 | 1.02 |
| SERINE PROTEASE | elastase-2 | 21 | KRPV\|KLLS | 2.41 | 0.61 | 1.01 |
| | cathepsin G | 24 | VKLL\|SG | 2.77 | 0.26 | 1.25 |

[a] Cleavage score generated by machine learning methods dependent by multiple features including local amino acid sequence profile, predicted secondary structure, solvent accessibility and predicted native disorder.

### 3.4 Analysis of ApoB-derived peptides *in vitro* digestion in simulated gastric and intestinal fluids

Allergenic proteins or peptides are generally more resistant to digestion with proteases with respect to non-allergenic ones [38]. Based on this, evaluation of protein stability in the gastro-intestinal tract is considered not only an indication of protein digestibility but also a putative indication of the absence of potential allergenic features [39]. For this reason, experiments were here performed to evaluate the stability of ApoB-derived peptides in Simulated Gastric Fluid (SGF) and Simulated Intestine Fluid (SIF) [40] by incubating peptides with pepsin (SGF) or trypsin (SIF) enzyme in 1:1 or 1:20 molar ratio, respectively. Once prepared, mixtures have been incubated for 0, 10, 30, 60, 120 and 180 min at 37 °C and then analysed by SDS-page (18%) followed by densitometric analysis of full-length peptides bands. As shown in **Figures 4A** and **B**, r(P)ApoB$_L^{Pro}$ was found to be significantly degraded by pepsin within 10 min of incubation (about 40% protein degradation) (**Figure 4A**), and degradation was found to be even more pronounced (about 80% protein degradation) upon treatment with trypsin (**Figure 4B**). Due to its shorter length, peptide r(P)ApoB$_S^{Pro}$ has been found to be more resistant to both pepsin and trypsin enzymes (**Figure 4A** and **B**). Indeed, only 40-50% peptide degradation was detected upon incubation with pepsin or trypsin even after 180 min of incubation (**Figure 4A** and **B**). In the case of r(P)ApoB$_L^{Ala}$ peptide, about 50% degradation has been detected upon incubation with pepsin (**Figure 4A**), whereas the peptide was found to be much more sensitive to trypsin, with about 80% degradation detected already upon 10 min of incubation (**Figure 4B**). This appears in disagreement with previously reported data indicating the presence in r(P)ApoB$_L^{Ala}$ peptide of 6 cleavage sites recognized by trypsin and 10 cleavage sites recognized by pepsin (**Figures 3A** and **B**). However, it has to be considered that in SGF and SIF media peptide r(P)ApoB$_L^{Ala}$ might assume local conformations that might interfere with protease cleavage by masking specific sites.

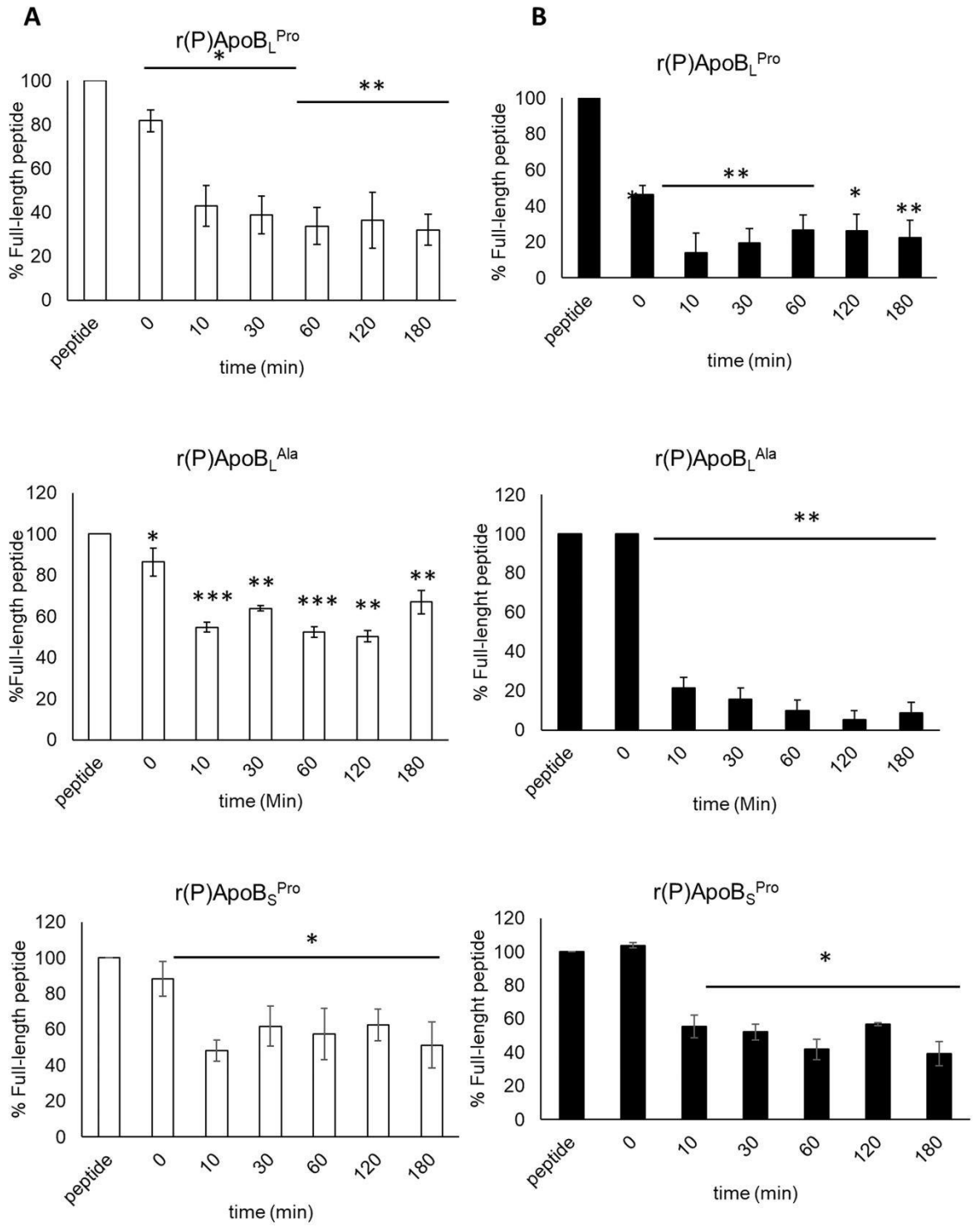


**Figure 4.** Analysis of ApoB-derived peptides hydrolysis in simulated gastric fluid (**A**, white bars) or in simulated intestine fluid (**B**, black bars). Graphs have been obtained upon SDS-PAGE and densitometric analyses of the intensity of the bands corresponding to full-length peptides in the absence or in the presence of pepsin (**A**) or trypsin (**B**). Experiments were performed in triplicate. Significant differences were indicated as *($P < 0.05$), **($P < 0.01$) or ***($P < 0.001$) for treated *versus* untreated samples.

## 4. Discussion

### 4.1 Host Defence Peptides as novel food bio-preservatives

Host Defence Peptides (HDPs), released upon proteolytic cleavage of precursor proteins, have gained great attention because of their broad-spectrum antimicrobial activity and anti-biofilm properties [23]. Furthermore, despite conventional antibiotics, HDPs general mechanism of action minimizes the rise of resistance phenotype development. This was found to be the case of antimicrobial ApoB-derived peptides that were found to be effective on food-borne pathogens while not inducing the development of resistance in bacterial strains generally causing skin infections [21,23]. Indeed, ApoB-derived peptides were found to be effective on both *Salmonella enteriditis* 706 RIVM and *Salmonella typhimurium* ATCC® 14028 bacterial strains with MIC values ranging from 2.5 to 5 μM [23], a value similar to those reported in the literature for different AMPs found to be effective on *Salmonella* strains and proposed as effective tools to counteract infections caused by multidrug resistant strains [41]. Here, we also demonstrated that a prolonged exposure of *Salmonella* strains to r(P)ApoB$_L^{Pro}$ peptide is not responsible for the development of resistance phenotype in contrast with what observed upon treatment with conventional antibiotic ciprofloxacin. ApoB-derived peptides were also found to be cytocompatible, since they were found not to affect the viability of human gastric carcinoma cells SNU-1 and of human colon-rectal adenocarcinoma cells HT-29, thus suggesting that they might not induce toxic effects upon consumption by humans. An example of antimicrobial peptide largely employed as a food preservative is represented by nisin, a peptide endowed with broad activity against Gram-positive bacteria and that was approved for human consumption by both US Food and Drug Administration (FDA) and by the European Food Safety Authority (EFSA) with its assigned E number being E 234 [42]. Nisin has been reported to act by inhibiting bacterial growth, by generating pores in cell membrane and by interrupting cell-wall biosynthesis through specific lipid II interaction [43], a mechanism similar to that reported for ApoB-derived peptides whose main target is represented by bacterial membranes. Indeed, we demonstrated that ApoB-derived peptides antimicrobial activity is dependent from their interaction with specific components of bacterial surfaces, such as LPS or LTA, which induce peptides to form β-sheet-rich amyloid-like structures [20,44]. Starting from these elements, in the future it will be possible to design variants of the antimicrobial peptides under study even more effective in counteracting bacterial infections and in preventing food contamination and spoilage. It has also to be highlighted that ApoB-derived peptides under study present some advantages over peptides conventionally employed in food preservation as nisin. Indeed, it has been widely reported that nisin is less effective in dairy foods with a neutral pH [45,46], probably due to a lack of peptide stability at neutral pH together with the possible development of resistance phenotype. Nisin stability and activity have been reported to be greatly

affected by pH with a maximum of solubility and stability detected at pH 3 [47,48], an aspect that strongly influences nisin applicability. ApoB-derived peptides, instead, were found to exert maximal antimicrobial activity at neutral pH, to remain active at pH 9 an to be affected by acidic pH [23]. This might suggest their applicability and effectiveness to prevent bacterial contaminations in conditions where nisin is less effective. It has been also described the development of resistance to nisin *in vitro* in *L. monocytogenes*, *Listeria innocua*, *Clostridium botulinum*, *Streptococcus thermophilus*, *S. aureus*, and *S. bovis* strains [49,50]. In the case of ApoB-derived peptides, instead, no resistance development was detected both upon prolonged exposure of *Salmonella* strains to r(P)ApoB$_L^{Pro}$ peptide, as here reported, and upon prolonged exposure of *A. baumannii* ATCC 17878 and *S. epidermidis* ATCC 35984 bacterial cells to r(P)ApoB$_L^{Pro}$, r(P)ApoB$_L^{Ala}$, and r(P)ApoB$_S^{Pro}$ peptides, as previously described [21]. This is a further important aspect evidencing a hypothetical advantage of ApoB-derived peptides over peptides conventionally used for food preservation and that opens interesting perspectives to their future applicability.

### 4.2 Evaluation of ApoB-derived peptides digestibility

To perform a further step towards ApoB-derived peptides applicability as food bio-preservatives, we also performed experiments to evaluate peptides digestibility. To this purpose, we performed as first an *in silico* analysis by using Expasy [51] and Prosper [52] tools, a score-based and a feature-based tool, respectively. By using these tools, multiple cleavage sites were predicted in ApoB-derived peptides. In particular, Prosper bioinformatic tool allowed us to analyse peptides susceptibility to 24 proteases comprising Aspartic (A), Cysteine (C), Metallo (M) and Serine (S) proteases from MEROPS database [53]. In order to increase the performance, analyses were performed on the basis of local amino acid sequences predicted secondary structure, solvent accessibility and predicted native disorder [54]. By this way, in each peptide, cleavage sites for five proteases were identified, *i.e.*, cathepsin K (cysteine proteases), metallopeptidase-3 and -9 (metalloproteases), elastase-2 and cathepsin G (serine proteases). These proteases are involved in key physiological processes, such as tissues remodelling (matrix metalloproteases) [55], regulation of bone resorption (cathepsin K largely expressed by osteoclasts) [56], epidermis skin barrier and digestion of extracellular matrix components and ingested bacteria (elastase-2 mainly produced by polymorphonuclear leukocytes and cathepsin G found in azurophil granules of neutrophils) [57,58,59]. In the case of r(P)ApoB$_L^{Ala}$ peptide, it was also identified a cleavage site for chymotrypsin A, a serine protease contributing to the digestion of food proteins in mammalian intestine [60]. Cleavage scores were also generated to evaluate the accuracy of PROSPER prediction and determined values were found to be high for chymotrypsin A (88.5 %), elastase-2 (82.9 %), matrix metallopeptidase-9 (81.2 %), cathepsin G (81.0 %), matrix metallopeptidase-3 (79.9 %) and cathepsin K (79.6 %). To integrate bioinformatic data

with experimental evidence, analyses were also performed to simulate the exposure of ApoB-derived peptides to gastrointestinal tract by using Simulated Gastric Fluid (SGF) and Simulated Intestine Fluid (SIF) models. By this way, we demonstrated that r(P)ApoB$_L^{Pro}$ peptide was hydrolysed within 10 min of incubation in both SGF (50% hydrolysis) and SIF (80% hydrolysis), whereas r(P)ApoB$_S^{Pro}$ was degraded after 180 min incubation in SGF (50% hydrolysis) and SIF (50% hydrolysis). r(P)ApoB$_L^{Ala}$ peptide was also found to be highly susceptible to degradation even if with some differences between SIF (50% degradation upon 10 min incubation) and SGC (80% degradation upon 10 min incubation). Similar analyses are reported in the literature for nisin, a polycyclic antibacterial peptide produced by the bacterium *Lactococcus lactis* and highly used as a food preservative [61,62]. It has been reported that nisin peptide is completely digested only when incubated in the small intestine simulated fluid, whereas, in oral and gastric digestion fluid, only 16% of the peptide is hydrolyzed [61,62]. When computer-aided designed peptides PepGAT and PepKAA have been analysed in SGF and SIF, PepGAT peptide was found to be readily degraded by pepsin and trypsin, whereas PepKAA was found to be completely degraded by trypsin only after 2 hours [63]. Hence, based on literature data, we can affirm that ApoB-derived peptides, once consumed by humans, should be rapidly digested, thus probably avoiding side effects. Even if some allergenic proteins have been found to be quickly degraded in the gastro-intestinal tract, probably because of specific environmental conditions that might alter proteases activity [29], it has to be highlighted that ApoB-derived peptides are of human origin and have been found to be neither toxic nor haemolytic when tested on eukaryotic mammalian cells.

### 4.3 Future perspectives

Based on the preliminary promising findings reported in the present manuscript, further experiments will be performed in the future to deepen on peptides' digestibility and allergenicity. Reported data appear to indicate peptides cytocompatibility, since no toxic effects were detected when peptides were analysed on stomach and intestinal cell lines under the experimental conditions tested. Furthermore, despite conventional antibiotics, ApoB-derived peptides were found not to induce resistance phenotype even after prolonged incubation with *Salmonella* cells. Preliminary data on peptides digestibility were also collected by performing bioinformatic analyses that revealed the high susceptibility of peptides to several proteases, as also confirmed by experiments in simulated gastric and intestinal fluids, thus suggesting peptide fast degradation upon ingestion. Hence, ApoB-derived peptides appear promising candidates to be employed as novel food bio-preservatives able to counteract bacterial infections without inducing resistance development. Based on this, future experiments will be also performed by incorporating peptides in edible films used to wrap food samples [24,64] and to prevent their contamination.

## 5. CONCLUSION

Finding natural antibacterial molecules rather than antibiotics or chemical additives to preserve food samples from contaminations is desired to meet consumers' needs. Currently, nisin, produced by microbial fermentation of *Lactococcus lactis*, is the only antimicrobial peptide widely utilized for the preservation of food [65]. However, several antimicrobial peptides have been found to possess features that make them suitable as natural food bio-preservatives [65]. Here, we demonstrated that ApoB-derived recombinant peptides are not toxic when tested on stomach and intestinal cell lines and don't induce resistance phenotype upon prolonged incubation with *Salmonella* cells. By bioinformatic analyses, peptides were also found to be susceptible to several proteases, as confirmed by experiments in simulated gastric and intestinal fluids, indicating that peptides, once consumed by humans, should be rapidly digested, thus probably avoiding side effects. Altogether, these findings open interesting perspectives to the future applicability of ApoB-derived peptides in food industry and to their employment in combination with other antimicrobial compounds, essential oils and polymeric nanoparticles to enhance the shelf-life of food samples.

### Conflicts of interest

The authors declare no competing financial interest.

### Data Availability Statement

All the used data are contained within the article.

### CRediT authorship contribution statement

**Eliana Dell'Olmo:** Conceptualization, Data curation, Formal analysis, Investigation, Methodology, Validation, Visualization, Writing - original draft, Writing - review & editing; **Katia Pane:** Data curation, Investigation, Methodology, Software, Validation, Writing - original draft; **Martina Schibeci**: Conceptualization, Data curation, Formal analysis, Investigation, Methodology; **Angela Cesaro:** Conceptualization, Data curation, Formal analysis, Investigation, Methodology; **Maria De Luca:** Conceptualization, Data curation, Formal analysis, Investigation, Methodology; **Shurooq Ismail**: Data curation, Formal analysis, Investigation, Methodology; **Rosa Gaglione**: Conceptualization, Data curation, Formal analysis, Investigation, Methodology, Validation, Visualization, Writing - original draft; **Angela Arciello:** Conceptualization, Data curation, Formal analysis, Validation, Funding acquisition, Project administration, Resources, Supervision, Writing - original draft, Writing - review & editing.

## References


[1] D.C. Pimenta, I. Lebrun, Peptides **2007**, *28*, 2403, https://doi.org/10.1016/j.peptides.2007.10.005.

[2] V.C. Wasinger, S.J. Cordwell, A. Poljak, J.X. Yan, A.A. Gooley, M.R. Wilkins, M.W. Duncan, R. Harris, K.L. Williams, I. Humphery-Smith, Electrophoresis **1995**, *16*, 1090, https://doi.org/10.1002/elps.11501601185.

[3] D.J. Autelitano, A. Rajic, A.I. Smith, M.C. Berndt, L.L. Ilag, M. Vadas, Drug Discov. Today **2006**, *11*, 306, https://doi.org/10.1016/j.drudis.2006.02.003.

[4] F. Iavarone, C. Desiderio, A. Vitali, I. Messana, C. Martelli, M. Castagnola, T. Cabras, Crit. Rev. Biochem. Mol. Biol. **2018**, *53*, 246, https://doi.org/10.1080/10409238.2018.1447543.

[5] N. Ueki, K. Someya, Y. Matsuo, K. Wakamatsu, H. Mukai, Biopolymers **2007**, 190, https://doi.org/10.1002/bip.20687.

[6] H.G. Boman, J. Intern. Med. **2003**, *254*, 197, https://doi.org/10.1046/j.1365-2796.2003.01228.x.

[7] T. Ganz, R.I. Lehrer, Curr. Opin. Immunol. **1994**, *6*, 584, https://doi.org/10.1016/0952-7915(94)90145-7.

[8] Y. Lai, R.L. Gallo, Trends Immunol. **2009**, *30*, 131, https://doi.org/10.1016/j.it.2008.12.003.

[9] S. Wang, X. Zeng, Q. Yang, S. Qiao, Int. J. Mol. Sci. **2016**, 17, https://doi.org/10.3390/ijms17050603.

[10] M. Zasloff, Nature **2002**, *415*, 389, https://doi.org/10.1038/415389a.

[11] O.N. Silva, K.C.L. Mulder, A.E.A.D. Barbosa, A.J. Otero-Gonzalez, C. Lopez-Abarrategui, T.M.B. Rezende, S.C. Dias, O.L. Franco, Front. Microbiol. **2011**, 2, https://doi.org/10.3389/fmicb.2011.00232.

[12] D.N. Karunaratne, G.K. Pamunuwa, in: Food Addit., InTech, **2017**, https://doi.org/10.5772/intechopen.70329.

[13] M.C. va. Putten, G.A. Kleter, L.J. Gilissen, B. Gremmen, H.J. Wichers, L.J. Frewer, Food Control. **2011**, *22*, 143, https://doi.org/10.1016/j.foodcont.2010.08.002.

[14] R. Gaglione, E. Pizzo, E. Notomista, C. de la Fuente-Nunez, A. Arciello, Curr. Top. Med. Chem. **2020**, *20*, 1324, https://doi.org/10.2174/1568026620666200427091454.

[15] R. Gaglione, E. Dell'Olmo, A. Bosso, M. Chino, K. Pane, F. Ascione, F. Itri, S. Caserta, A. Amoresano, A. Lombardi, H.P. Haagsman, R. Piccoli, E. Pizzo, E.J.A. Veldhuizen, E. Notomista, A. Arciello, Biochem. Pharmacol. **2017**, *130*, 34, https://doi.org/10.1016/j.bcp.2017.01.009.

[16] E. Dell'Olmo, R. Gaglione, A. Cesaro, V. Cafaro, W. Teertstra, H. de Cock, E. Notomista, H. HP, E. Veldhuizen, A. Arciello, Appl. Microbiol. Biotechnol., **2021**, *105*, 1953, https://doi.org/10.1007/S00253-021-11114-3.

[17] R. Gaglione, K. Pane, E. Dell'Olmo, V. Cafaro, E. Pizzo, G. Olivieri, E. Notomista, A. Arciello, N. Biotechnol. **2019**, 51, https://doi.org/10.1016/j.nbt.2019.02.004.

[18] R. Gaglione, A. Cesaro, E. Dell'Olmo, B. Della Ventura, A. Casillo, R. Di Girolamo, R. Velotta, E. Notomista, E.J.A. Veldhuizen, M.M. Corsaro, C. De Rosa, A. Arciello, Sci. Rep. **2019**, 9, https://doi.org/10.1038/s41598-019-43063-3.

[19] R. Gaglione, A. Cesaro, E. Dell'olmo, R. Di Girolamo, L. Tartaglione, E. Pizzo, A. Arciello, Int. J. Mol. Sci. **2020**, 21, https://doi.org/10.3390/ijms21062049.

[20] R. Gaglione, G. Smaldone, A. Cesaro, M. Rumolo, M. De Luca, R. Di Girolamo, L. Petraccone, P. Del Vecchio, R. Oliva, E. Notomista, E. Pedone, A. Arciello, Pharm. **2021**, *14*, 631, https://doi.org/10.3390/PH14070631.

[21] A. Cesaro, M.D.T. Torres, R. Gaglione, E. Dell'Olmo, R. Di Girolamo, A. Bosso, E. Pizzo, H.P. Haagsman, E.J.A. Veldhuizen, C. de la Fuente-Nunez, A. Arciello, ACS Nano **2022**, *16*, 1880, https://doi.org/10.1021/ACSNANO.1C04496/SUPPL_FILE/NN1C04496_SI_001.PDF.

[22] A. Arciello, Curr. Top. Med. Chem. **2020**, *20*, 1235, https://doi.org/10.2174/1568026620142005190828l4.

[23] E. Dell'Olmo, R. Gaglione, M. Sabbah, M. Schibeci, A. Cesaro, R. Di Girolamo, R. Porta, A. Arciello, Food Microbiol. **2021**, *99*, 103804, https://doi.org/10.1016/J.FM.2021.103804.

[24] E. Dell'Olmo, R. Gaglione, A. Arciello, R. Piccoli, V. Cafaro, A. Di Maro, S. Ragucci, R. Porta, C.V.L. Giosafatto, Biochim. Biophys. Acta. Gen. Subj. **2021**, 1865, https://doi.org/10.1016/J.BBAGEN.2020.129803.

[25] M. De Luca, R. Gaglione, B. Della Ventura, A. Cesaro, R. Di Girolamo, R. Velotta, A. Arciello, Int. J. Mol. Sci. **2022**, *23*, 5219. https://doi.org/10.3390/ijms23095219.

[26] I. Wiegand, K. Hilpert, R.E.W. Hancock, Nat. Protoc. **2008**, *3*, 163, https://doi.org/10.1038/nprot.2007.521.

[27] Platella, C. Gaglione, R. Napolitano, E. Arciello, A. Pirota, V. Doria, F. Musumeci, D. Montesarchio, D. Int. J. Mol. Sci. **2021**, *22*, 10624. https://doi.org/10.3390/ijms221910624

[28] K.R. Roesler, A.G. Rao, J. Agric. Food Chem. **2001**, *49*, 3443, https://doi.org/10.1021/jf010209b.

[29] J.D. Astwood, J.N. Leach, R.L. Fuchs, Nat. Biotechnol. **1996**, *14*, 1269, https://doi.org/10.1038/nbt1096-1269.

[30] U.K. Laemmli, Nature **1970**, *227*, 680, https://doi.org/10.1038/227680a0.

[31] E. Giraud, A. Cloeckaert, D. Kerboeuf, E. Chaslus-Dancla, Antimicrob. Agents Chemother.

**2000**, *44*, 1223, https://doi.org/10.1128/AAC.44.5.1223-1228.2000.

[32] X. Wang, Y. Wang, Y. Zhou, J. Li, W. Yin, S. Wang, S. Zhang, J. Shen, Z. Shen, Y. Wang, Emerg. Microbes Infect. **2018**, *7*, https://doi.org/10.1038/S41426-018-0124-Z.

[33] J. Ahn, M.J. Cao, Y.Q. Yu, J.R. Engen, Biochim. Biophys. Acta. **2013**, *1834*, 1222, https://doi.org/10.1016/J.BBAPAP.2012.10.003.

[34] R.J. Simpson, CSH Protoc. **2006** pdb.prot4550, https://doi.org/10.1101/PDB.PROT4550.

[35] D.J. Anderson, J.J. Engemann, L.J. Harrell, Y. Carmeli, L.B. Reller, K.S. Kaye, Antimicrob. Agents Chemother. **2006**, *50*, 1715, https://doi.org/10.1128/AAC.50.5.1715-1720.2006.

[36] R.D. Ekmay, C.N. Coon, G.S. Ladics, R.A. Herman, Regul. Toxicol. Pharmacol. **2017**, *89*, 240, https://doi.org/10.1016/j.yrtph.2017.07.024.

[37] H.D. Williams, P. Sassene, K. Kleberg, J.C. Bakala-N'Goma, M. Calderone, V. Jannin, A. Igonin, A. Partheil, D. Marchaud, E. Jule, J. Vertommen, M. Maio, R. Blundell, H. Benameur, F. Carrière, A. Müllertz, C.J.H. Porter, C.W. Pouton, J. Pharm. Sci. **2012**, *101*, 3360, https://doi.org/10.1002/jps.23205.

[38] A. Priyadarshini, G. Rajauria, C.P. O'Donnell, B.K. Tiwari, Crit. Rev. Food Sci. Nutr. **2019**, *59*, 3082, https://doi.org/10.1080/10408398.2018.1483890.

[39] J.H. Song, R.J. Murphy, R. Narayan, G.B. Davies., Philos. Trans. R. Soc. Lond. B. Biol. Sci. **2009**, *364*, 2127, https://doi.org/10.1098/RSTB.2008.0289.

[40] A.G. Atanasov, S.B. Zotchev, V.M. Dirsch, C.T. Supuran, Nat. Rev. Drug Discov. **2021**, *20*, 200, https://doi.org/10.1038/s41573-020-00114-z.

[41] R.P. Dassanayake, B.M. Atkinson, A.S. Mullis, S. M. Falkenberg, E. M. Nicholson, E. Casas, B. Narasimhan, S.M.D. Bearson. Scientific Reports **2021**, *11*, 19276, https://doi.org/10.1038/s41598-021-98860-6.

[42] M. Younes, P. Aggett, F. Aguilar, R. Crebelli, B. Dusemund, M. Filipič, M.J. Frutos, P. Galtier, U. Gundert-Remy, G.G. Kuhnle, C. Lambré, J.C. Leblanc, I.T. Lillegaard, P. Moldeus, A. Mortensen, A. Oskarsson, I. Stankovic, I. Waalkens-Berendsen, R.A. Woutersen, M. Wright, L. Herman, P. Tobback, F. Pizzo, C. Smeraldi, A. Tard, A. Papaioannou, D. Gott, EFSA J. **2017**, *15*, e05063, https://doi.org/10.2903/j.efsa.2017.5063.

[43] A. Prince, P. Sandhu, P. Ror, E. Dash, S. Sharma, M. Arakha, S. Jha, Y. Akhter, M. Saleem. Scientific Reports **2016**, *6*, 37908, https://doi.org/10.1038/srep37908.

[44] D.M. Monti, F. Guglielmi, M. Monti, F. Cozzolino, S. Torrassa, A. Relini, P. Pucci, A. Arciello, R. Piccoli. Eur Biophys J. **2010**, *39*, 1289, https://doi.org/10.1007/s00249-010-0582-2.

[45] A. Sobrino-Lopez, O. Martín-Belloso. Int. Dairy J. **2008**, *18*, 329, https://doi.org/10.1016/j.idairyj.2007.11.009.

[46] A. Gharsallaoui, N. Joly C. Oulahal, P. Degraeve. Crit. Rev. Food Sci. Nutr. **2016**, *56*, 1262, https://doi.org/10.1080/10408398.2013.763765.

[47] W. Liu, J.N. Hansen, Appl. Environ. Microbiol. **1990**, 56, 2551.

[48] E.A. Davies, H.E. Bevis, R. Potter, J. Harris, G.C. Williams, J. Delves-Broughton. Lett. Appl. Microbiol. **1998**, *27*, 186, https://doi.org/10.1046/j.1472-765X.1998.t01-1-00401.x.

[49] G. Kaur, R.K. Malik, S.K. Mishra, T.P. Singh, A. Bhardwaj, G. Singroha, S. Vij, N. Kumar. Microb. Drug Resist. **2011**, *17*, 197, https://doi.org/10.1089/mdr.2010.0054.

[50] H. Zhou, J. Fang, Y. Tian, X.Y. Lu. Ann. Microbiol. **2014**, *64*, 413, https://doi.org/10.1007/s13213-013-0679-9

[51] E. Gasteiger, A. Gattiker, C. Hoogland, I. Ivanyi,R. D. Appel, A. Bairoch, Nucleic Acids Res. **2002**, *31*, 3784, https://doi.org/10.1093/NAR/GKG563.

[52] J. Song, H. Tan, A.J. Perry, T. Akutsu, G.I. Webb, J.C. Whisstock, R.N. Pike, PLoS One

**2012**, *7*, 50300, https://doi.org/10.1371/JOURNAL.PONE.0050300.

[53] N.D. Rawlings, F.R. Morton, C.Y. Kok, J. Kong, A.J. Barrett, Nucleic Acids Res. **2008**, *36*, D320, https://doi.org/10.1093/NAR/GKM954.

[54] J. Song, H. Tan, A.J. Perry, T. Akutsu, G.I. Webb, J.C. Whisstock, R.N. Pike, PLoS One **2012**, *7*, e50300, https://doi.org/10.1371/JOURNAL.PONE.0050300.

[55] G.A. Cabral-Pacheco, I. Garza-Veloz, C.C.D. La Rosa, J.M. Ramirez-Acuña, B.A. Perez-Romero, J.F. Guerrero-Rodriguez, N. Martinez-Avila, M.L. Martinez-Fierro, Int. J. Mol. Sci. **2020**, *21*, 9739, https://doi.org/10.3390/IJMS21249739.

[56] B.R. Troen, Ann. N. Y. Acad. Sci. **2006**, *1068*, 165, https://doi.org/10.1196/ANNALS.1346.018.

[57] A.A. Belaaouaj, Kwang Sik Kim, S.D. Shapiro, Science **2000**, *289*, 1185, https://doi.org/10.1126/SCIENCE.289.5482.1185.

[58] C. Bonnart, C. Deraison, M. Lacroix, Y. Uchida, C. Besson, A. Robin, A. Briot, M. Gonthier, L. Lamant, P. Dubus, B. Monsarrat, A. Hovnanian, J. Clin. Invest. **2010**, *120*, 871, https://doi.org/10.1172/JCI41440.

[59] L. Ottonello, A.L. Epstein, M. Mancini, P. Dapino, F. Dallegri, J. Leukoc. Biol. **2004**, *75*, https://doi.org/10.1189/jlb.0403133.

[60] D. Mosztbacher, A. Demcsák, M. Sahin-Tóth, Pancreatology **2020**, *20*, 288, https://doi.org/10.1016/J.PAN.2019.12.020.

[61] R. Gough, P.M. O'Connor, M.C. Rea, B. Gómez-Sala, S. Miao, C. Hill, A. Brodkorb, LWT - Food Sci. Technol. **2017**, *86*, 530, https://doi.org/10.1016/j.lwt.2017.08.031.

[62] B. Jarvis, R.R. Mahoney, J. Dairy Sci. **1969**, *52*, 1448, https://doi.org/10.3168/jds.S0022-0302(69)86771-8.

[63] P.F.N. Souza, L.S.M. Marques, J.T.A. Oliveira, P.G. Lima, L.P. Dias, N.A.S. Neto, F.E.S. Lopes, J.S. Sousa, A.F.B. Silva, R.F. Caneiro, J.L.S. Lopes, M. V. Ramos, C.D.T. Freitas, Biochimie **2020**, *175*, 132, https://doi.org/10.1016/J.BIOCHI.2020.05.016.

[64] A. Cesaro, R. Gaglione, M. Chino, M. De Luca, R. Di Girolamo, A. Lombardi, R. Filosa, A. Arciello, A. Biomedicines **2022**, *10*, 1301, https://doi.org/10.3390/biomedicines10061301

[65] M. Rai, R. Pandit, S. Gaikwad, G. Kövics. J Food Sci Technol. **2016**, *53*, 3381, doi: 10.1007/s13197-016-2318-5.

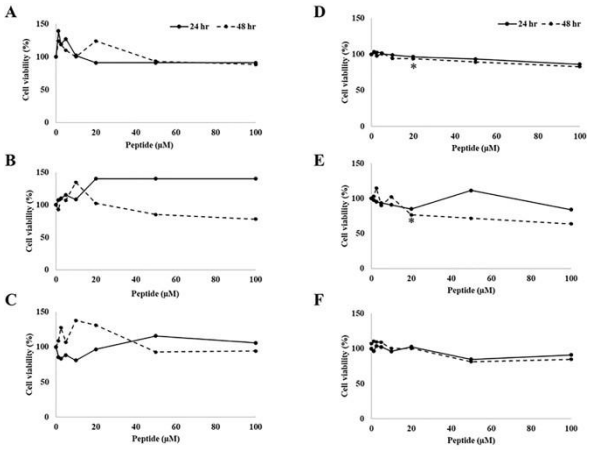


Figure 1. Effects of r(P)ApoBLPro (A, D), r(P)ApoBLAla (B, E) or r(P)ApoBSPro (C, F) on the viability of HT-29 (A, B, C) and SNU-1 (D, E, F) cell lines. MTT reduction assays were performed by treating cells with increasing concentrations (0-100 μM) of each peptide for 24 and 48 h. Experiments were performed in triplicate with triplicate determinations. Significant differences were indicated as *($P < 0.05$) for treated versus untreated samples.

338x190mm (300 x 300 DPI)

A

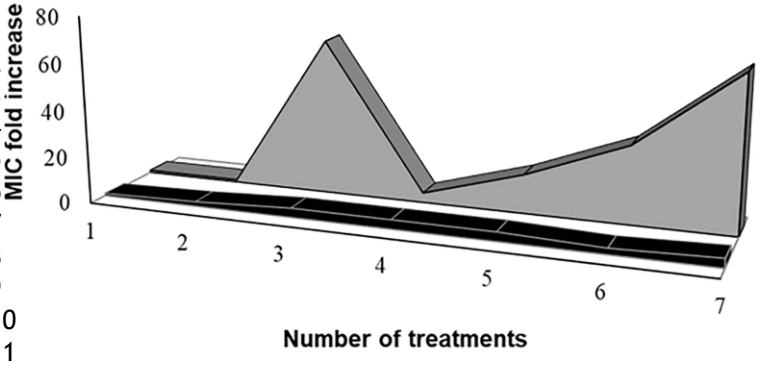
MIC fold increase
80
60
40
20
0
1
2
3
4
5
6
7
Number of treatments

B

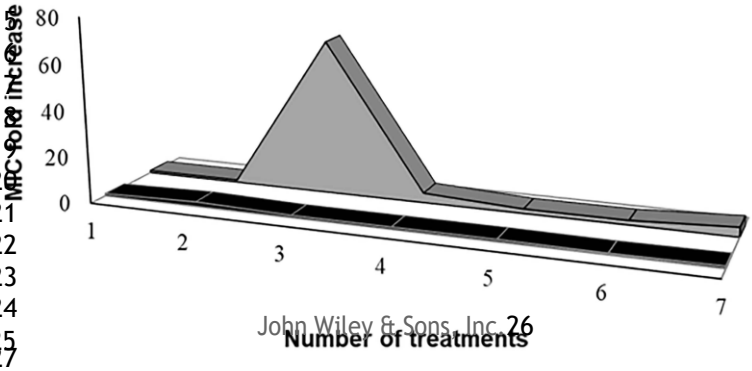
MIC fold increase
80
60
40
20
0
1
2
3
4
5
6
7
Number of treatments

**Table 1. MIC values obtained at time 0 and after several rounds of treatment of bacterial cells with ciprofloxacin or r(P)ApoB$_L^{Pro}$ peptide**

| | CIPROFLOXACIN | | | | r(P)ApoB$_L^{Pro}$ | | | |
|---|---|---|---|---|---|---|---|---|
| | *S. typhimurium* ATCC 14028 | | *S. enteriditis* 706 RIVM | | *S. typhimurium* ATCC 14028 | | *S. enteriditis* 706 RIVM | |
| **Number of treatments** | **MIC (µg/ml)** | **Fold increase** | **MIC (µg/ml)** | **Fold increase** | **MIC (µM)** | **Fold increase** | **MIC (µM)** | **Fold increase** |
| 1 | 0.3 | 1 | 0.3 | 1 | 2.5 | 1 | 5 | 1 |
| 2 | 0.3 | 1 | 0.3 | 1 | 5 | 2 | 5 | 1 |
| 3 | 20 | 67 | 20 | 67 | 10 | 4 | 5 | 1 |
| 4 | 1.25 | 4 | 1.25 | 4 | 10 | 4 | 5 | 1 |
| 5 | 5 | 17 | 0.6 | 2 | 10 | 4 | 5 | 1 |
| 6 | 10 | 33 | 0.6 | 2 | 10 | 4 | 5 | 1 |
| 7 | 20 | 67 | 1.25 | 4 | 10 | 4 | 5 | 1 |

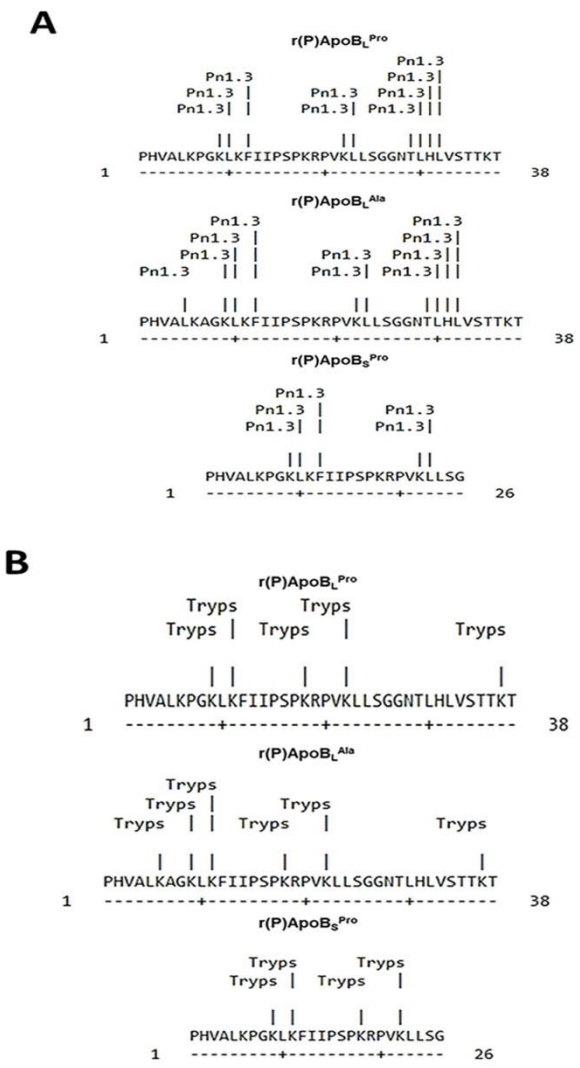


Figure 3. In silico identification of pepsin cleavage sites (A) and trypsin cleavage sites (B) in ApoB-derived peptides sequences. Analyses have been performed by using Peptide Cutter tool on ExSPAsy database. The total number and the position of pepsin and trypsin cleavage sites are shown in r(P)ApoBLPro, r(P)ApoBLAla, and r(P)ApoBSPro.

190x338mm (300 x 300 DPI)

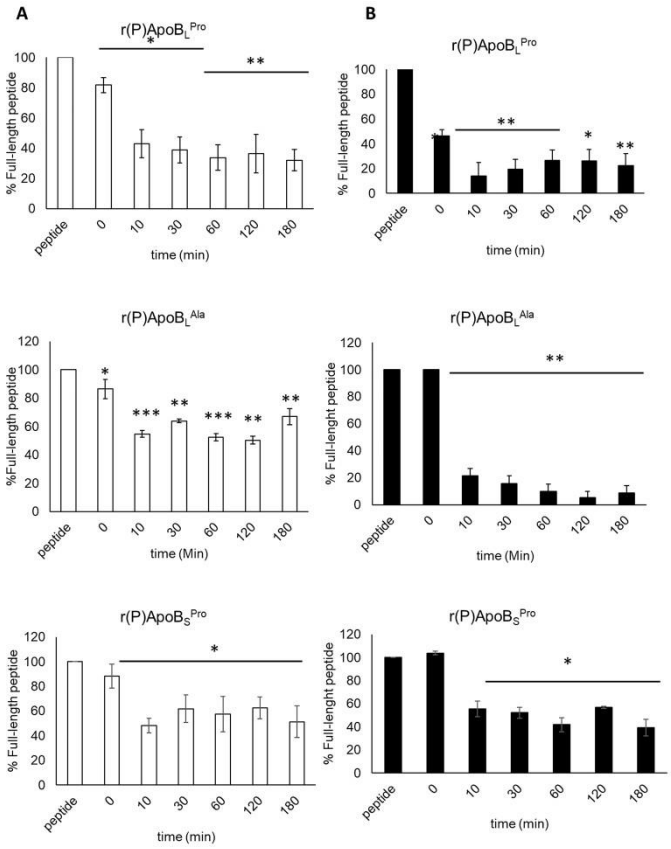


Figure 4. Analysis of ApoB-derived peptides hydrolysis in simulated gastric fluid (A, white bars) or in simulated intestine fluid (B, black bars). Graphs have been obtained upon SDS-PAGE and densitometric analyses of the intensity of the bands corresponding to full-length peptides in the absence or in the presenceof pepsin (A) or trypsin (B). Experiments were performed in triplicate. Significant differences were indicated as *(P < 0.05), **(P < 0.01) or ***(P < 0.001) for treated versus untreated samples.

483x860mm (200 x 200 DPI)